

DISS. ETH NO. 23419

# **FUNCTIONS OF HUMAN CACTIN IN PRE-mRNA SPLICING AND CHROMOSOME STABILITY**

A thesis submitted to attain the degree of

DOCTOR OF SCIENCES of ETH ZURICH

(Dr. sc. ETH Zurich)

presented by

**ISABELLA MARTINA YVONNE ZANINI**

MS sc. in Biology, University of Zurich, Switzerland

born on 09.02.1985

citizen of Bellinzona, Ticino, Switzerland

accepted on the recommendation of

Prof. Dr. Claus M. Azzalin, examiner  
Prof. Dr. Massimo Lopes, co-examiner  
Prof. Dr. Vikram Panse, co-examiner

2016





## SUMMARY

Cactin proteins are evolutionarily conserved, essential nuclear proteins implicated in different molecular pathways apparently unrelated to each other, including control of gene expression, inflammatory response, cell cycle progression, development and embryogenesis, and pre-mRNA splicing. A screen of a *S. pombe* deletion library performed in our laboratory identified fission yeast Cactin (Cay1) as a regulator of telomeric chromatin. Further analyses showed that Cay1 regulates telomere length and telomeric transcription via stabilisation of the telomeric protein Rap1, principally by promoting Rap1 pre-mRNA splicing. The C-terminal domain, which has been shown to mediate protein-protein interactions in different organisms, is 46% identical in Cay1 and human Cactin (hCactin), suggesting that Cay1 and hCactin are orthologs. We show that hCactin is an essential nuclear protein necessary for preserving genome stability, chromosome integrity and promoting cell proliferation in human cells. Differently from its fission yeast ortholog Cay1, hCactin does not participate in maintaining telomere homeostasis in human cells. We provide evidence that hCactin sustains pre-mRNA splicing and it physically interacts with the ATPase/RNA helicase DHX8 and with the SR protein SRRM2. Importantly, these factors function with hCactin in promoting pre-mRNA splicing of the cohesin regulatory factor Sororin. Deregulated Sororin pre-mRNA splicing in hCactin-depleted cells leads to cohesion loss and premature sister chromatid separation, as Sororin overexpression in the same cells reverses these phenotypes. hCactin depletion also leads to accumulation of DNA damage and impaired cell proliferation independently of Sororin splicing defects. In addition, hCactin physically interacts with the cullin protein CUL7 and enhances its stability. hCactin interaction with a multitude of proteins involved in independent cellular pathways is likely to explain the pleiotropic phenotypes observed upon its depletion in human cells.



## RIASSUNTO

Le proteine della famiglia Cactin sono proteine essenziali conservate durante l'evoluzione. Diversi studi hanno dimostrato il coinvolgimento di queste proteine in processi molecolari apparentemente indipendenti tra loro, quali il controllo dell'espressione genica, la risposta infiammatoria, la promozione del ciclo cellulare, lo sviluppo e l'embriogenesi ed il processo di trasformazione dell'acido ribonucleico precursore (pre-mRNA) nell'acido ribonucleico messaggero (mRNA) mediante uno specifico meccanismo chiamato splicing del pre-mRNA. Il nostro laboratorio, tramite lo screening di un'intera biblioteca di soppressioni geniche nel lievito *S. pombe*, ha individuato la proteina Cactin Cay1 quale regolatore della cromatina telomerica. Ulteriori analisi hanno dimostrato che Cay1 regola lunghezza e trascrizione dei telomeri stabilizzando la proteina telomerica Rap1, principalmente promuovendo il processo di splicing. Alcuni studi hanno suggerito che la porzione terminale della proteina Cactin possa promuovere l'interazione tra proteine in diversi organismi. Questa regione è identica al 46% in Cay1 e nella proteina umana Cactin (hCactin), suggerendo che Cay1 e hCactin siano ortologhi. In questa tesi documentiamo che hCactin è una proteina nucleare necessaria alla proliferazione cellulare e alla salvaguardia dell'integrità cromosomica e della stabilità genomica nelle cellule umane. A differenza di Cay1, hCactin non partecipa direttamente alla conservazione dell'omeostasi telomerica nelle cellule umane. Forniamo invece prova della partecipazione di hCactin nella promozione dello splicing del mRNA tramite l'interazione fisica con l'ATPasi/RNA elicasi DHX8 e la proteina SRRM2. Nello specifico, queste proteine sembrerebbero funzionare con hCactin nel promuovere lo splicing di Sororin, una proteina che regola la coesione tra i cromatidi fratelli. Nelle cellule umane con indotta insufficienza della proteina hCactin si osserva una deregolamentazione del processo di splicing di Sororin e una conseguente prematura separazione dei cromatidi fratelli. Per quanto l'overespressione di Sororin compensi per la perdita di coesione, l'accumulazione di danni all'acido deossiribonucleico (DNA) e la compromissione della proliferazione cellulare non sono compensati dal ripristino dei livelli di Sororin nelle cellule carenti di hCactin. Dimostriamo inoltre che hCactin interagisce fisicamente con la proteina Cullin7 promuovendone la stabilità. Proponiamo quindi che simili interazioni tra hCactin e proteine coinvolte in diversi processi cellulari spieghino i fenotipi pleiotropici associati all'insufficienza di hCactin nelle cellule uman



## AKNOWLEDGEMENTS

I'm particularly grateful to my supervisor Prof. Claus Azzalin for offering me the possibility to work in his lab as a PhD candidate and for providing great supervision during these years. His passion for science and his continuous support motivated me throughout this experience and strengthened my interest for scientific research.

I would like to thank the current and past members of the Azzalin lab for providing such a pleasant working atmosphere, for the productive scientific discussions, and for sharing ideas and expertise. I'm appreciative of the collaborative work that was done towards this thesis and to Luca Lorenzi who studied Cactin in fission yeast laying the foundation for my PhD project. A special thank goes to Rajika Arora for her precious help and continuous encouragement.

I'm grateful to my doctoral thesis committee members Prof. Massimo Lopes, Prof. Paola Picotti, Prof. Vikram Panse, Prof. Matthias Peter, and Prof. Fabrizio d'Adda di Fagagna for investing time and interest in profitable discussions, providing important inputs and criticisms during the course of my PhD.

I also would like to thank colleagues and member of the Institute of Biochemistry (IBC) for the nice working atmosphere and for sharing expertise and materials, and the MLS PhD program for providing a number of interesting training activities.

I'm also grateful to Rajika, Corinne and Richard for their friendship and for sharing happy and gloomy days in the lab. A special thanks goes to my friend Lorenza for sharing ups and downs during these years. Many thanks also to Kai for his precious encouragement and helpful discussions.

Non da ultimo ci tengo a ringraziare la mia famiglia, soprattutto i miei genitori per il loro affetto e il costante incoraggiamento. Un grazie speciale a Lorenzo per il suo importante appoggio e per aver condiviso questi anni importanti al mio fianco.



# TABLE of CONTENT

LIST OF FIGURES .....	11
LIST OF TABLES .....	14
1 DECLARATION OF CONTENTS.....	15
2 INTRODUCTION .....	17
2.1 The eukaryotic family of Cactin proteins.....	17
2.2 Sister chromatid cohesion in eukaryotes.....	26
2.3 Pre-mRNA splicing .....	35
2.4 CUL7 protein.....	44
3 AIM OF THE STUDY .....	49
4 RESULTS.....	51
4.1 Phenotypes associated to hCactin depletion .....	53
4.2 Human Cactin is essential for Sororin pre-mRNA splicing.....	75
4.3 Human Cactin and its interactome .....	83
5 DISCUSSION .....	109
5.1 Human Cactin is an essential nuclear protein .....	109
5.2 Human Cactin safeguard genome stability .....	109
5.3 Human Cactin promotes cell proliferation.....	112
5.4 Human Cactin supports pre-mRNA splicing .....	114
5.5 Human Cactin and its interactome .....	117
5.6 Conservation of function between Cactin in fission yeast (Cay1) and hCactin.....	122

5.7	Human Cactin and the immune response .....	126
5.8	Conclusion.....	127
5.9	Outlook.....	129
6	MATERIAL AND METHODS .....	131
6.1	Human cell lines.....	131
6.2	Cell culture, cell transfection and cell treatments.....	132
6.3	Protein extraction and western blotting .....	135
6.4	Indirect immunofluorescence and DNA <i>in-situ</i> hybridisation .....	137
6.5	Flow cytometric analysis.....	138
6.6	Pulse Field Gel Electrophoresis for DSB detection.....	139
6.7	Metaphase spread.....	140
6.8	Nuclei acids analysis .....	141
6.9	Streptavidin One-Step purification for MS analysis .....	144
6.10	Co-Immunoprecipitation.....	145
7	BIBLIOGRAPHY .....	147
8	CURRICULUM VITAE.....	169



## LIST OF FIGURES

Figure 1: Conservation of Cactin protein throughout the evolution.....	18
Figure 2: Conserved protein domains of Cactin protein.....	19
Figure 3: Cay1 deletion results in increased telomere transcription and elongated telomeres as a consequence of reduced Rap1 protein levels. ....	25
Figure 4: Mitotic phases and sister chromatid separation. ....	27
Figure 5: The ring model of the cohesin complex. ....	29
Figure 6: Dual mode of cohesin binding.....	31
Figure 7: Schematic representation of the two-step mechanism of pre-mRNA splicing. ....	36
Figure 8: Canonical cross-intron assembly and disassembly pathway of the spliceosome. ....	37
Figure 9: Model for the exon definition.....	38
Figure 10: Schematic representation of pre-mRNA splicing control exerted by cis-acting sequences.....	40
Figure 11: Kinetic model of cotranscriptional splicing. ....	42
Figure 12: Human Cactin is nuclear and chromatin bound. ....	52
Figure 13: hCactin depletion results in cell cycle arrest. ....	54
Figure 14: hCactin depletion induces abnormal nuclear morphologies. ....	55
Figure 15: Abnormal nuclear morphology may be the consequence of aberrant mitosis.....	56
Figure 16: hCactin depletion induces accumulation of DNA damage. ....	58
Figure 17: DNA damage checkpoint activation in hCactin-depleted cells. ....	60
Figure 18: Metaphase spread analysis of hCactin-depleted cells ....	61
Figure 19: Cell cycle arrest, appearance of abnormal nuclei, accumulation of DNA damage and increased frequency of aberrant metaphases are true outcome of Cactin depletion. ....	63
Figure 20: Depletion of hCactin impairs cell proliferation shortly after transfection. ...	65

<b>Figure 21: hCactin-depleted cells experience a hindered G1/S transition of the first cell cycle after transfection.....</b>	<b>66</b>
<b>Figure 22: hCactin depletion impairs cell proliferation of immortalised human fibroblasts.....</b>	<b>68</b>
<b>Figure 23: Depletion of hCactin in RPE-1 cells affects the G-1 transition of the first cell cycle after transfection.....</b>	<b>69</b>
<b>Figure 24: Depletion of hCactin does not affect levels of shelterin proteins or telomere length. ....</b>	<b>71</b>
<b>Figure 25: hCactin depletion does not impact on telomere homeostasis in RPE-1 cells. ....</b>	<b>72</b>
<b>Figure 26: hCactin-depleted cells do not specifically accumulate DNA damage at telomeres.....</b>	<b>73</b>
<b>Figure 27: hCactin depletion leads to a mild and general pre-mRNA splicing defect. ..</b>	<b>74</b>
<b>Figure 28: hCactin depletion affects Sororin pre-mRNA splicing.....</b>	<b>76</b>
<b>Figure 29: hCactin depletion leads to retention of Sororin intron 1. ....</b>	<b>78</b>
<b>Figure 30: Sororin cDNA overexpression.....</b>	<b>79</b>
<b>Figure 31: Sororin overexpression rescues the mitotic defects associated to hCactin depletion. ....</b>	<b>80</b>
<b>Figure 32: Sororin overexpression is not sufficient to rescue DNA damage and cell cycle defect associated with hCactin depletion. ....</b>	<b>82</b>
<b>Figure 33: Streptavidin One-Step purification of hCactin protein complexes for MS analysis.....</b>	<b>84</b>
<b>Figure 34: Validation of some hCactin interactions. ....</b>	<b>87</b>
<b>Figure 35: Depletion of hCactin interactome and Sororin pre-mRNA splicing.....</b>	<b>89</b>
<b>Figure 36: Human Cactin and DHX8 and SRRM2 may synergise to promote Sororin pre-mRNA splicing.....</b>	<b>91</b>
<b>Figure 37: Depletion of hCactin, DHX8 and SRRM2 impact on cell cycle progression, accumulation of DNA damage and abnormal nuclear morphology to different extent. ....</b>	<b>93</b>
<b>Figure 38: Depletion of CUL7 does not affect Sororin pre-mRNA splicing.....</b>	<b>95</b>
<b>Figure 39: Human Cactin is not a substrate of CRL7. ....</b>	<b>96</b>

<b>Figure 40: Reduced CUL7 protein levels observed upon hCactin depletion are not a clear consequence of CUL7 protein destabilisation. ....</b>	<b>97</b>
<b>Figure 41: Depletion of hCactin leads to a mild defect in CUL7 pre-mRNA splicing. ....</b>	<b>99</b>
<b>Figure 42: Depletion of Cul7 affects the G1/S transition similarly to hCactin depletion. ....</b>	<b>101</b>
<b>Figure 43: Depletion of hCactin induces c-Fos transcripts accumulation similarly to CUL7-depleted cells.....</b>	<b>103</b>
<b>Figure 44: CUL7 compensation system.....</b>	<b>105</b>
<b>Figure 45: CUL7 overexpression does not rescue the phenotypes associated to hCactin depletion.....</b>	<b>106</b>
<b>Figure 46: Speculative model for functions of hCactin in promoting chromosome stability.....</b>	<b>128</b>

## LIST OF TABLES

<b>Table 1: Brief description of known functions associated to the interactors of hCactin identified by MS. ....</b>	<b>85</b>
<b>Table 2: Commercial cell lines.....</b>	<b>131</b>
<b>Table 3: Plasmids for stable integration.....</b>	<b>131</b>
<b>Table 4: Generated stable cell lines.....</b>	<b>132</b>
<b>Table 5: Generated DOX-inducible Flp-In T-Rex 293 cell lines.....</b>	<b>132</b>
<b>Table 6: Generated DOX-inducible cell lines by random integration. ....</b>	<b>132</b>
<b>Table 7: shRNA sequences.....</b>	<b>133</b>
<b>Table 8: siRNA sequences.....</b>	<b>133</b>
<b>Table 9: Plasmids for transient transfections. ....</b>	<b>134</b>
<b>Table 10: Compounds used for cell culture treatments.....</b>	<b>134</b>
<b>Table 11: Antibodies used for WB analysis.....</b>	<b>136</b>
<b>Table 12: Antibodies used for IF analysis. ....</b>	<b>138</b>
<b>Table 13: Fluorescent labelled probes used for DNA FISH analysis.....</b>	<b>138</b>
<b>Table 14: Antibodies used for flow cytometric analysis. ....</b>	<b>139</b>
<b>Table 15: Running parameters of PFGE for DSB detection.....</b>	<b>140</b>
<b>Table 16: Primers used for RT-PCR analysis, previously designed (Watrin et al., 2014). .....</b>	<b>142</b>
<b>Table 17: Primers used for qRT-PCR analysis. Sororin and c-Fos primers were previously designed (Watrin et al., 2014) (Gu et al., 2013).....</b>	<b>143</b>
<b>Table 18: Antibodies used for IP and Co-IP analyses. ....</b>	<b>145</b>

## 1 DECLARATION OF CONTENTS

I declare that this doctoral thesis has been written by myself, Isabella Martina Yvonne Zanini.

The data contained in this thesis represents unpublished work of myself as well as of current and former members of the research group of Prof. Claus M. Azzalin (Institute of Biochemistry, ETH Zurich, 8093 Zürich, Switzerland), as listed below.

Metaphase spread and TRF analyses shown in **Figures 19G** and **24B** were performed by Catherine Brun; northern blot and TRF analyses shown in **Figure 25** were performed by Harry Wischnewski; IF-FISH analysis shown in **Figure 26** was performed by the semester student Federica Richina under my supervision; Purification and MS analysis of hCacin interactors shown in **Figure 33** was performed in collaboration with Luca Lorenzi.

**Figures 27B, 28A and B** and **41A** are the result of collaboration between our group and Dr. Charlotte Sonesson (Institute of Molecular Life Sciences, University of Zurich, 8057 Zürich, Switzerland).



## 2 INTRODUCTION

### 2.1 The eukaryotic family of Cactin proteins

#### The discovery of Cactin

In 1999 a polypeptide of 758 aminoacids (aa) named NY-REN-24 was discovered as an antigen recognized by autologous antibodies in patients with renal-cell carcinoma (Scanlan et al., 1999). This finding suggests that this protein is involved in promoting cancer cell proliferation. Shortly after, the NY-REN-24 ortholog in *D. melanogaster* was identified as a novel Cactus-interactor, and named Cactin (Lin et al., 2000). Cactus is one of the five genes that compose the intracellular part of the *Drosophila* Rel pathway, commonly referred to as the NF- $\kappa$ B signalling pathway. It is preserved in both invertebrates and vertebrates and plays an important role in the immune response and during development (Govind, 1999). Cactus (I $\kappa$ B) is found in complex with the morphogen Dorsal (NF- $\kappa$ B). Upon signalling Cactus and Dorsal proteins are phosphorylated, resulting in ubiquitin-mediated proteasomal degradation of Cactus and the nuclear translocation of Dorsal, which functions as a transcription factor (TF). This promotes expression of specific genes either involved in the immune response (Wu and Anderson, 1998) or contributing to the dorsoventral axis formation during embryogenesis (Govind et al., 1993). Yeast two-hybrid and co-immunoprecipitation analyses showed that Cactin directly interacts with Cactus through the highly conserved C-terminal domain of Cactin. Although Cactus and Dorsal are known to coexist in a complex, Cactin failed to co-immunoprecipitate with Dorsal (Lin et al., 2000). Lin and colleagues reported that the overexpression of Cactin in a *cactus*<sup>A2</sup> heterozygous background exacerbates the ventralized phenotype and the embryonic lethality associated with Cactus haploinsufficiency, suggesting that Cactin positively regulates Dorsal functions.

#### Conservation of Cactin

Cactins are essential proteins highly conserved throughout eukaryotes (**Fig. 1**). In the last 15 years Cactin has been studied in several model organisms, yet the molecular function exerted by this protein is still poorly characterized. With the exception of the *Saccharomyces cerevisiae* subphylum, in which no protein with sequence similarity has been found, Cactins share a considerable sequence identity, principally within the Cactin-mid and the Cactin C-terminal

domains (**Fig. 2**). The C-terminal domain, which shares the highest sequence identity among Cactin proteins, has been proposed to mediate protein-protein interaction in *Drosophila melanogaster* (Lin et al., 2000) and oligomerisation in *Toxoplasma gondii* (Szatanek et al., 2012). Lin and colleagues have suggested that the C-terminal domain, which is rich in prolines and includes several positively charged residues, may interact with metal ions and possibly have enzymatic function. The less conserved N-terminal part of Cactin, comprising the Mid-domain, contains a putative number of serine- and arginine-rich (SR) domains and two coiled-coil domains that may also function in self-association or in interaction with other proteins (Lin et al., 2000). Human Cactin contains two bipartite nuclear localisation signals (NLSs) in its N-terminal part, which has been shown to be essential for its nuclear localization (Atzei et al., 2010a). Cactin is also known to localize to the nucleus in *T. gondii*, *Arabidopsis thaliana*, *Schizosaccharomyces pombe*, and *Caenorhabditis elegans*, and Cactin nuclear localization has been shown to be crucial for some of its functions (Baldwin et al., 2013; Lorenzi et al., 2015; Szatanek et al., 2012; Tannoury et al., 2010). Considering that Cactin in *D. melanogaster* contains three predicted NLSs, Cactin nuclear localisation is expected to be essential, at least for some of its functions, in every organism. Lastly, a number of supposed phosphorylation sites are distributed along Cactin protein sequence, but their functional relevance has not been tested yet.

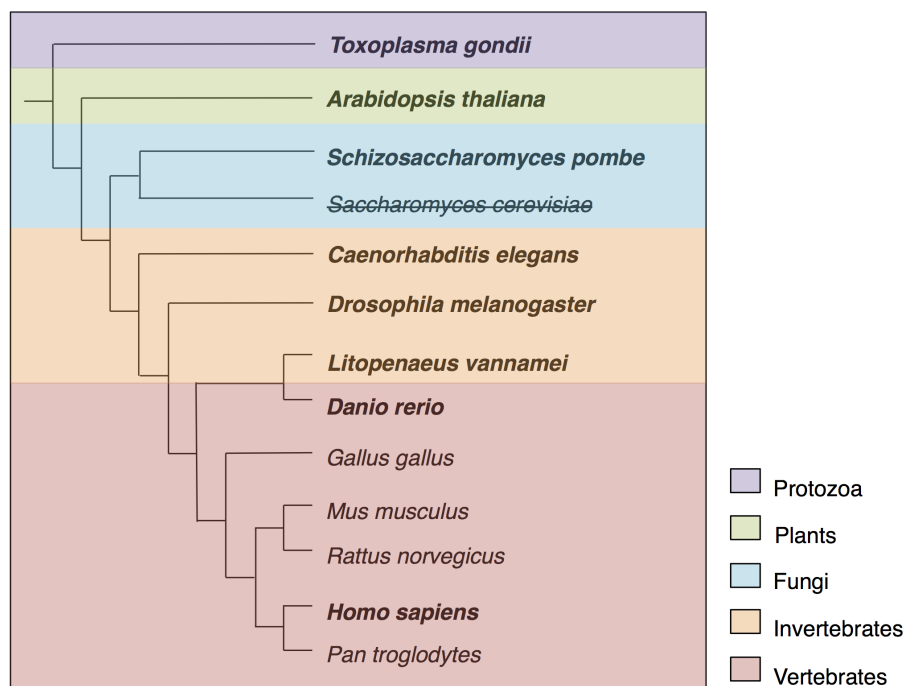


**Figure 1: Conservation of Cactin protein throughout the evolution.**

Simplified phylogenetic tree representing organisms where Cactin is conserved. Branch lengths are arbitrary. Species in bold represent organisms in which Cactin has been studied.





**Figure 2: Conserved protein domains of Cactin protein.**  
Protein sequence alignment made using the Clustal Omega software (www.uniprot.org). Conserved domains of Cactin protein are highlighted and schematically represented on the right.

### **Cactin in early development and cell viability**

Cactin seems to be necessary for development in different organisms, as Cactin insufficiency leads to embryonic lethality in *A. thaliana* (Baldwin et al., 2013) and *Danio rerio* (Atzei et al., 2010b), results in larval development arrest in *C. elegans* (Tannoury et al., 2010), and compromises neural development in *D. melanogaster* (Sepp et al., 2008). Moreover, Cactin seems to be essential for organism and cell viability, since Cactin depletion leads to a high mortality rate in *Litopenaeus vannamei* (Zhang et al., 2014), induces irreversible cell cycle arrest in *T. gondii* (Szatanek et al., 2012) and is required for *S. pombe* cell cycle progression in the cold (Hayles et al., 2013; Lorenzi et al., 2015).

The effects of Cactin deficiency on development processes and cell viability in different organisms suggest that Cactin is an essential protein and, considering the selective pressure exerted on the C-terminal portion of Cactin protein throughout evolution, that at least some of its functions are likely to be conserved.

### **Cactin in vertebrates and evidence of function in transcriptional regulation**

The NF- $\kappa$ B signalling in zebrafish is known to play an important role in the anteriorposterior axis formation interfering with the notochord development (Correa et al., 2004). Atzei and colleagues showed that maternal expression of Cactin correlates with the maternal expression of Toll-like receptors and associated adaptor proteins (Atzei et al., 2010b), which are known to be upstream regulators of NF- $\kappa$ B (van der Sar et al., 2006). Moreover, Cactin knockdown by morpholino oligonucleotides impairs posterior body morphogenesis and neural development, and results in high embryonic lethality (Atzei et al., 2010b). Atzei and colleagues highlighted the functional role of Cactin in zebrafish early development, providing the first evidence that Cactin is essential during vertebrate development.

hCactin was shown to participate in the modulation of the NF- $\kappa$ B signalling pathway in response to proinflammatory stimuli (Atzei et al., 2010a). While overexpression of hCactin inhibits the NF- $\kappa$ B-dependent gene expression upon both endogenous and exogenous proinflammatory stimuli, hCactin depletion through short hairpin RNA (shRNA) enhances NF- $\kappa$ B signalling. Thus, differently from what was observed in *D. melanogaster*, in human cells hCactin seems to negatively regulate the NF- $\kappa$ B function. Furthermore, hCactin depletion also augments the activation of interferon regulatory transcription factors IRF3 and IRF7 in response to endotoxins, whereas it reduces the MEKK1-dependent activation of c-Jun TF, suggesting that

hCactin controls independent transcriptional programs (Atzei et al., 2010a). Atzei and colleagues reported that hCactin failed to interact with the canonical cytoplasmic I $\kappa$ B proteins but interacts with the nuclear I $\kappa$ BL protein, a nuclear I $\kappa$ B-related protein that displays a similar regulation of the NF- $\kappa$ B signalling pathway in response to proinflammatory stimuli (Chiba et al., 2011). I $\kappa$ BL and hCactin exhibit a comparable inhibitory effect on NF- $\kappa$ B and the overexpression of both proteins did not further augment this inhibitory effect, suggesting that hCactin and I $\kappa$ BL function in an epistatic relationship in regulating the NF- $\kappa$ B-mediated inflammatory response (Atzei et al., 2010a).

Recently, yeast two-hybrid screening and co-immunoprecipitation analyses showed that Cactin interacts with the tripartite motif-containing protein with TRIM39 (Suzuki et al., 2015), whose E3 ligase activity can promote substrate protein degradation (Zhang et al., 2012a) or protein stabilization (Lee et al., 2009). Like other TRIM proteins, TRIM39 is involved in inflammatory response, specifically by regulating the interferon type 1 (INF-1) signalling pathway (Kurata et al., 2013). Moreover, a single nucleotide polymorphism (SNP) on the exon 9 of TRIM39 gene has been reported to be one of the genetic factors in Behcet's syndrome, a rare disease characterized by chronic inflammation of small vessels (systemic vasculitis) (Kurata et al., 2010). Suzuki and colleagues showed that TRIM39 physically binds and stabilises hCactin in the nucleus in order to suppress the NF- $\kappa$ B signalling pathway. hCactin, but not TRIM39, mRNA and protein levels are significantly increased upon cell stimulation with tumour necrosis factor  $\alpha$  (TNF $\alpha$ ), suggesting that hCactin is part of a negative feedback loop within the NF- $\kappa$ B signalling pathway. Upon TNF $\alpha$  stimulation TRIM39 overexpression substantially suppresses NF- $\kappa$ B, whereas TRIM39 depletion significantly activates NF- $\kappa$ B signalling pathway (Suzuki et al., 2015). It has been shown that the mitogen-activated protein kinases (MAPKs) are involved in TLR-induced immune response by transcriptionally regulating several NF- $\kappa$ B target genes (Jin et al., 2011). However, TRIM39 and hCactin are not involved in the MAPK signalling pathway; rather they appear to be negative regulators of inflammatory responses (Suzuki et al., 2015).

Interestingly, TRIM39 and I $\kappa$ BL are proteins encoded by the human major histocompatibility complex (MHC) locus located on chromosome 6, which comprises more than 100 genes related to the immune response. I $\kappa$ BL is encoded by the (MHC) class III region, which codes for a plethora of factors that do not have antigen-presenting capacity but are involved in other immune response (Xie et al., 2003). Large-scale yeast two-hybrid analysis also revealed that hCactin interacts with two proteins encoded by the human major histocompatibility complex (MHC) class III region: the RNA binding protein NELF-E, a subunit of the negative elongation factor complex that represses

transcription elongation by RNA polymerase II, and LST1/f, a leukocyte specific transcript 1 variant of unknown function (Lehner et al., 2004).

### **Emerging role for Cactin in control of transcriptional programs**

A genome-wide RNA interference (RNAi) screen identified Cactin and NELF-E, together with other factors involved in transcriptional regulation, as regulators of mitochondrial citrate synthase activity in *D. melanogaster*, providing evidence of a pleiotropic function for fly Cactin (Chen et al., 2008).

The Rel pathway is not conserved in *C. elegans* (Pujol et al., 2001) and its defence mechanism against bacterial or fungal pathogens does not depend on a Toll pathway (Aballay et al., 2003). Still Cactin is well conserved in worms, suggesting additional targets for this protein. In *C. elegans* a genome-wide RNAi screen identified Cactin/Cacn-1 as an essential gene for larval development and regulation of the distal tip cell (DTC) migration during gonad morphogenesis (Tannoury et al., 2010). Cell migration is a fundamental process for embryonic development and for immune system function in the adult organism. Tannoury and colleagues showed that, in order to control DTC migration, Cacn-1 is expressed in different tissues at different times in the larvae, and that the genetic interaction between Cacn-1 and the Rac GTPase is important for controlling DTC pathfinding. Moreover, Cacn-1 has been shown to participate in the Wnt/ $\beta$ -catenin signalling pathway (LaBonty et al., 2014), which controls cell proliferation and differentiation (Teo and Kahn, 2010). During larval development Cacn-1 seems to negatively regulate the activity of the transcription factor POP-1, a major regulator of gene expression (Maduro et al., 2002) and cell fate determination (Herman, 2001), suggesting a function for Cactin in transcriptional control independent of the Toll-pathway (LaBonty et al., 2014).

A genetic screen for temperature-sensitive (ts) growth defects in the human protozoan pathogen *Toxoplasma gondii*, which also lacks the Rel pathway, identified a G1-arrested mutant that carries a point mutation in the CACTIN gene (Szatanek et al., 2012). The point mutation results in a Tyrosine to Histidine change in the highly conserved C-terminal domain of Cactin and causes an irreversible G1 arrest, suggestive of a defect in a general process essential for G1 progression. In addition to the expected expression of G1-associated genes, further genome-wide expression profiling of this mutant revealed the unexpected expression of several genes associated with the extracellular state and the bradyzoite tissue cyst stage (Szatanek et al., 2012), in particular genes encoding several apicomplexan AP2 transcription factors, which directly control expression of genes involved in growth and stage differentiation (Painter et al., 2011). Szatanek and colleagues also demonstrated that Cactin is present in an oligomeric complex and the

aforementioned point mutation in Cactin probably leads to Cactin protein misfolding. A critical function exerted by the N-terminal half of Cactin protein was also emphasised, since the C-terminal domain could not rescue the G1 arrest in the mutant parasites (Szatanek et al., 2012). Szatanek and colleagues provided evidence of Cactin functioning as a scaffold protein regulating many key signalling pathways through promotion of protein complex formation. Although there is still limited understanding of the molecular function exerted by Cactin, an important function in controlling different transcriptional programs is likely to be conserved among Cactin proteins.

### **Evidence of Cactin function in promoting pre-mRNA splicing**

Bioinformatic analysis predicted SR domains in *D. melanogaster* and human Cactin (Boucher et al., 2001). SR domains are characteristic of SR factors functioning in pre-mRNA splicing (Graveley and Maniatis, 1998). Consistently, several studies have suggested a link between Cactin proteins and pre-mRNA splicing. An affinity-tag purification analysis of native spliceosome intermediates and large-scale proteomic analysis identified hCactin as a component of the catalytically active spliceosome (Bessonov et al., 2008; Jurica et al., 2002; Rappsilber et al., 2002; Zhou et al., 2002). *In vitro* analysis of *D. melanogaster* nuclear extracts confirmed that Cactin is part of the spliceosomal complex (Herold et al., 2009), further suggesting a conservation of function from fly to human. Furthermore, a large-scale proteomic analysis of human protein-protein interactions disclosed that hCactin and the RNA-binding protein RNPS1 form a complex in cells (Ewing et al., 2007). RNPS1 is an auxiliary component of the exon junction complex (EJC) deposited at splice junctions on mRNAs and involved in several mRNA metabolic processes including nuclear export and RNA surveillance (Lee and Tarn, 2013; Lykke-Andersen et al., 2001; Nott et al., 2004). In *A. thaliana* Cactin localises to nuclear speckles and co-localises with two splicing factors: the SR proteins RSP31 and SR45 (Baldwin et al., 2013). Interestingly, SR45 is the ortholog of the human RNPS1, again strengthening the idea of a conservation of function among the members of the Cactin family. Moreover, yeast two-hybrid analyses revealed that *Arabidopsis* Cactin interacts with putative components of the spliceosome (Baldwin et al., 2013) and *Drosophila* Cactin interacts with the splicing core factor SmB (Giot et al., 2003). Additionally, the hCactin interactor IkBL has been shown to associate with the spliceosomal complex and control alternative splicing of immune-related genes (An et al., 2013; Bessonov et al., 2008).

A screening of a fission yeast deletion library performed in our laboratory identified Cactin ortholog in fission yeast Cay1 (Cactin in fission yeast 1) as a

regulator of telomeric transcript cellular levels (Lorenzi et al., 2015). Telomeres are nucleoprotein complexes situated at the end of the linear eukaryotic chromosomes, comprising arrays of G-rich DNA tandem repeats and the multiprotein complex shelterin (de Lange, 2009; Jain and Cooper, 2010). The shelterin complex protects telomeres from aberrant DNA processing, promotes telomeric DNA replication, and regulates the accessibility of telomerase to telomeres (de Lange, 2005). Although telomeres are known to be constitutive heterochromatin loci and are enriched in repressive chromatin marks, they are transcribed into different long-noncoding RNA (lncRNA) species. Among these, the lncRNA TERRA (telomeric repeat-containing RNA) has been first discovered in human cells as a G-rich telomeric transcript synthesised by the RNA polymerase II (RNAPII) starting from the subtelomeric tract (Azzalin et al., 2007). The telomeric transcriptome in fission yeast, comprising TERRA, the TERRA antisense transcript ARIA, and two antiparallel subtelomeric transcripts ARRET and  $\alpha$ -ARRET, is regulated at the transcriptional and post-transcriptional level (Bah et al., 2012). We showed that *cay1* $\Delta$  cells present increased telomeric transcription and elongated telomeres as a consequence of alleviated heterochromatin silencing and deregulated telomerase activity (**Fig. 3D, 3E**) (Lorenzi et al., 2015). The shelterin protein Rap1 is known to negatively regulate telomerase and to restrict the accessibility of RNAPII to the TERRA transcription start site (Bah et al., 2012; Cooper et al., 1997; Greenwood and Cooper, 2012). In *cay1* $\Delta$  cells Rap1 mRNA and protein levels are reduced as a consequence of inefficient Rap1 pre-mRNA splicing and slightly decreased Rap1 protein stability (**Fig. 3A, 3B, 3C**). Overexpression of Rap1 is sufficient to revert the telomeric defects associated with *cay1* $\Delta$ , demonstrating that Cay1 restricts telomere transcription and telomere elongation by controlling Rap1 levels in cells. Furthermore, *cay1* $\Delta$  cells accumulate unprocessed Tf2 retrotransposon RNA, which can also result from compromised pre-mRNA splicing (Lorenzi et al., 2015). In the cold, *cay1* $\Delta$  cells suffer from growth retardation and chromosomal aberration in a Rap1-independent manner (Lorenzi et al., 2015). Our data in fission yeast provide first evidence of Cactin promoting pre-mRNA splicing and possibly controlling a plethora of important cellular processes.

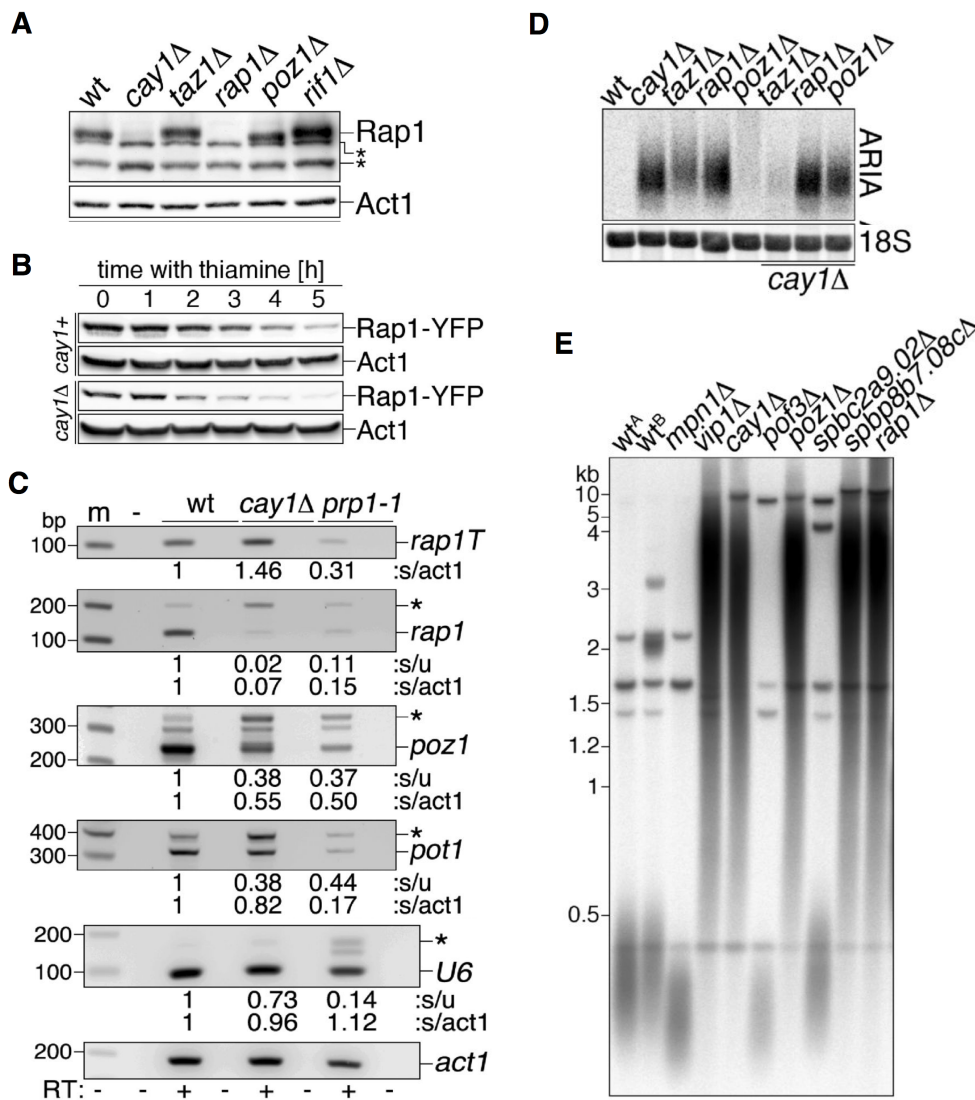


**Figure 3: Cay1 deletion results in increased telomere transcription and elongated telomeres as a consequence of reduced Rap1 protein levels.**

**A)** Western blot analysis showing reduced Rap1 protein levels in *cay1Δ* cells. **B)** WB analysis of cycloheximide-treated cells shows Rap1 protein destabilisation in *cay1Δ* cells. **C)** RT-PCR analysis indicating compromised Rap1 pre-mRNA splicing in *cay1Δ* cells. **D)** Northern blot analysis shows augmented amounts of the telomeric transcript ARIA in *cay1Δ* cells. **E)** Southern blot analysis revealing elongated telomeres in *cay1Δ* cells. Modified from Lorenzi et al., 2015.

## 2.2 Sister chromatid cohesion in eukaryotes

In order to proliferate the cell needs to duplicate and distribute its chromosomes and its cellular components into two daughter cells. These tasks are tightly regulated and restricted to specific phases of the cell cycle. The organelles and cytosolic components are duplicated at every cell cycle during the G1 phase. This process requires an elevated rate of transcription and translation processes. During the subsequent S phase cells duplicate their entire DNA. If properly replicated, the resulting sister chromatids are then segregated during mitosis into the two genetically identical daughter cells formed through cytokinesis (**Fig. 4**). Correct segregation is achieved thanks to the action of the spindle apparatus, which firstly captures condensed chromosomes in a bipolar manner and successively moves into opposite directions pulling apart sister chromatids. Although this process is tightly controlled by a plethora of factors that ensure proper spindle-kinetochore attachment and regulate progression through mitosis, it largely depends on proper sister chromatid cohesion (Krenn and Musacchio, 2015).

The chromosome structure in eukaryotes is maintained thanks to three important protein complexes, called structural maintenance of chromosome (SMC) complexes, which associate with chromatin and modulate important processes involved in chromatin dynamics and maintenance (Jeppsson et al., 2014). The protein complex cohesin exerts an essential function in maintaining sister chromatid cohesion (Michaelis et al., 1997). Additionally, it also promotes homologous recombination (Birkenbihl and Subramani, 1995), modulates transcriptional rates (Tonkin et al., 2004) and participates in chromosome condensation (Guacci et al., 1997) (Mehta et al., 2013; Peters et al., 2008). Condensin is the key complex involved in chromosome condensation (Hirano et al., 1997), and it has also been linked to transcriptional silencing (Chuang et al., 1994). Lastly, Smc5/6 is crucial for DNA repair (Fousteri and Lehmann, 2000), it promotes replication (Torres-Rosell et al., 2007) and regulates mitotic chromosomal organisation (Gallego-Paez et al., 2014).



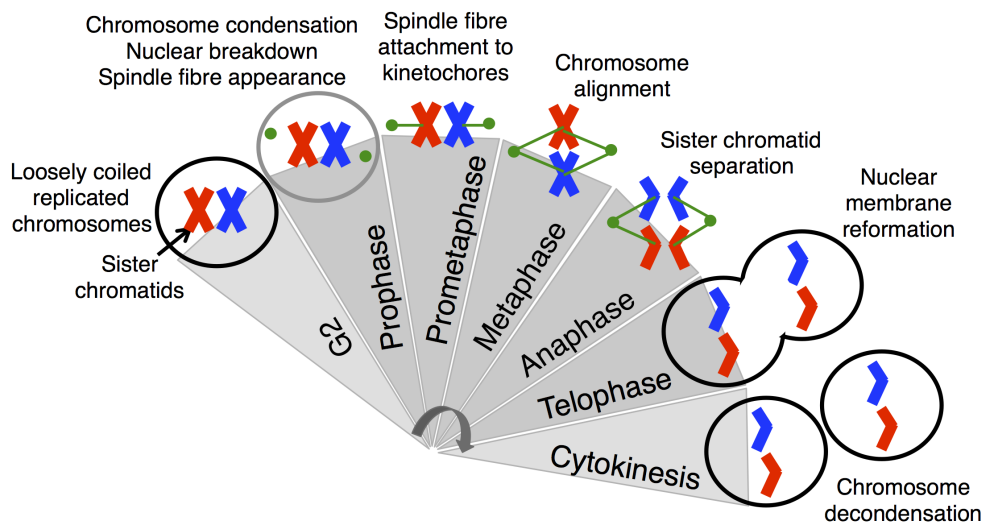


**Figure 4: Mitotic phases and sister chromatid separation.**

The mitotic phases and the important steps of chromosome segregation are schematically represented. For simplicity only two chromosomes are shown (blue and red). Spindle poles and spindle fibres are shown in green. Circles around chromosomes represent nuclear membrane.

### Mitotic cohesin is the key factor of sister chromatid cohesion

Cohesin is a protein complex composed of a well-conserved cohesin core complex and a number of less conserved cohesin-associated proteins that exert regulatory function. The cohesin core complex is composed of Smc1 and Smc3, two large ATPases members of the SMC family that associate through their hinge domains (Haering et al., 2002). The ATPase heads of Smc1 and Smc3 are connected by the kleisin Scc1 (Schleiffer et al., 2003). In vertebrates, somatic cells contain two sets of cohesin core subunits comprising either the stromalin antigens 1 (SA1) or 2 (SA2) (Losada et al., 2000; Sumara et al., 2000). Three cohesin-associated proteins are known to be part of the cohesin. One of them is the conserved HEAT repeats-containing protein Pds5 (precocious separation of sisters 5), which associates with Cohesin<sup>SA1</sup> or Cohesin<sup>SA2</sup> core subunits and is thought to contribute to cohesion and condensation (Hartman et al., 2000). In vertebrates there are two Pds5 homologs (Pdsf5A and Pdsf5B), resulting in at least four different cohesins (Losada et al., 2002; Sumara et al., 2000). The second protein known to associate with cohesin core complex is the poorly conserved repetitive sequences-containing protein Wap1. Its function in vertebrate is dispensable for sister chromatid cohesion but essential for cohesin removal from chromatin (Gandhi et al., 2006; Kueng et al., 2006). The third cohesin-

regulatory factor is Sororin, a small protein only conserved in vertebrates. It was initially discovered as a substrate of the anaphase-promoting complex/cyclosome (APC/C) (Rankin et al., 2005). However, Sororin has been shown to be required for chromatid cohesion independent of the APC/C (Diaz-Martinez et al., 2007).

### **Cohesin loading and positioning onto DNA**

Sister chromatid cohesion and cohesin loading are strictly dependent mechanisms. Cohesin loading always requires the activity of the chromatin-bound protein Adherin (also called Scc2; Scc2/4 in human), which help in recruiting cohesin to specific loci (Ciosk et al., 2000; Watrin et al., 2006). The Smc1/3-mediated ATP hydrolysis is also necessary to transiently open the cohesin ring and allow loading onto DNA (Arumugam et al., 2003). In *Xenopus* egg extracts Adherin is recruited to chromatin by interaction with the pre-replicative complexes (pre-RCs), whose assembly has also been shown to participate in cohesin loading (Takahashi et al., 2004). Interestingly, tethering Adherin to a chromosomal locus where it is normally not bound is not sufficient for recruiting cohesin, implying a more sophisticated mechanism (Hu et al., 2011).

For a long time it has been thought that cohesins can directly bind to DNA through their ATPase heads. However, the ring-like structure formed by Smc1, Smc3 and Scc1 (Gruber et al., 2003) and the observation that a proteolytic cleavage of Scc1 is required to remove cohesin from chromatin (Hauf et al., 2001) led to the cohesin ring model (**Fig. 5**). This model predicts that cohesin embraces chromatin in a ring, principally interacting with DNA by topological entrapment, implying either that the replication fork machinery goes through the cohesin ring or that the cohesin ring transiently opens during passage of the replication machinery (Gruber et al., 2003; Haering et al., 2002).

In different organisms cohesin has been shown to preferentially bind to certain loci within the genome. In *Drosophila melanogaster* cohesin localizes at RNA polymerase II (RNAPII) transcribed genes (Misulovin et al., 2008), whereas yeast cohesin preferentially binds to intergenic regions and the transcription machinery slides it towards other loci (Lengronne et al., 2004). In mammals, cohesin binding sites are mostly in intergenic regions, but cohesin also binds within intronic sequences and in regions directly up- or downstream of genes (Parelho et al., 2008). Despite differences, eukaryotic cohesin seems to bind DNA in a sequence-independent manner. However, in human cells cohesin binding sites correlate with binding sites of the zinc-finger protein CTCF, but CTCF binding sites do not correlate with adherin binding sites (Parelho et al., 2008). Although, CTCF is not essential for cohesin loading on chromatin

(Wendt et al., 2008) and cohesin is not required for CTCF recruitment to its binding sites (Rubio et al., 2008), new evidence suggests that CTCF is mostly required to reposition cohesin to its binding sites, but the corresponding molecular mechanism remains elusive (Ohlsson et al., 2010). In every organism analysed so far cohesin binds to centromeres. Human centromeres are composed of major and minor satellite repeat sequences. The minor satellites are important for kinetochore assembly, whereas the heterochromatic major satellites are enriched for Heterochromatin Protein 1  $\alpha$  (HP1 $\alpha$ ) and cohesin (Bernard et al., 2001; Guenatri et al., 2004). In fission yeast recruitment of cohesin to heterochromatic region has been shown to be Swi6/HP1-dependent (Nonaka et al., 2002). In human cells perturbation of HP1 recruitment on chromatin leads to defects in sister chromatid cohesion (Inoue et al., 2008), but HP1 is not directly recruiting cohesin at centromeres (Serrano et al., 2009).

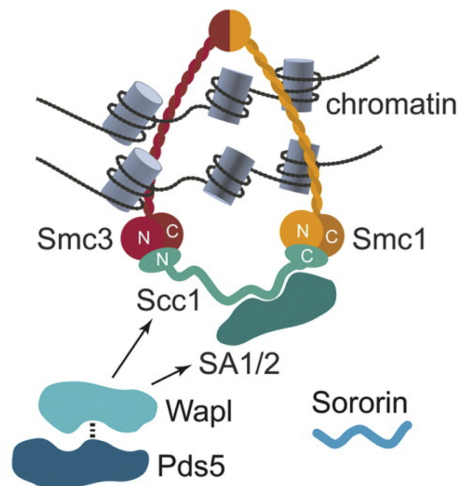


**Figure 5: The ring model of the cohesin complex.**

According to the ring model cohesin embraces dsDNA and is entrapped onto chromatin in a topological manner. Modified from Peters et al., 2008.

### Regulation of sister chromatid cohesion

Cohesion is established in S phase as the replication fork progresses (Song et al., 2012), but it can also be established in G2 in response to DNA damage to promote DNA repair (Strom et al., 2007; Unal et al., 2007).

In metazoan cohesin complexes are bound to chromosomes from telophase until the onset of anaphase and are found in either a dynamic or a stable state (binary mode of cohesin binding) (**Fig. 6**) (Gause et al., 2010; Gerlich et al., 2006). From telophase until the onset of S phase, Wap1 counteracts the

Scc2/4-dependent loading of cohesin, generating a pool of cohesin with weak interactions (Gandhi et al., 2006; Kueng et al., 2006). During replication the acetyltransferases Eco1 (Esco1 and Esco2 in human) acetylates Smc3 neutralising the Wap1-mediated cohesin removal (Rolef Ben-Shahar et al., 2008; Rowland et al., 2009; Zhang et al., 2008), generating a pool of cohesin stably bound to chromatin (Gerlich et al., 2006) and promoting replication fork progression (Terret et al., 2009). In vertebrates Sororin is also required to repress Wap1 action on cohesin (Lafont et al., 2010; Nishiyama et al., 2010), importantly preventing cohesin removal during G2 (Diaz-Martinez et al., 2007; Schmitz et al., 2007). This prevention mechanism is important for proper chromosome condensation (Lavoie et al., 2004), which occurs in two steps: the first step, which happens between G2 and metaphase, is thought to depend on cohesin, whereas the second step entirely depends on condensin function.

During mitosis cohesin is removed from chromatin in a 2-step process (Kueng et al., 2006). During the first step, referred to as the prophase pathway, cohesin-associated proteins (Pds5, Sororin) and factors involved in cohesin loading (Scc2/4, CTCF) are displaced from chromatin (Gandhi et al., 2006; Watrin et al., 2006; Wendt et al., 2008). The activity of different cell cycle-regulated kinases, like CDK1, Plk1, and AuroraB, is required for this step (Losada et al., 2002; Sumara et al., 2000). Consequently, the bulk of cohesin is removed from chromosome arms by the proteolytic action of Wap1 (Gandhi et al., 2006), whereas cohesin at centromeres remains protected by the action of Sgo1 (Tang et al., 2004) and protein phosphatase 2A (PP2A) (Riedel et al., 2006). At the onset of anaphase the second step, referred to as cohesin cleavage, takes place. The APC/C, which is inhibited by the spindle checkpoint until metaphase, becomes active leading to ubiquitin-mediated degradation of many substrates (Hagting et al., 2002; Hauf et al., 2001). One important APC/C substrate is Securin, which is the inhibitor of the cysteine protease Separase (Waizenegger et al., 2002). Activated Separase cleaves Scc1, inducing the release of cohesin from centromeres and residual cohesin from chromosome arms. Thus, Separase activity results in sister chromatid separation (Uhlmann et al., 2000). As soon as the cohesin dissociates from DNA the class I histone deacetylase family member Hos1 (HDAC8 in human) deacetylates Smc3, allowing recycling of cohesin factors and the re-assembly of new cohesin in G1 (Borges et al., 2010). While many cohesin subunits are recycled, cohesin-associated factors that have been degraded, like cleaved Scc1 and Sororin, need to be re-synthesised in every cell cycle in G1 (Nishiyama et al., 2010; Uhlmann et al., 2000).

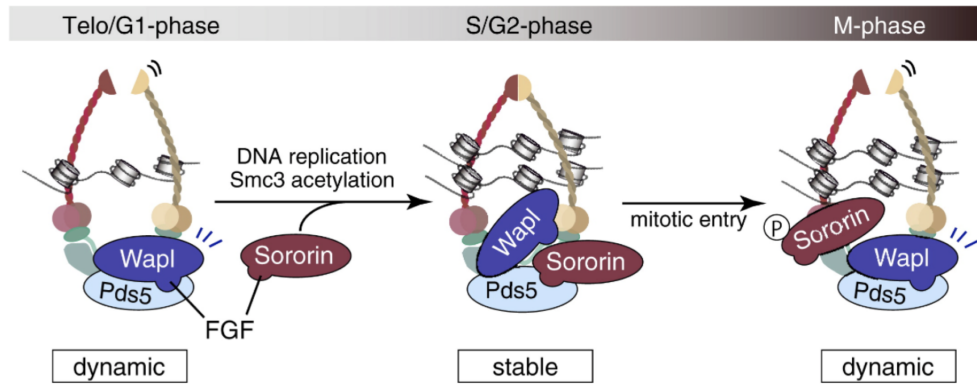


**Figure 6: Dual mode of cohesin binding.**

Cohesin loaded in telophase is dynamic and is dispensable for cohesion. During S phase Sororin stabilises cohesin ensuring proper sister chromatid cohesion until the end of G2, where bulk cohesin is removed from chromosome arms by the action of Wapl. Modified from Nishiyama et al., 2010.

### Cohesin in DNA damage control

Mutants for the Scc1 ortholog in budding yeast (Rad21) and Wapl ortholog in fission yeast (Rad61) have been shown to be hypersensitive to DNA damage (Birkenbihl and Subramani, 1992; Game et al., 2003). In budding yeast, cohesin mutants are defective in DNA damage repair, but not in DNA damage response (DDR) and checkpoint activation, suggesting that sister chromatid cohesion is important for proper DNA damage repair (Sjogren and Nasmyth, 2001). Upon DNA damage, cohesin accumulate at chromatin surrounding double strand breaks (DSBs) in an Scc2/4-dependent manner, suggesting *de-novo* loading of cohesin at these sites (Strom et al., 2004). Cohesin loading in G2 is not only observed at DNA damage sites, it can also occur genome-wide (Unal et al., 2004) in response to ATM (ataxia telangiectasia mutated) kinase-dependent Scc1 phosphorylation, suggesting that Scc1 is a key target of the DDR (Heidinger-Pauli et al., 2008). In vertebrates, cohesin recruitment to DSBs depends on the Smc5/6 complex (Potts et al., 2006). Sororin has been shown to be essential for DSBs repair, suggesting a requirement of cohesin in a stable binding state and proper sister chromatid cohesion (Schmitz et al., 2007). Upon DNA damage, both ATR (ataxia telangiectasia mutated- relates) and ATM kinases phosphorylate Smc1 and Smc3 (Kim et al., 2002; Yazdi et al., 2002). This shows a requirement of cohesin for the in intra-S and G2/M DNA damage checkpoint (Watrin and Peters, 2009). Although Sororin is thought to be dispensable for DDR and checkpoint activation, it is essential for spindle checkpoint activation, stressing its important function in preventing premature sister chromatid separation in early mitosis (Diaz-Martinez et al.,

2007). Lastly, cohesin has been shown to prevent end joining of distant DNA double-strand ends in S/G2 phases, thereby promoting homologous recombination in G2; this mechanism also requires the participation of the cohesin-regulatory factor Sororin (Gelot et al., 2016).

### **Cohesin in transcriptional control**

In vertebrates cohesin is loaded on chromatin in telophase and removed from DNA in prophase (Gerlich et al., 2006; Sumara et al., 2000), although sister chromatid cohesion is established during the S phase and endures until anaphase. Moreover, in mammals cohesin is expressed in every cell type, including terminally differentiated post-mitotic neurons, suggesting a function for cohesin beyond sister chromatid cohesion (Wendt et al., 2008). In fission yeast cohesin promotes transcriptional termination between convergent genes (Gullerova and Proudfoot, 2008). On the contrary, in *D. melanogaster* cohesin is known to repress gene expression by binding with paused RNA polymerases, preventing transcriptional elongation (Fay et al., 2011). Additional genetic analyses performed in model organisms suggested a function for cohesin in chromatin structure and gene expression (Dorsett, 2007). Moreover, mutations in cohesin factors or in cohesin regulators lead to developmental abnormalities in *C. elegans*, *D. melanogaster*, zebrafish and mice (Benard et al., 2004; Horsfield et al., 2007; Schuldiner et al., 2008; Zhang et al., 2007). Cohesinopathies like Cornelia de Lange syndrome (CdLS) and Roberts/SC phocomelia are human development disorders that can be the consequence of mutations in cohesin or cohesin-associated genes (Krantz et al., 2004; Tonkin et al., 2004). Remarkably, CdLS is characterized by upper limb malformation and mental retardation, but cell lines derived from CdLS patients show normal sister chromatid cohesion and cell proliferation. In budding yeast and human cells, cohesin is even known to influence translation by increasing the transcription rate or rRNA (Bose et al., 2012). Although it is still unclear how cohesin controls gene expression, there is evidence of a conservation of function in transcriptional control. In mammals cohesin has been shown to regulate expression of  $\beta$ -globin (Chien et al., 2011) and cohesin depletion leads to transcriptional deregulation of the imprinted H19/Igf2 locus (Wendt et al., 2008). Intriguingly, both loci are under the control of CTCF, which is thought to function as a transcriptional insulator (Ohlsson et al., 2010; Wallace and Felsenfeld, 2007). As already mentioned, cohesin and CTCF binding sites correlate. Although CTCF is not required for cohesin loading on chromatin, CTCF depletion abolishes cohesin loading on CTCF binding sites suggesting that CTCF is required for proper positioning of cohesin on DNA. Experiments in cultured mammalian cells suggest that some CTCF/cohesin-binding sites function as insulator or transcriptional regulatory

elements, proposing a long-range DNA-DNA loop model (Chien et al., 2011). However, other investigations have identified a CTCF-independent pathway of cohesin-mediated gene regulation (Kagey et al., 2010; Sofueva et al., 2013). Cohesin depletion has been shown to cause a global perturbation of chromosomal insulation, leading to topological domain decompaction (Lavoie et al., 2004). Considering that cohesin does not exert an inhibitory function on polymerase binding to promoters and does not physically block transcriptional elongation (Fay et al., 2011), it seems that cohesin is required to maintain the chromosomal structure necessary to control the transcriptional program. In fact, mild cohesin depletion leads to altered gene expression without affecting sister chromatid cohesion or chromosome segregation, suggesting that strong cohesin binding to chromatin may be essential for regulating transcription (Dorsett, 2011). The binary mode of cohesin binding could adapt functional differences exerted by the same cohesin complex.

## **Sororin**

In *D. melanogaster*, a putative Sororin ortholog called Dalmatin has been identified. Dalmatin function is required during development (Prokopenko et al., 2000), and is important for mitotic spindle assembly (Goshima et al., 2007) and sister chromatid cohesion (Nishiyama et al., 2010; Somma et al., 2008). Similarly to Sororin, Dalmatin depletion leads to premature sister chromatid separation and spindle checkpoint activation, suggesting that this cohesin-associated factor may also be evolutionarily conserved in invertebrates. Furthermore, based on sequence alignment, it has been proposed that budding yeast Eco1 is the yeast ortholog of Sororin (Zhang and Pati, 2012). Sororin protein levels are tightly regulated during the different stages of the cell cycle, being translated towards the end of the G1 and degraded at the onset of mitosis putatively in an APC/C-dependent manner (Rankin et al., 2005; Zhang et al., 2011). Sororin localizes to the nucleus and associates to chromatin during S and G2 phases, and upon phosphorylation becomes cytosolic in prophase (Nishiyama et al., 2010). 30 putative phosphorylation sites have been identified on Sororin, suggesting that Sororin is tightly regulated at the post-translational level during the cell cycle (Zhang et al., 2011). To date, the only two identified kinases involved in Sororin phosphorylation are CDK1/Cyclin-B and ERK (Dreier et al., 2011; Nguyen et al., 2010), but there are indications that Sororin may also be a Plk1 (Polo-like kinase 1) substrate (Zhang et al., 2011). Interestingly, Sororin seems to re-associate with chromatids in late anaphase and telophase before being degraded at the onset of G1 (Dreier et al., 2011; Zhang et al., 2011). Apart from its function along chromosome arms, Sororin also localizes to centrosomes and spindle poles, suggesting that it may also be involved, like

cohesin, in centriole-engagement (Schockel et al., 2011). Sororin depletion leads to premature sister chromatid separation and cell cycle arrest at prometaphase (Rankin et al., 2005). Sororin is essential for stable cohesin binding and sister chromatid cohesion during S and G2 phases (Nishiyama et al., 2010; Schmitz et al., 2007), and studies in *Xenopus* egg extracts have revealed that Sororin is also required for chromosome separation (Rankin et al., 2005).

Sororin is a cohesin-regulatory factor that has been co-purified with several cohesin-core and cohesin-associated factors. However, the way in which Sororin interacts with cohesin remains elusive. Sororin loading on chromatin coincides with Eco1-dependent acetylation of Smc3, and a reduced rate of DNA replication or impairment of Smc3 acetylation also reduces Sororin loading (Lafont et al., 2010). However, it is still unclear if Smc3 acetylation serves primarily for cohesin loading or Sororin recruitment.

Sororin plays a crucial role in the dual model binding of cohesin, principally counteracting the cohesin-releasing activity of Wap1 and stabilizing cohesin in its stable mode during the S phase and in particular in G2 (Nishiyama et al., 2010). Both Wap1 and Sororin contain FGF motifs that seem to mediate interaction with the cohesin-associated factor Pds5, suggesting that Wap1 and Sororin may compete with each other for Pds5 binding (Shintomi and Hirano, 2009). Furthermore, Sororin has been shown to regulate resolution of sister chromatid cohesion. Phosphorylation of Sororin in early mitosis seems to promote Plk1-dependent phosphorylation of the cohesin subunits SA1 and SA2, leading to its chromatin dissociation in a non-proteolytic manner (Hauf et al., 2001; Zhang et al., 2011).

Although Sororin seems to be dispensable for the cohesin-dependent activation of the DDR, it is required for DNA DSBs repair as it ensures stable association of cohesin and consequent sister chromatid cohesion, thereby contributing to the activation of the G2/M checkpoint (Watrin and Peters, 2009). Furthermore, Sororin has recently been shown to be essential for cohesin to prevent end joining of distant DNA double-strand ends and chromosomal rearrangements (Gelot et al., 2016). Last but not least, stable cohesin binding has been proposed to be an essential mechanism for ensuring control of the transcriptional program, highlighting the probable important contribution of Sororin in transcriptional control (Nguyen et al., 2010).



### 2.3 Pre-mRNA splicing

The majority of eukaryotic genes are expressed as precursor messenger RNAs (pre-mRNAs) and subsequently converted to mRNAs through pre-mRNA splicing, a mechanism that excises noncoding sequences, called introns, and ligates coding sequences, called exons (Will and Luhrmann, 2011). In metazoans, some exons are constitutively spliced, whereas many others are alternatively spliced, generating different mRNA species from the same pre-mRNA. The mechanism of alternative splicing is predominantly used in higher eukaryotes and significantly contributes to expanding the human transcriptome and thus proteome (Nilsen and Graveley, 2010). Aberrant pre-mRNA splicing is linked to several human diseases. In certain cases it directly causes the disorder and in other cases it contributes to its malignancy (Ward and Cooper, 2010). Recently an important role of pre-mRNA splicing in tumorigenesis has emerged (Grosso et al., 2008). The pre-mRNA splicing process is catalysed by the spliceosome, a large and highly dynamic ribonucleoprotein (RNP) complex. In almost all eukaryotes two unique spliceosomes coexist: the U2-dependent spliceosome (major spliceosome), which splices U2-type introns, and the less abundant U12-dependent spliceosome (minor spliceosome), which splices the U12-type introns (Patel and Steitz, 2003). This introduction focuses on the major spliceosome.

#### Spliceosome assembly and splicing catalysis

The catalytic core of the canonical spliceosome is composed by five different small nuclear ribonucleoprotein (snRNP) complexes, which consist of one or two snRNAs (U1, U2, U4/U6, and U5), a group of seven Sm proteins (B/B', D3, D2, D1, E, F, and G), and a variable number of particle-specific proteins (LSm) (Will and Luhrmann, 2011). Additionally, a large number of accessory non-snRNP proteins (more than 200 proteins in metazoans) are associated with the spliceosome (Jurica and Moore, 2003). An extensive network of protein-protein interactions influences the snRNA-snRNA interactions, leading to structural and compositional rearrangements in the spliceosome (Hegele et al., 2012). These rearrangements are fundamental for proper spliceosome assembly and catalysis. Although the spliceosome is thought to be a ribozyme, the energy generated by a number of spliceosome-associated ATPases and GTPases is of particular importance for structural changes (Hacker et al., 2008).

An essential step in the splicing cycle is the intron definition. Short conserved sequences at the 5' splice site (ss), 3' ss and branch site (BS) of an intron

contribute to defining its boundaries on the pre-mRNA. In higher eukaryotes the BS is followed by a polypyrimidine tract (PPT), which is also involved in this process. Furthermore, short and divergent cis-acting pre-mRNA elements, which are exonic and intronic splicing enhancers (ESEs and ISEs) or silencer (ESSs and ISSs), modulate splicing by binding trans-acting regulatory proteins (Wang and Burge, 2008). Intron removal is achieved in a two-step mechanism characterized by two consecutive transesterification reactions (**Fig. 7**) (Moore and Sharp, 1993). During the first step the 5' ss of the intron is cleaved and ligated to the BS forming a lariat. During the second step the 3' ss of the intron is cleaved, the two adjacent exons are ligated, and the intron is released.

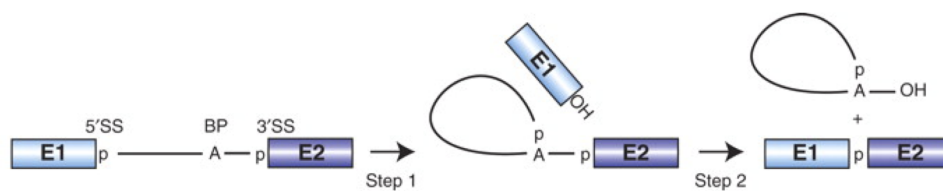


**Figure 7: Schematic representation of the two-step mechanism of pre-mRNA splicing.**

Boxes represent exons, whereas solid lines represent introns. Branch point site is indicated with the letter A. Phosphate and hydroxyl groups involved into the transesterification reactions are shown. Modified from Will and Lührmann, 2011.

In order to correctly function the spliceosome needs to be properly assembled on the mRNA in a space- and temporal-controlled manner (Staley and Woolford, 2009). If the intron length does not exceed ~250 nucleotides, the spliceosome assembly occurs across the intron (**Fig.8**) (Fox-Walsh et al., 2005). During the first step the U1 snRNP is recruited to the 5' ss of an intron and the splicing-associated factors SF1 and U2AF interact with the BS and PPT, respectively, forming the earliest spliceosomal complex (E complex). In the second step the U2 snRNP associates with the BS creating the prespliceosome (A complex). During the third step the pre-assembled U4/U6-U5 tri-snRNP is recruited, forming the precatalytic spliceosome (B complex). The fourth step is characterized by major rearrangements in RNA-RNA and RNA-protein interactions. Destabilization and release of the U1 and U4 snRNPs allows the formation of the activated spliceosome ( $B^{\text{act}}$  complex). The spliceosome becomes catalytically activated ( $B^*$  complex) upon the association of the ATPase/RNA helicase DHX16/Prp2, promoting the first step of splicing. After rearrangements, the  $B^*$  complex is converted into the catalytically active spliceosome (C complex), which catalyses the second step of splicing. At this point the intron RNA is released followed by spliceosome dissociation and snRNP recycling (Brow, 2002; Will and Lührmann, 2011).

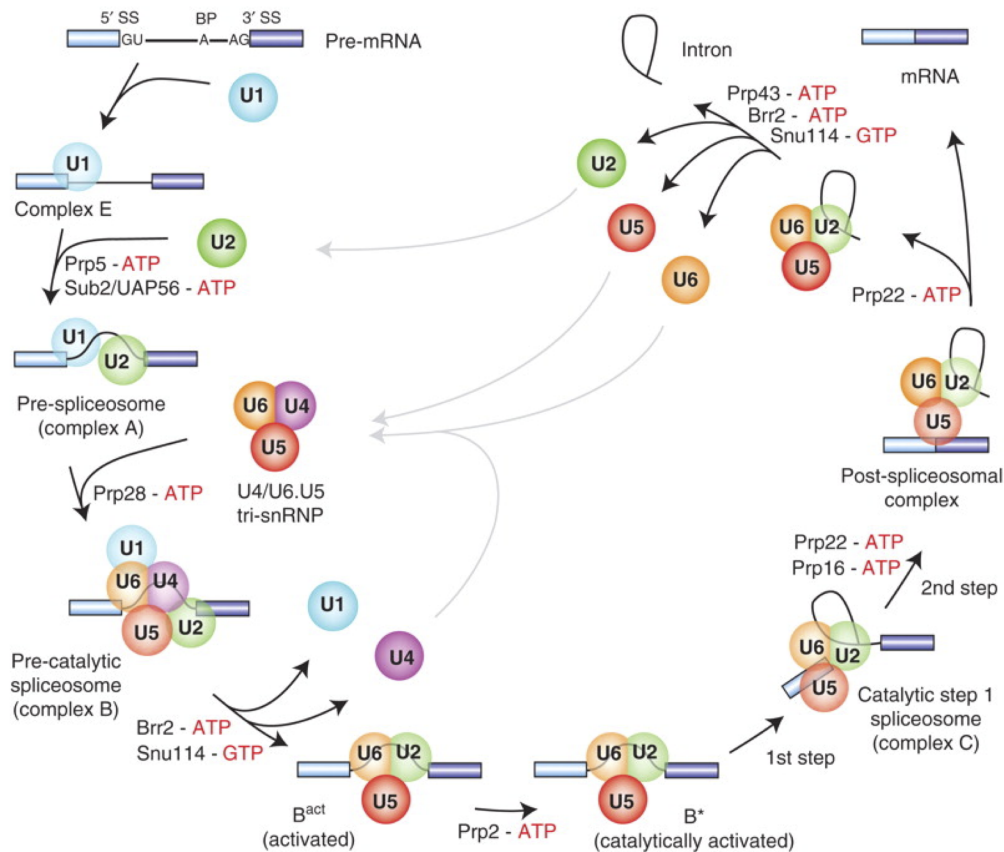


**Figure 8: Canonical cross-intron assembly and disassembly pathway of the spliceosome.**

The ordered interactions of the snRNPs are shown. Spliceosomal components are named according to the metazoan nomenclature. Stages at which the DExD/H-box RNA ATPases/helicases associate to the spliceosome to facilitate rearrangements are indicated. Modified from Will and Lührmann, 2011.

In mammals the intron length often exceeds ~250 nt. Therefore the spliceosome first assembles across an exon in a mechanism called exon definition (**Fig. 9**) (Berget, 1995; Xiao et al., 2007). In this case the U1 snRNP binds to the 5' ss of an intron, promoting association of U2AF with the PPT/3' ss of the upstream intron. The U2 snRNP is subsequently recruited to the BP of the upstream intron, forming a prespliceosome complex across an exon. This complex is further stabilized by the recruitment of regulatory proteins belonging to the SR protein family to the enhancer sequences within the exon (ESEs) (Hoffman and Grabowski, 1992; Reed, 2000). Since the splicing process occurs across an intron there may be a switch from an exon-defined to an intron-defined spliceosomal complex. Although this switch is thought to play an important role during alternative splicing (Sharma et al., 2008), its mechanism is not yet completely understood (Schneider et al., 2010).

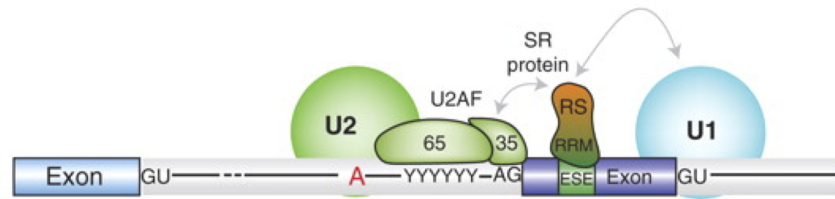


**Figure 9: Model for the exon definition.**

The principal interactions are shown. Branch point site is indicated with the letter A. Interaction between an exonic splicing enhancer sequence (ESE) and the RRM domain of a SR protein is shown. Modified from Will and Lührmann, 2011.

### Regulation of the splicing process

The spliceosome seems to use a single active site for both catalytic steps, suggesting that the catalytic active spliceosome exists in two discrete conformational states. Several studies in yeast support this idea (Query and Konarska, 2004; Villa and Guthrie, 2005) and demonstrations that the catalytic steps of splicing are reversible further corroborate it (Tseng and Cheng, 2008). As already mentioned, in the spliceosome a dynamic network of RNA-RNA interactions is built. While RNA-RNA secondary interactions within the spliceosome are well characterised, the dynamics of the RNA tertiary interactions and their role during the catalytic steps of splicing are poorly understood. Several analyses support the idea that the U2-U6 base-paired snRNA complex forms the active site of the spliceosome, consistent with the notion of spliceosomes being ribozymes (Wachtel and Manley, 2009). A large number of spliceosome-associated proteins transiently bind to the spliceosome, modulating snRNA-snRNA, RNA-protein and protein-protein interactions required for proper spliceosome assembly and splicing catalysis (Newman and Nagai, 2010). Studies in budding yeast have identified roughly 90 spliceosome-associated proteins with homologs in higher eukaryotes, putatively representing proteins required for constitutive splicing (Fabrizio et al., 2009). Conserved DExD/H-box family members with ATPases and RNA helicases activity are essential for the sequential structural rearrangements in the spliceosome (Staley and Guthrie, 1998). They transiently associate with the spliceosome and generate the energy necessary to promote conformational changes and displacement of factors through their RNA unwinding activity (see **Fig. 8**). A number of these DExD/H-box proteins are also key factors that ensure the fidelity of the splicing process, facilitating the discard of aberrant splicing intermediates (Liu and Cheng, 2015). In higher eukaryotes, members of the SR protein family are involved in both protein-

protein and protein-RNA interactions via their positively charged SR (serine- and arginine-rich) domains, contributing to snRNA/pre-mRNA base pairing during intron definition, and to other regulatory mechanisms late in the splicing cycle (Shen and Green, 2004, 2006). Phosphorylation events are particularly important in higher eukaryotes where the essential role of SR protein phosphorylation and dephosphorylation in splicing has been deeply investigated (Soret and Tazi, 2003). PP1/PP2A phosphatase-mediated dephosphorylation of spliceosomal proteins has been shown to facilitate important conformational changes in the spliceosome during the transition from the first to the second step of splicing for the catalytic step of splicing (Shi et al., 2006). SR proteins are not conserved in yeast and very few splicing-associated phosphorylation events are known to occur in this organism, suggesting a limited number of regulatory switches during splicing (Fabrizio et al., 2009). It has also emerged that other post-translational modifications contribute to the splicing process. Acetylation of spliceosomal components is required for spliceosome assembly and activation (Kuhn et al., 2009), whereas ubiquitination has been proposed to regulate RNA unwinding processes during spliceosome activation and disassembly (Bellare et al., 2008).

Roughly half of the spliceosome-associated proteins found in metazoans have no homolog in yeast and are thought to be involved in alternative splicing (Fabrizio et al., 2009) and to link pre-mRNA splicing to other molecular mechanisms involved in transcription and RNA fate (Maniatis and Reed, 2002). Many of these factors are not required for the splicing of every pre-mRNA, suggesting target-specificity (Wahl et al., 2009). Thus, the complex composition of the metazoan spliceosome reflects the variety of pre-mRNA substrates and its plasticity in maintaining the cellular homeostasis.

### **Pre-mRNA splicing and control of gene expression**

The splicing process is primarily regulated by cis-acting pre-mRNA elements and spliceosome-associated RNA-binding proteins. However, several other mechanisms, like chromatin modifications (Zhou et al., 2014), small RNA pathway components and RNA-RNA interactions (Huang and Li, 2014; Kishore and Stamm, 2006), RNA polymerase II (RNAPII) speed and alternative splicing patterns (Dujardin et al., 2014) are known to influence splicing.

In budding yeast splice sites are characterized by highly conserved sequences, reflecting the fact that the large majority of introns are constitutively spliced in this organism (Will and Luhrmann, 2011). In contrast, in metazoans, these splice sites are represented by degenerated sequences that are the prerogative of alternative splicing (Nilsen and Graveley, 2010). In

fact, the rate of alternative splicing correlates with the organismal complexity and offers an additional mechanism to control gene expression (Chen et al., 2014). Not surprisingly, alternative splicing is tightly regulated during developmental stages (Barberan-Soler and Zahler, 2008; Revil et al., 2010). Several cancer transcriptome analyses have highlighted the recurrence of somatic mutations in genes encoding spliceosome proteins involved in the 3' ss recognition process and in SR proteins (Hahn and Scott, 2012). Overexpression of mutant spliceosome proteins, mimicking the mutant proteins found in cancer cells, alters the splicing pattern leading to alternative spliced transcripts (Brooks et al., 2014). Also, overexpression of wt splicing factor SFSR1 has been shown to induce tumours in mice, suggesting that this factor acts as an oncogene and that overexpression of splicing factors can directly promote cancer (Karni et al., 2007).

There are three distinct groups of proteins known to modulate splice site selection and alternative splicing: the heterogeneous nuclear RNPs (hnRNPs), the SR proteins, and tissue-specific RNA-binding proteins. In general, hnRNPs work as splicing repressors and SR proteins as splicing activators. Tissue-specific factors have been shown to act as either activators or repressors (Lee and Rio, 2015). Regulation of alternative splicing directly depends on cis-acting regulatory elements. In fact, regulatory proteins function by interacting with exonic/intronic splicing enhancer/silencer elements, promoting exon inclusion/exclusion (**Fig. 10**) (Wang and Burge, 2008). Importantly, the intron/exon definition mechanism is modulated by non-snRNPs, namely hnRNPs and SR proteins, suggesting that an important regulation of the splicing process occurs early in the spliceosome assembly (McManus and Graveley, 2011). It has also recently emerged that trans-acting small RNAs contribute to the control of alternative splicing (Allo et al., 2009).

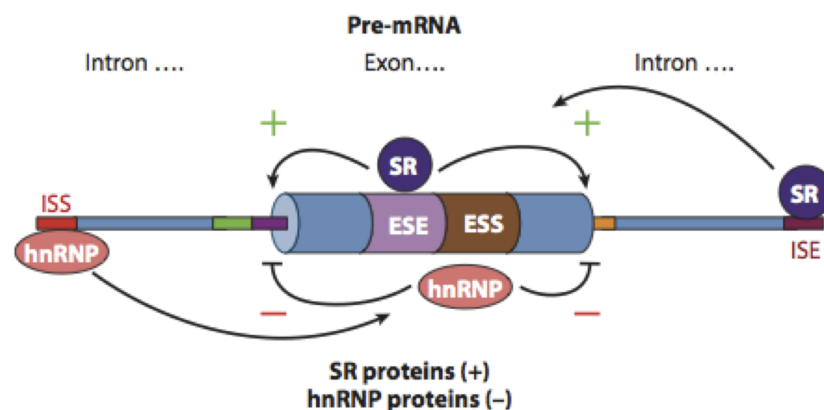


**Figure 10: Schematic representation of pre-mRNA splicing control exerted by cis-acting sequences.**

Intronic/exonic splicing enhancers usually interact with SR proteins promoting splicing of nearby splice sites, whereas intronic/exonic splicing silencers typically interact with hnRNPs inhibiting splicing of nearby splice sites. Modified from Lee and Rio, 2015.

The discovery of looped structures formed on nascent transcripts prior to their releases in dipteran embryos provided evidence of cotranscriptional splicing more than 30 years ago (Beyer et al., 1981). However, studies in budding yeast led to the hypothesis that spliceosome assembly occurs cotranscriptionally, but most genes are spliced post-transcriptionally because the majority of the yeast genes are too short for cotranscriptional catalysis (Tardiff et al., 2006). More recent studies instead demonstrated that the majority of the yeast genes are spliced cotranscriptionally, suggesting that the polymerase pauses and allows time to splice (Alexander et al., 2010; Carrillo Oesterreich et al., 2010). In *D. melanogaster* and human cell lines the majority of intron-containing genes are at least partially spliced cotranscriptionally and nascent transcripts stay associated with chromatin until splicing is accomplished (Ameur et al., 2011; Khodor et al., 2011). The key player that coordinates transcription with splicing is the DNA-dependent RNA polymerase II (RNAPII), which diverges from the other eukaryotic RNA polymerases by its C-terminal repeat domain (CTD). CTD plays a crucial role in the regulation of RNAPII activity. In fact, post-translational modifications of CTD link transcription with numerous RNA processing events (de Almeida and Carmo-Fonseca, 2008; Hsin and Manley, 2012). CTD has been shown to directly interact with spliceosome proteins and it has been proposed to dock them to the nascent transcript (Hirose et al., 1999). Moreover, interaction between CTD and SR proteins seems to be important for constitutive and alternative splicing in metazoans (Yuryev et al., 1996). Analyses of RNAs containing alternative 3' splice sites revealed that RNAPII elongation rates effectively influence splice site selection in alternatively spliced genes (Kornblihtt et al., 2004), leading to the kinetic model of cotranscriptional splicing (**Fig. 11**). Decreased elongation rates or pausing of RNAPII favours the inclusion of exons holding weak 3' splice sites, whereas normal elongation rates without pausing favours exon skipping (Merkhofer et al., 2014).

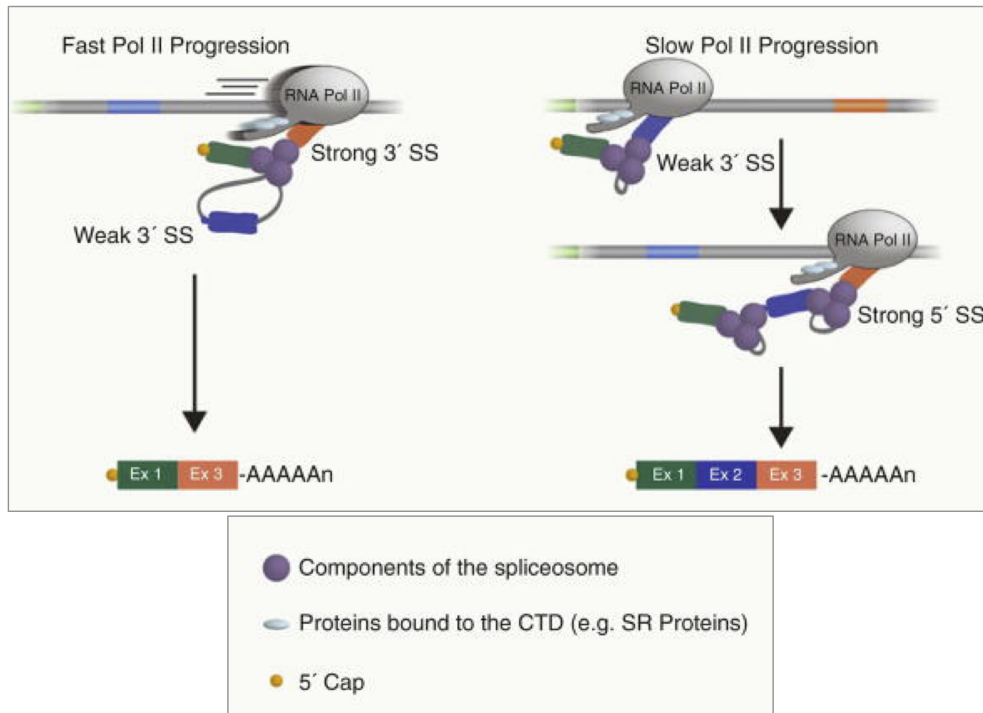


**Figure 11: Kinetic model of cotranscriptional splicing.**

Elongation rate of RNA polymerase II modulates the cotranscriptional alternative splicing. Modified from Merkhofer et al., 2014.

A contribution of nucleosome positioning has been proposed to regulate RNAPII transcriptional rates and influence alternative splicing (Schwartz et al., 2009; Tilgner et al., 2009). Promoters and transcription factors (TFs) can also influence alternative splicing (Cramer et al., 1997). Thus, recruitment and kinetics of cotranscriptional splicing seem to be interconnected processes. As already mentioned, SR proteins associate with the RNAPII cotranscriptionally, promoting transcriptional elongation (Lin et al., 2008). Interestingly, SR proteins also bind to intron-less genes and to histones, further stressing their important function in transcriptional control (Loomis et al., 2009). Moreover, the pre-initiation complex (PIC) formation is known to be enhanced by a functional 5' ss (Damgaard et al., 2008), and U1 snRNA associates with the TFIIF regulatory subunit of RNAPII (Kwek et al., 2002), influencing transcriptional initiation.

Chromatin dynamics also emerged to influence splicing patterns. Chromatin-binding and chromatin-remodelling proteins have been reported to interact with splicing factors linking them to specific histone modifications (Ameur et al., 2011). Recent analyses in mammals have revealed that splicing can directly promote establishment or maintenance of histone H3K36me<sub>3</sub>, a mark



of active transcription, stressing the idea that cotranscriptional splicing is an important mechanism for controlling gene expression (Kim et al., 2011).

### **DExD/H-box protein DHX8**

Several DExD/H-box ATPases/RNA helicases (referred to as pre-mRNA processing factors in budding yeast) are crucial enzymes for the splicing process. They generate energy required for structural and compositional rearrangements in the spliceosome, promoting one or more steps of the splicing cycle (see **Fig. 8**). DExD/H-box proteins involved in the splicing process include DDX46 (Prp5), hnRNPX (Sub2), DDX23 (Prp28), snRNP200 (Brr2), DHX16 (Prp2), DHX38 (Prp16), DHX8 (Prp22) and DHX15 (Prp43) (Will and Luhrmann, 2011).

DHX8/Prp22 is a DEAH-box protein that associates with the spliceosome slightly before the second transesterification reaction of the splicing process (Company et al., 1991). It possesses an ATPase, an RNA-binding and a dsRNA-helicase activity *in vitro*, but is thought to unwind RNA structures or dissociate RNA-protein complexes within the spliceosome (Schwer and Gross, 1998; Tanaka and Schwer, 2005; Wagner et al., 1998).

DHX8/Prp22 is known to exert distinct functions during splicing. First, it directly interacts with the 3' splice site, promoting 3' splice site selection in an ATP-independent manner and contributing to the alignment of reactive groups necessary for the second step of splicing (McPheeters et al., 2000; Schwer, 2008; Schwer and Gross, 1998). Second, DHX8/Prp22 promotes mRNA release from the spliceosome in an ATP-dependent manner (McPheeters et al., 2000; Ohno and Shimura, 1996; Schwer, 2008; Wagner et al., 1998). Additionally, DHX8/Prp22 has also been shown to ensure the fidelity of exon-ligation by inhibiting the splicing and promoting discard of aberrant intermediates. This function depends on ATP-hydrolysis and RNA-helicase activity, but the exact mechanism is still unclear (Mayas et al., 2006). DHX8 is essential for embryonic development and oogenesis in zebrafish (English et al., 2012) and *D. melanogaster* (Klusza et al., 2013), respectively, whereas DHX8 depletion in human cells leads to mitotic spindle disorganization and abnormalities in nuclear structure/shape (Klusza et al., 2013).

### **SR proteins and SRRM2**

SR proteins are essential metazoan spliceosome factors that contain one or two RNA-recognition motifs (RRMs) and a serine- and arginine-rich (SR) C-terminal domain. These factors are required at early stages of the splicing cycle, contributing to splice site recognition and spliceosomal assembly, and at late stages, participating in RNA fate (e.g. RNA quality control mechanism,

RNA export and RNA translation) (Shepard and Hertel, 2009). They are also involved in alternative selection of 5' ss during alternative splicing (van Der Houven Van Oordt et al., 2000).

The serine/arginine repetitive matrix 2 (SRRM2 or SRm300) is usually found in complex with SRRM1 (SRm160). The SRRM1/2 complex is a co-activator subunit of the spliceosome that remains associated with mRNA after intron excision (Blencowe et al., 2000). It binds at sites upstream from exon-exon junctions as part of the exon junction complex (EJC) (Wagner et al., 2004). EJCs remain associated with the mRNAs and influence mRNA translation, surveillance and localization (Le Hir et al., 2001; Le Hir et al., 2000; Le Hir and Seraphin, 2008). SRRM1 promotes 3' end cleavage of pre-mRNA and its overexpression leads to intron-retention (McCracken et al., 2002). Moreover, SRRM1 is known to promote mRNA export in an ATP-dependent but SRRM2-independent manner (Wagner et al., 2004). SRRM1 is not conserved in budding yeast, whereas Cwc21 is thought to be a poorly conserved ortholog of SRRM2. Cwc21 plays a critical role in the catalytic centre of the spliceosome (Grainger et al., 2009), promoting 3' ss selection and second step conformational changes (Gautam et al., 2015). Lastly, the SRRM2 ortholog in *C. elegans* exerts a crucial function during development by influencing the transcription machinery (Fontrodona et al., 2013). In humans SRRM1 has been shown to interact with cohesin (McCracken et al., 2005), whereas several studies have proposed a role of SRRM2 in alternative splicing modulation (Shehadeh et al., 2010; Wojcechowskyj et al., 2013).

## 2.4 CUL7 protein

Cullins are structurally related proteins that share a conserved cullin domain located at their C-termini (Sarikas et al., 2011). Cullin proteins function as molecular scaffolds for the assembly of Cullin-RING complexes containing the ring-finger protein ROC1 (also called Rbx1) that exerts Ubiquitin-ligase (E3) activity (Chen et al., 2000). ROC1 binds to the C-terminal portion of Cullin and recruits the Ubiquitin-conjugating enzyme (E2), whereas the Cullin-specific substrate receptor is recruited through adaptor proteins to the N-terminal portion of Cullin (Pickart, 2001). The Cullin-RING ligase (CRL) complex directly transfers Ubiquitin (Ub) protein from the E2 Ub-conjugating enzyme to a substrate protein without forming a covalent intermediate. In addition Cullins also promote the ROC1-mediated substrate ubiquitination by the action of a regulatory protein Nedd8. Nedd8 is an Ub-like protein that binds to a conserved Lys residue in the C-terminus of Cullins and controls CRLs activity promoting conformational changes (Ohh et al., 2002).

In comparison with other Cullins, Cullin7 (CUL7) presents some atypical features. In fact CUL7 is a large Cullin protein that is only conserved in vertebrates (Skaar et al., 2013). Beside the highly conserved cullin domain, CUL7 also contains a DOC domain of unknown function, similar to the DOC1 domain of APC/C, and a CPH domain for p53 binding, conserved only in CUL7, CUL9 and HERC2 proteins (Kaustov et al., 2007). CUL7 forms a large CRL complex (CRL7) similar to the SCF (SKP1-CUL1-F-box protein ROC1) complex, which is composed by the adapter protein Skp1, the scaffold protein Cullin1, and the ring finger protein ROC1 (Wu et al., 2000). The single substrate receptor known to be associated with the CRL7 is the WD40 repeat-containing F-box protein Fbxw8, indicating remarkable specificity of CRL7 towards its substrates (Dias et al., 2002).

### **Proteolytic functions of CRL7**

CRL7 has been shown to be involved in the proteasomal degradation of CyclinD (Okabe et al., 2006). CyclinD is known to be overexpressed in many tumours and to be crucial for G1 progression in normal cells (Alt et al., 2000). Okabe and colleagues reported that the stability of CyclinD is controlled through the MAPK signalling pathway, and that CyclinD is degraded every cell cycle in S phase, allowing cancer cell proliferation. CyclinD degradation is mediated by the SCF or the CRL7 proteolytic action via direct interaction between CyclinD and the substrate receptor Fbxw8 (Ponyeam and Hagen, 2012). Ponyeam and Hagen have shown that CRL7 is an atypical CRL, where CUL7 interacts with the adapter protein Skp1 in an indirect manner via Fbxw8. Fbxw8 binds to CUL1 through its F-box domain, whereas the interaction between Fbxw8 and CUL7 is anomalously mediated by the WD40 domain of the substrate receptor. Thus Skp1 can simultaneously bind both CUL1 and CUL7 leading to heterodimerisation between CUL7 and CUL1 (Ponyeam and Hagen, 2012). This may be a mechanism to enhance the proteolytic activity of SCF complex towards specific substrates.

CRL7 has also been reported to mediate the proteasomal degradation of the insulin receptor substrate 1 (IRS1) upon IRS1 phosphorylation by mTOR (mechanistic target of rapamycin) kinase, inducing ERK/MAPK signalling (Destefano and Jacinto, 2013; Xu et al., 2012; Xu et al., 2008). However, Xu and colleagues have also shown that CUL7<sup>-/-</sup> mouse embryonic fibroblasts (MEFs) rapidly arrest in G1 with phenotypic features similar to oncogene-induced senescence. Other studies further corroborated the implication of CRL7 in a not fully understood mTOR-dependent feedback mechanism that influences the insulin-signalling pathway (Scheufele et al., 2014). Furthermore, the large T-antigen (LT) of the SV40 virus has been shown to impair CRL7-mediated degradation of IRS1, post-transcriptionally interfering

with the Ub-mediated signalling pathway and sustaining the MAPK signalling pathway (Hartmann et al., 2014). Hartmann and colleagues reported that LT interacts with the C-terminal portion of CUL7 downstream of its conserved cullin domain where Nedd8 is covalently conjugated.

### **Non-proteolytic functions of CUL7**

In a screen CUL7 was identified as an inhibitor of Myc-mediated apoptosis (Kim et al., 2007), an intrinsic mechanism that eliminates precancerous cells overexpressing the Myc oncoprotein (Evan et al., 1992). Kim and colleagues showed that CUL7 directly interacts with the tumour suppressor p53 *in vitro* and *in vivo*, cooperating with the Myc-mediated transformation. Importantly, Skp1 and Fbxw8 seem to be dispensable for this interaction, and CUL7-mediated p53 inhibition is not the consequence of Ub-mediated p53 degradation (Jung et al., 2007). Jung and colleagues also showed that the CUL7-p53 interaction inhibits p53 in a non-proteolytic manner and that interaction between p53 and CUL7 does not seem to influence p53 localization, but it may promote p53 oligomerisation. Induction of DNA damage leads to the accumulation of CUL7 mRNA and protein levels in a p53-independent manner and enhances CUL7-p53 interaction *in vivo*. Moreover, how CUL7 responds to DNA damage is not directly mediated by the DNA damage response kinases ATM and ATR (Jung et al., 2007). In support of the idea that CUL7 promotes proliferation through binding and inhibiting p53 in a non-proteolytic manner, some studies reported that CUL7 is overexpressed and promotes cell proliferation in several p53 proficient breast and lung cancers (Guo et al., 2014; Men et al., 2015).

The cytoskeletal adaptor protein OBSL1 (obscurin-like 1) functions as a regulator of CUL7 during Golgi morphogenesis by physically interacting with CUL7 and localizing it to the Golgi apparatus in dendritic cells (Litterman et al., 2011). CUL7 has been found to interact with OBSL1 and the p53-binding protein of unknown function CCDC8 (coiled-coil domain-containing 8) (Dai et al., 2011) to form the 3-M complex (Yan et al., 2014). Mutually exclusive mutation in one of these genes causes the 3-M syndrome in humans, a hereditary disease characterized by pre- and post-natal growth retardation as a consequence of abnormal p53 function and growth hormone (GH) and insulin-like growth factors (IGF) resistance or deficiency (Hanson et al., 2012). Yan and colleagues reported that the 3-M complex is essential for normal microtubule dynamics and maintenance of genome integrity since loss of 3-M gene function sensitizes cells to microtubule damage and CUL7 depletion impairs progression through mitosis as a consequence of misaligned chromosome in metaphase and defects in cytokinesis (Yan et al., 2014). In the 3-M complex, CCDC8 mediates the localization of CUL7 to the

centrosomes, whereas OBSL1 is required to maintain proper levels of CUL7 mRNA and protein. Importantly, the substrate receptor Fbxw8 is also part of the 3-M complex and the E3 ligase activity of CUL7 is required to accomplish functions of the 3-M complex (Yan et al., 2014). Li and colleagues showed that the 3-M complex majorly functions in preserving Survivin, an inhibitor of apoptosis protein (IAP) that plays a fundamental role in proliferation (Li et al., 2014). Survivin is also part of the chromosomal passenger complex (CPC), where it mediates its recruitment to mitotic chromosomes in order to control multiple steps of mitosis (Watanabe, 2010), and has been shown to regulate microtubule dynamics through a not yet understood CPC-independent mechanism (Rosa et al., 2006).

The 3-M complex binds via CUL7 to Cullin9 (CUL9), a cytoplasmic protein that binds p53 and shares high sequence identity with CUL7 (Kaustov et al., 2007). CUL9 depletion rescues the mitotic and microtubule defects associated with CUL7 or OBSL1 depletion, suggesting a genetic interaction in maintaining genome integrity (Li et al., 2014). Survivin is a substrate for CUL9, which targets Survivin for proteasomal degradation. The other components of the CRL formed by CUL9 are currently unknown. Li and colleagues propose that the 3-M complex sequesters CUL9 by heterodimerisation with CUL7, thus preventing Survivin degradation.

The 3-M pathway seems to safeguard against genome instability during chromosome segregation, but does not appear to be part of the spindle assembly checkpoint (SAC) complex, since SAC and 3-M complexes are genetically different, have distinct targets, and the 3-M complex evolved much more recently. A 3-M protein interactome analysis followed by network analysis identified a 3-M network comprising roughly 100 proteins linked to mRNA splicing/processing (Hanson et al., 2012). Using an exogenous insulin receptor (INSR) minigene-based system, Hanson and colleagues have shown that downregulation of 3-M factors promotes the inclusion of exon 11, similarly to that observed in fibroblasts derived from 3-M patients compared to control cells. Overexpression of 3-M factors in fibroblasts established from 3-M patients leads to the exclusion INSR exon 11, suggesting causality between the 3-M complex function and alternative splicing of the insulin receptor mRNA (Hanson et al., 2012).



### 3 AIM OF THE STUDY

Cactins are essential proteins largely conserved throughout eukaryotes. In the last decade, investigations of different model organisms have revealed Cactins' involvement in several apparently unrelated pathways. In particular, Cactins have been shown to participate in the control of gene expression (Atzei et al., 2010a; Szatanek et al., 2012), inflammatory response (Atzei et al., 2010a; Suzuki et al., 2015), cell cycle progression (Szatanek et al., 2012), development (Atzei et al., 2010b; Tannoury et al., 2010), and embryogenesis (Baldwin et al., 2013; Lin et al., 2000). We have shown that the *Schizosaccharomyces pombe* Cactin ortholog constrains telomere length and telomeric transcription by regulating levels of the telomeric protein Rap1 (Lorenzi et al., 2015). Yet, the molecular functions associated to Cactin proteins remain elusive.

Driven by our discovery in fission yeast, we aimed to gain insight into the molecular function of human Cactin (hCactin). Correspondingly, we investigated a possible conservation of function between hCactin and its putative ortholog in fission yeast *Cay1*.





## 4 RESULTS

### Human Cactin is a nuclear protein

It has been shown that Cactins are nuclear proteins (Atzei et al., 2010a; Baldwin et al., 2013; Tannoury et al., 2010). Through an indirect immunofluorescence analysis (IF) we confirmed that endogenous hCactin was predominantly nuclear (**Fig. 12A**). By western blot (WB) analysis of fractionated cellular extracts we showed that a considerable portion of hCactin was chromatin-associated (**Fig. 12B**).

Using retroviral infection we generated U2OS, HeLa, and HEK293T cell lines with a stably integrated empty vector (pB\_EV) or vector constitutively expressing a 3'UTR-less, HA-tagged version of hCactin (pB\_Cac). Similarly to what shown for endogenous hCactin, we also showed by IF analysis performed on pre-extracted samples, that the majority of the ectopically expressed HA-Cactin was nuclear and chromatin bound in both HeLa and U2OS pB\_Cac cell lines (**Fig. 12C**).

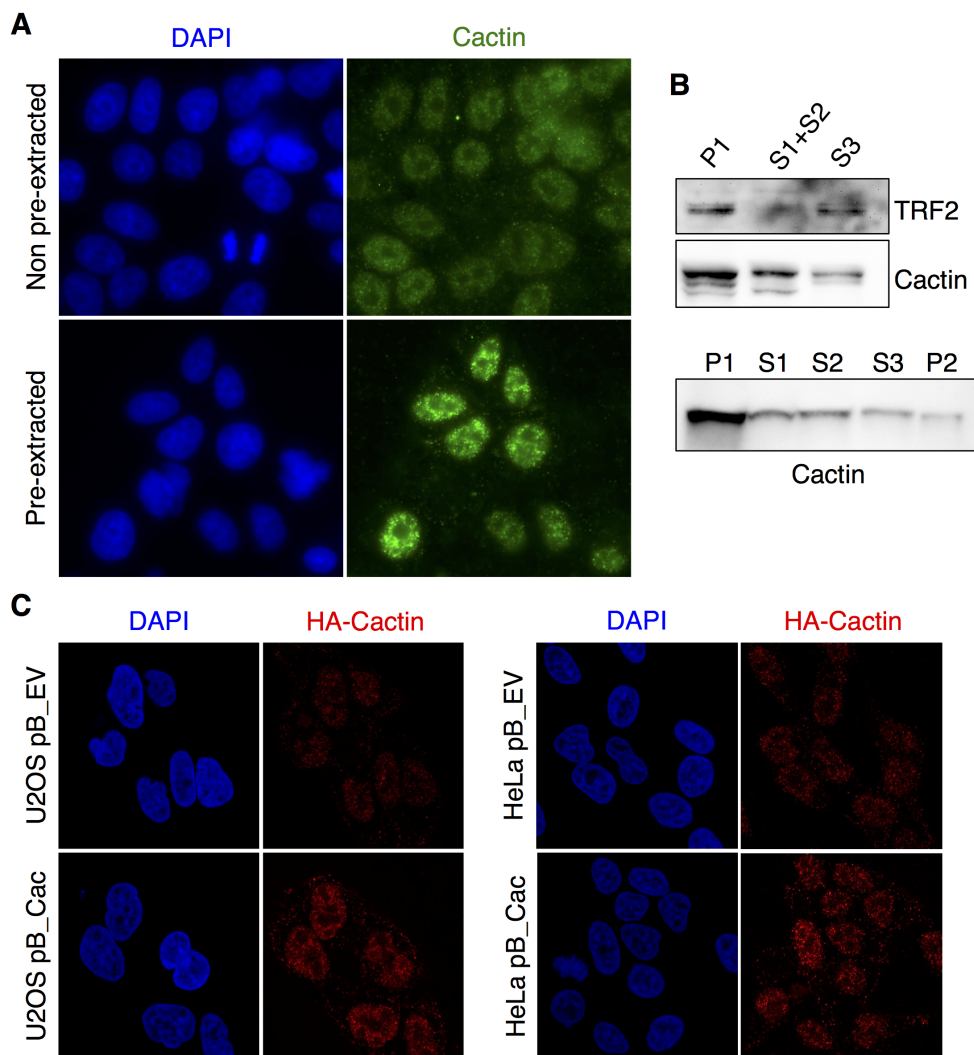


**Figure 12: Human Cactin is nuclear and chromatin bound.**

**A)** IF analysis of non pre-extracted or pre-extracted HeLa cells using an anti-Cactin antibody. Pictures were taken on a fluorescence microscope with 60x magnification. **B)** WB analysis of fractionated HEK293T protein extracts. P1 represents total extract, S1 cytoplasmic soluble fraction, S2 nucleoplasmic soluble fraction, S3 nuclear non-soluble fraction, and P2 final pellet upon extraction series. **C)** IF analysis of pre-extracted U2OS and HeLa cells stably expressing HA-tagged hCactin (pB\_Cac) or empty vector control cells (pB\_EV) using an anti-HA antibody. Pictures were taken on a confocal microscope with 60x magnification.

## 4.1 Phenotypes associated to hCactin depletion

### Human Cactin depletion in cancer cells results in a terminal cell cycle arrest

In order to examine the effect of hCactin deficiency, we depleted hCactin in cancer cells by shRNA (small hairpin RNA). U2OS cells were transfected with either a control shRNA (shCtrl) or five independent shRNAs targeted against the coding sequence (shCac\_A; shCac\_B; shCac\_C) or the 3'UTR (shCac\_D; shCac\_E) of hCactin mRNA. A considerable reduction in hCactin protein levels was achieved three days after transfection with all five hCactin shRNAs (**Fig. 13A**). Moreover, flow cytometric analysis of propidium iodide (PI) stained cells showed a similar cell cycle arrest 72h after transfection with all five hCactin shRNAs (**Fig. 13B**).

Given that hCactin depletion by shRNAs in HeLa cells quickly resulted in cell death, we decided to deplete hCactin by siRNAs (small interfering RNAs), which allowed us to follow hCactin depletion without having to wait for selection of positively transfected cells as we had to do with shRNA plasmid transfection. Indeed, transfection of both U2OS and HeLa cells with either a control siRNA (siCtrl) or two independent siRNAs targeted against the 3'UTR of hCactin mRNA (siCac\_D; siCac\_E) resulted in a gradual reduction of hCactin protein levels (**Fig. 13C**). Flow cytometric analysis of hCactin-depleted U2OS and HeLa cells revealed a progressive cell cycle arrest from 24h to 72h after transfection (**Fig. 13D**). hCactin-depleted cells accumulated in G2/M- and partially in G1-phase 48h after transfection, while S phase was essentially abolished. We can conclude that hCactin is an essential protein and its depletion results in a clear cell cycle arrest in cancer cells.

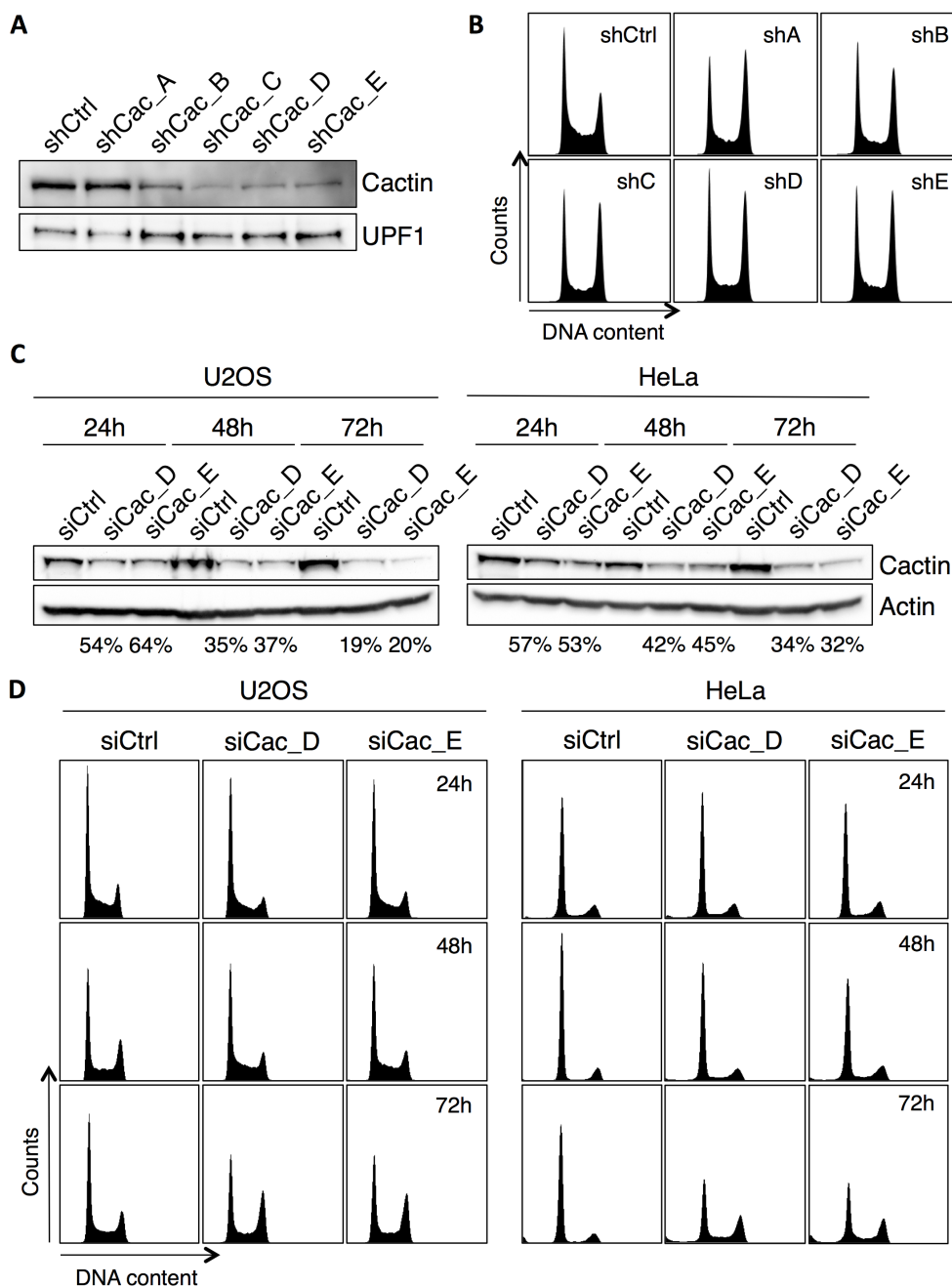


**Figure 13: hCactin depletion results in cell cycle arrest.**

**A)** WB analysis for hCactin depletion using protein extracts of U2OS cells transfected with shCtrl or hCactin shRNAs and harvested 72h after transfection. **B)** Flow cytometric analysis for DNA content of U2OS cells transfected as in A. shCac\_A-E are named in the plots as shA-E. **C)** WB analyses for hCactin depletion using protein extracts of U2OS and HeLa cells transfected with siCtrl or two independent hCactin siRNAs and harvested at given time after transfection. Quantifications of residual hCactin signal are indicated. **D)** Flow cytometric analyses for DNA content of U2OS and HeLa cells transfected as in C.

## Human Cactin depletion affects the nuclear morphology of cancer cells

We observed that transfection of U2OS cells with shCac\_C and shCac\_D leads to accumulation of nuclei with abnormal morphologies (**Fig. 14A**). Nuclei loosed their typical rounded shape, accumulating large nucleoli and appearing lobed, multilobed or fragmented (**Fig. 14B**). This phenotype was reproducible in both U2OS and HeLa cells depleted for hCactin by siRNAs (siCac\_D; siCac\_E) (**Fig. 14C**). Remarkably, already 24h after transfection with hCactin siRNAs there was a statistically significant increase of cells harbouring an abnormal nuclear shape.

Using western blot and IF analyses we promptly excluded the possibility that this nuclear phenotype was a consequence of reduced amount of Lamin proteins (Lamin A/C and Lamin B1) (**Fig. 15A**) or mislocalized Lamin A within the cell nucleus (**Fig. 15B**).

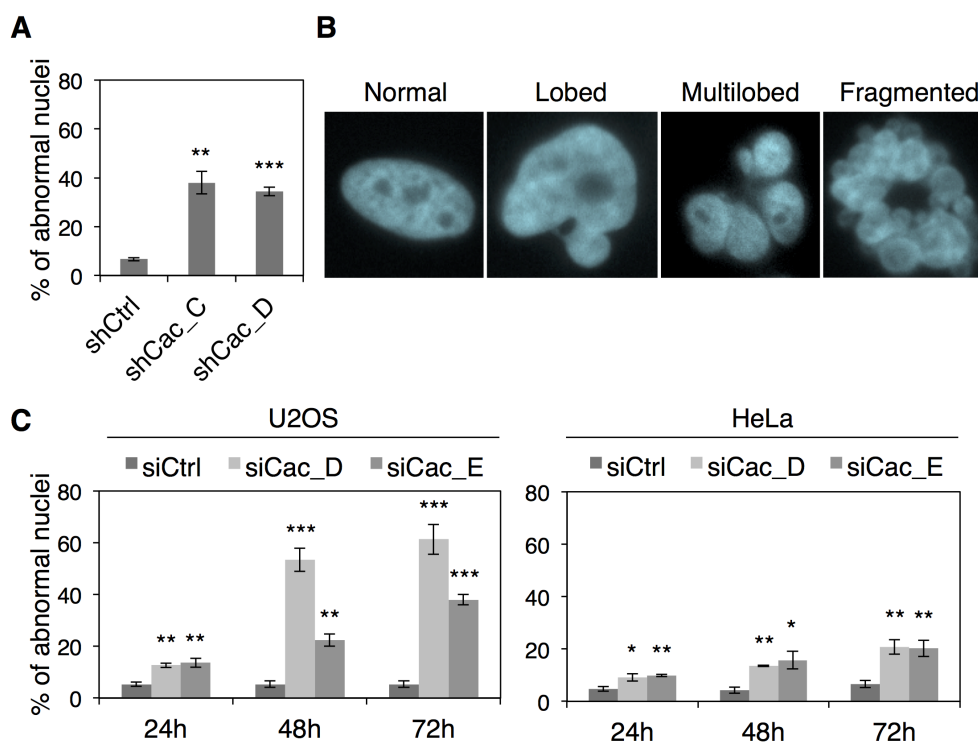


**Figure 14: hCactin depletion induces abnormal nuclear morphologies.**

**A)** Quantifications of abnormal nuclei in U2OS transfected with shCtrl or hCactin shRNAs and processed 72h after transfection. **B)** Examples of DAPI-stained nuclei with abnormal morphologies observed upon hCactin depletion in U2OS cells. **C)** Quantifications of abnormal nuclei in U2OS and HeLa cells transfected with siCtrl or hCactin siRNAs and fixed at given time after transfection. Pictures were taken on a fluorescence microscope with 60x magnification. Error bars represent SEMs. Stars represent significant changes vs. shCtrl or siCtrl based on t-test: \*  $p < 0.05$ ; \*\*  $p < 0.01$ ; \*\*\*  $p < 0.001$ .

In order to investigate whether the accumulation of abnormal nuclei was a consequence of anomalous mitotic division, we subjected hCactin siRNAs-treated HeLa cells to flow cytometric analysis to simultaneously quantify DNA content and the common mitotic marker pH3 (phosphorylated Histone 3). This analysis revealed an accumulation of mitotic cells upon hCactin depletion proportional to the accumulation of cells with a 4N DNA content at 48h and 72h after transfection (**Fig. 15C**).

Taken together, these data suggest that hCactin depletion affects the nuclear morphology of cancer cells before cell cycle arrest and that abnormally shaped nuclei may be a consequence of aberrant mitosis or cell death.

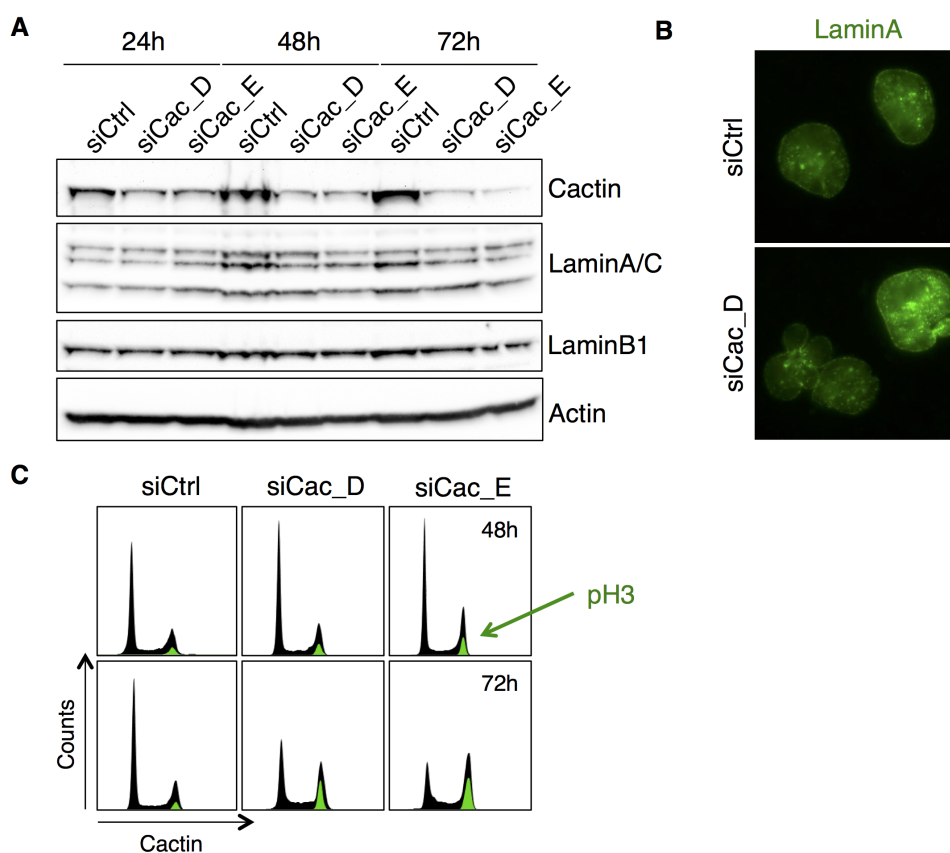


**Figure 15: Abnormal nuclear morphology may be the consequence of aberrant mitosis.**

**A)** WB analysis for hCactin depletion and Lamins using protein extracts of U2OS cells transfected with siCtrl or hCactin siRNAs and processed at given time after transfection. **B)** Representative pictures of LaminA IF analysis performed in U2OS cells transfected as in A. Nuclear localisation and nuclear speckles of LaminA are visible in both conditions. Pictures were taken on a fluorescence microscope with 60X magnification. **C)** Flow cytometric analysis for DNA content and pH3 of HeLa cells transfected with siCtrl or hCactin siRNAs and harvested at given time after transfection. pH3-positive portion of the cell population is shown in green.

## Human Cactin depletion in cancer cells leads to accumulation of DNA damage

Another interesting phenotype we observed in association to hCactin depletion in cancer cells was the accumulation of DNA damage, quantified by IF analysis using an antibody specific for the DNA damage marker 53BP1 (p53-binding protein 1). For our quantifications we considered as positive cells the ones with more than five 53BP1 foci per nucleus. In U2OS cells transfected with shCac\_C or shCac\_D the frequencies of 53BP1-positive cells were 2- to 3-fold higher than in shCtrl-treated cells (**Fig. 16A**). Time course analysis performed in both U2OS and HeLa cells transfected with either siCtrl or hCactin siRNAs indicated that accumulation of DNA damage only occurred from 48h after transfection (**Fig. 16B**). Furthermore, pulse-field gel electrophoresis (PFGE) analysis of DNA double strand breaks (DSBs) revealed that 72h after transfection at least a portion of the accumulated DNA damage was composed of DSBs in both hCactin-depleted U2OS and HeLa cells (**Fig. 16C**). We can thus conclude that hCactin contributes to prevent genomic instability.

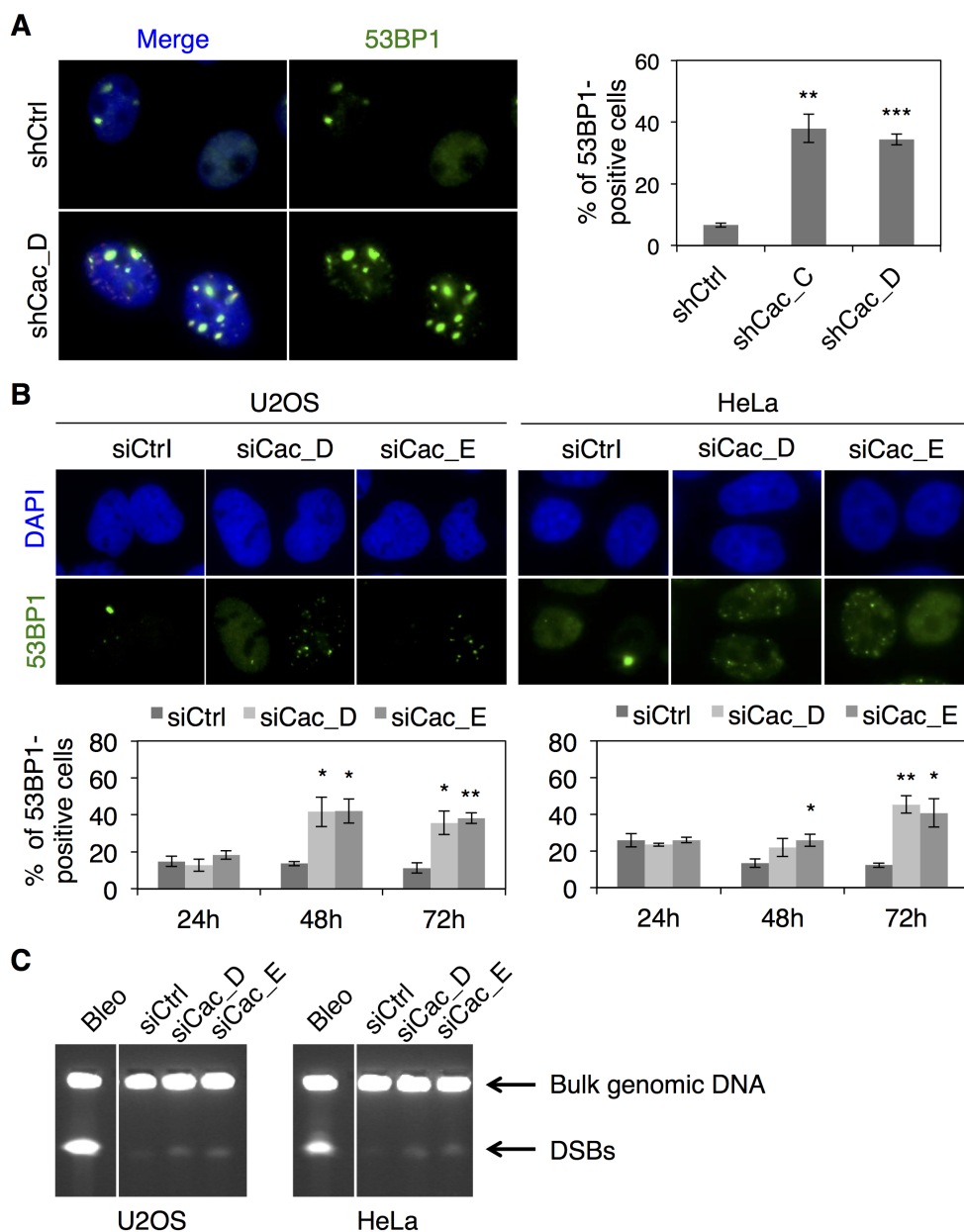


**Figure 16: hCactin depletion induces accumulation of DNA damage.**

**A)** Representative pictures and IF analysis quantifications of U2OS cells transfected with shCtrl or hCactin shRNAs for DNA damage accumulation and processed 72h after transfection. Nuclei presenting more than 5 foci of the DNA damage marker 53BP1 were considered as positive. **B)** Same as in A for a time course analysis in U2OS and HeLa cells transfected with siCtrl hCactin siRNAs. **C)** PFGE for DSBs detection of U2OS and HeLa cells transfected as in B. As positive control cells were treated with Bleomycin. Pictures were taken on a fluorescence microscope with 60x magnification. Error bars represent SEMs. Stars represent significant changes vs. shCtrl or siCtrl based on t-test: \*  $p < 0.05$ ; \*\*  $p < 0.01$ ; \*\*\*  $p < 0.001$ .



## **DNA damage accumulation is not the primary cause of the cell cycle arrest experienced by hCactin-depleted cells**

In order to investigate whether the accumulation of DNA damage and DSBs was the cause of the cell cycle arrest observed upon hCactin depletion, we examined the activation of the canonical DNA damage checkpoint. U2OS cells were transfected with siCtrl or hCactin siRNAs and cell extracts collected at different time points (24h, 48h, and 72h) were subjected to western blot analysis. Surprisingly, we never detected a clear activation of the ATM (ataxia telangiectasia mutated) kinase or the ATR (ataxia telangiectasia mutated-related) kinase as gauged by the phosphorylation state of their downstream targets KAP1 (KRAB-associated protein 1) and Chk1 (checkpoint kinase 1) (**Fig. 17A**).

Aiming to assess the capability of hCactin-depleted cells to activate the DNA damage checkpoint, we treated hCactin-depleted U2OS by siRNAs with the topoisomerase-I inhibitor camptothecin (CPT) for 16h before cell harvesting. Flow cytometric analysis of cell cycle progression clearly showed that 48h after transfection both siCtrl-treated and hCactin-depleted cells accumulated in S phase upon CPT treatment (**Fig. 17B**). Furthermore, western blot analysis for canonical DNA damage checkpoint activation indicated that 48h after transfection hCactin-depleted U2OS cells clearly activate the DNA damage checkpoint upon CPT treatment (**Fig. 17C**). However, 72h after transfection hCactin-depleted cells seemed to respond less than siCtrl-treated cells to CPT treatment and the DNA damage checkpoint was no longer activated. We showed that from 48h after transfection hCactin-depleted cells accumulated in G2/M and S phase was essentially abolished. CPT is known to induce DNA topological stress in cells that are undergoing replication, leading to fork stalling and fork collapse (Ray Chaudhuri et al., 2012). The DNA damage checkpoint is a signalling pathway that functions in promoting genome stability by arresting the cell cycle progression providing time for DNA repair. In response to CPT an intra-S phase checkpoint or a G2 checkpoint is usually activated (Ciccia and Elledge, 2010). Therefore, we propose that 72h after transfection hCactin-depleted cells were no longer proliferating.

Altogether, these data suggest that the accumulation of DNA damage is not the cause of cell cycle arrest experienced by hCactin-depleted cancer cells.

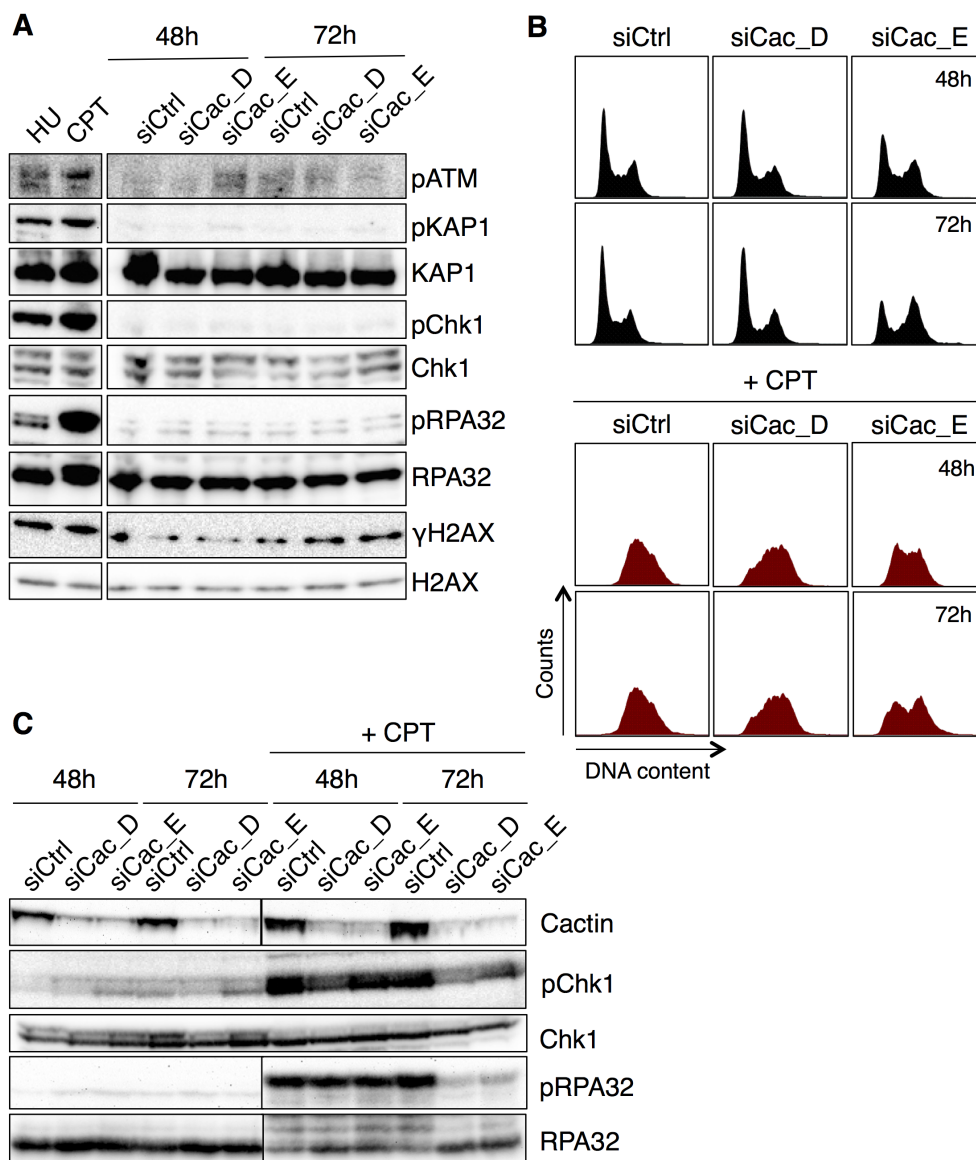


**Figure 17: DNA damage checkpoint activation in hCactin-depleted cells.**

**A)** WB analysis for DNA damage checkpoint activation upon hCactin depletion using protein extracts of U2OS cells transfected with siCtrl or hCactin siRNAs and harvested at given time after transfection. **B)** Flow cytometric analysis for DNA content of U2OS cells transfected as in A or transfected and treated with CTP 16h before harvesting. **C)** WB analysis for DNA damage checkpoint activation using protein extracts of U2OS cells treated as in B.

### Human Cactin-depleted cancer cells accumulate aberrant chromosomal structures

Aiming to better characterize the phenotypes associated to hCactin depletion in cancer cells, we enriched U2OS and HeLa cells previously transfected with siCtrl or hCactin siRNAs in metaphase and performed metaphase spread analysis. For both cell lines, approximately 80 to 90% of metaphases from

hCactin-depleted cells showed abnormal chromosomal morphologies 72h after transfection (**Fig. 18A and B**). Roughly 40% of metaphases presented a number of prematurely separated sister chromatids, approximately 20% showed completely separated sister chromatids, while another 20% exhibited strongly condensed chromosomes.

Thus, hCactin-depleted cancer cells accumulate aberrant chromosomal structures, which may contribute to the cell cycle arrest observed upon hCactin depletion.

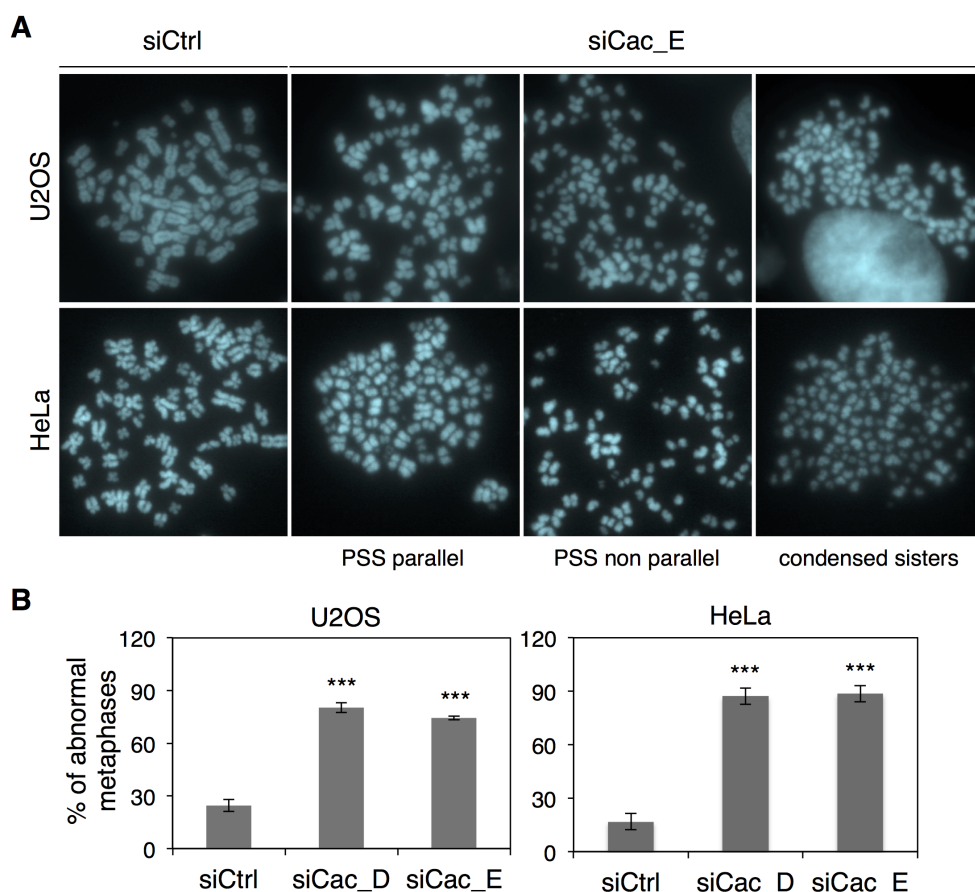


**Figure 18: Metaphase spread analysis of hCactin-depleted cells**

**A)** Representative pictures of metaphase chromosomes from U2OS and HeLa cells transfected with siCtrl or hCactin siRNAs and treated with Colcemid 72h after transfection. In hCactin-depleted cells the majority of the metaphase spreads looked abnormal, presenting premature sister chromatid separation (PSS) and condensed sister chromatids. Pictures of DAPI-stained metaphases were taken on a fluorescence microscope with 60x magnification.

**B)** Quantifications of abnormal metaphase spreads observed in cells treated as in A. Error bars represent SEMs. Stars represent significant changes vs. shCtrl or siCtrl based on t-test: p<\*\*\* 0.001.

**Cell cycle arrest, abnormal nuclear morphology, accumulation of DNA damage, and aberrant mitotic chromosomal structures are true consequences of hCactin depletion**

In order to exclude possible off-targets of the RNA oligonucleotides targeted against hCactin mRNA, we performed compensation experiments. U2OS cells with stably integrated empty vector (pB\_EV) or vector constitutively expressing 3'UTR-less, HA-tagged hCactin (pB\_Cac) were transfected with either a control shRNA (shCtrl) or an shRNAs targeted against the 3'UTR of hCactin mRNA (shCac\_D). As expected, western blot analysis demonstrated that the HA-tagged version of hCactin is insensitive to shCac\_D (**Fig. 19A**). Flow cytometric analysis showed no changes in cell cycle distribution between U2OS pB\_Cac cells transfected with shCtrl or shCac\_D, while an accumulation of cells in G2/M was appreciable in U2OS pB\_EV cell transfected with shCac\_D (**Fig. 19B**). IF analysis also indicated that U2OS pB\_Cac cells transfected with shCac\_D accumulated neither nuclei with abnormal morphology nor DNA damage, whereas there was a statistically significant increase of abnormal nuclei and 53BP1-positive cells in U2OS pB\_EV cells treated with the same shRNA (**Fig. 19C and D**).

In parallel experiments, HEK293T pB\_EV and HE293T pB\_Cac cells were transfected with either shCtrl or shCac\_D and subjected to metaphase spread analysis 96h after transfection. This analysis showed that the aberrant mitotic structures did not appear in HEK293T pB\_Cac cells transfected with shCac\_D, while they were present in HEK293T pB\_EV cells transfected with the same shRNA (**Fig. 19 E, F and G**).

Altogether, these data validated that the cell cycle arrest, the appearance of nuclei with abnormal morphology, the accumulation of DNA damage, and the increased frequency of aberrant metaphases are true outcome of hCactin depletion.

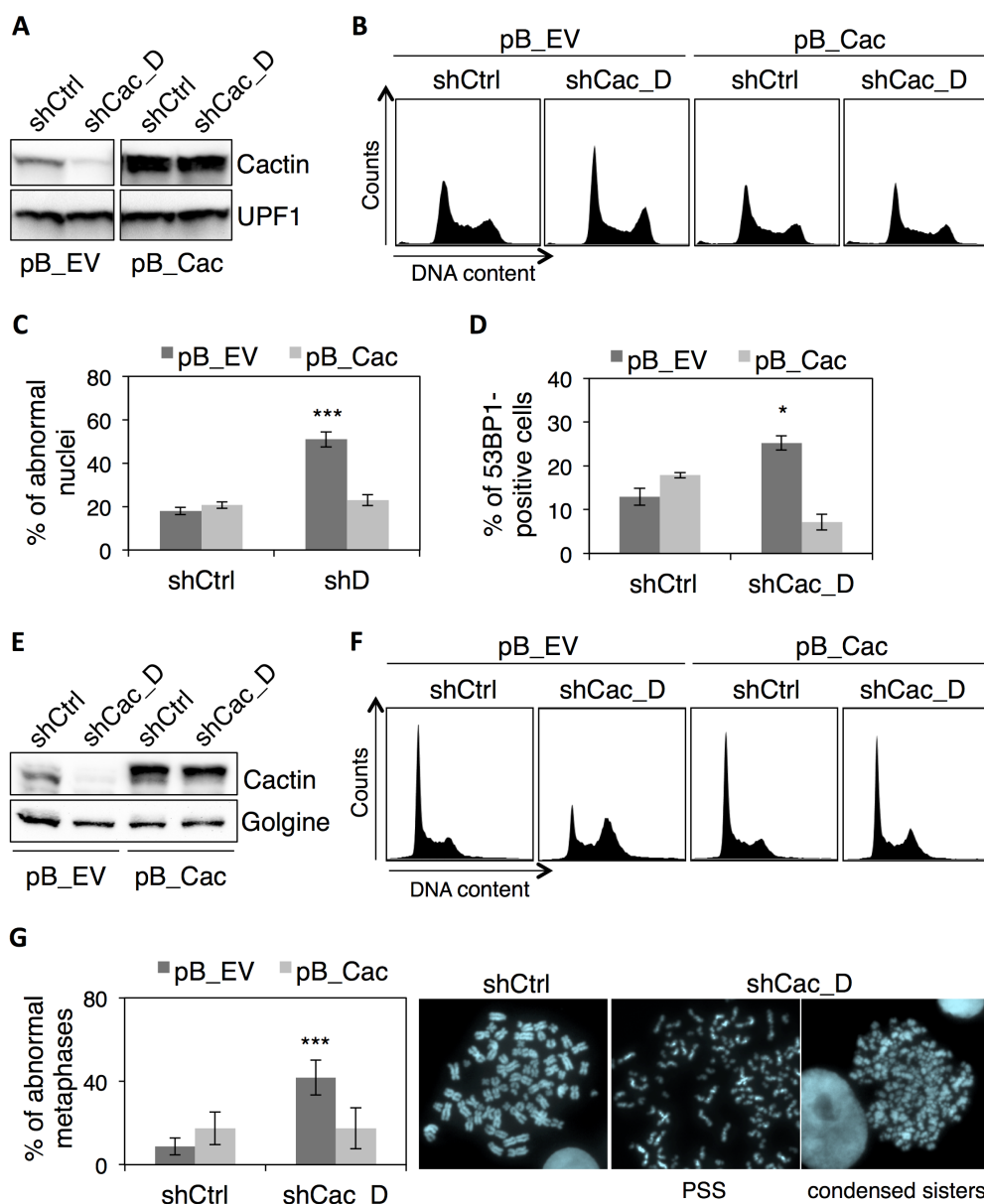


**Figure 19: Cell cycle arrest, appearance of abnormal nuclei, accumulation of DNA damage and increased frequency of aberrant metaphases are true outcome of Cactin depletion.**

**A)** WB analysis for hCactin depletion using protein extracts of U2OS cells stably expressing a 3'UTR-less and HA-tagged hCactin (pB\_Cac) or empty vector control cells (pB\_EV), transfected with shCtrl or shCac\_D and processed 72h after transfection. **B)** Flow cytometric analysis for DNA content of U2OS pB\_EV and pB\_Cac cells transfected as in A. **C)** Quantifications of nuclei presenting abnormal morphology observed in U2OS pB\_EV and pB\_Cac transfected as in A. **D)** Quantifications of 53BP1-positive cells observed in U2OS pB\_EV and pB\_Cac transfected as in A. Cells presenting more than 5 foci of 53BP1 were considered as positive. **E)** WB analysis for hCactin depletion using protein extracts of HEK293T pB\_Cac or pB\_EV cells transfected with shCtrl or shCac\_D and harvested 4 days after transfection. **F)** Flow cytometric analysis for DNA content of HEK293T pB\_EV and pB\_Cac cells transfected as in E. **G)** Quantifications of abnormal metaphase spreads observed in HEK293T pB\_EV and pB\_Cac cells transfected as in E and treated with

Colcemid for 3h before harvesting. Examples of metaphases spreads observed in HEK293T pB\_EV cells are shown. hCactin-depleted cells presented elevated number of metaphases with premature sister chromatid separation (PSS) and condensed chromatids. DAPI-stained metaphases were taken on a fluorescence microscope with 60x magnification. Error bars represent SEMs. Stars represent significant changes vs. shCtrl or siCtrl based on t-test: \*  $p < 0.05$ ; \*\*  $p < 0.01$ ; \*\*\*  $p < 0.001$ .

### **Human Cactin depletion compromises proliferation of both cancer cells and immortalized fibroblasts**

To better dissect the effect of hCactin depletion on cell proliferation, we performed a flow cytometric analysis of DNA content, incorporation of the nucleotide analog EdU (5'-ethynyl-2'-deoxyuridine), and phosphorylation of the Histone 2AX ( $\gamma$ H2AX) as a marker of DNA damage (**Fig. 20A**). U2OS and HeLa cells were transfected with either siCtrl or hCactin siRNAs in a time-course of 2 to 3 days. Transfected cells were pulse labelled with EdU for 30 min before collection. Both U2OS and HeLa cells depleted for hCactin showed a marked reduction in EdU incorporation rate already at 24h after transfection, when no accumulation of DNA damage was detectable (**Fig. 20 B**) and hCactin protein levels were only reduced by roughly 50% (see **Fig. 13C**). Thus, hCactin depletion strongly affected the cell cycle progression shortly after transfection.

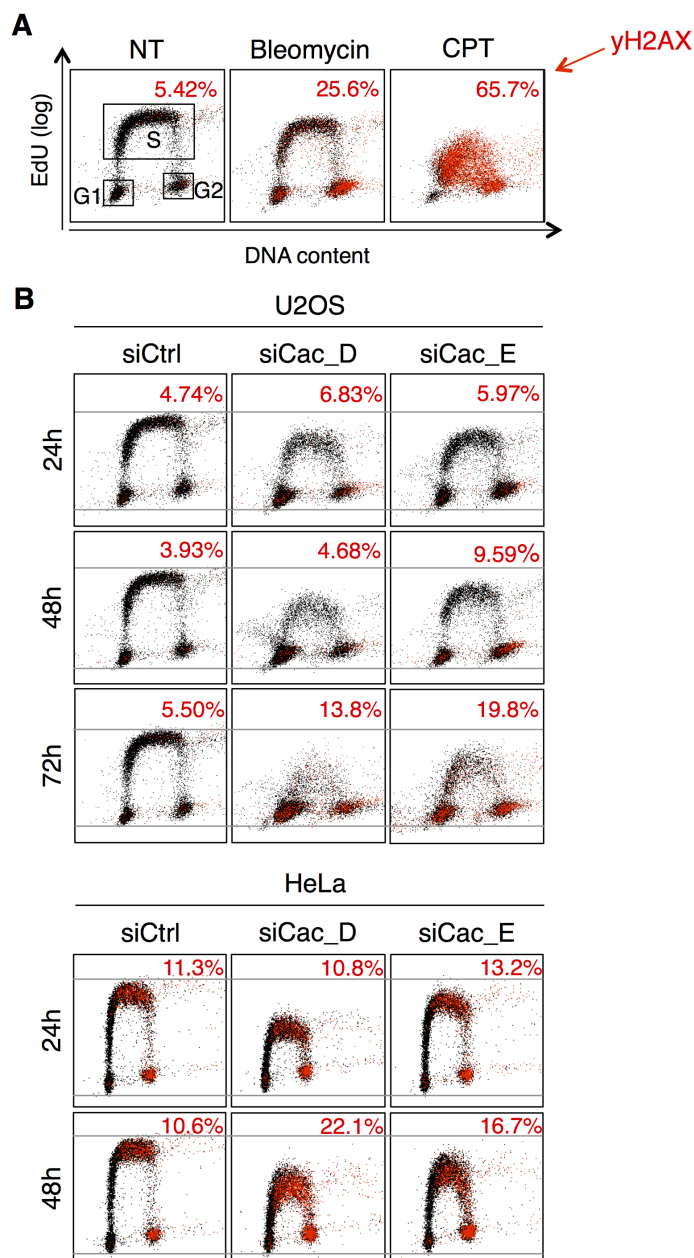


**Figure 20: Depletion of hCactin impairs cell proliferation shortly after transfection.**

Flow cytometric analysis for DNA content, halogenated nucleotide EdU incorporation and activation of the DNA damage marker  $\gamma$ H2AX. **A)** Control profiles of U2OS cell untreated or treated with the DNA-damaging compounds Bleomycin or Campthothecin (CPT). Different cell cycle phases are distinguishable as shown in untreated sample, whereas portion of cell population positive for  $\gamma$ H2AX is shown in red. **B)** Flow cytometric profiles of U2OS and HeLa cells transfected with siCtrl or hCactin siRNAs and pulse labelled with EdU for 30 min before harvesting at indicated time.

In order to explore whether hCactin-depleted cells already experienced proliferation problems during the first round of replication after transfection, we performed a cell synchronization experiment. U2OS cells were synchronized in G1/S with thymidine for 20h (thymidine block), released for 4h and

transfected with either siCtrl or hCactin siRNAs, and then synchronized in G2/M with nocodazole for 10h (nocodazole block) (**Fig. 21A and B**). Afterwards, mitotic cells were released in fresh media, collected at different time points, and subjected to flow cytometric analysis of cell cycle progression. Remarkably, hCactin-depleted cells clearly showed a hindered G1/S entry and a consequent slow down in the cell cycle progression compared to siCtrl-treated cells (**Fig. 21C**). Hence, we can conclude that hCactin depletion impairs cancer cell proliferation by affecting the re-start of a new cycle of replication right after transfection and way before accumulation of DNA damage.

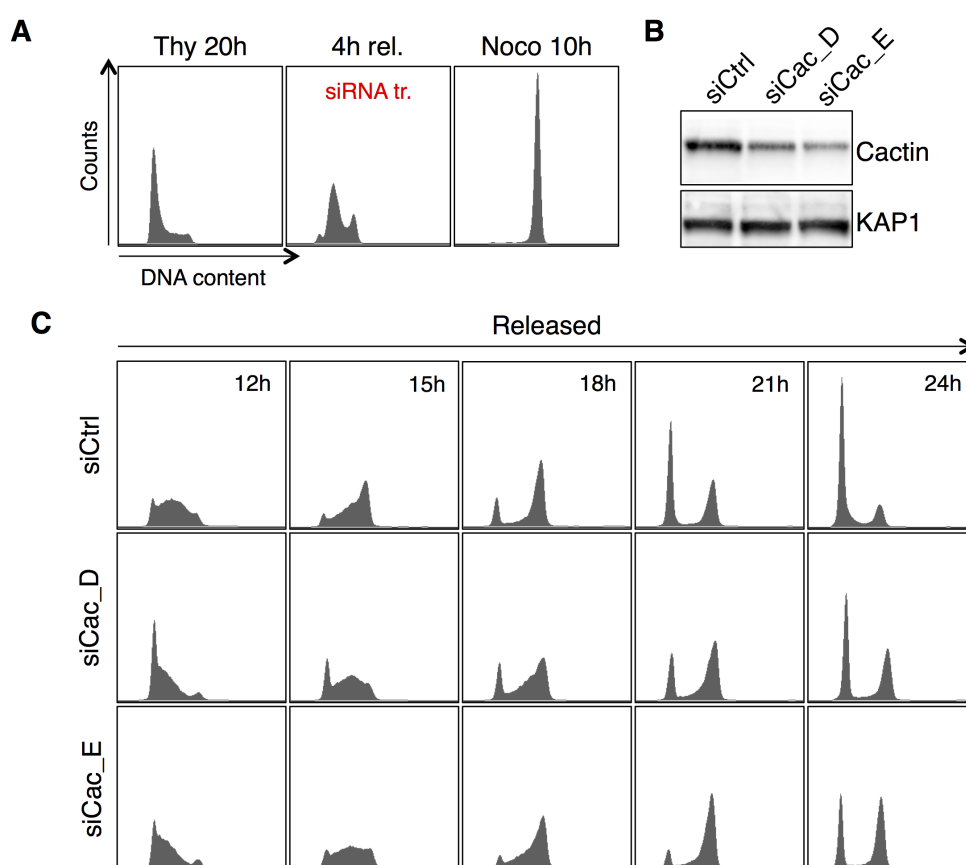


**Figure 21: hCactin-depleted cells experience a hindered G1/S transition of the first cell cycle after transfection.**

**A)** Flow cytometric analysis for DNA content of U2OS cells synchronised in G1/S by Thymidine block, released in normal media and transfected with siCtrl or hCactin siRNAs, and synchronised again in mitosis by Nocodazole block. **B)** Western blot analysis for hCactin depletion using protein extracts of U2OS cells synchronised and transfected as in A and harvested by mitotic shake-off. **C)** Flow cytometric analysis for DNA content of U2OS cells synchronised and transfected as in A. Upon mitotic shake-off cells were released in normal media and harvested at the indicated time.



To verify whether the aforementioned phenotypes associated with hCactin depletion were only a prerogative of cancer cells, we depleted hCactin by siRNAs in telomerase-immortalized RPE-1 cells (**Fig. 22A**). 48h after transfection flow cytometric analysis of cell cycle progression revealed a marked reduction of cells in S phase upon hCactin depletion. 72h after transfection hCactin-depleted fibroblasts were almost completely arrested in G1 (**Fig. 22B**).

Differently from cancer cells, flow cytometric analysis of DNA content, EdU incorporation, and  $\gamma$ H2AX showed that hCactin-depleted RPE-1 cell population had a gradually reduced number of proliferating cells without presenting either sign of replication stress (deduced from EdU incorporation) or accumulation of DNA damage ( $\gamma$ H2AX) (**Fig. 22C**). Activation of the canonical DNA damage checkpoint was also excluded by western blot (**Fig. 22D**).

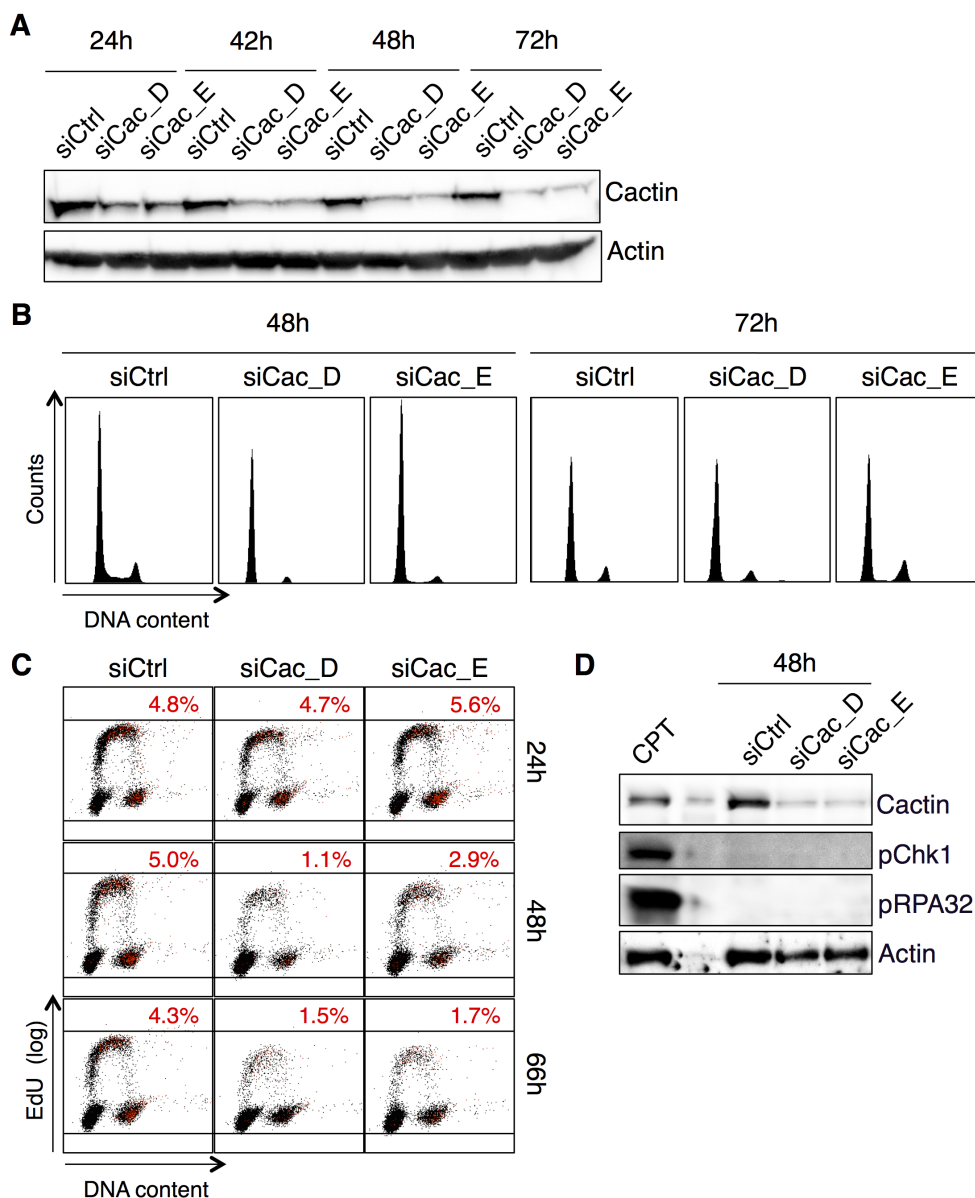


**Figure 22: hCactin depletion impairs cell proliferation of immortalised human fibroblasts.**

**A)** WB analysis for hCactin depletion using protein extracts of RPE-1 cells transfected with siCtrl or hCactin siRNAs and harvested at the indicated time. **B)** Flow cytometric analysis for DNA content of RPE-1 cells transfected as in A. **C)** Flow cytometric analysis for DNA content, halogenated nucleotide EdU incorporation and activation of the DNA damage marker  $\gamma$ H2AX. RPE-1 cells were transfected as in A and pulse labelled with EdU for 30 min before harvesting at the indicated time. **D)** WB analysis for DNA damage checkpoint activation using protein extracts of RPE-1 cells transfected as in A and harvested at the indicated time.

In order to determine whether RPE-1 fibroblasts also presented a proliferation defect during the first cell cycle after depletion we performed flow cytometric experiments after synchronizing cells by serum starvation. Serum-starved RPE-1 fibroblasts were transfected in absence of serum with either siCtrl or

hCactin siRNAs. 48h after transfection cells were released in fresh media for another 24h. While siCtrl-transfected fibroblasts re-started cycling nicely, only few hCactin-depleted fibroblasts re-entered the cell cycle (**Fig. 23A**).

To investigate whether RPE-1 cells, like U2OS cells, presented a proliferation defect shortly after depletion we repeated the aforementioned experiment releasing serum-starved fibroblasts 24h after transfection with siRNAs and collecting samples every 3h from 17h to 35h after release (41h-76h after transfection). Compared to siCtrl-transfected fibroblasts, hCactin-depleted RPE-1 cells showed a hindered G1/S transition that slowed down their progression during the first cell cycle (**Fig. 23B and C**).

Thus, hCactin depletion strongly impaired the proliferation capacity of RPE-1 cells, resembling what we observed in cancer cells.

Taken together, these data indicate that depletion of hCactin primarily impacts on cell proliferation in both cancer cells and immortalized fibroblasts.

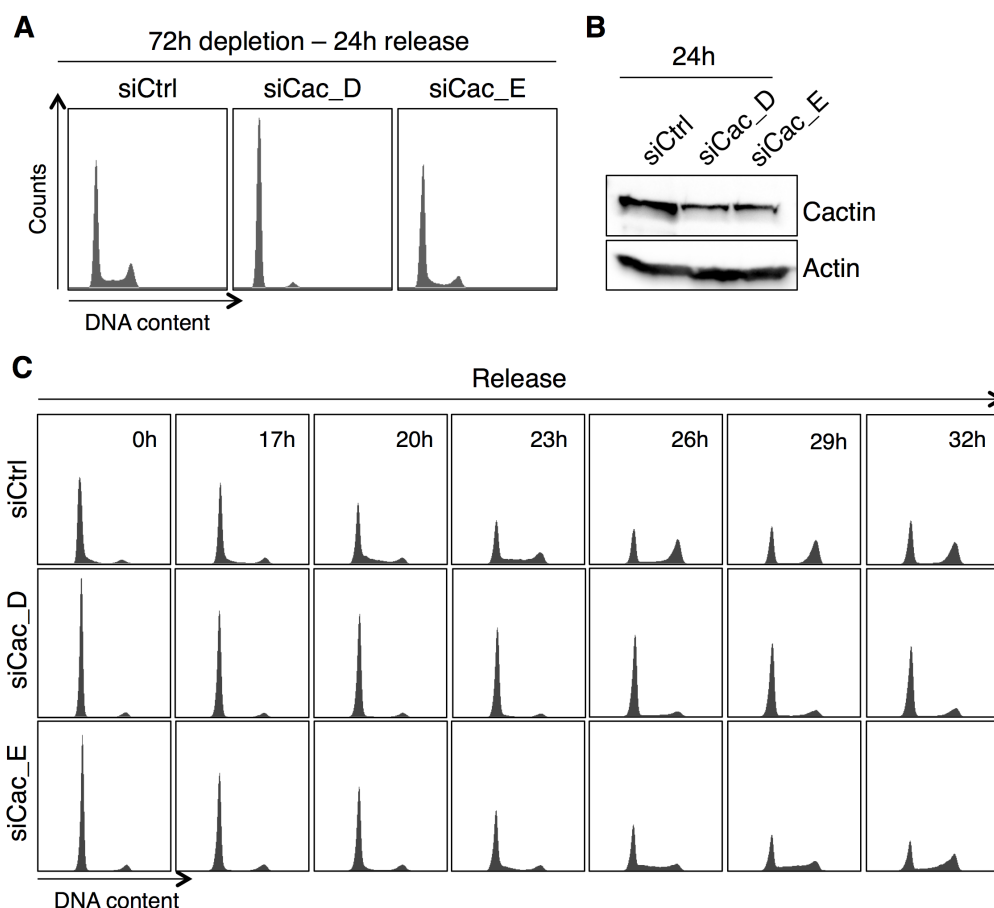


**Figure 23: Depletion of hCactin in RPE-1 cells affects the G-1 transition of the first cell cycle after transfection.**

**A)** Flow cytometric analysis for DNA content of RPE-1 cells transfected during serum-starvation with siCtrl or hCactin siRNAs and stimulated into fresh media 48h after transfection for 24h. **B)** WB analysis for hCactin depletion using protein extracts of RPE-1 cells transfected during serum-starvation with siCtrl or hCactin siRNAs and harvested 24h after

transfection. **C)** Flow cytometric analysis for DNA content of RPE-1 cells transfected as in B and stimulated into fresh media 24h after transfection. Cells were harvested at indicated time upon stimulation.

### **Human Cactin depletion does not compromise telomere homeostasis**

Our lab has previously shown that the *Schizosaccharomyces pombe* Cactin ortholog *Cay1* restricts telomere length and telomeric transcription by regulating levels of the telomeric protein Rap1 (Lorenzi et al., 2015). We thus decided to investigate whether hCactin depletion also had an effect on telomere homeostasis. First we examined whether the levels of the main telomeric proteins that compose the telomeric shelterin complex (de Lange, 2005) were altered upon hCactin depletion. Protein extracts from both U2OS and HeLa cells transfected with either siCtrl or hCactin siRNAs were subjected to western blot analysis. None of the examined shelterin proteins (namely: TRF1, TRF2, RAP1, and TPP1) showed changes in levels 48h and 72h after hCactin depletion in both cell lines (**Fig. 24A**).

We then isolated genomic DNA from HEK293T pB\_EV and pB\_Cac cells transfected with either shCtrl or shCac\_D and maintained in culture for 96h to measure telomere length. Southern blot analysis of terminal restriction fragment (TRF) lengths revealed no detectable change in telomere length upon hCactin depletion or overexpression (**Fig. 24B**).

Thus, differently from fission yeast, hCactin depletion in cancer and immortalized cells did not have a direct effect on shelterin composition and telomere length. Nonetheless, we cannot exclude mild changes in telomere length that would not be disclosed by Southern blot based-approach that we used.

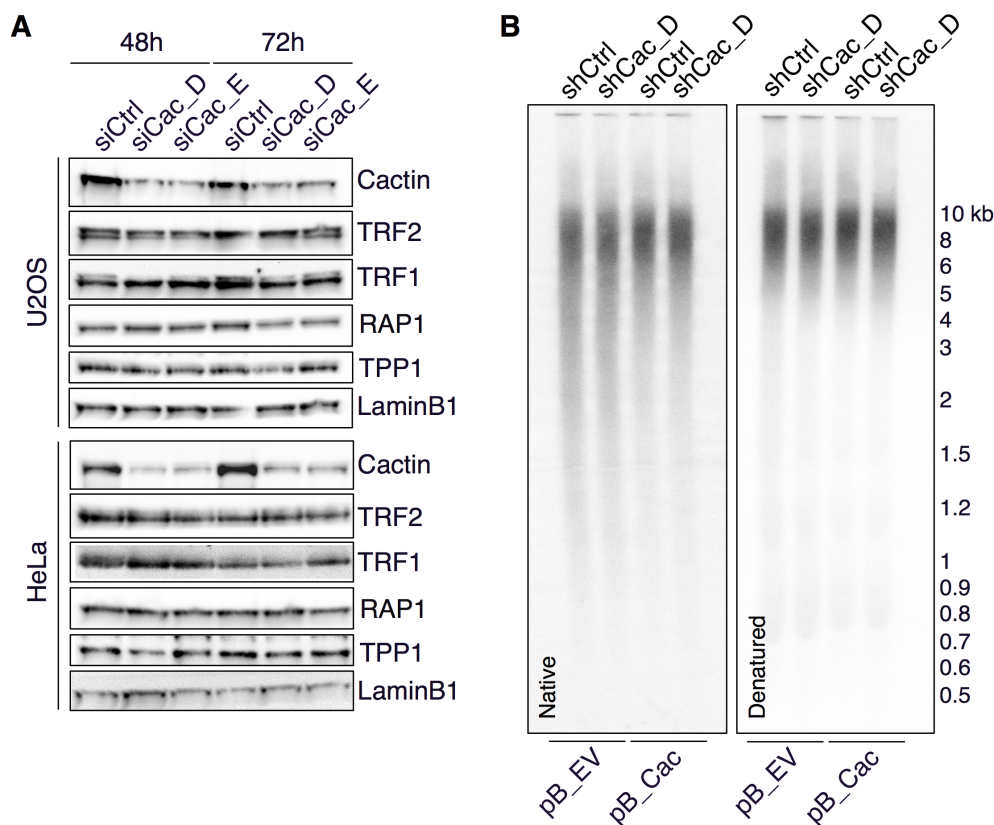


**Figure 24: Depletion of hCactin does not affect levels of shelterin proteins or telomere length.**

**A)** WB analysis for hCactin depletion and shelterin proteins using protein extracts of U2OS and HeLa cells transfected with siCtrl or hCactin siRNAs and harvested at indicated time after transfection. **B)** TRF analysis using genomic DNA of HEK293T cells stably expressing HA-tagged hCactin (pB\_Cac) or empty vector control cells (pB\_EV) transfected with shCtrl or shCac\_D and harvested 4 days after transfection. Hybridisation with a telomeric probe in native and denatured conditions is shown.

Fission yeast *cay1Δ* strain presents increased levels of telomeric transcripts as a consequence of alleviated telomeric heterochromatin. Total RNA was isolated from RPE-1 fibroblasts transfected with siCtrl or hCactin siRNAs and subjected to northern blot analysis for the telomeric transcript TERRA (telomeric repeat-containing RNA) (Azzalin et al., 2007). As with telomere length, we could not detect any clear changes in amounts of TERRA upon hCactin depletion and compared with siCtrl-treated fibroblasts (**Fig. 25A**).

It has been reported that rapid telomere shortening and telomere loss can promptly induce a cell cycle arrest (Saretzki et al., 1999). We considered the hypothesis that immortalized fibroblasts RPE-1 depleted for hCactin experienced a G1 arrest as a consequence of rapid telomere shortening. Thus, we transfected RPE-1 cells with either siCtrl or hCactin siRNAs, and isolated genomic DNA 24h and 48h after transfection for TRF analysis.

Southern blot analysis revealed no change in telomere length or in the intensity of the telomeric signal between hCactin-depleted and siCtrl-transfected fibroblasts (**Fig. 25B**). Thus, hCactin depletion did not substantially affect either telomeric heterochromatin or telomere length of immortalized fibroblasts.

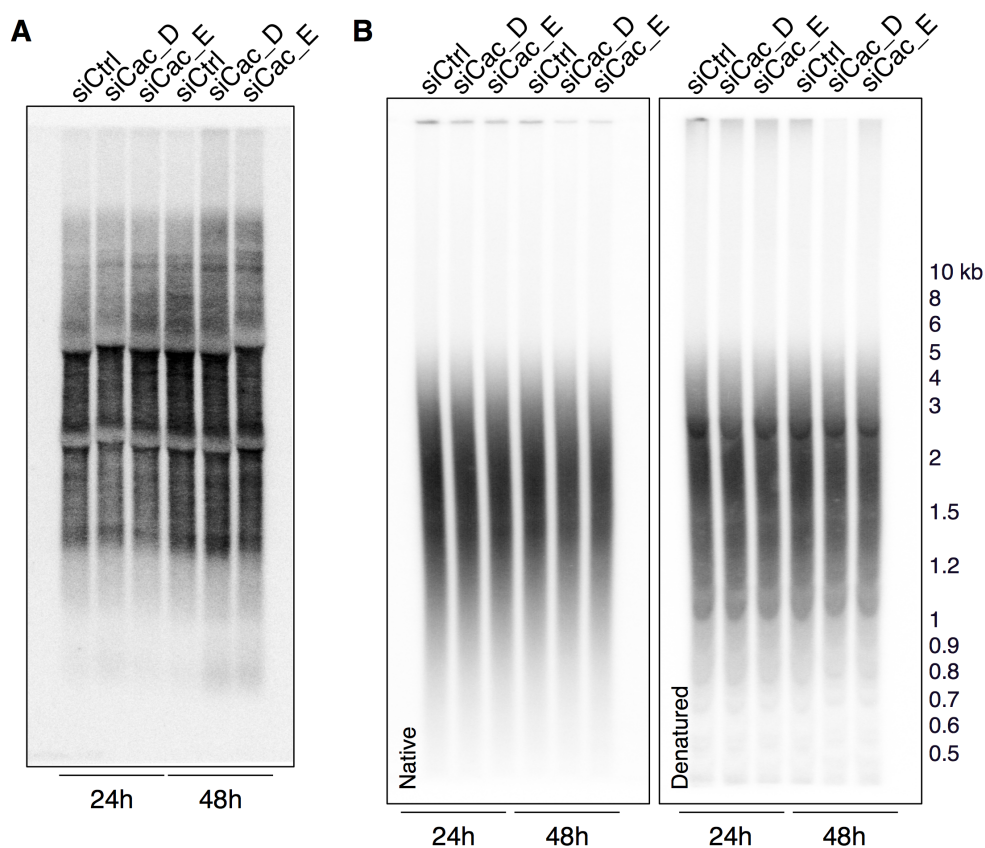


**Figure 25: hCactin depletion does not impact on telomere homeostasis in RPE-1 cells.**

**A)** Northern blot analysis for TERRA transcript using total RNA extracts of RPE-1 cells transfected with siCtrl or hCactin siRNAs and harvested at indicated time after transfection. **B)** TRF analysis using genomic DNA of RPE-1 cells transfected as in A. Hybridisation with a telomeric probe in native and denatured conditions is shown.

Furthermore, DNA damage at telomeres is known to be irreparable and to induce cell cycle arrest and cellular senescence in primary fibroblasts (Fumagalli et al., 2012; Rossiello et al., 2014). We considered the hypothesis that hCactin-depleted cells accumulate DNA damage at telomere thereby impairing cell proliferation. We performed DNA fluorescence in situ hybridization (FISH) combined with IF analysis to monitor accumulation of the DNA damage marker 53BP1 at telomeres upon hCactin depletion in U2OS cells. As a specificity-control we decided to monitor the co-localization of 53BP1 protein with repetitive centromeric DNA. Quantifications revealed that

48h after transfection U2OS cells treated with the radiomimetic drug bleomycin (positive control for DNA damage induction) or transfected with siCac\_E accumulated more DNA damage at telomeres compared to centromeres (**Fig. 26**). However, transfection with either siCtrl or siCac\_E led to a comparable accumulation of DNA damage at telomeres. This confirmed previous reports showing that telomeres tend to accumulate DNA damage as a general response to cell transfection (Ho et al., 2008). Taken together, these data indicate that hCactin depletion does not compromise telomere homeostasis in both cancer cells and immortalized fibroblasts.

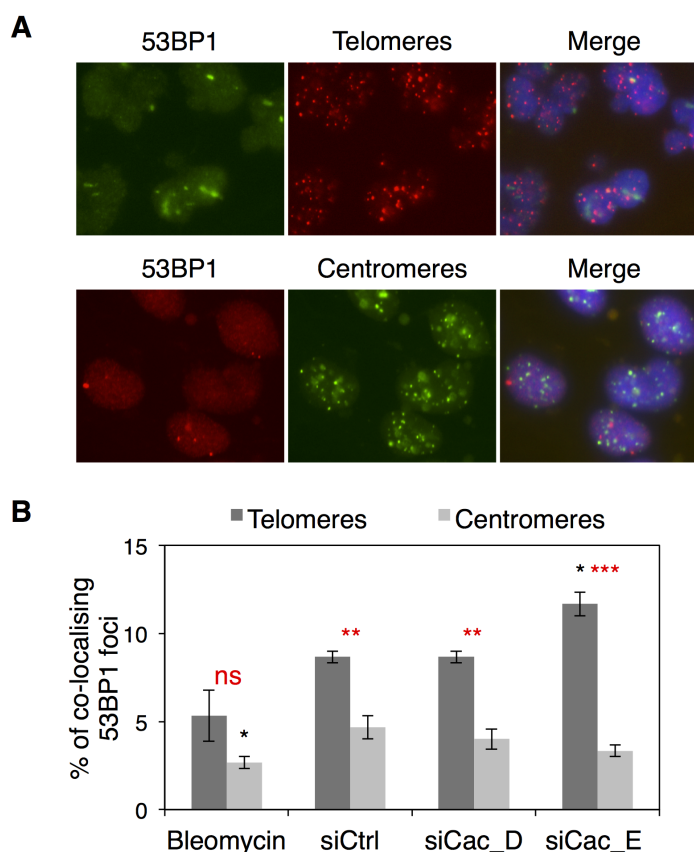


**Figure 26: hCactin-depleted cells do not specifically accumulate DNA damage at telomeres.**

**A)** Images representing the different fluorescent signals used for the analysis in B. IF analysis for DNA damage accumulation using the common 53BP1 marker and FISH analysis for telomeric or centromeric repeats on interphase nuclei. **B)** Quantifications of co-localising IF and FISH signals in U2OS cells transfected with siCtrl or hCactin siRNAs and processed 48h after transfection. As positive control cells were treated with Bleomycin. Error bars represent SEMs. Black stars represent significant changes vs. siCtrl, whereas red stars represent significant changes at telomeres vs. centromeres based on t-test: \*  $p < 0.05$ ; \*\*  $p < 0.01$ ; \*\*\*  $p < 0.001$ .

## Human Cactin depletion leads to a global splicing defect

In addition to telomeric transcripts, fission yeast *cay1Δ* cells also present elevated cellular levels of all *Tf2* retrotransposons and long terminal repeats (LTRs) dispersed throughout the fission yeast genome (Lorenzi et al., 2015). Moreover, *cay1Δ* cells suffer from inefficient splicing of several pre-mRNAs. We thus isolated and deep-sequenced total RNA collected from U2OS transfected with shCtrl or hCactin shRNAs (**Fig. 27A**). Although, many retrotransposons families were up- or down-regulated upon hCactin depletion, the high number and complexity of repetitive sequences dispersed throughout the human genome did not allow us to firmly conclude on a possible direct involvement of hCactin in controlling retrotransposons expression. However, transcriptome analysis disclosed a mild and general splicing defect in hCactin-depleted samples, represented by retention of intronic reads (**Fig. 27B**). In accordance with these findings, hCactin has previously been co-purified with the catalytically active spliceosome complex C (Jurica et al., 2002) and shown to co-localize with evolutionary conserved spliceosome factors in *Arabidopsis thaliana* (Baldwin et al., 2013). It seems therefore likely that hCactin directly supports pre-mRNA splicing by interacting with the spliceosome.

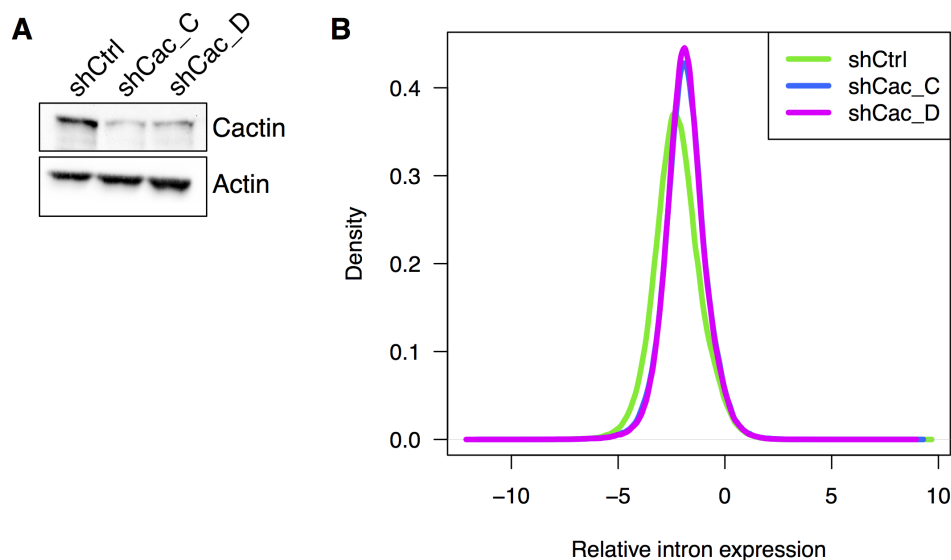


**Figure 27: hCactin depletion leads to a mild and general pre-mRNA splicing defect.**

**A)** WB analysis for hCactin depletion using protein extracts of U2OS cells transfected with shCtrl or hCactin shRNAs and harvested 48h after transfection. **B)** Distribution of relative intron expression estimates for expressed introns in each of the three conditions generated by bioinformatic analysis of the RNA-sequencing data obtained from cells as in A. The relative intron expression is defined as the log-ratio between the estimated intron expression and the estimated expression of the corresponding gene.



## 4.2 Human Cactin is essential for Sororin pre-mRNA splicing

### Human Cactin depletion compromises Sororin pre-mRNA splicing in cancer cells

Recent publications have highlighted the requirement of pre-mRNA splicing factors for sister chromatid cohesions (van der Lelij et al., 2014) (Sundaramoorthy et al., 2014). It has been shown that the splicing machinery majorly contributes to sister chromatid cohesion by promoting pre-mRNA splicing of the cohesin complex regulatory factor Sororin (Watrin et al., 2014). Hence, it seems that Sororin is particularly susceptible to dysfunctional pre-mRNA splicing, in fact, also single depletion of accessories splicing factors impairs Sororin pre-mRNA splicing process, leading to defective sister chromatid cohesion (Oka et al., 2014).

Having established that human Cactin-depleted cancer cells accumulate prematurely separated sister chromatid, we asked whether hCactin-depleted cells also presented a defect in Sororin pre-mRNA splicing. Data from our transcriptome analysis showed a clear enrichment of intronic reads mapping to Sororin (CDCA5) gene locus in hCactin-depleted U2OS cells (**Fig. 28A**). In particular, hCactin-depleted U2OS had a stronger retention of intronic reads corresponding to the first and the third introns of Sororin pre-mRNA (**Fig. 28B**). Consistently, quantitative real-time polymerase chain reaction (qRT-PCR) analyses in HeLa cells revealed a significant accumulation of Sororin pre-mRNA species 72h after transfection with either hCactin siRNAs or shRNA targeting the SF3A-3 (splicing factor 3A subunit 3) mRNA (**Fig. 28C**). Pre-mRNA splicing defects generally result in the accumulation of pre-mRNA species and a reduction of mRNA levels. Despite accumulation of Sororin pre-mRNA species, our qRT-PCR analysis revealed increased amounts of Sororin mRNA in hCactin-depleted or in shSF3a-3-transfected cells (**Fig. 28C**). As previously suggested (Oka et al., 2014; Sundaramoorthy et al., 2014), retention of Sororin intron 1 causes a translational frame shift, generating a stop codon in either intron 2 or exon 3. Mis-spliced Sororin mRNA may not be degraded, but exported and translated into a non-functional truncated Sororin protein.

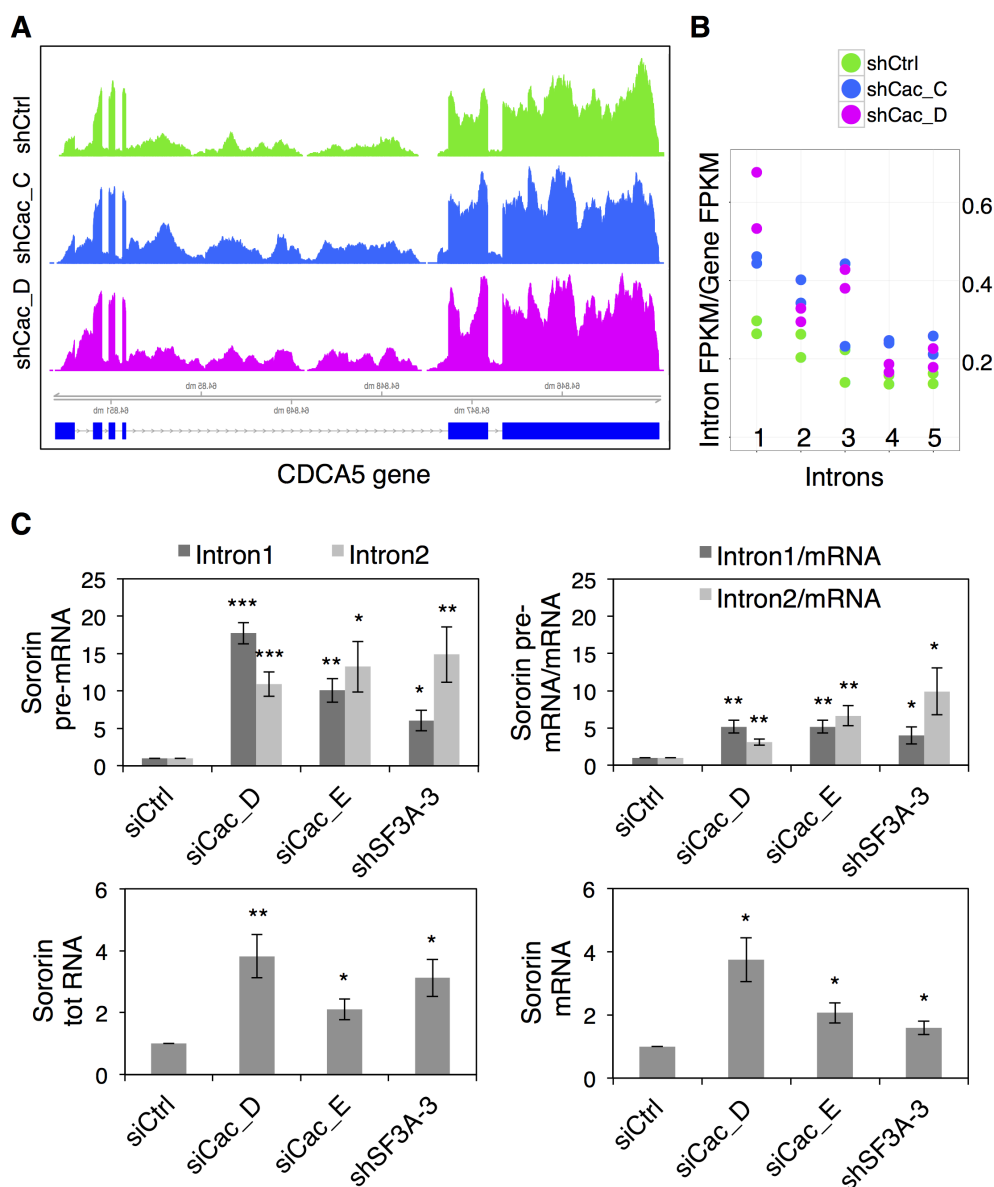


**Figure 28: hCactin depletion affects Sororin pre-mRNA splicing.**

**A)** Read coverage of the Sororin (CDCA5) gene in three representative samples obtained by bioinformatic analysis of the RNA sequencing data obtained from total RNA extracts of U2OS cells transfected with shCtrl or hCactin shRNAs and harvested 48h after transfection (see Fig. 27). **B)** Relative intron expression for each Sororin intron was calculated by dividing its (fragments per kilobases per million reads mapped, FPKM) estimated expression with the estimated expression for the corresponding gene. **C)** qRT-PCR analyses for Sororin transcripts using total RNA extracts of HeLa cells transfected with siCtrl or hCactin siRNAs and harvested 72h after transfection. As positive control for compromised splicing cells were transfected with an shRNA targeted against the spliceosome factor SF3A-3. Error bars represent SEMs. Stars represent significant changes vs. siCtrl based on t-test: \*  $p < 0.05$ ; \*\*  $p < 0.01$ ; \*\*\*  $p < 0.001$ .

In order to gain more insight into the effect of hCactin depletion on Sororin pre-mRNA splicing, we performed RT-PCR analyses for different Sororin introns. These experiments revealed that intron 5 of Sororin pre-mRNA was retained in HeLa cell transfected with hCactin siRNAs similarly to cells transfected with shSF3A-3, while retention of intron 1 was especially increased in hCactin-depleted cells (**Fig. 29A**). Notably, with the latter set of primers we also saw reduced levels of Sororin mRNA with spliced intron 1. Furthermore, northern blot analysis showed accumulation of Sororin pre-mRNA in both hCactin-depleted and SF3A-3-depleted HeLa cells, whereas appearance of a smeary band due to intron(s) retention was visible only in hCactin-depleted samples (**Fig. 29B**). As a proof of principle we performed RT-PCR analysis for Sororin intron 1 in HEK293T cells expressing a 3'UTR-less and HA-tagged version of hCactin (pB\_Cac) or in empty vector control cells (pB\_EV), transfected with either shCtrl or shCac\_D and cultured for 72h after transfection. Overexpression of the shRNA-insensitive Cactin ORF clearly rescued the retention of Sororin intron 1 upon hCactin depletion (**Fig. 29C**). Taken together, these data show that hCactin is essential for Sororin pre-mRNA splicing.

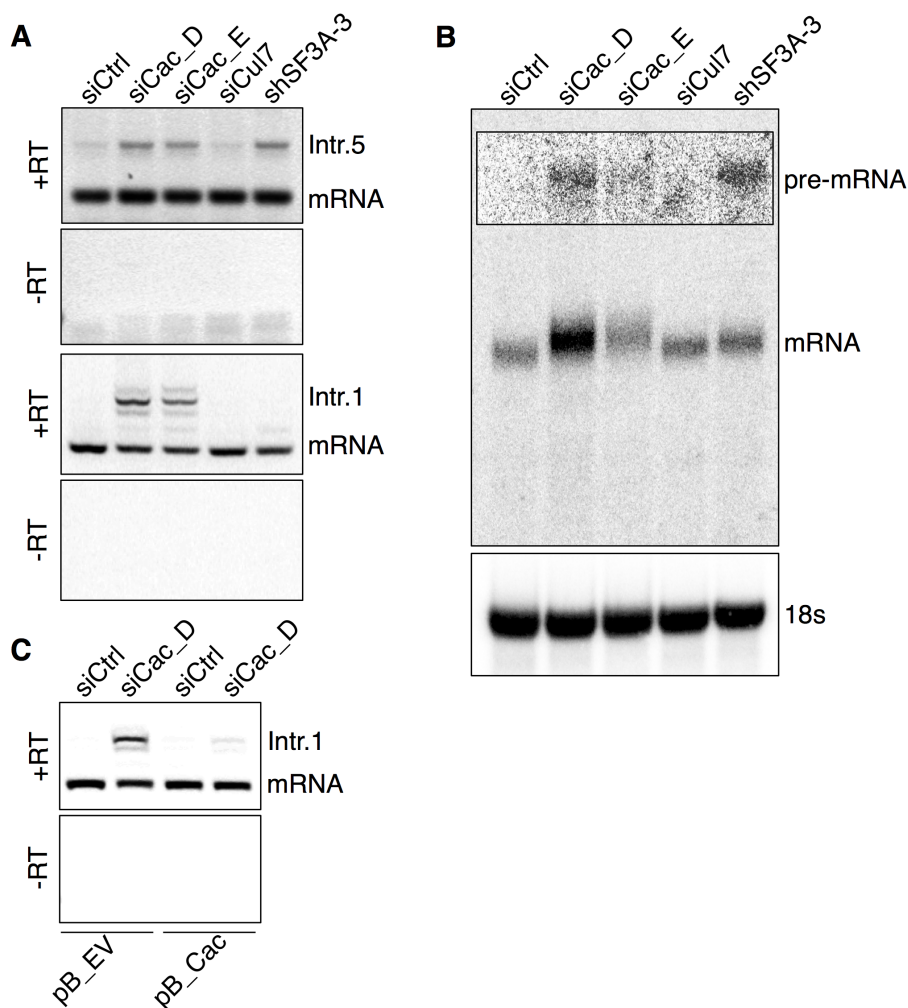


**Figure 29: hCactin depletion leads to retention of Sororin intron 1.**

**A)** RT-PCR analyses for Sororin intron 5 and intron 1 using total RNA extracts of HeLa cells transfected with siCtrl or hCactin siRNAs and harvested 72h after transfection. As positive control for splicing defects cells were transfected with shSF3A-3. siCul7-transfected cells represents a negative control. **B)** Northern blot analysis for Sororin transcripts using RNA extracts of HeLa cells transfected as in A. 18s represents the loading control. To detect pre-mRNA species the inset of the blot was auto contrasted. **C)** RT-PCR analysis for Sororin intron1 using RNA extracts of HEK293T cells expressing a HA-tagged version of hCactin (pB\_Cac) or empty vector control cells (pB\_EV) transfected with shCtrl or shCac\_D and harvested 72h after transfection.

### Ectopic expression of Sororin cDNA rescues the mitotic defect induced by hCactin depletion in cancer cells

In order to test whether the accumulation of abnormal chromosome structures in hCactin-depleted cells was a direct consequence of reduced amounts of properly spliced Sororin, we used lentiviral infection to generate HeLa cell lines with stably integrated empty vector (pL\_EV) or vector expressing Sororin

cDNA (pL\_Sor) under the control of a doxycycline- (DOX) inducible promoter. HeLa pL\_EV and HeLa pL\_Sor were transfected with siCtrl or hCactin siRNA and maintained for 72h in absence or presence of DOX. Upon induction, qRT-PCR analysis showed a 15- to 20-fold increase of Sororin mRNA levels in HeLa pL\_Sor cells transfected with siCtrl and siCac\_E (Fig. 30).

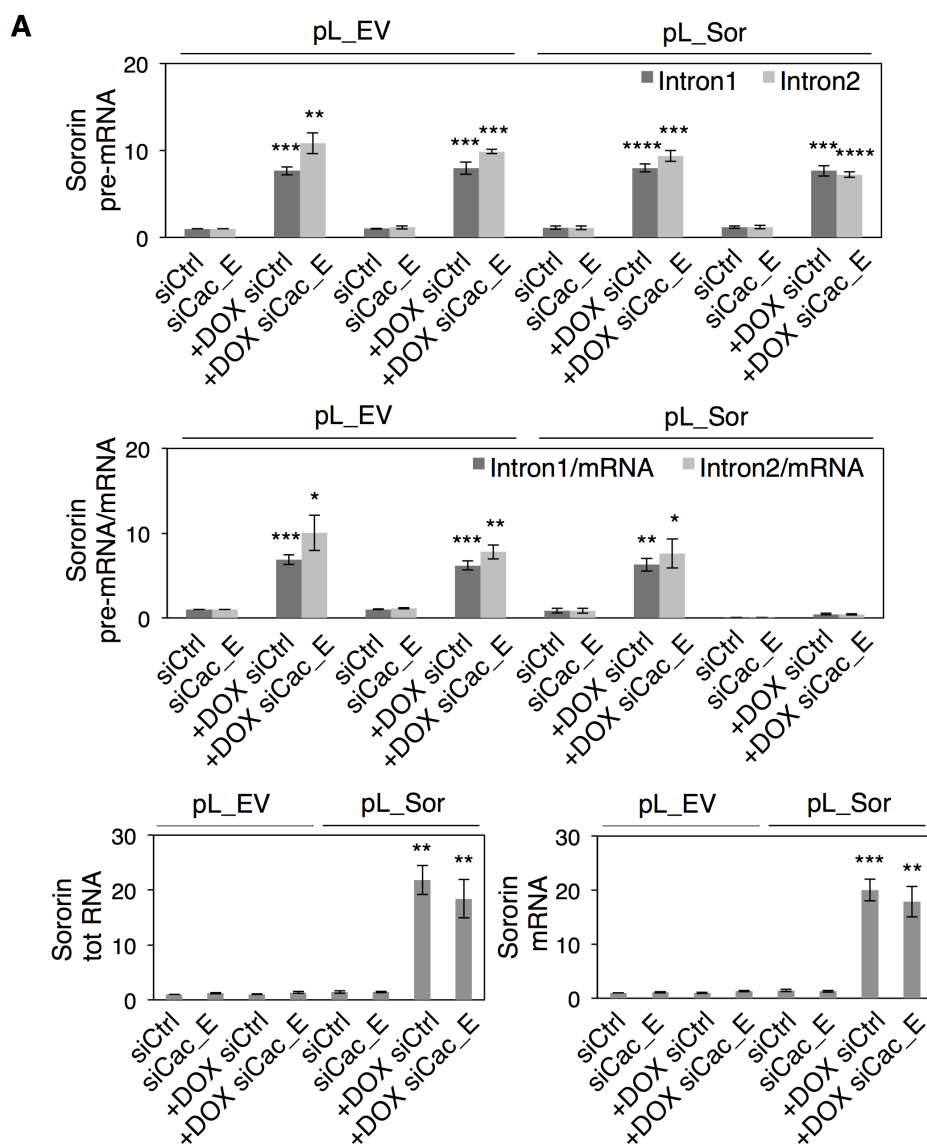


**Figure 30: Sororin cDNA overexpression.**

**A)** qRT-PCR analyses for Sororin transcripts using RNA extracts of HeLa cells overexpressing Sororin cDNA in a DOX-inducible manner (pL\_Sor) or empty vector control cells (pL\_EV) transfected with siCtrl or siCac\_E and harvested 72h after transfection. Error bars represent SEMs. Stars represent significant changes vs. siCtrl based on t-test: \* p<0.05; \*\* p<0.01; \*\*\* p<0.001; \*\*\*\* p<0.0001.

Moreover, northern blot analysis revealed a DOX-dependent expression of Sororin cDNA in both siCtrl- and siCac\_D-treated HeLa pL\_Sor cells (**Fig. 31A**). As expected, a splicing defect of endogenous Sororin pre-mRNA was still detectable upon hCactin depletion in induced HeLa pL\_Sor. Metaphase spread analysis showed a nearly total rescue of the abnormal chromosomal structure accumulated upon hCactin depletion in HeLa pL\_Sor cells cultured in presence of DOX (**Fig. 31B**). Thus, we conclude that the mitotic defects observed upon hCactin depletion are a direct consequence of reduced levels of properly spliced Sororin mRNA.

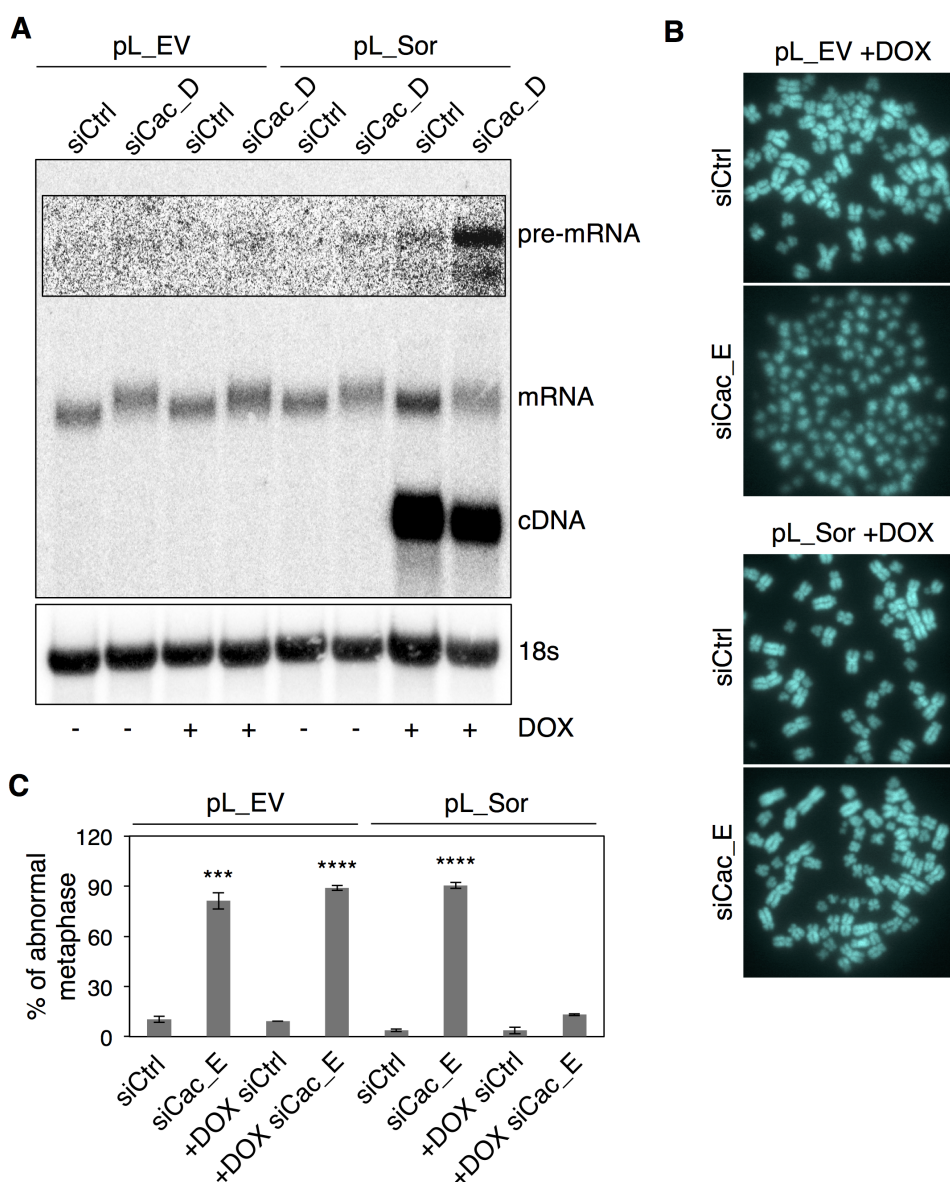


**Figure 31: Sororin overexpression rescues the mitotic defects associated to hCactin depletion.**

**A)** Northern blot analysis for Sororin transcripts using RNA extracts of HeLa cells overexpressing Sororin cDNA in a DOX-inducible manner (pL\_Sor) or empty vector control cells (pL\_EV) transfected with siCtrl or siCac\_E and harvested 72h after transfection. 18s

represents the loading control. To detect pre-mRNA species the inset of the blot was auto contrasted. **B)** Representative images of metaphase spreads of HeLa pL\_Sor or pL\_EV transfected as in A and treated with Colcemid 72h after transfection observed in different conditions. **C)** Quantifications of abnormal metaphase spreads observed in HeLa pL\_Sor and pL\_EV transfected and treated as described in A and B. Images of DAPI-stained metaphases were taken on a fluorescence microscope with 60x magnification. Error bars represent SEMs. Stars represent significant changes vs. siCtrl based on t-test: \*  $p < 0.05$ ; \*\*  $p < 0.01$ ; \*\*\*  $p < 0.001$ ; \*\*\*\*  $p < 0.0001$ .

### **Sororin cDNA overexpression ameliorates the cell cycle defect and reduces the abnormal nuclei observed upon hCactin, but does not prevent accumulation of DNA damage**

We investigated whether the overexpression of Sororin and the consequent restoration of sister chromatid cohesion were sufficient for a full recovery from the different cellular defects induced by hCactin depletion. Flow cytometric analysis of cell cycle progression revealed an alleviation of the cell cycle defect observed upon hCactin depletion in HeLa pL\_Sor cells cultured in the presence of DOX (**Fig. 32A**). HeLa pL\_Sor cells cultured in the presence of DOX also showed a reduction of abnormal nuclear morphology and nuclear fragmentation observed upon hCactin depletion (**Fig. 32B**) However, Sororin cDNA overexpression in hCactin-depleted cells did not prevent accumulation of DNA damage (**Fig. 32C**). Taken together, these data showed that Sororin downregulation clearly had a strong impact on cell proliferation. Nevertheless, Sororin overexpression was not sufficient to sustain proliferation of hCactin-depleted cells, suggesting that DNA damage and premature sister separation are not causally linked.

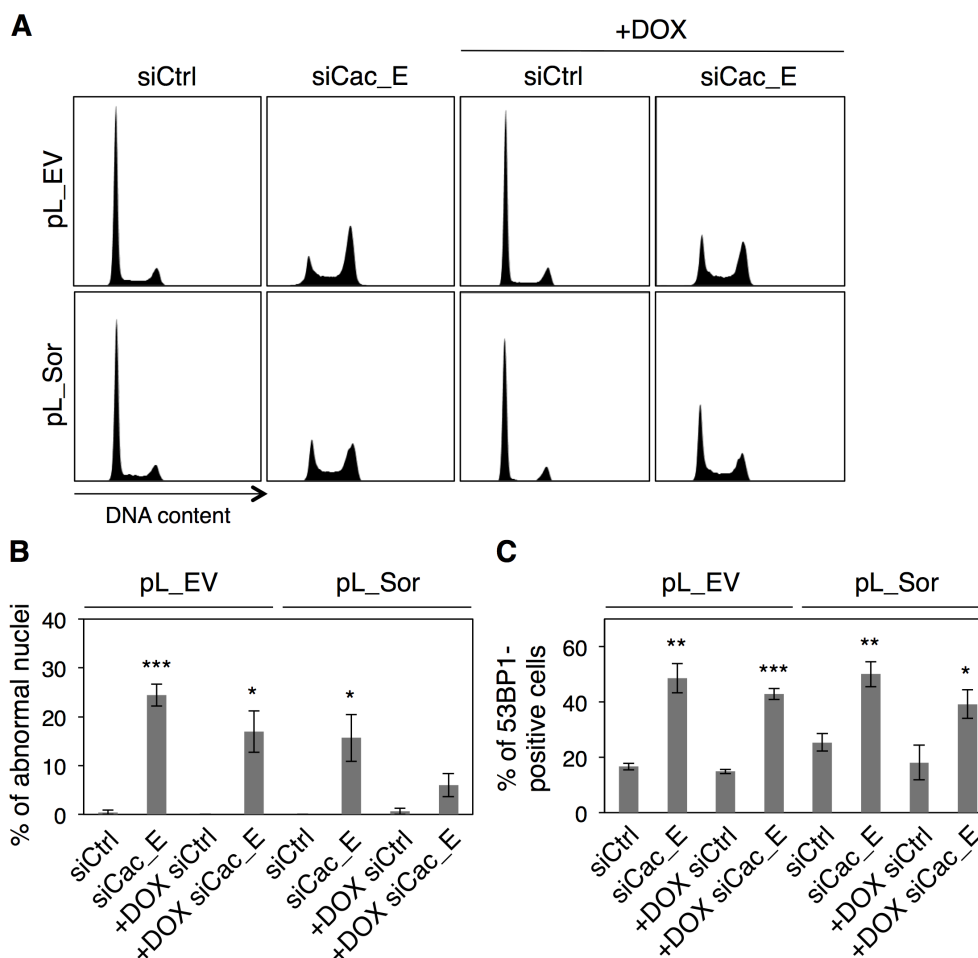


**Figure 32: Sororin overexpression is not sufficient to rescue DNA damage and cell cycle defect associated with hCactin depletion.**

**A)** Flow cytometric analysis for DNA content of HeLa cells overexpressing Sororin cDNA in a DOX-inducible manner (pL\_Sor) transfected with siCtrl or siCac\_E and cultured in absence or presence of DOX for 72h before processing. **B)** Quantification of abnormal nuclei observed in HeLa pL\_Sor or empty vector control cells (pL\_EV) transfected and cultured as in A. **C)** Quantification of IF analysis for the DNA damage marker 53BP1 performed in HeLa pL\_Sor and pL\_EV transfected and cultured as in A. Cells with more than 5 foci of 53BP1 were considered as positive. Error bars represent SEMs. Stars represent significant changes vs. siCtrl based on t-test: \*  $p < 0.05$ ; \*\*  $p < 0.01$ ; \*\*\*  $p < 0.001$ .



### 4.3 Human Cactin and its interactome

#### Mass spectrometric analysis for hCactin interactors

Human Cactin has been previously co-purified with the spliceosome (complex C) (Jurica et al., 2002; Rappsilber et al., 2002; Zhou et al., 2002), and a large-scale analysis for protein-protein interactions identified hCactin as a putative interactor of RNPS1 (RNA binding protein S1) (Ewing et al., 2007), a well-characterized accessory splicing factor. Beside these strong indications of hCactin being part of the spliceosome, analyses in different model organisms did not highlight a possible molecular function linked to pre-mRNA splicing process for Cactin proteins. Moreover, hCactin has also been shown by co-immunoprecipitation (CoIP) analysis to physically interact with the I $\kappa$ B-like protein (NFKBIL) (Atzei et al., 2010a) and possibly with other proteins encoded in the major histocompatibility complex class III (MHCIII) region of chromosome 6 (Lehner et al., 2004). More recently, the interaction between hCactin and TRIM39, a member of the tripartite motif-containing family with E3 ligase activity, has also been disclosed (Suzuki et al., 2015) supporting the finding that hCactin participates in the innate immune response (Atzei et al., 2010a).

Aiming to gain insight into the molecular function of hCactin, we performed mass spectrometric (MS) analysis for the hCactin interactome. We generated a Flp-In T-Rex 293 cell line (Flp-In\_Cac) overexpressing a Strep-HA-tagged version of hCactin under control of a DOX-inducible promoter. Cell extracts from Flp-In\_Cac cells grown in the presence or absence of DOX for 48h were subjected to in-column purification of Strep-HA-Cactin protein complexes (**Fig. 33A**). Protein complexes were first trapped in a column containing resin with immobilized Strep-Tactin and subsequently eluted with the competitor Biotin. Purified protein complexes were sent for MS analysis (**Fig. 33B**). A list of putative hCactin-interactors was generated by comparing identified purification products in induced and non-induced samples (**Fig. 33C**). A short description of the molecular functions attributed to the putative hCactin interactors is listed above (**Table 1**).

Interestingly, among these hCactin interactors only a few of them have been reported to be involved in the pre-mRNA splicing process. Furthermore, several putative hCactin interactors have been shown to interact with each other. Unfortunately, neither I $\kappa$ B-like nor TRIM39 have been found to interact with hCactin in our MS analysis.

In conclusion, hCactin seems to interact with proteins involved in different molecular pathways. Although some of these putative interactors have been

reported to be involved with pre-mRNA splicing, none is part of the spliceosome core complex.

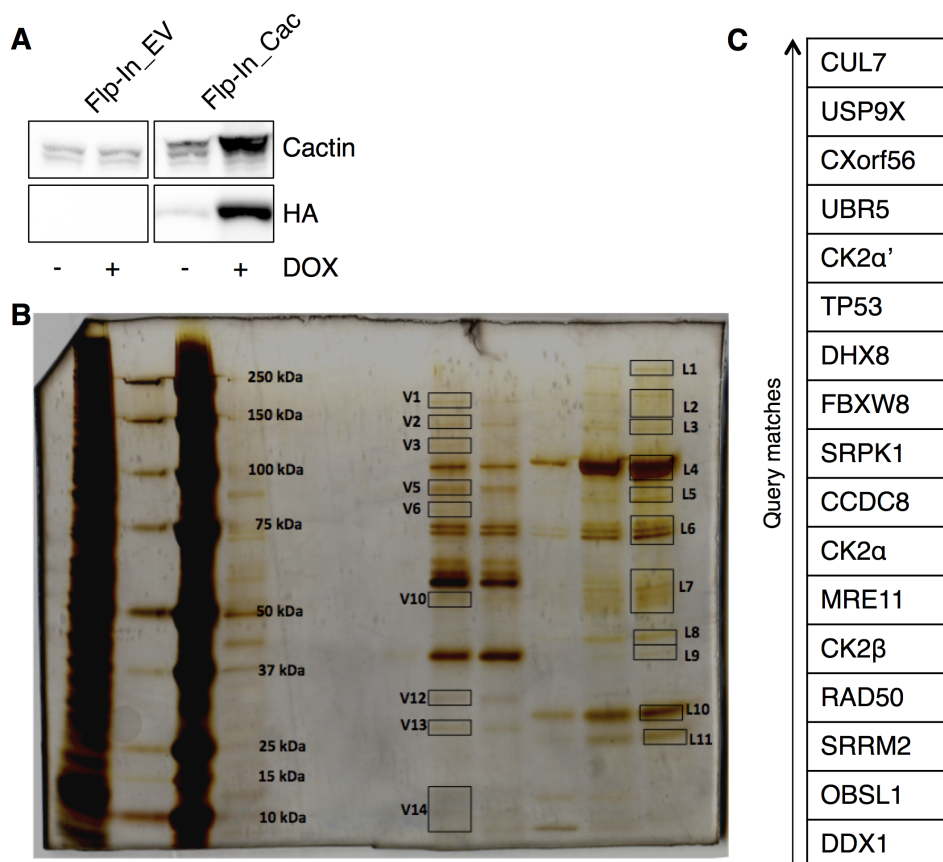


**Figure 33: Streptavidin One-Step purification of hCactin protein complexes for MS analysis.**

**A)** WB analysis for Strep-HA Cactin expression using protein extracts of Flp-In T-Rex 293 cells overexpressing a Strep-HA-tagged hCactin in a DOX-inducible manner (Flp-In\_Cac) or empty vector control cells (Flp-In\_EV) cultured in presence or absence of DOX for 24h before harvesting. **B)** Silver staining of the electrophoresed proteins eluted from One-Step purification of Flp-In\_Cac or Flp-In\_EV protein extracts upon culture in presence of DOX for 24h. Bands L1-L11 were cut as positive hCactin interactors and subjected for MS analysis. **C)** Putative hCactin interactors identified by MS analysis are listed from highest to lowest query matches.

Protein	Function
CUL7	It belongs to the Cullin family of scaffolding proteins and is part of an E3-ubiquitin ligase complex. It is known to interact with Fbxw8, p53, CUL9, OBSL1 and CCDC8 and to be implicated in carcinogenesis and in the 3-M syndrome. (Dias et al., 2002) (Jung et al., 2007; Li et al., 2014; Yan et al., 2014). (Hanson et al., 2012) (Guo et al., 2014; Men et al., 2015)
USP9X	Ubiquitin-specific peptidase associated encoded on the X chromosome, known to escapes X-inactivation. Loss of function leads to developmental delay and congenital malformations. It has been associated with Turner syndrome and is implicated in carcinogenesis. (Murtaza et al., 2015)

CXorf56	Uncharacterized protein of unknown function that has been linked to mental retardation. (Thunstrom et al., 2015).
UBR5	Progesterin-induced protein that belongs to the HECT family of E3 ubiquitin ligases. It is involved in DDR, proliferation and differentiation, and tumorigenesis. (Bradley et al., 2014; Chen et al., 2013; Henderson et al., 2006)
CK2 $\alpha$	Catalytic subunit of the ubiquitous serine/threonine protein kinase Casein kinase 2. It is involved in many different cellular processes. It has been implicated in carcinogenesis. (Trembley et al., 2009; Xu et al., 1999)
p53	Tumorsuppressor protein with transcriptional activation function. It responds to diverse cellular stresses inducing cell cycle arrest, DNA repair, apoptosis, senescence, and metabolic changes. A large number of cancers mutate p53 gene. (Kruiswijk et al., 2015)
DHX8	DEAH-box ATPase/RNA helicase that associates to the spliceosome and promotes the splicing process by helping structural rearrangements within the catalytic core, the mRNA release and ensuring the fidelity of exon-ligation process. (Mayas et al., 2006; Ohno and Shimura, 1996; Schwer, 2008)
Fbxw8	It belongs to the F-box protein family and functions as substrate receptor in the SCF and CRL7 E3 ubiquitin ligase complexes. It has been implicated in cell proliferation and differentiation and in carcinogenesis. (Lin et al., 2011; Okabe et al., 2006; Tsunematsu et al., 2006; Tsutsumi et al., 2008)
SRPK1	Seine/arginine protein kinase specific for the SR family of splicing factors. It is thought to contribute to splicing by regulating intracellular localization of splicing factors. It seems to play a role in alternative splicing regulation and in carcinogenesis. (Giannakouros et al., 2011; Goncalves et al., 2016)
CCDC8	Coiled-coil domain-containing protein of unclear function. It works as co-factor in p53-mediates apoptosis and it seems to play a role in growth. It is implicated in the 3-M syndrome. (Hanson et al., 2012)
CK2 $\alpha'$	Catalytic subunit of the ubiquitous serine/threonine protein kinase Casein kinase 2. It is involved in many different cellular processes. It has been implicated in carcinogenesis. (Trembley et al., 2009; Xu et al., 1999)
Mre11	Nuclear protein with 3' to 5' exonuclease and endonuclease activity involved in homologous recombination and DSB repair. (Rein and Stracker, 2014)
CK2 $\beta$	Regulatory subunits of the serine/threonine protein kinase Casein kinase 2. It is involved in many different cellular processes, like cell cycle control, apoptosis and circadian rhythms. It has been implicated in carcinogenesis. (Trembley et al., 2009; Xu et al., 1999)
Rad50	Essential protein that forms a complex with Mre11 and Nbs1 and is involved in homologous recombination and DSB repair. (Rein and Stracker, 2014)
SRRM2	SR protein that functions in the spliceosome. It is part of a splicing co-activator complex that localizes with the EJC on the mRNA and is directly involved in promoting splicing activity. (Grainger et al., 2009)
OBSL1	Cytoskeletal adaptor protein, member of the obscurin family. It is implicated in the 3-M syndrome. (Geisler et al., 2007; Huber et al., 2010)
DDX1	DEAD box protein and putative RNA helicase of unclear function that has been involved in RNA transport and anti-viral innate immunity. (Fullam and Schroder, 2013; Perez-Gonzalez et al., 2014)

**Table 1: Brief description of known functions associated to the interactors of hCactin identified by MS.**

### Validation of some hCactin interactors

Small-scale purification of Strep-HA-Cac followed by western blot analysis confirmed the physical interaction of Strep-HA-Cac with the endogenous CUL7 (**Fig. 34A**), which represents the most enriched interactor in our MS analysis.

In order to exclude artifactual interactions created during the purification process or by the overexpression of Strep-HA-Cactin, we decided to further validate this interaction. While CoIP analysis performed with ectopically expressed MYC-tagged CUL7 and HA-tagged Cactin clearly showed the interaction between these two proteins (**Fig. 34B**), CoIP analysis using antibodies directed against the endogenous proteins only showed a weak interaction between hCactin and CUL7 (**Fig. 34C**). It seems possible that interactions between hCactin and CUL7 are transient or weak.

We also performed CoIP analysis using ectopically expressed and tagged versions of Casein kinase 2 (CK2) subunits (CK2 $\alpha$ -HA; HA-CK2 $\alpha$ '; MYC-CK2 $\beta$ ) and Cactin-FLAG. These experiments confirmed the interactions between hCactin and the CK2 holoenzyme (**Fig. 34D**).

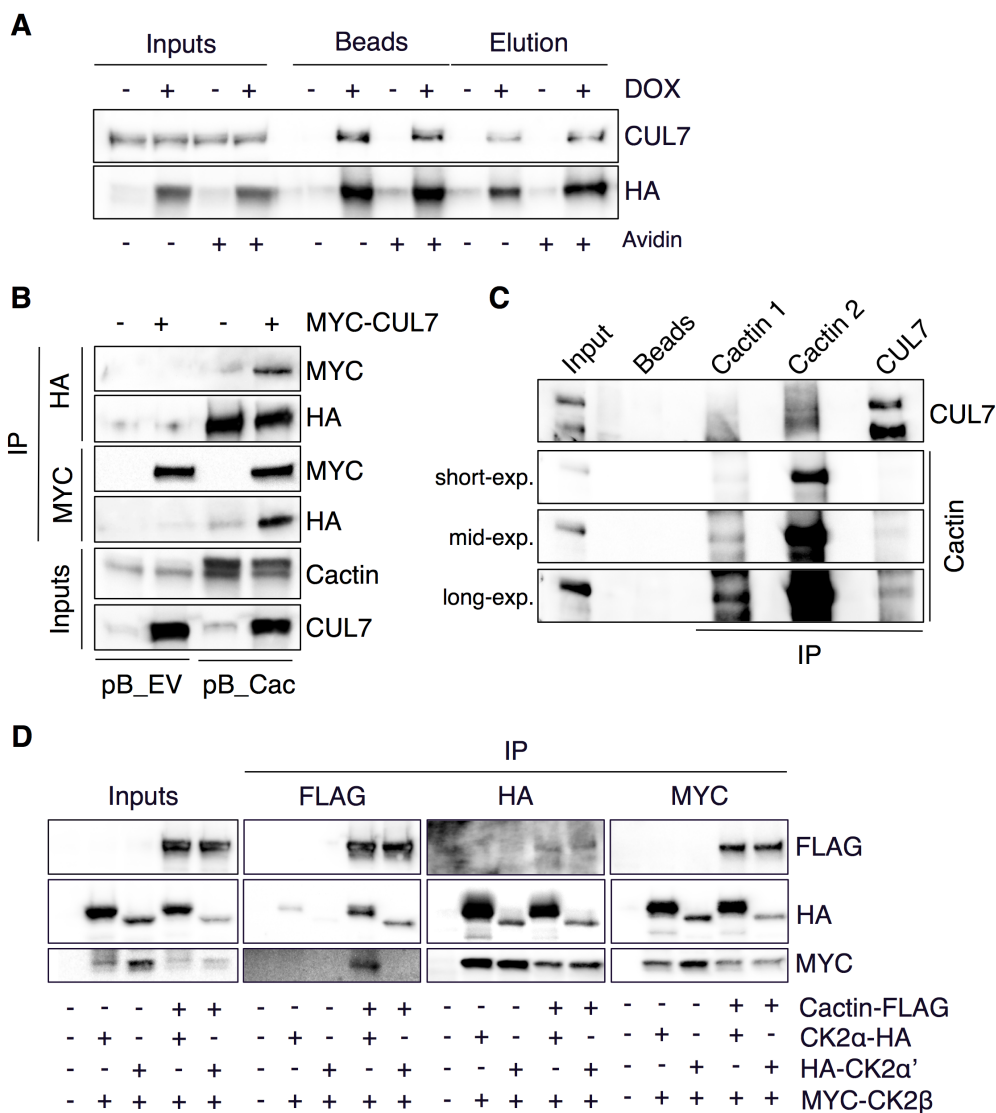


**Figure 34: Validation of some hCactin interactions.**

**A)** WB analysis of small-scale co-purification of Strep-HA-tagged Cactin and CUL7. Flp-In T-Rex 293 cells overexpressing Strep-HA Cactin (Flp-In\_Cac) in a DOX-inducible manner cultured in presence of DOX for 24h were subjected to Streptavidin One-Step purification in presence or absence of Avidin. Protein complexes were either eluted with Biotin or extracted in Laemmli buffer from Streptactin beads. **B)** WB analysis using co-immunoprecipitation (CoIP) products of exogenous HA-tagged Cactin (HA-Cactin) and MYC-tagged CUL7 (MYC-CUL7). HEK293T cells overexpressing HA-tagged Cactin (pB\_Cac) or empty vector control cells (pB\_EV) were transiently transfected with pcDNA3\_MYC-CUL7 plasmids and processed 48h later. Immunoprecipitation (IP) was carried on with anti-HA or anti-MYC antibodies. **C)** WB analysis using CoIP of endogenous hCactin and CUL7 from HEK293T cells. IP was performed using two different anti-Cactin and an anti-CUL7 antibodies. **D)** WB analysis using co-immunoprecipitation (CoIP) products of exogenous FLAG-tagged Cactin (Cactin-FLAG), MYC-tagged CK2β (MYC-CK2β), HA-tagged CK2α (CK2α-HA) and CK2α' (HA-CK2α'). HEK293T cells were transiently transfected with pcMV6\_Cac, pZW6, pZW16 and pZW12 plasmids and processed 48h later. Immunoprecipitation (IP) was carried on with anti-FLAG, anti-HA or anti-MYC antibodies

### Some hCactin interactors promote Sororin pre-mRNA splicing

With the aim to better understand the function exerted by hCactin during the pre-mRNA splicing process, we chose to use Sororin mRNA splicing as a functional readout. We depleted 11 different putative hCactin interactors obtained in our MS analysis in HeLa cells using siRNAs, and tested the depletion 72h after transfection by qRT-PCR (**Fig. 35A**). Interestingly, cells depleted for either DHX8 (DEAH-box helicase 8) or SRRM2 (serine/arginine repetitive matrix 2) showed Sororin intron 1 retention in RT-PCR analysis, similarly to what we observed upon hCactin depletion (**Fig. 35B**). Similarly, northern blot analysis revealed that DHX8-depleted HeLa cells exhibited Sororin intron(s) retention to a similar extent of hCactin-depleted cells, whereas SRRM2-depleted cells showed a milder yet clear defect (**Fig. 35C**). Thus, we can conclude that among the identified interactors of hCactin, the RNA helicase DHX8 and the RNA binding protein SRRM2 are required for Sororin pre-mRNA splicing.

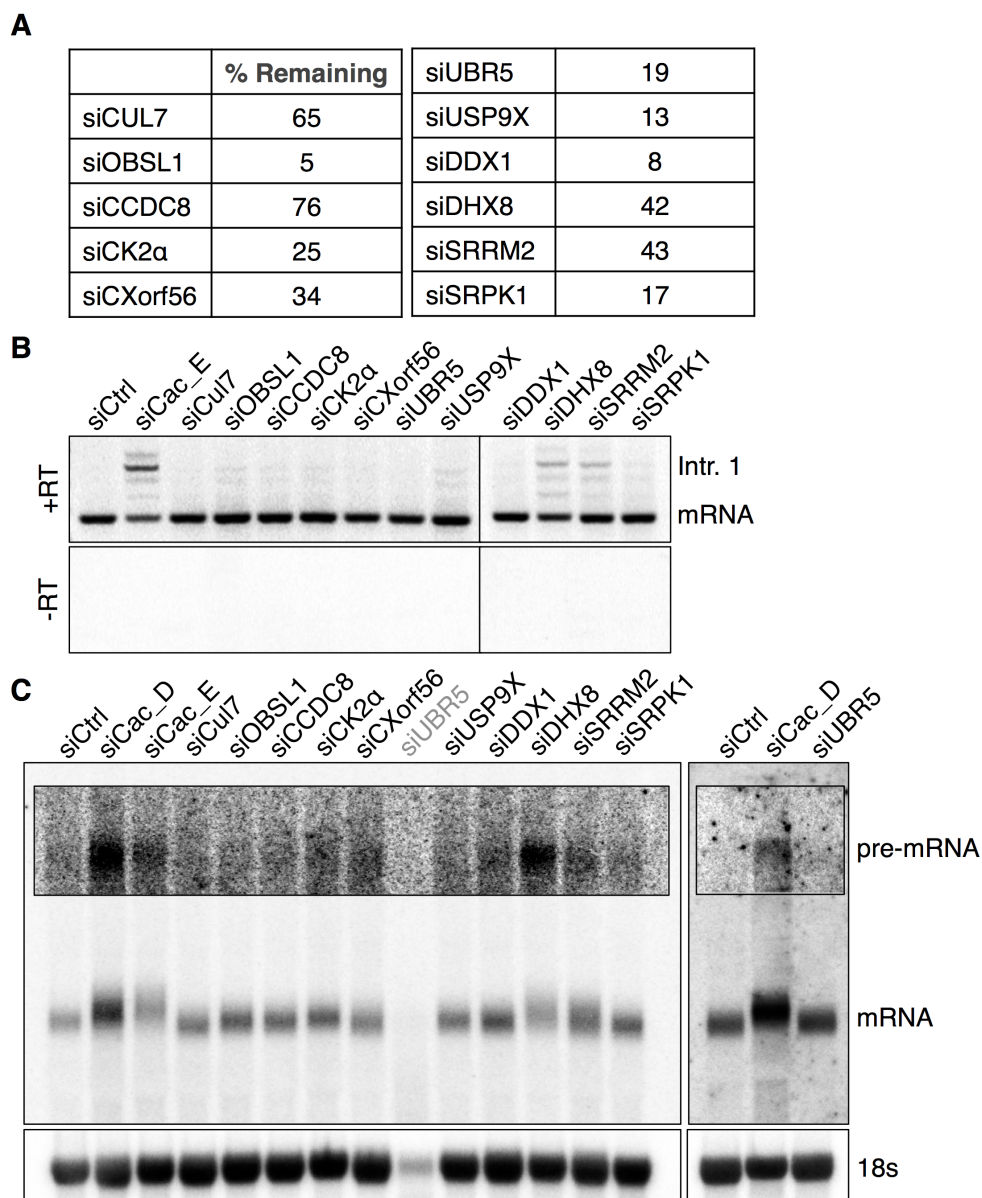


**Figure 35: Depletion of hCactin interactome and Sororin pre-mRNA splicing.**

**A)** Protein levels remaining upon siRNA depletion according to qRT-PCR analysis. HeLa cells were transfected with the indicated siRNAs and harvested 72h after transfection. **B)** RT-PCR analysis for Sororin intron 1 using RNA extracts of HeLa cells transfected as in A. **C)** Northern blot analysis for Sororin transcripts using RNA extracts of HeLa cells transfected as in A. 18s represents loading control. To detect pre-mRNA species the indicated inset of the blot was auto contrasted.

### **DHX8 supports Sororin pre-mRNA splicing within the same genetic pathway of hCactin**

In order to gain an insight into the mechanism of Sororin pre-mRNA splicing driven by hCactin, we analysed the effects of hCactin and DHX8 or hCactin and SRRM2 co-depletions on Sororin pre-mRNA splicing. HeLa cells were transfected with different combinations of siRNAs, and expression levels of the aforementioned factors were checked by western blot or qRT-PCR analysis 72h after transfection (**Fig. 36A and B**). hCactin protein levels were similarly reduced in both single and co-depletion experiments. Despite some variations among replicate experiments, mRNA levels of DHX8 and SRRM2 showed a similar reduction in both single and co-depletion experiments. Parallel northern blot analysis revealed that the combination of hCactin and DHX8 depletions did not exacerbate Sororin intron(s) retention, while hCactin and SRRM2 co-depletion clearly worsened this phenotype (**Fig. 36C**). In particular, co-depletion of hCactin and SRRM2 clearly accumulated Sororin pre-mRNA. In line with the northern blot analysis, RT-PCR analysis revealed that HeLa cells depleted for both hCactin and DHX8 experienced retention of Sororin intron 1 comparable to the respective single depletions, whereas combination of hCactin and SRRM2 depletions exacerbated this phenotype compared to single depletions (**Fig. 36D**).



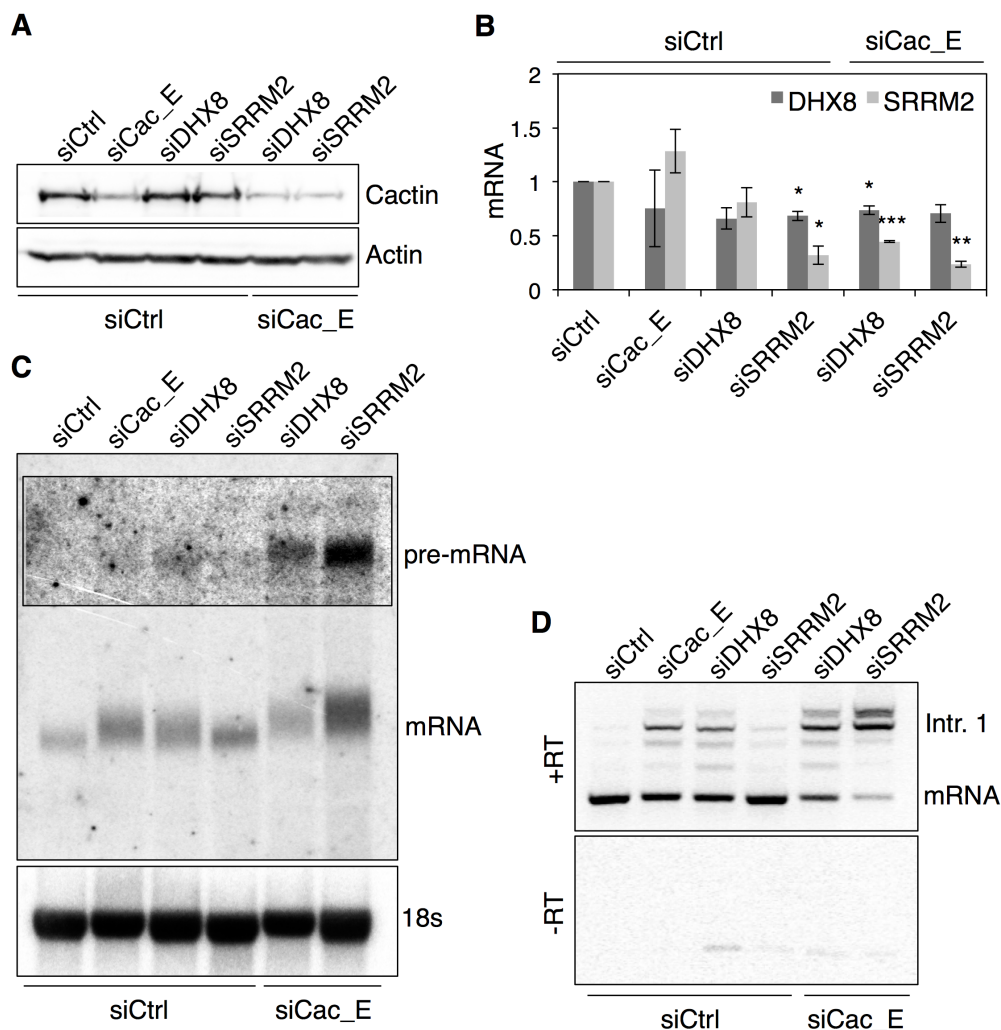


**Figure 36: Human Cactin and DHX8 and SRRM2 may synergise to promote Sororin pre-mRNA splicing.**

**A)** WB analysis for hCactin depletion using protein extracts of HeLa cells transfected with the indicated combinations of siRNAs and harvested 72h after transfection. **B)** qRT-PCR analysis for DHX8 and SRRM2 mRNA levels using RNA extracts of HeLa cells transfected as in A. **C)** Northern blot analysis for Sororin transcripts using RNA extracts of HeLa cells transfected as in A. 18s represents loading control. To detect Sororin pre-mRNA species blot was auto contrasted. **D)** RT-PCR analysis for Sororin intron 1 using RNA extracts of HeLa cells transfected as in A. Error bars represent SEMs. Stars represent significant changes vs. siCtrl based on t-test: \*  $p < 0.05$ ; \*\*  $p < 0.01$ ; \*\*\*  $p < 0.001$ .

Metaphase spread analysis indicated that DHX8-depleted HeLa cells accumulated a number of metaphases with abnormal chromosomal morphologies similarly to hCactin-depleted cells, while SRRM2-depleted HeLa cells presented way less (~50% less) metaphases with chromosomal abnormalities compared to hCactin-depleted cells (**Fig. 37A**). Remarkably, DHX8 and hCactin co-depletion in HeLa cells presented similar numbers of

abnormal metaphases to the respective single depletions, whereas SRRM2 and hCactin-co-depleted HeLa cells showed an additive effect reaching up to 90% of abnormal metaphases.

Notably, DHX8 mRNA levels seemed to be only slightly reduced in both single and co-depletion experiments. Yet DHX8 single depletion was sufficient to induce Sororin pre-mRNA splicing defects comparable to hCactin single depletion.

Taken together, these data suggest that hCactin and DHX8, but not SRRM2, support Sororin pre-mRNA splicing in an epistatic relationship. We cannot exclude that SRRM2 and hCactin work in the same pathway as well, and that co-depletion of these factors results in a stronger impairment of the pathway compared to single depletions due to low efficiency of SRRM2 protein depletion achieved with our siRNA.

### **Cell cycle arrest, accumulation of DNA damage and nuclear abnormalities induced by hCactin depletion may arise from different causes**

In order to better characterize the interaction between hCactin and DDX8 or SRRM2, we investigated the phenotypes associated with hCactin-depletion that we could not compensate by Sororin overexpression, in single- and co-depletion experiments.

Flow cytometric analysis of cell cycle progression disclosed a marked G2/M accumulation of HeLa cells depleted for DHX8 72h after transfection, which is reminiscent of the cell cycle defect observed upon hCactin depletion. In contrast, 72h after transfection cells transfected with SRRM2 siRNA slightly accumulated in G1 (**Fig. 37B**). Interestingly, while co-depletion of hCactin and DHX8 did not have an additive effect on the cell cycle perturbation, co-depletion of hCactin and SRRM2 clearly showed a cell cycle arrest resembling hCactin-depleted cells.

Furthermore, IF analysis for accumulation of the DNA damage marker 53BP1 disclosed that DHX8-depleted HeLa cells accumulated DNA damage to a similar extent of hCactin-depleted cells 72h after transfection. In reverse, SRRM2-depleted cells did not accumulate DNA damage as compared to siCtrl-treated cells (**Fig. 37C**). Co-depletion of hCactin and DHX8 did not increase the amount of 53BP1-positive cells compared to single depletions, while co-depletion of hCactin and SRRM2 induced more DNA damage compared to hCactin single depletion, suggesting an exacerbation of the phenotype.

Taken together, these data suggest that hCactin and DHX8 function in the same pathway, which is not only required for Sororin pre-mRNA splicing, but is also essential for cell cycle progression and suppression of DNA damage.

SRRM2, on the other side, appears to be required only when hCactin function is compromised.

Interestingly, the accumulation of nuclei with abnormal morphology appeared comparable in hCactin, DHX8, and SRRM2 single depletions (**Fig. 37D**). Moreover, co-depletion of hCactin and DHX8 led to an exacerbation of the number of abnormal nuclei, whereas co-depletion of hCactin and SRRM2 did not show additive effect on nuclear morphology, resembling single-depleted cells. Thus, the effect on nuclear morphology observed upon hCactin depletion seems to arise from impairment of a pathway involving primarily hCactin and SRRM2, while DHX8 requirements become evident only upon functional inactivation of hCactin.

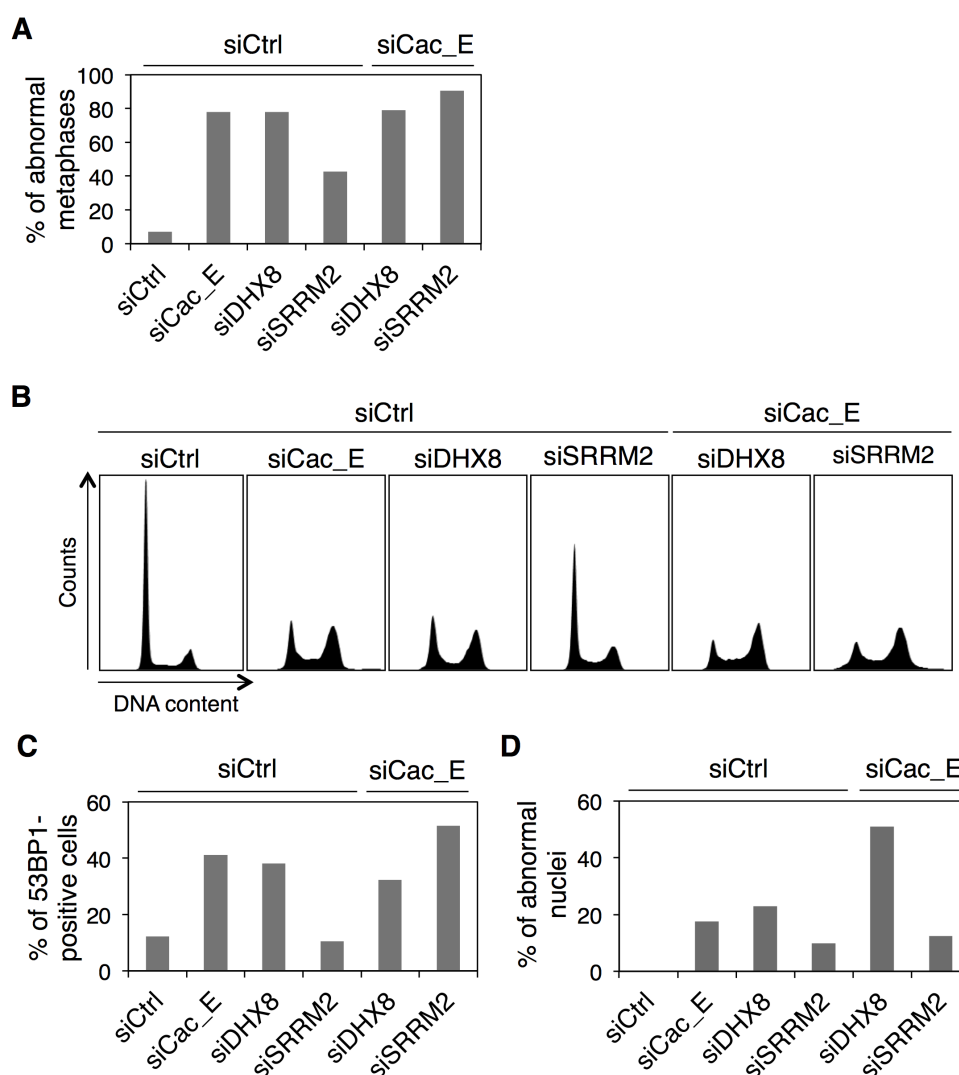


**Figure 37: Depletion of hCactin, DHX8 and SRRM2 impact on cell cycle progression, accumulation of DNA damage and abnormal nuclear morphology to different extent.**

**A)** Quantifications of abnormal metaphase spread observed in HeLa cells transfected with the indicated combination of siRNAs and treated with Colcemid 72h after transfection. **B)** Flow cytometric analysis for DNA content of HeLa cells transfected as in A and harvested 72h after transfection. **C)** Quantifications of IF analysis for DNA damage accumulation using the DNA

damage marker 53BP1 of HeLa cells transfected as in A. Cells with more than 5 foci of 53BP1 were considered as positive. **D)** Quantifications of abnormal nuclei observed in HeLa cells transfected as in A.

### **Human Cactin and CUL7 physically interact, but CUL7 is not required for Sororin pre-mRNA splicing**

According to our MS analysis, hCactin interacts with several factors (see **Fig. 33D**). Among these are the scaffold protein CUL7 and the CUL7 interactors OBSL1 (cytoskeletal adaptor protein obscurin-like 1) and CCDC8 (coiled-coil domain containing 8); CUL7, OBSL1 and CCDC8 are known to form the 3-M complex. Mutually exclusive mutations in one of these genes have been shown to cause the 3M-syndrome, which is characterized by abnormal p53 function and growth retardation (Hanson et al., 2012). Recent reports have proposed that the 3-M complex functions in maintaining microtubule stability and contributes to promote cell survival by suppressing the activity of another E3 ligase complex comprising by Cullin 9 (CUL9) (Li et al., 2014; Yan et al., 2014).

As mentioned already above, CoIP of ectopically expressed and endogenous proteins confirmed that hCactin and CUL7 physically interacted (see **Fig. 34A, B and C**). However, RT-PCR and northern blot analyses (see **Fig. 29A and B, 35 B and C**) revealed that CUL7 did not impact on Sororin pre-mRNA splicing. qRT-PCR analysis also confirmed these data (**Fig. 38**), suggesting that hCactin might be involved in cellular processes other than pre-mRNA splicing and involving CUL7.

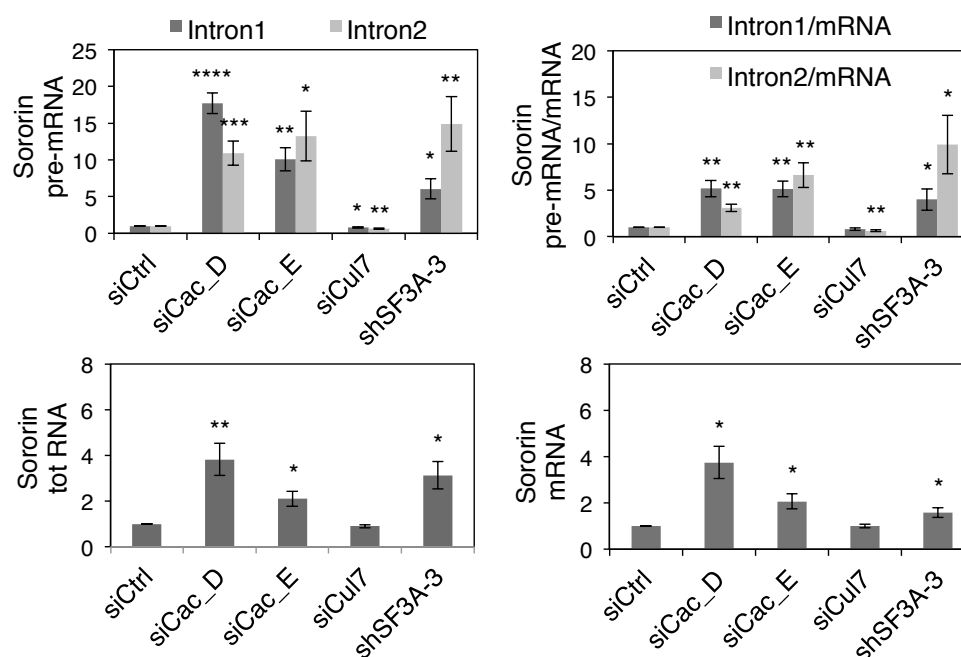


**Figure 38: Depletion of CUL7 does not affect Sororin pre-mRNA splicing.**

qRT-PCR analysis for Sororin transcripts using RNA extracts of HeLa cells transfected with siCtrl, hCactin siRNAs or siCul7 and harvested 72h after transfection. As positive control for impaired pre-mRNA splicing cells were transfected with shSF3A-3. Error bars represent SEMs. Stars represent significant changes vs. siCtrl based on t-test: \*  $p < 0.05$ ; \*\*  $p < 0.01$ ; \*\*\*  $p < 0.001$ ; \*\*\*\*  $p < 0.0001$ .

### Human Cactin is not a substrate for the CUL7 E3 ligase complex

The scaffold protein CUL7 has been shown to assemble a large Cullin ring E3 ligase complex (CRL7) similar to the SCF complex (Skp, Cullin, F-box containing complex) formed by the scaffold protein Cullin 1 (CUL1). Indeed the small RING domain protein Rbx1 and the adaptor protein Skp1 can be assembled in both the CRL7 and SCF complex (Pickart, 2001). So far, the Fbxw8 (F-box and WD repeat containing 8) is the only substrate-receptor that has been identified for CRL7, suggesting high substrate-specificity (Dias et al., 2002). Substrates of the ubiquitin E3 ligase complexes are generally polyubiquitinated and targeted for proteasomal degradation (Pickart, 2001). Since, in our MS analysis, we found several proteins known to be part of the CRL complex, we hypothesised that hCactin may be a substrate for the CRL7 complex. Therefore, we checked whether hCactin protein levels were elevated in absence of CUL7. HeLa cells were transfected with siCtrl, hCactin siRNAs, or siRNA targeted against CUL7 mRNA (siCul7), lysed and subjected to western blot analysis. While CUL7 protein levels were extremely reduced in siCul7-transfected cells, we did not observe any difference in hCactin protein

levels at 48h or 72h after transfection (**Fig. 39A**). Unexpectedly, CUL7 protein levels were particularly reduced upon hCactin depletion (discussed below). We also performed CoIP analysis of endogenous hCactin and CUL7 from untreated HEK293T cells and HEK293T cells treated for 2h with the proteasome inhibitor MG132. CoIP results did not show any further stabilization of the physical interaction between hCactin and CUL7 upon inhibition of the proteasome (**Fig. 39B**). Furthermore, we subjected immunoprecipitated endogenous hCactin from untreated and MG132-treated HEK293T cells to western blot analysis with an antibody raised against Ubiquitin (**Fig. 39C**). While a smear, representing polyubiquitinated proteins, was visible in the MG132 input, there was no enrichment of polyubiquitinated hCactin in either condition. However, a band around 110 kDa was visible, which could represent hCactin monoubiquitinated species. Taken together, these data suggest that hCactin is not a canonical substrate of CUL7-mediated polyubiquitination.

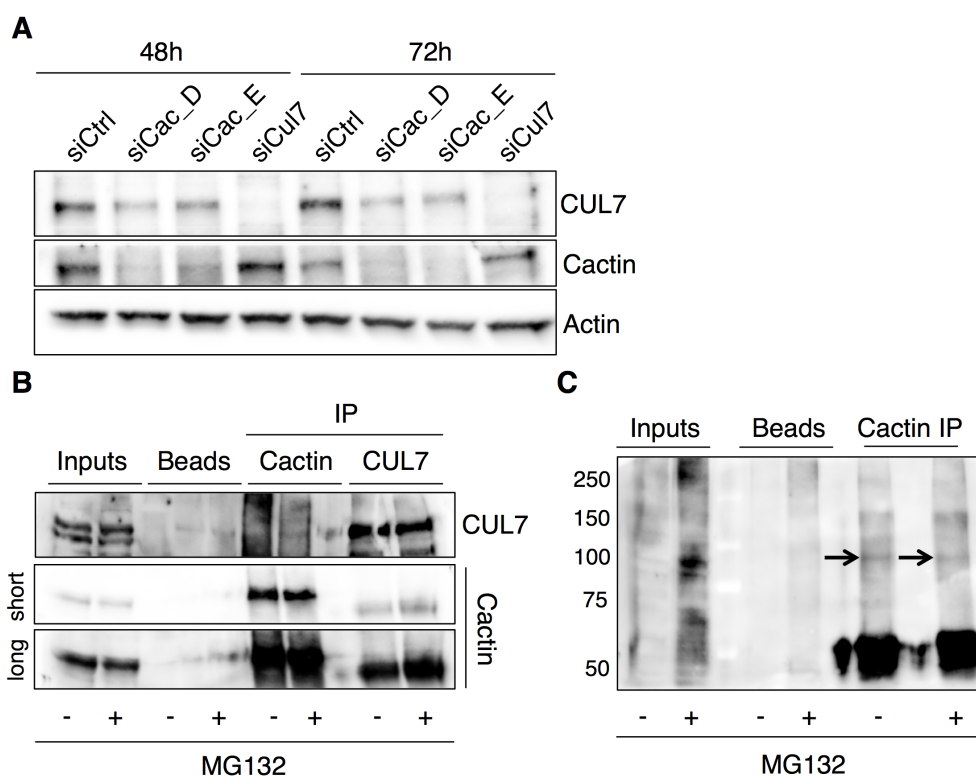


**Figure 39: Human Cactin is not a substrate of CUL7.**

**A)** WB analysis for hCactin protein levels using protein extracts of HeLa cells transfected with siCtrl, hCactin siRNAs or siCul7 and harvested at given time after transfection. **B)** WB analysis using co-immunoprecipitation (CoIP) products of endogenous hCactin and CUL7. HeLa cells were treated with MG132 for 2h to possibly stabilise hCactin in complex with CUL7 and immunoprecipitation (IP) was carried on with anti-Cactin or anti-CUL7 antibodies. **C)** WB analysis for polyubiquitination using endogenous hCactin IP products and an anti-Ubiquitin antibody. HeLa cells were treated with MG132 for 2h to accumulate polyubiquitinated proteins

and cell extracts were subjected to IP with an anti-Cactin antibody. Arrows indicated putative monoubiquitinated hCactin.

### Human Cactin depletion leads to reduced CUL7 protein levels

As mentioned above, we noticed that hCactin-depleted cells had reduced levels of CUL7 protein. In order to exclude off-target effects of the hCactin siRNAs, we performed a compensation experiment in HeLa pB\_EV and HeLa pB\_Cac cells transfected with either siCtrl or siCac\_D. Western blot analysis performed 48h after transfection verified that CUL7 levels were normal in HeLa pB\_Cac cells depleted for endogenous hCactin (**Fig. 40A**).

We then wondered whether CUL7 protein stability was compromised in hCactin-depleted cells. HeLa cells were transfected with either siCtrl or siCac\_D and 48h later treated with the protein translation inhibitor cycloheximide. Protein samples were collected every 2h over a time-course of 6h. Although CUL7 protein levels seemed to decay slightly faster within the first 2 hours of the time course in cells depleted for hCactin, signal quantifications did not reveal any statistically significant difference in CUL7 half-life among different conditions (**Fig. 40B and C**).

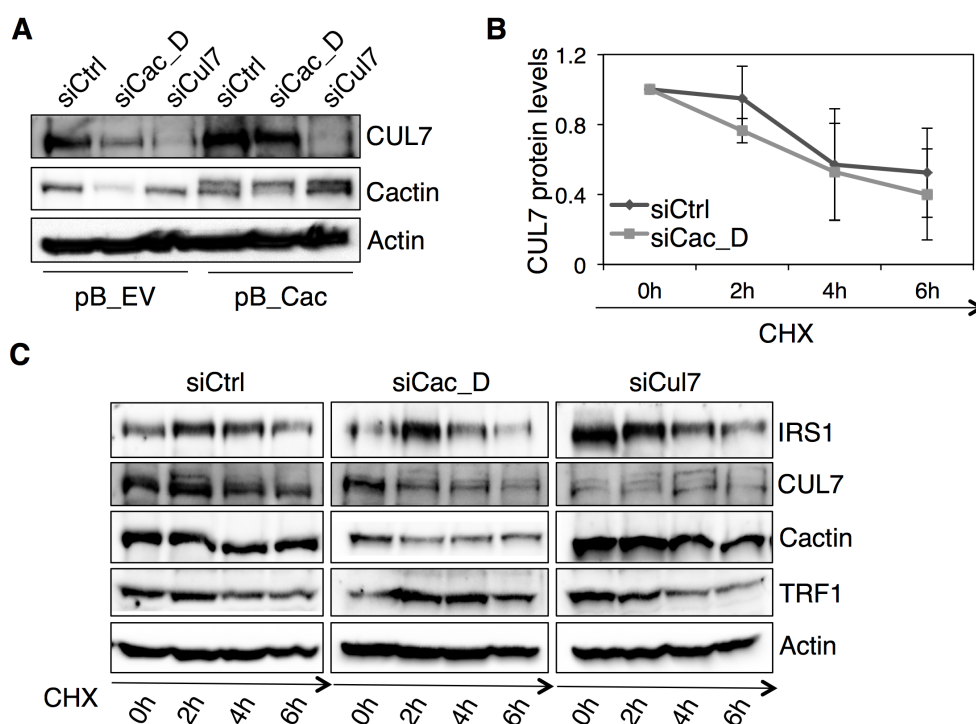


**Figure 40: Reduced CUL7 protein levels observed upon hCactin depletion are not a clear consequence of CUL7 protein destabilisation.**

**A)** WB analysis for CUL7 protein levels using protein extracts of HeLa cells overexpressing a HA-tagged Cactin (pB\_Cac) or empty vector control cells (pB\_EV) transfected with siCtrl, siCac\_D or siCul7 and harvested 72h after transfection. **B)** Graphic representation of CUL7

protein stability in different conditions calculated by WB signal intensity. HeLa cells were transfected with siCtrl or siCac\_D and 72h after transfection were treated with Cycloheximide for 6h. Cells were harvested at given time points and protein extracts were subjected to WB analysis. Error bars represent SEMs. **C)** Example of WB analysis for CUL7 protein stability using cell extracts of HeLa cells transfected and treated as in B.

We then set up to test whether the reduced CUL7 protein levels were a consequence of impaired CUL7 pre-mRNA splicing. Data from our transcriptome analysis showed a mild enrichment of intronic reads mapping to CUL7 gene locus in hCactin-depleted cells (**Fig. 41A**). RT-PCR analysis confirmed a milder accumulation of pre-mRNA species compared to shSF3A-3 control cells (**Fig. 41B**). qRT-PCR analysis revealed that CUL7 mRNA levels were reduced by 0.5-0.6 fold 72h after transfection with siCac\_E in HeLa cells (**Fig. 41C**). HeLa cells transfected with siCul7 or shSF3A-3 presented a similar reduction in CUL7 mRNA levels. Although HeLa cells transfected with siCac\_D did not show a statistically significant reduction of CUL7 mRNA, a similar trend upon hCactin depletion was found. Moreover, CUL7 pre-mRNA species accumulated in siCac\_D-transfected cells at a similar extent to shSF3A-3-treated cells, while siCac\_E-transfected HeLa cells only showed a statistically significant accumulation of CUL7 pre-mRNA specie retaining intron 1, but not specie retaining intron 4.

Taken together, these data suggest that, despite some indications of a possible destabilization of CUL7 protein, reduced CUL7 protein levels observed in hCactin-depleted cells may be a consequence of defects in CUL7 pre-mRNA splicing.



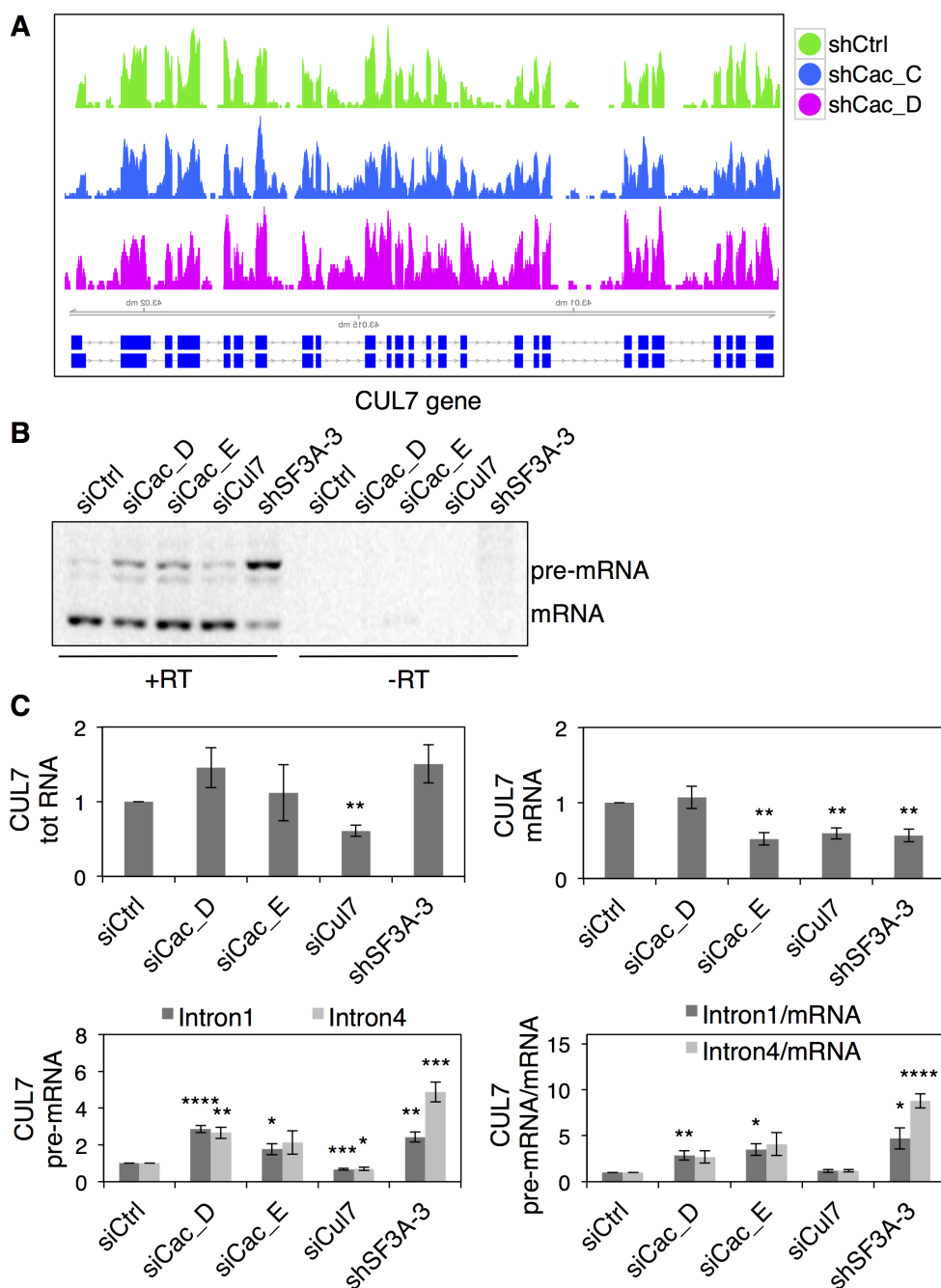


**Figure 41: Depletion of hCactin leads to a mild defect in CUL7 pre-mRNA splicing.**

**A)** Read coverage of the CUL7 gene in three representative samples obtained by bioinformatic analysis of the RNA sequencing data obtained from total RNA extracts of U2OS cells transfected with shCtrl or hCactin shRNAs and harvested 48h after transfection (see Fig. 27). **B)** RT-PCR analysis for CUL7 intron retention using RNA extracts of HeLa cells transfected with siCtrl, hCactin siRNAs or siCul7 and harvested 72h after transfection. As positive control for compromised splicing cells were transfected with an shRNA targeted against the spliceosome factor SF3A-3. **C)** qRT-PCR analyses for CUL7 transcripts using total RNA extracts of HeLa cells transfected as in B. Error bars represent SEMs. Stars represent significant changes vs. siCtrl based on t-test: \*  $p < 0.05$ ; \*\*  $p < 0.01$ ; \*\*\*  $p < 0.001$ ; \*\*\*\*  $p < 0.0001$ .

### **Both Cactin- and CUL7-depleted cancer cells show a hindered G1/S transition**

It has been shown that, differently from primary cells, degradation of CyclinD at the onset of S phase is a prerogative for cancer cell survival, and that compromised regulation of CyclinD protein levels lead to hindered G1/S transition (Alt et al., 2000; Okabe et al., 2006). Moreover, CyclinD is a substrate of both the SCF complex and CUL7 via the substrate-receptor Fbxw8 (Ponyeam and Hagen, 2012). Considering that hCactin-depleted cells presented a compromised G1/S transition, we investigated whether this could be a consequence of deregulated CyclinD protein levels due to reduced CUL7 protein. First we used western blot to check whether total amounts of CyclinD were altered upon hCactin or CUL7 depletion. U2OS cells transfected with siCtrl, hCactin siRNAs, or siCul7 for 72h did not show any accumulation of CyclinD (**Fig. 42A**). In order to examine whether CyclinD expression was altered upon hCactin depletion we synchronized U2OS cells with a thymidine block followed by a nocodazole block. Cells were transfected during the release from the thymidine block with siCtrl, hCactin siRNA, or siCul7 for 4h. Nocodazole-enriched mitotic cells were then released into normal medium and collected every 3h over a time course of 18h. Flow cytometric analysis of cell cycle progression and western blot analysis of CyclinD protein amounts were performed. Flow cytometric analysis revealed that both hCactin- and CUL7-depleted cells experience a hindered G1/S transition compared to control cells (**Fig. 42C**). However, CyclinD was expressed to a similar extent and at the right cell cycle stage in both hCactin- and CUL7-depleted cells (**Fig. 42B**).

It has been demonstrated that the substrate-receptor Fbxw8 mediates dimerization between the SFC complex and CUL7 and that this dimerization may enhance the proteolytic activity mediated by the SCF complex (Ponyeam and Hagen, 2012). Western blot analysis of HeLa cells transfected with either siCtrl or hCactin siRNAs clearly showed that CUL1 protein levels were not affected upon hCactin depletion (see **Fig. 42A**).

Thus, from these data we can conclude that hCactin and CUL7 depletions lead to impaired G1/S transition, but that this phenotype is not a consequence of deregulated CyclinD expression.

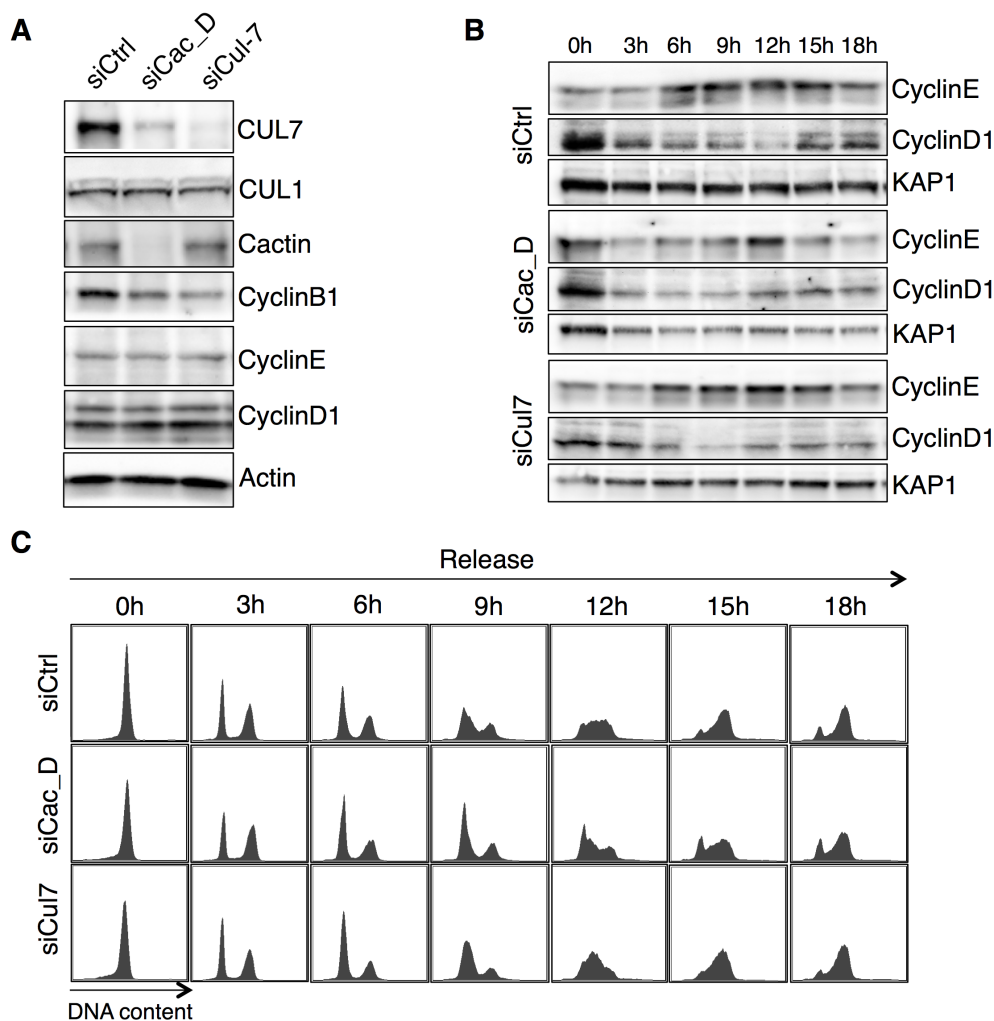


**Figure 42: Depletion of Cul7 affects the G1/S transition similarly to hCactin depletion.**

**A)** WB analysis using protein extracts of U2OS cells transfected with siCtrl, siCac\_D or siCul7 and harvested 72h after transfection. **B)** WB analysis for CyclinD1 levels using protein extracts of U2OS cells synchronised by subsequent Thymidine and Nocodazole blocks and transfected with siCtrl, siCac\_D or siCul7 after Thymidine block. Cells were collected by mitotic shake-off and released in fresh media. Released cells were harvested at indicated time. **C)** Flow cytometric analysis of U2OS cells transfected and treated as in B.

### **Both hCactin- and CUL7-depleted cancer cells present an accumulation of c-Fos transcript**

The insulin receptor substrate 1 (IRS1) is a known substrate for CUL7 (Xu et al., 2012; Xu et al., 2008). However, whether the ubiquitin-mediated degradation of this substrate is mediated by CUL7 alone is not clear. Interferences with the insulin pathway also impact the MAPK/ERK (mitogen-activated protein kinase) pathway, in turn leading to cell growth and survival defects (Scheufele et al., 2014). We assumed that reduced levels of CUL7 upon hCactin depletion led to up-regulation of IRS1 levels, consequently altering the MAPK downstream target proto-oncogene c-Fos (human homolog of the retroviral oncogene v-Fos), as previously described (Hartmann et al., 2014).

First we started investigating whether the IRS1 protein levels are altered in HeLa cells transfected with siCtrl, siCac\_D, or siCul7. Western blot analysis of whole cell extracts did not show any accumulation of IRS1 upon hCactin depletion (**Fig. 43A**). Notably, we did not observe accumulation of IRS1 in CUL7-depleted HeLa cells. We went on testing whether IRS1 protein was stabilized upon hCactin depletion by transfecting HeLa cells with siCtrl, siCac\_D, or siCul7 and then treating them with cycloheximide for 6h. Protein samples were collected every 2h during cycloheximide treatment and subjected to western blot analysis. Quantification of western blot analysis did not show stabilization of IRS1, either in hCactin- or in CUL7-depleted cells (**Fig. 43B**, see **Fig. 40C**).

On the other side, qRT-PCR analysis for c-Fos transcripts revealed a roughly 2-fold increase of c-Fos mRNA levels in hCactin- and CUL7-depleted HeLa cells (**Fig. 43C**). While pre-mRNA levels of c-Fos were 2-fold higher upon CUL7-depletion, suggesting increased transcriptional rates, the levels of c-Fos pre-mRNA were increased by about 6-fold upon hCactin depletion. Pre-mRNA/mRNA ratios showed that hCactin-depleted cells also presented a c-Fos pre-mRNA splicing defect.

These data show that hCactin depletion promotes accumulation of c-Fos transcripts similarly to what observed in CUL7-depleted cells, possibly suggesting an activation of the c-Fos proto-oncogene. However, the molecular details leading to c-Fos transcript accumulation upon hCactin depletion remain elusive.

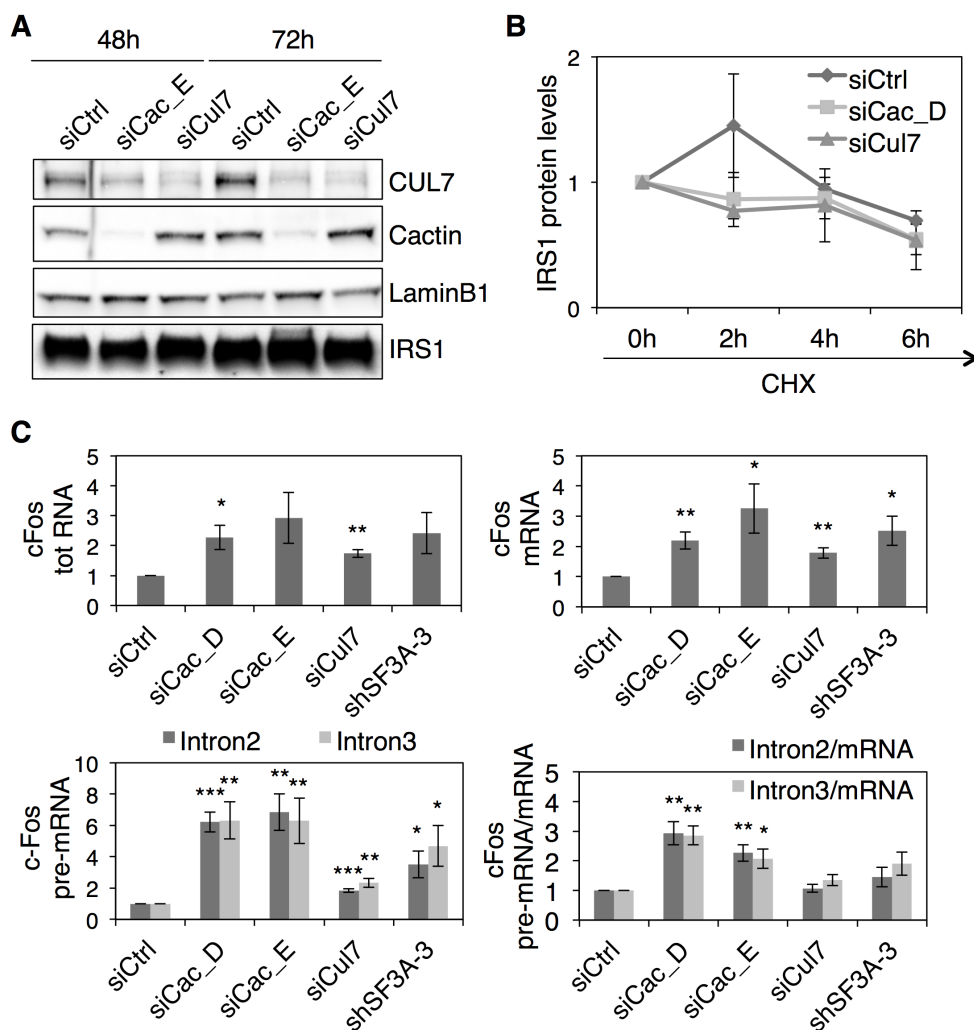


**Figure 43: Depletion of hCactin induces c-Fos transcripts accumulation similarly to CUL7-depleted cells.**

**A)** WB analysis for IRS1 protein levels using protein extracts of HeLa cells transfected with siCtrl, siCac\_D or siCul7 and harvested 72h after transfection. **B)** Graphic representation of IRS1 protein stability in different conditions calculated by WB signal intensity. HeLa cells were transfected with siCtrl or siCac\_D and 72h after transfection were treated with Cycloheximide for 6h. Cells were harvested at indicated time and protein extracts were subjected to WB analysis. Example of WB analysis for IRS1 protein stability using cell extracts of HeLa cells transfected and treated are shown in Fig. 40C. **C)** qRT-PCR analysis for c-Fos transcripts using RNA extracts of HeLa cells transfected as in A. Error bars represent SEMs. Stars represent significant changes vs. siCtrl based on t-test: \*  $p < 0.05$ ; \*\*  $p < 0.01$ ; \*\*\*  $p < 0.001$ .

### **CUL7 overexpression in hCactin-depleted cancer cells does not rescue any principal phenotype associated with hCactin depletion**

To directly test whether and to what extent CUL7 deficiency contributed to the different defects observed in hCactin-depleted cells, we set up a complementation system where Cul7 levels could be restored in absence of hCactin. We used lentiviral infection to generate HeLa cell lines with stably integrated empty vector (pL\_EV) or vector expressing a MYC-tagged version of CUL7 (pL\_CUL7) under the control of a DOX-inducible promoter. Western blot analysis showed that the overexpression of MYC-CUL7 was able to maintain CUL7 protein levels to at least the endogenous level upon siCul7 and siCac\_E treatment (**Fig. 44A**). Unfortunately, IF analysis revealed that our inducible system was leaky and that MYC-CUL7 was non-homogeneously expressed throughout the cell population. Consequently, we decided to restrict our analysis only to pL\_EV and pL\_CUL7 cells treated with DOX, discarding data from non-induced cells.

As expected, qRT-PCR analysis of DOX-treated pL\_EV HeLa cells displayed reduced CUL7 mRNA levels upon hCactin and CUL7 depletion 72h after transfection (**Fig. 44B**). On the contrary, DOX-treated pL\_CUL7 cells presented at least 10-fold more CUL7 mRNA in each condition confirming the strength of the induction. CUL7 pre-mRNA/CUL7mRNA ratio demonstrated that hCactin-depleted pL\_EV HeLa cells suffered from a CUL7 pre-mRNA splicing defect and such defect was compensated by CUL7 overexpression in DOX-treated pL\_CUL7 cells.

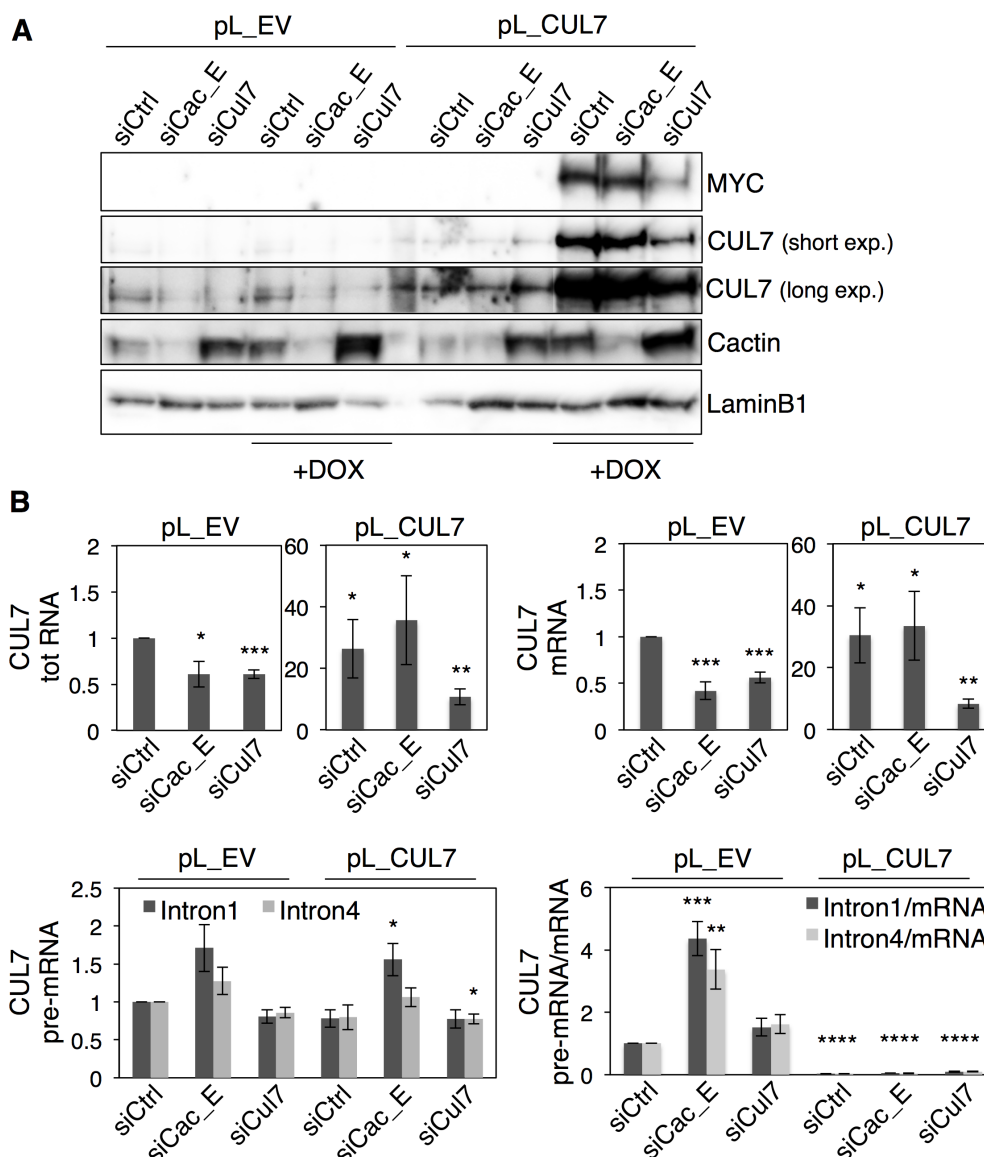


**Figure 44: CUL7 compensation system.**

**A)** WB analysis of CUL7 protein levels using protein extracts of HeLa cells overexpressing MYC-tagged CUL7 in a DOX-inducible manner (pB\_CUL7) or empty vector control cells (pL\_EV). Cells were cultured in presence or absence of DOX, transfected with siCtrl, siCac\_E or siCul7 and harvested 72h after transfection. **B)** qRT-PCR analysis of CUL7 transcripts using RNA extracts of HeLa pL\_CUL7 or pL\_EV cultured in presence of DOX and transfected as in A. Error bars represent SEMs. Stars represent significant changes vs. siCtrl +DOX based on t-test: \*  $p < 0.05$ ; \*\*  $p < 0.01$ ; \*\*\*  $p < 0.001$ ; \*\*\*\*  $p < 0.0001$ .

Flow cytometric analysis revealed that siCul7-transfected pL\_EV HeLa cells presented a broader G1 peak that could embody a slight accumulation of cells at the G1/S boundary without any sign of cell cycle arrest 72h after depletion (**Fig. 45A**). Importantly, CUL7 overexpression did not ameliorate the cell cycle progression of hCactin-depleted cells. Similarly, CUL7 overexpression in

hCactin siRNA-transfected cells did not prevent accumulation of DNA damage (**Fig. 45B**), abnormal nuclei (**Fig. 45C**) and aberrant metaphases (**Fig. 45D**). Altogether, these data indicate that reduced CUL7 protein levels in hCactin-depleted cells do not contribute to the appearance of the main phenotypes associated with hCactin deficiency.

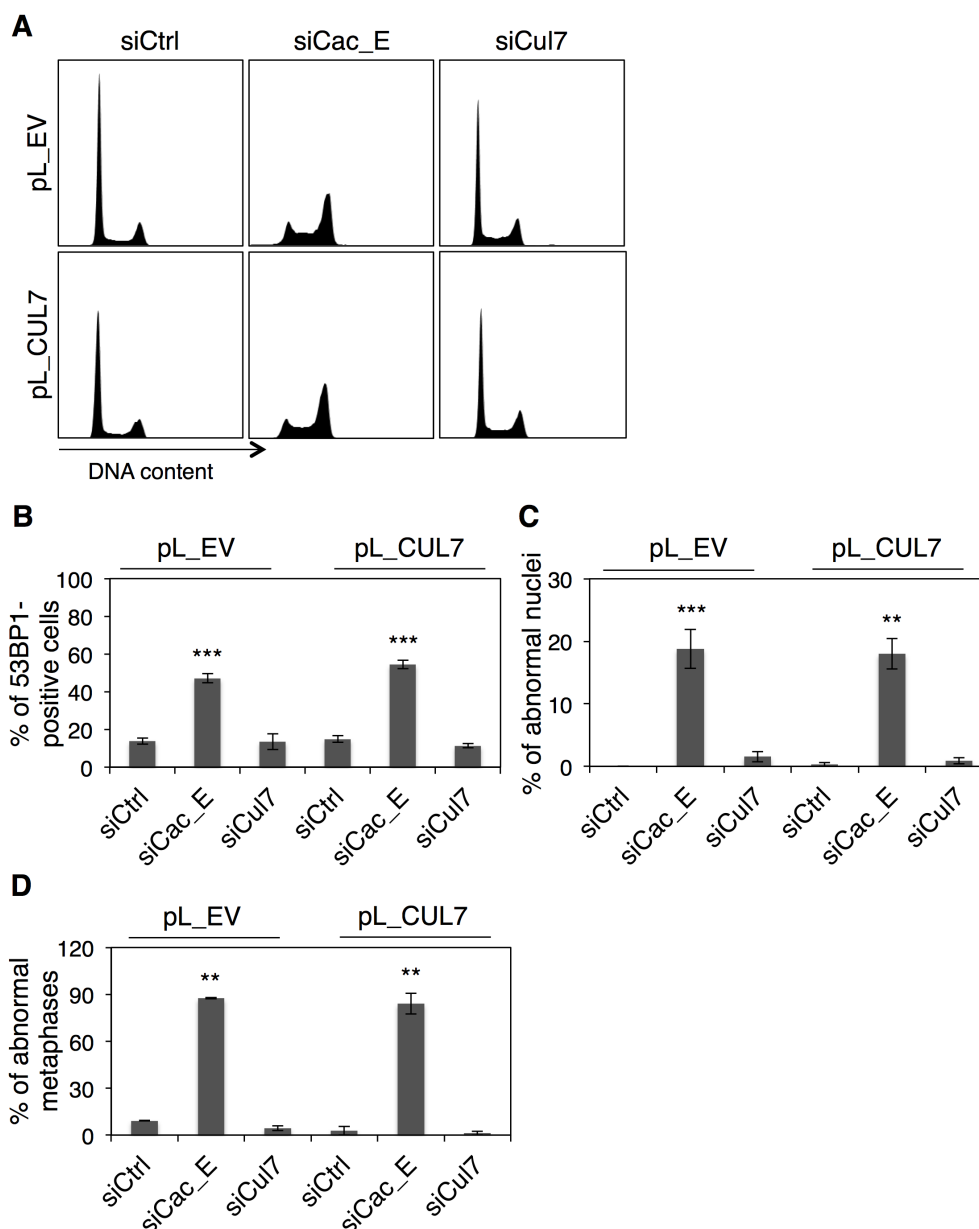


**Figure 45: CUL7 overexpression does not rescue the phenotypes associated to hCactin depletion.**

**A)** Flow cytometric analysis for DNA content of HeLa cells overexpressing a MYC-tagged CUL7 (pL\_CUL7) in a DOX-dependent manner or empty vector control cells (pL\_EV). Cells were grown in presence of DOX, transfected with siCtrl, siCac\_E or siCul7 and processed 72h after depletion. **B)** Quantifications of IF analysis for DNA damage accumulation observed in HeLa pL\_CUL7 and pL\_EV cells cultured and transfected as in A. Cells presenting more than 5 foci of the DNA damage marker 53BP1 were considered as positive. **C)** Quantifications of DAPI stained abnormal nuclei observed in HeLa pL\_CUL7 and pL\_EV cells cultured and



transfected as in A. **D)** Quantifications of aberrant metaphase spreads observed in HeLa pL\_CUL7 and pL\_EV cells cultured and transfected as in A. 72h after transfection cells were treated with Colcemid for metaphase spread analysis. Error bars represent SEMs. Stars represent significant changes vs. siCtrl +DOX based on t-test: \*  $p < 0.05$ ; \*\*  $p < 0.01$ ; \*\*\*  $p < 0.001$ .



## 5 DISCUSSION

### 5.1 Human Cactin is an essential nuclear protein

With exception of the simple eukaryote *Schizosaccharomyces pombe*, Cactins have been shown to be essential proteins in many organisms (Atzei et al., 2010b; Baldwin et al., 2013; Lin et al., 2000; Tannoury et al., 2010; Zhang et al., 2014). On one side the necessity of Cactin in higher eukaryotes to develop and survive highlights the importance of this protein, but on the other side the embryonic lethality associated to Cactin depletion has hindered the capability to investigate its molecular function.

We observed that human Cactin depletion resulted in cell cycle arrest within a few days, which highlights the importance of hCactin-associated function(s) for cell proliferation. Previous analyses in different model organisms have shown that Cactins are nuclear proteins (Baldwin et al., 2013; Lorenzi et al., 2015; Szatanek et al., 2012; Tannoury et al., 2010). Not surprisingly, the Cactin protein sequence contains at least one putative nuclear localization sequence (NLS). Our analyses confirmed that hCactin was prevalently nuclear and showed that a portion of it was chromatin bound.

### 5.2 Human Cactin safeguard genome stability

#### Human Cactin and nuclear morphologies

Human Cactin depletion in cancer cells led to abnormal nuclear morphologies 24h after transfection. This phenotype has been observed and associated with defective nuclear organization (Mattioli et al., 2008). Lamins are crucial components of the inner nuclear membrane, which play a fundamental role in chromatin organization. Laminopathies, like the Hutchinson-Gilford Progeria syndrome, are characterized by mutations that interfere with modifications of the Lamin precursor (Prolamin) leading to non-functional or mislocated Lamins (Camozzi et al., 2014). Among different phenotypes, fibroblasts derived from Progeria patients and LaminA/C-depleted cells are characterized by nuclei with abnormal morphologies (Bridger and Kill, 2004). Our analyses showed that hCactin-depleted cells presented regular amounts of Lamin proteins (Lamin A/C, and LaminB1), and that Lamin A/C was normally

distributed within the nucleus. We consequently excluded a contribution of Lamin proteins to the observed nuclear phenotype upon hCactin depletion.

Abnormal nuclear morphologies have also been associated with mitotic instability and defects in DNA condensation (George et al., 2014). Through flow cytometric analysis we showed that hCactin-depleted cells accumulated in G2/M and were largely positive for phosphorylated H3 (pH3) staining. Moreover, we observed that at least half of the nuclei presenting abnormal morphology were positive for the replication accessory protein PCNA (data not shown). Although PCNA can be retained after DNA synthesis at DNA repair loci or at under-replicated and premature condensed chromosome regions (Ando et al., 2001), our data suggested that abnormal nuclear morphologies are at least partially generated in S phase shortly after hCactin depletion.

Interestingly, we did not observe abnormal nuclei in hCactin-depleted RPE-1 cells. The majority of these cells were dramatically impaired in cell cycle progression shortly after transfection, supporting that the abnormal nuclei observed in hCactin-depleted cells are most likely generated upon active cell division, possibly during the S phase.

### **Human Cactin and DNA damage**

Our analyses revealed that hCactin-depleted cancer cells clearly accumulated DNA damage starting from 48h after depletion, and that 72h after transfection the accumulated DNA damage corresponded at least partially to double strand breaks (DSBs). Accumulation of DNA damage, and in particular of DSBs, in checkpoint-proficient cells usually triggers activation of the DNA damage response (DDR). In general, the sensor MRN complex (MRE11, Rad50, NBS1), localized at sites of DSBs, activates the ATM kinase, which initiates a multitude of phosphorylation events required for cell cycle arrest and DNA repair. Accordingly, cells arrest in G2 principally as a response to phosphorylation of Chk2 (checkpoint kinase 2), and activate proteins involved in DNA repair accumulating at sites of damage. DSBs are not the only DNA lesions that can trigger a cell cycle arrest. In fact, accumulation of single-stranded DNA (ssDNA), which is rapidly coated by RPA (replication protein A), directly activates the ATR kinase leading to a temporary cell cycle arrest primarily through phosphorylation of Chk1 (checkpoint protein 1). ATR also activates a number of other downstream targets dedicated to stabilize and eventually restart replication forks and to promote DNA repair (Ciccia and Elledge, 2010).

Intriguingly, we did not observe a clear activation of the canonical DNA damage checkpoints despite accumulation of DNA damage and DSBs in both U2OS and HeLa cells depleted for hCactin. Although hCactin-depleted cells

were able to activate the DDR in response to CPT treatment shortly after depletion, 72h after siRNA transfection these cells were no longer proliferating and, unable to activate the DDR. From these data we concluded that the accumulation of DNA damage was not the cause of the cell cycle arrest experienced by hCactin-depleted cells.

At the end of G2 non-repaired DNA lesions are transferred to the next G1 phase in the so-called 53BP1 nuclear bodies (Lukas et al., 2011) in order to be repaired by non-homologous end-joining (NHEJ), a fast and error prone mechanism that does not require recombination between homologous chromatids (Ciccia and Elledge, 2010). Eventually, a persistent DDR and irreparable DNA lesions initiate the irreversible p53-mediated cell cycle arrest, which culminates in apoptosis or senescence (Lakin and Jackson, 1999; Purvis et al., 2012). Compared to siCtrl-transfected cells, we noticed that both hCactin-depleted U2OS and HeLa cells presented a reduced amount of cells with 53BP1 nuclear bodies (data not shown), suggesting that the accumulated DNA damage upon hCactin depletion is not transmitted to the next G1. Moreover, our flow cytometric analysis disclosed that hCactin-depleted cells accumulated phosphorylated H2AX ( $\gamma$ H2AX) in late S/G2 phase and before arresting in G2/M. It is still unclear which mechanism prevents hCactin-depleted cells to progress through mitosis. Interestingly, the majority of cells having abnormal nuclear morphology did not accumulate DNA damage, suggesting that these two phenotypes are independent or generated in different phases of the cell cycle.

As already mentioned, hCactin depletion in RPE-1 cells resulted in a clear cell cycle arrest with cells accumulating in G1. Moreover, hCactin-depleted RPE-1 cells did not accumulate any DNA damage and, consequently, did not activate the DDR. It would be interesting to understand which molecular pathway prevents RPE-1 cells from entering a new cell cycle thus avoiding genomic instability.

### **Human Cactin and chromosome structure**

Through metaphase spread analysis we showed that hCactin-depleted cancer cells accumulated abnormal chromosomal structures, in particular prematurely separated sister chromatids and extremely condensed chromosomes. We observed a similar phenotype upon hCactin-depletion by shRNA in the immortalized human embryonic kidney cell line (HEK293T). This result revealed that generation of abnormal chromosomal structures upon hCactin depletion is not a prerogative of cancer cells. Furthermore, preliminary analysis of hCactin-depleted RPE-1 fibroblasts treated with caffeine in order to bypass cell cycle arrest resulted in the appearance of similar chromosomal structures 48h after depletion (data not shown). Since HEK293T cells have

been immortalized with the SV40 T-antigen, they have a weak checkpoint compared to the RPE-1 cells that have been immortalized by expressing the catalytic subunit of telomerase. It is likely that primary cell lines, and in general full checkpoint-proficient immortalized cells, sense cellular perturbation induced by hCactin depletion much earlier than cancer and checkpoint-weakened cell lines. It would be worth identifying which perturbation caused by hCactin depletion triggers this early checkpoint in RPE-1 cells.

### 5.3 Human Cactin promotes cell proliferation

Cancer cells depleted for hCactin started a new round of replication with a low rate of nucleotide incorporation shortly after transfection, when only a mild depletion of hCactin protein was achieved. This phenotype has previously been described and associated with DNA replication stress (Neelsen et al., 2013a; Neelsen et al., 2013b). Yet, cells experiencing DNA replication stress in general accumulate  $\gamma$ H2AX on chromatin, whereas hCactin depleted cells accumulated  $\gamma$ H2AX only 48h after transfection. This result suggests that hCactin depletion affects cancer cell proliferation before the accumulation of evident chromatin-associated defects.

Flow cytometric analysis of synchronized U2OS cells revealed that hCactin depletion impacted cell proliferation shortly after depletion, affecting the G1/S transition of the first cell cycle after transfection. Moreover, hCactin depletion in RPE-1 cells resulted in a strong G1 arrest. Intriguingly, neither a reduced nucleotide incorporation rate nor accumulation of DNA damage was observed in hCactin-depleted RPE-1 cells. In addition, hCactin-depleted quiescent RPE-1 cells released from serum-starvation 48h after transfection were not able to re-enter the cell cycle, whereas hCactin-depleted quiescent RPE-1 cells released from serum-starvation shortly after transfection presented a hindered G1/S transition. Despite phenotypic differences between cancer cells and immortalized fibroblasts, we can conclude that hCactin-depletion primarily impacts on cell proliferation.

Cell proliferation is tightly regulated during the G1 phase of the cell cycle by different pathways that preserve cellular homeostasis (Duronio and Xiong, 2013). Quiescent cells and cells exiting mitosis are kept in an anti-proliferative status principally by the inhibitory activity of the pRB (retinoblastoma) proteins on the E2F transcription factors. Extracellular mitogenic signals activate the canonical MAPK (Ras-Raf-MEK-ERK mitogen-activated protein kinase) pathway to promote transcription of the G1 cyclins (D-type) via AP-1 (activator protein 1) transcription factors (e.g. Jun, c-Fos), driving cells into a new cell cycle (Albanese et al., 1995; Morrison, 2012). Cytokine signalling, mitogen-

induced NF- $\kappa$ B pathway, and Wnt signalling are examples of other pathways known to stimulate D-type cyclins (Kopan, 2012; Nusse, 2012). In proliferating cells there is a peak of CyclinE expression at the G1/S transition, which is controlled by the pRB-E2F pathway, but can also directly respond to growth factors coordinating cell cycle progression with cell differentiation. It has also been shown that G1 cyclins are regulated by the ubiquitin-proteasome system. Of particular importance is the regulation of CyclinE mediated by the SCF complex in response to antiproliferative signals (Clurman et al., 1996). Post-transcriptional regulation of cyclin-dependent kinases (CDKs) and transcriptional regulation of CDK inhibitors (CKIs) are also important mechanisms used by cells to prevent re-entry into the cell cycle. For instance, p21 and INK4 are well known CKIs that respond to a variety of stresses blocking cell cycle progression and preventing genome instability (Donjerkovic and Scott, 2000).

Our analysis revealed that CyclinD1 protein levels were similar in siCtrl and hCactin siRNA-treated cancer cells (see below). However, the complex network of pathways involved in proliferation control suggests that a multitude of factors need to be produced and activated via different mechanisms. Intriguingly, hCactin-depleted cancer cells presented elevated levels of c-Fos (see below) and c-Myc transcripts (data not shown), suggesting a cellular attempt to promote cell proliferation.

Functional inactivation of Cactin in *Toxoplasma gondii* (TgCactin) causes irreversible G1 arrest within the fast proliferating infectious stage (Szatanek et al., 2012). Interestingly, gene expression analysis has revealed the expression of several genes typically associated with slow proliferating or extracellular stages, suggesting that TgCactin is involved in transcriptional control. Moreover, it has been shown that hCactin interacts with TRIM39, and that this interaction stabilizes hCactin protein levels (Suzuki et al., 2015). TRIM39 is known to play a role in the regulation of the immune response (Kurata et al., 2013), but it also contributes to cell cycle progression and to the DNA damage response through the stabilization of p21 (Zhang et al., 2012b). It is possible that hCactin-depletion deregulates the transcriptional pattern required for G1/S transition. A more detailed investigation of the G1/S transition upon hCactin-depletion would help in clarifying the role of hCactin in cell proliferation.

## 5.4 Human Cactin supports pre-mRNA splicing

### Human Cactin and pre-mRNA splicing

It is worth mentioning that the way we prepared the library for deep sequencing was not ideal to specifically look at pre-mRNAs as total RNA was used. Thus, one could repeat the same experiment using more appropriate protocols for example by using only nuclear RNA as a starting material. Nevertheless, bioinformatic analysis of our next generation sequencing data showed mild accumulation of reads mapping to intronic sequences and a slight decrease of reads mapping to exons in hCactin-depleted U2OS cells, suggestive of a mild and general splicing defect. Moreover, previous independent reports have highlighted the involvement of hCactin in pre-mRNA splicing: hCactin has been co-purified with the catalytically active spliceosome (Jurica et al., 2002; Rappsilber et al., 2002; Zhou et al., 2002); MS analysis disclosed that hCactin interacts with the spliceosome-associated factor RNPS1 (Ewing et al., 2007); Cactin co-localizes with evolutionary conserved splicing factors in *Arabidopsis* (Baldwin et al., 2013); Cactin in fission yeast (Cay1) supports Rap1 pre-mRNA splicing (Lorenzi et al., 2015). Altogether these data suggest that Cactins play a direct role in pre-mRNA splicing.

### Pre-mRNA splicing and genomic stability

Recent discoveries have shown that in higher eukaryotes pre-mRNA splicing occurs predominantly cotranscriptionally, and that core and accessory splicing factors are co-ordinately enriched at the transcription sites on chromatin (Merkhofer et al., 2014). Thus, the observation that a portion of hCactin was chromatin bound is in accordance with the idea that hCactin works as an accessory splicing factor (discussed below).

Cells depleted for spliceosome factors are characterized by interphase lobed nuclei and nuclear fragmentation (Sundaramoorthy et al., 2014). Our analysis of hCactin-depleted HeLa cells revealed that a considerable number of interphase nuclei were morphologically abnormal and underwent fragmentation. Thus, the accumulation of altered nuclear morphology in hCactin-depleted cells may be a consequence of perturbed pre-mRNA splicing; this in turn might affect cell cycle progression. Depletion of spliceosome factors also leads to prolonged mitosis, which is partially due to premature sister chromatid separation and consequently impaired chromosome segregation (Oka et al., 2014; Sundaramoorthy et al., 2014; van der Lelij et al., 2014; Watrin et al., 2014). Depletion of hCactin led to similar accumulation of metaphases with abnormal chromosomal structure, reminiscent of what was observed upon depletion of spliceosome factors.



Notably, depletion of the pre-mRNA splicing factor CDC5L (cell division cycle 5-like) leads to impaired kinetochore-microtubule attachment and accumulation of DNA damage, which in turn activates the spindle assembly checkpoint or results in mitotic catastrophe (Mu et al., 2014). Mitotic catastrophe is a cell death event usually characterized by spontaneous premature condensation, abnormal mitosis, and nuclear fragmentation (Castedo et al., 2004). Because we did not directly test the activation of the spindle assembly checkpoint in hCactin-depleted cells, we cannot exclude that hCactin depletion hinders the kinetochore-microtubule attachment resulting in mitotic catastrophe.

We have shown that hCactin-depleted cells experienced a reduced replication rate and accumulated DNA damage. The splicing factor Clf1s is known to associate with origins of replication and to play a role in DNA replication in budding yeast (Zhu et al., 2002), whereas the human DNA replication licensing factor MCM7 is thought to be essential for pre-mRNA splicing (Chen et al., 2015). Moreover, DNA replication stress can promote alternative pre-mRNA splicing (Ratray et al., 2013), suggesting interplay between DNA replication and pre-mRNA splicing factors. Depletion of spliceosome factors has been previously associated with increased genome instability and accumulation of DNA damage (Li and Manley, 2005), and the evidence that pre-mRNA splicing process occurs cotranscriptionally highlights a direct link between pre-mRNA splicing and genome stability. In fact, defects in RNA processing have been proposed to promote RNA:DNA hybrids formation and to stabilize R-loops, influencing the transcription pattern and creating replication barriers (Chan et al., 2014).

Depletion of hCactin perturbs cell proliferation in both cancer cells and immortalized fibroblasts. It has been shown that up-regulation of the splicing factor SRSF1 in breast cancers influences alternative splicing of target genes involved in apoptosis and cell proliferation (Anczukow et al., 2012). Consequently, anti-apoptotic isoforms that are unable to properly interact with the pro-apoptotic factors and isoforms that promote cell proliferation are generated, sustaining cancer cell transformation. It is easy to imagine a scenario where compromised pre-mRNA splicing, as a consequence of hCactin depletion, leads to limited production of important factors and prerequisite isoforms required for cell proliferation and survival.

In conclusion, impaired pre-mRNA splicing can lead to an accumulation of DNA damage, compromised metaphase spindle assembly, premature sister chromatid cohesion, and prolonged mitotic arrest. Taking the phenotypes observed upon hCactin depletion into consideration, it is likely that hCactin associates with the spliceosome and contributes to its function. However, the core components of the spliceosome are highly conserved in eukaryotes, whereas Cactin ortholog in budding yeast is missing. This brings us to the

conclusion that hCactin is a putative accessory splicing factor. Yet, the exact molecular function exerted by hCactin remains elusive.

### **Human Cactin is essential for Sororin pre-mRNA splicing and sister chromatid cohesion**

As mentioned, recent publications have emphasised the requirement of pre-mRNA splicing factors for sister chromatid cohesion. Sundaramoorthy and colleagues reported that depletion of splicing factors disrupts sister chromatid cohesion in interphase (Sundaramoorthy et al., 2014). They also showed that splicing factors are dispensable for cohesin loading onto chromatin, but essential for stable association of cohesin with chromatin in G2. In G2 binding of the cohesin complex to chromatin strongly depends on the regulatory protein Sororin, which counteracts Wap1's cohesin releasing activity (Nishiyama et al., 2010).

HeLa cells depleted for hCactin clearly presented a Sororin splicing defect, particularly evident as retention of intron 1. Previous works made a similar observation upon depletions of either core or accessory splicing factors (Oka et al., 2014; Sundaramoorthy et al., 2014; van der Lelij et al., 2014; Watrin et al., 2014). Yet, our analyses showed that depletion of the splicing factor SF3A-3 induced accumulation of complete Sororin pre-mRNA species accompanied with clearly reduced Sororin mRNA levels. This discrepancy remains to be further investigated.

It has been proposed that retention of Sororin intron 1 causes a translational frame shift, generating a full length Sororin mRNA that contains a premature stop codon in exon 3 or intron 2 if retained. This mRNA may be exported and translated producing a truncated and non-functional Sororin protein (Sundaramoorthy et al., 2014). Interestingly, cohesin-core components and other cohesin-associated factors do not present increased intron retention upon depletion of splicing factors (Ando et al., 2001; Sundaramoorthy et al., 2014; van der Lelij et al., 2014), suggesting that the compromised splicing process selectively affects Sororin pre-mRNA splicing. Differently from other cohesin-associated proteins, Sororin is phosphorylated and degraded through APC/C-mediated proteasomal degradation at the end of the cell cycle, allowing cohesin complex release and sister chromatid separation (Rankin et al., 2005). Therefore, every cell cycle, newly synthesised Sororin needs to associate with the acetylated Smc3 cohesin subunit during progression of the S phase ensuring sister chromatid cohesion until the end of the cell cycle (Zhang et al., 2008). This could explain why Sororin pre-mRNA is particularly affected by pre-mRNA splicing defects compared to other cohesin factors.

Sororin overexpression almost completely rescued the abnormal chromosomal morphology of hCactin-depleted metaphases. However, Sororin

overexpression was not sufficient to prevent accumulation of DNA damage and to completely restore normal cell cycle progression hCactin-depleted cells. Similarly, it has been reported that Sororin overexpression does not restore mitotic progression in cells depleted for spliceosome factors (Sundaramoorthy et al., 2014; van der Lelij et al., 2014; Watrin et al., 2014). Moreover, upon depletion of the spliceosome factor SNW1, splicing of both Sororin and APC2 (APC/C subunit) pre-mRNAs is compromised, and overexpression of both Sororin and APC2 is necessary in order to restore cohesion defects in SNW1-depleted cells (van der Lelij et al., 2014). Van der Lelij and colleagues have proposed that the mitotic arrest experienced by SNW1-depleted cells is partially due to reduced APC/C activity as a consequence of limited amounts of APC2.

A prolonged mitotic arrest has been shown to result in mitotic slippage and consequently cell death, either in mitosis or during the next cell cycle (Rieder and Maiato, 2004). In this light, mitotic catastrophe can be considered as a mechanism induced in mitotic-incompetent cells to avoid genomic instability, ultimately resulting in apoptosis, necrosis or senescence (Vitale et al., 2011). A prolonged mitotic arrest has also been proposed to be the cause of "cohesion fatigue", which is defined as being a gradual reduction of cohesion as a consequence of cohesin complex disruption through physical tension generated by the mitotic spindle (Daum et al., 2011). In the case of cohesion fatigue, chromatid separation reactivates the spindle checkpoint, which further delays mitotic progression until mitotic slippage or apoptosis occurs (Gorbsky, 2013). Taking in consideration that cohesion is essential for proper G2/M checkpoint activation (Watrin and Peters, 2009), cohesin loss may explain why hCactin-depleted cells were strongly arrested in G2/M but were unable to activate the DNA damage checkpoint.

## 5.5 Human Cactin and its interactome

### MS analysis identified novel hCactin interactors

Cactin was originally discovered in *D. melanogaster* as a physical interactor of the I $\kappa$ B protein Cactus, which is involved in the establishment of the dorso-ventral polarity of the embryo, in muscle development, and in humoral immunity (Lin et al., 2000). Ten years later, the conservation of interaction between hCactin and the cytoplasmic I $\kappa$ B proteins in human cells has been disproved (Atzei et al., 2010a). However, hCactin physically interacts and co-localises with the nuclear I $\kappa$ B-like (I $\kappa$ BL) protein, encoded within the major histocompatibility complex (MHC) region of chromosome 6. Large-scale yeast

two-hybrid analysis disclosed the interaction between hCactin and two other proteins encoded within the MHC: the nuclear elongation factor NELF-E and the uncharacterized protein LST1/f (Lehner et al., 2004). To add to the complexity of Cactin interactome, hCactin has been co-purified with the spliceosome complex C (Jurica et al., 2002) and with the accessory splicing factor RNPS1 (Ewing et al., 2007). More recently, *A. thaliana* Cactin has been shown to co-localise with the ortholog of RNPS1 SR45 (Baldwin et al., 2013). Finally, hCactin was also reported to physically interact with TRIM39, which is involved in inflammatory signalling pathways and encoded within the MHC (Suzuki et al., 2015).

Our MS analysis identified several novel putative hCactin interactors. Among them only a few were reported to be involved in pre-mRNA splicing. RNPS1 was detected with poor queries match and, unfortunately, NFKBIL, NELF-E, LST-1, and TRIM39 were not identified. This discrepancy may have arisen partly because the overexpressed Strep-HA-tagged Cactin lacked regulatory 5' and 3'UTR sequences that may lead to false-positive interaction or could favour some interactions over others. Also, we used a standard protein extraction protocol followed by in-column purification generally used for MS analysis that may not be efficient in extracting the chromatin-bound portion of hCactin. Thus, limitations in our procedure might have influenced the readout. Nevertheless, our analysis proved useful to identify novel factors (i.e. DHX8, SRRM2 and members of the 3-M complex), whose interaction with hCactin appears to be physiologically relevant.

### **Human Cactin, the ATPase/RNA helicase DHX8 and the SR protein SRRM2**

Depletion of either hCactin or DHX8 leads to impaired Sororin pre-mRNA splicing, aberrant metaphases, accumulation of DNA damage, and cell cycle arrest. Because simultaneous depletion of hCactin and DHX8 did not exacerbate these phenotypes, we conclude that hCactin and DHX8 promote efficient Sororin pre-mRNA splicing, genome stability and cell cycle progression in an epistatic relationship.

Although depletion of the RNA binding protein SRRM2 also disturbed Sororin pre-mRNA splicing, SRRM2-depleted cells presented a less severe phenotype compared to hCactin-depleted cells. Co-depletion of hCactin and SRRM2 showed an additive effect on Sororin pre-mRNA splicing and associated phenotypes, suggesting that hCactin and SRRM2 function independently in promoting pre-mRNA splicing. Although mRNA levels of SRRM2 and protein levels of hCactin were considerably reduced in single and co-depletion experiments, the use of siRNAs to deplete proteins is limiting for testing genetic interactions. In fact, we cannot exclude that combining

incomplete depletions of hCactin and SRRM2 results in a stronger effect on a common pathway promoting Sororin pre-mRNA splicing; this second hypothesis is further supported by the direct interaction between hCactin and SRRM2. Also we cannot disregard the possibility that hCactin interacts with DHX8 and SRRM2 in two independent complexes associated to the spliceosome, thereby interfering with Sororin pre-mRNA splicing at different steps of the splicing process. DHX8 and SRRM2 co-depletion experiments would help in testing these possibilities.

Amongst the phenotypes tested, accumulation of nuclei with abnormal morphology appeared to be comparable in hCactin, DHX8, and SRRM2 single depletions. While co-depletion of hCactin and DHX8 exacerbated the number of abnormal nuclei, co-depletion of hCactin and SRRM2 did not show additive effect. This suggests that abnormal nuclear morphology is not linked to the other observed phenotypes (defects in Sororin pre-mRNA splicing, DNA integrity, premature sister chromatid separation and cell cycle proliferation). Perturbation of a so far unclear pathway, in which hCactin and SRRM2 function in an epistatic relationship, could be the cause leading to abnormally shaped nuclei. However, it is also possible that abnormality in nuclear morphology is a general feature of impaired pre-mRNA splicing. In this case altered transcriptional control and chromatin organization or even mitotic catastrophe could lead to nuclear shape abnormality, independently from the exact step of splicing process that may be compromised. Again, DHX8 and SRRM2 co-depletion experiments would help clarify this point.

A large number of molecular events and splicing factors and co-factors need to be precisely coordinated in order to generate a functional, properly spliced mRNA (Will and Luhrmann, 2011). In brief, the splicing process occurs in two distinct and consecutive steps: during the first step the 5' end of the intron is cleaved and a lariat structure is formed; during the second step the 3' end of the intron is cleaved and the exons are ligated. At the end of the second step the spliced RNA is released, the lariat is discarded and degraded, and the spliceosome components are recycled for a new splicing cycle. The ATP-dependent RNA helicase DHX8 is essential to allow efficient release of the spliced mRNA from the spliceosome (Company et al., 1991; Ohno and Shimura, 1996). The budding yeast ortholog of DHX8 scPrp22 has been shown to sustain the second step of splicing, facilitating the 3' splice site (3'ss) selection by promoting structural rearrangements within the catalytic core of the spliceosome (Schwer, 2008). scPrp22 also guarantees the fidelity of exon ligation by promoting removal of atypical splicing intermediates (e.g. intron containing intermediates ) (Mayas et al., 2006; Wlodaver and Staley, 2014). The RNA binding protein SRRM2 is part of a splicing co-activator subunit that co-localizes on the spliced mRNAs with the exon junction complex (EJC) (Blencowe et al., 2000; Wagner et al., 2004), which is known

to coordinate several pathways involved in RNA localization, translation and surveillance (Le Hir and Seraphin, 2008). Although depletion of SRRM2 in human cells does not compromise splicing (Blencowe et al., 2000), the budding yeast SRRM2 ortholog scCwc21 has been shown to function within the catalytic core of the spliceosome (Grainger and Beggs, 2005), promoting the 3' ss selection during the second step of splicing (Gautam et al., 2015). Interestingly, the binding partner of SRRM2, SRRM1, is known to associate with the mitotic cohesin complex, although SRRM1 depletion did not disclose any defects in sister chromatid cohesion (McCracken et al., 2005). Although our MS analysis did not find SRRM1 as putative hCactin interactors, it would be interesting to see if hCactin-depletion interferes with the interaction between SRRM2 and SRRM1.

In summary, using Sororin pre-mRNA splicing as a readout we identified two hCactin interactors that likely function with hCactin within the spliceosome. Both DHX8 and SRRM2 contribute to the second step of the splicing process, primarily promoting the 3' ss selection. Additionally, both factors are involved in mRNA release from the spliceosome, putatively impacting on its fate. Although it is still unclear how hCactin functions within the spliceosome, published results and our data strongly suggest that hCactin also promotes the second step of splicing. Furthermore, preliminary observation revealed that hCactin chromatin association was RNase sensitive (data not shown), suggesting that hCactin interacts with chromatin through directly or indirectly binding to RNA. We speculate that hCactin works as a platform for protein-protein and protein-RNA binding interactions during the splicing process.

### **Cooperation between hCactin and the 3-M complex may foster alternative pre-mRNA splicing**

Consistent with the hypothesis that hCactin participates in independent biological pathways, we have found that it physically interacts with the scaffold protein CUL7 and that CUL7 is not required for Sororin pre-mRNA splicing. We have excluded that CUL7 promotes hCactin degradation through CUL7-dependent ubiquitination, although we observed possible monoubiquitinated hCactin species dependent on CUL7. While polyubiquitination is known to mediate proteasomal degradation, monoubiquitination has been shown to dictate protein localization or function, and to regulate protein-protein interactions (Schnell and Hicke, 2003). Preliminary analysis revealed that hCactin re-localises to the nucleoli upon CUL7 depletion (data not shown). This suggests that indeed CUL7 might impose modifications on hCactin proteins in order to regulate its nuclear localization.

While hCactin protein levels are not affected by CUL7 depletion, CUL7 protein levels were substantially reduced upon hCactin depletion. Protein stability and

qRT-PCR analysis revealed only very mild defects in CUL7 protein degradation and CUL7 pre-mRNA splicing when Cactin was depleted, and it seems unlikely that those defects can explain the dramatic drop in total CUL7 protein levels. It is therefore possible that hCactin regulates CUL7 levels through other mechanisms, for example by supporting CUL7 mRNA translation. A study from Jun Yan and colleagues has shown that depletion of OBSL1, a factor comprised within the 3-M complex together with CUL7 and CCDC8, reduces both CUL7 mRNA and protein levels (Yan et al., 2014). Thus, hCactin could also stabilize CUL7 through mechanisms shared with OBSL1.

CUL7 depletion did not induce any particular phenotype reminiscent of what observed upon hCactin depletion. However, during the first cell cycle shortly after transfection, both hCactin- and CUL7-depleted cells presented a delayed G1/S transition. Although the CUL7 substrate receptor Fbxw8 is implicated in the degradation of CyclinD and in G1/S transition in cancer cells (Okabe et al., 2006), we excluded that the observed G1/S slow down was a consequence of defective CyclinD protein regulation.

Another reported substrate of CUL7 is the insulin receptor substrate 1 (IRS1) (Xu et al., 2008), which is known to be an important mediator of the insulin/insulin-like growth factor 1 (IGF1) signalling pathway (Dearth et al., 2007). *Cul7*<sup>-/-</sup> mouse embryonic fibroblasts (MEFs) accumulate IRS-1 and activate its downstream pathways Akt and MEK/ERK (Scheufele et al., 2014). However, these MEFs grow very slowly, showing phenotypes previously associated with oncogene-induced senescence. Upon hCactin or CUL7 depletion our analyses did not detect any accumulation of IRS1 protein, but disclosed a similar accumulation of c-Fos transcript, a known target of MAPK signalling induced by IRS1 stabilization (Hartmann et al., 2014). However, CUL7 overexpression failed to rescue the accumulation of c-Fos transcripts upon hCactin depletion (data not shown). Considering that we also observed accumulation of c-Myc, a known antagonist of the p53-dependent apoptotic pathway (Kim et al., 2007), upon hCactin depletion (data not shown), it remains intriguing that cells completely arrested in G2/M activate a signalling pathway associated to cell proliferation.

Upon induction of DNA damage expression levels of CUL7 are known to increase and CUL7 associates to p53 limiting its pro-apoptotic function in a non-proteolytic manner (Jung et al., 2007). Our MS analysis also disclosed p53 as a putative hCactin interactor; we hypothesised that the interaction between hCactin and CUL7 may impact on p53 function.

CUL7 overexpression did not ameliorate any of the defects associated with hCactin depletion (e.g. accumulation of DNA damage, aberrant chromosomal structure and impaired cell cycle proliferation). Thus we exclude a major

contribution of reduced CUL7 protein levels to the phenotypes associated to hCactin depletion.

CRL7 has been shown to play an important role in preventing microtubule and genome instability within the 3-M complex (Yan et al., 2014). Li and colleagues have shown that the 3-M complex binds the large Cullin protein CUL9 via CUL7, thus preventing the CUL9-mediated proteolytic function towards Survivin (Li et al., 2014). Survivin is a known inhibitor of apoptosis (IAP) that is also part of the chromosomal passenger complex (CPC) (Watanabe, 2010) and promotes microtubule dynamics in a CPC-independent but 3-M complex-dependent manner (Rosa et al., 2006). Survivin has been shown to recruit the CPC to mitotic chromosomes controlling several mitotic steps contributing to the spindle checkpoint and preventing mitotic catastrophe (Lens et al., 2003). Thus, it would be interesting to check the status of Survivin in hCactin-depleted cells.

Taking in consideration that hCactin and CUL7 physically interact and that the other members of the 3-M complex were also identified by our MS analysis as putative hCactin interactors, it is possible that hCactin is either part of the 3-M complex or is important for its function. Recently it has been proposed that the 3-M complex is involved in alternative pre-mRNA splicing (Hanson et al., 2012). Hanson and colleagues showed that overexpression of the 3-M complex results in the exclusion of exon 11 of an exogenous insulin receptor (INSR) minigene, while downregulation of the 3-M complex promotes the inclusion of this exon. Although the causality between this observation and the 3-M syndrome still need to be proved, 3-M patient fibroblasts also presented a significant inclusion of the exon 11 of the INSR minigene (Hanson et al., 2012). Thus, it is possible that hCactin interacts with the 3-M complex in order to promote its putative function in alternative splicing regulation.

## **5.6 Conservation of function between Cactin in fission yeast (Cay1) and hCactin**

### **Human Cactin depletion does not impact on telomere homeostasis**

Work from our lab showed that the hCactin ortholog in *Schizosaccharomyces pombe* Cay1 limits telomere length and telomeric transcription by affecting levels of the telomeric protein Rap1 (Lorenzi et al., 2015). Despite other phenotypes, the *cay1*-deleted (*cay1* $\Delta$ ) *S. pombe* strain is characterized by two evident telomeric defects: elongated telomeres and elevated telomeric transcription, which is a consequence of relaxed heterochromatin. These telomeric defects are the outcome of reduced amounts of Rap1 protein,



predominantly occurring as a result of Rap1 pre-mRNA splicing defects. A slight decrease in Rap1 protein stability has also been determined in the *cay1Δ* strain (Lorenzi et al., 2015).

Our analysis did not reveal changes in the amounts of the telomeric shelterin protein complex in hCactin-depleted cells. The fact that depletion of hCactin did not affect Rap1 protein levels excludes a straight conservation of function between Cay1 and hCactin and may also be related to functional changes associated with Rap1 protein during evolution (Kabir et al., 2010). Budding yeast Rap1 (scRap1) has been identified as a DNA binding protein that is associated with both activator and silencer elements at different loci of the genome (e.g. ribosomal genes, mating type silencer elements, telomeres) (Kanoh and Ishikawa, 2003; Shore and Nasmyth, 1987). It contains protein domains that serve for DNA binding, protein-protein interaction, and transcriptional control. Fission yeast Rap1 (spRap1) already differs from scRap1 in regards to some protein motifs and sequence conservation. Intriguingly, spRap1 principally binds to telomeres via interaction with another shelterin component called Taz1 (Kanoh and Ishikawa, 2001). Human Rap1 (hRap1) has been initially identified as an interactor of the shelterin protein TRF2 (the ortholog of spTaz1). Like spRap1, hRap1 associates with telomeres via its interaction with TRF2 (Li et al., 2000). While ablation of scRap1 and spRap1 leads to elongated telomeres, a similar phenotype is not observed in human or mouse cells deficient for hRap1.

Our analyses did not disclose any change in telomere length or perturbations of telomere transcription upon hCactin depletion, indicating that hCactin does not directly contribute to maintenance of telomere homeostasis. However, it has to be taken in account that hCactin depleted cancer and HEK293T cells died within 3-4 days of hCactin depletion and this interval may not be long enough to generate detectable changes at telomeres. Similarly, hCactin-depleted RPE-1 cells arrested shortly after siRNA transfection possibly preventing the appearance of signatures of genomic/telomeric instability.

Furthermore, accumulation of DNA damage at telomeres in primary fibroblasts has been shown to be irreparable and to drive cells into premature senescence, suggesting that telomeres serve as a sensor for exogenous and endogenous DNA damaging agents contributing to safeguard genome stability (Fumagalli et al., 2012; Rossiello et al., 2014). It has also been reported that prolonged mitotic arrest in primary and cancer cells induces dissociation of TRF2 from telomeres, leading to telomeric DNA damage accumulation and DNA damage checkpoint activation (Hayashi et al., 2012). However, we find that hCactin-depleted cells do not specifically accumulate DNA damage foci at telomeres compared to siCtrl-treated cells, excluding that damaged telomeres contribute to the cell cycle arrest provoked by hCactin depletion.

In summary, we can conclude that, differently from fission yeast Cay1, hCactin does not affect Rap1 levels and telomere homeostasis, and that the pleiotropic phenotypes associated to hCactin depletion do not derive from compromised telomere integrity.

### **A basic conservation of function between Cay1 and hCactin has likely been preserved**

It clearly emerges that Cactin is required for efficient splicing of different pre-mRNAs in different organism. We have shown that hCactin is required for general pre-mRNA splicing and that Sororin pre-mRNA is particularly affected by hCactin depletion. Although analyses performed in the *cay1Δ S. pombe* strain did not disclose a general splicing defect, they suggested that, different telomeric factors suffered pre-mRNA splicing defects in *cay1Δ* cells (Lorenzi et al., 2015). While in fission yeast Cay1 is specifically necessary for Rap1 splicing, in humans it seems that assembling a proper telomere cap does not depend on hCactin-mediated pre-mRNA splicing. Yet, there might be conserved clusters of pre-mRNAs that require Cactin for efficient splicing.

Notably, cohesin proteins are conserved from yeast to humans. In both organisms the loading and unloading of cohesin complexes onto and from DNA through the cell cycle is similar. During S phase a portion of cohesin becomes stably bound by Eso1/Eso2-dependent acetylation of the cohesin subunit Pms3/Smc3, whereas at the end of the cell cycle Wpl1/Wap1 stimulates the removal of cohesin (Zhang et al., 2008). In human cells Smc3 acetylation is a requisite for replication fork progression and Sororin association to the cohesin complex (Song et al., 2012), whereas in fission yeast Pms3 acetylation is dispensable but contributes to the essential Eso1 activity that counteracts Wpl1 (Feytout et al., 2011). Sororin is conserved in vertebrates, but clear homologues in lower eukaryotes have not been found. However, it has been proposed that Eco1 is the yeast ortholog of Sororin (Zhang and Pati, 2012). Like in human cells, fission yeast cohesin complexes stably bound to chromosomes are not uniformly distributed. A major part co-localizes with the heterochromatin protein Swi6, the ortholog of human HP1 (Nonaka et al., 2002). Differently from humans, the fission yeast genome contains few and well-defined heterochromatic regions. Among them are telomeres that have been shown to be important for meiotic division (Klutstein et al., 2015). Thus, function in controlling cohesin components or regulation of sister chromatid cohesion may be conserved from Cay1 to hCactin.

Our data showed that hCactin and the RNA helicase DHX8 function in the same pathway to promote Sororin pre-mRNA splicing, and probably the splicing of other genes. Between DHX8 and its ortholog in fission yeast spPrp22 there is a conservation of function, and the fidelity control

mechanism exerted by spPrp22 is involved in transcriptional control of the telomerase (Kannan et al., 2013). Interestingly, DHX8 is indirectly involved in the selective regulation of p21 mRNA splicing and expression under stress conditions, suggesting a contribution of DHX8 in both pre-mRNA splicing and transcriptional control (Chen et al., 2011). Although our yeast two-hybrid screen did not reveal any physical interaction between Cay1 and spPrp22, it would be worth analysing whether Cay1 and spPrp22 genetically interact.

Our lab has shown that *cay1* $\Delta$  cells have a reduced proliferation rate compared to wild-type (wt) cells, resulting in a slight increase of cell length, suggestive of a G2/M checkpoint activation (Lorenzi et al., 2015). This phenotype was exacerbated when *cay1* $\Delta$  cells were grown in the cold, with the appearance of clearly elongated cells and chromosomal bridges between dividing nuclei. Similarly, hCactin-depleted cells experienced a cell cycle arrest independently of Sororin and sister-chromatid cohesion. This likeness in phenotype is suggestive of a conservation of function between Cay1 and Cactin in controlling chromosome integrity.

Our MS analysis identified several putative hCactin interactors. Many of these interactors, like CUL7, are proteins only conserved in higher eukaryotes, highlighting the fact that hCactin may have acquired additional functions during evolution that are not exerted by Cay1.

Interestingly, it has been shown that hRap1 also exerts a non-telomeric function, binding to several Rap1-binding sites dispersed throughout the genome (Martinez et al., 2013; Martinez et al., 2010). hRap1 depletion leads to significant upregulation of a distinct set of genes, suggesting that hRap1 is a transcriptional regulator. Furthermore, cytoplasmic hRap1 binds to the I $\kappa$ B kinase (IKKs), contributing to the activation of the NF $\kappa$ B signalling pathway (Teo et al., 2010). Although a direct interaction between hCactin and the I $\kappa$ B has been disproved (Atzei et al., 2010a), recent work has shown that hCactin is involved in a negative feedback loop response of the NF $\kappa$ B signalling pathway (Suzuki et al., 2015). Hence, during evolution of the immune system in higher eukaryotes, orthologs of the genetically interacting spRap1 and Cay1 may have evolved autonomous and extra-telomeric functions within the NF $\kappa$ B signalling pathway. Moreover, Cay1 interacts with histone deacetylases (HDACs) that are well known to participate in transcriptional control (Lorenzi et al., 2015). Thus, despite molecular differences, functions in controlling transcription are most likely also conserved.

## 5.7 Human Cactin and the immune response

Human Cactin has been initially characterized as a negative regulator of the Toll-like receptors (TLRs), the primary sensors of the innate immune system (Atzei et al., 2010a). hCactin has been shown to repress TLR-responsive genes, thus inhibiting the NF- $\kappa$ B and interferon (INF) regulatory signalling pathways. Moreover, Atzei and colleagues have shown that hCactin physically interacts and co-localises with the I $\kappa$ B-like (I $\kappa$ BL) protein. This interaction is thought to be critical for the inhibitory function of hCactin on the innate immune response, although the exact molecular mechanism exerted by hCactin in this context is not clear.

Recent work in the white shrimp *L. vannamei* has also made an attempt to characterize the role of Cactin in the immune response (Zhang et al., 2014). However, upon Cactin depletion a high mortality rate was observed and results regarding induction of immune-related genes are poorly indicative.

TRIM39, a tripartite motif-containing protein with E3 ligase activity, stabilises hCactin through physical interaction (Suzuki et al., 2015). TRIM39 is known to participate in the inflammatory signalling pathway and in the regulation of INF-1 response (Kurata et al., 2010). Suzuki and colleagues proposed that the TRIM39-mediated stabilization of hCactin is part of a positive feedback-loop where hCactin is induced by the NF- $\kappa$ B after TNF- $\alpha$  stimulation (Tumour necrosis factor  $\alpha$ ) and negatively regulates the NF- $\kappa$ B signalling pathway (Suzuki et al., 2015).

To contextualise our finding within the entire information on the connections between Cactins from different organisms and the immune response, it is likely that hCactin functions as a transcription regulator. Indeed, the immune response is often regulated through transcriptional feedback loops and hCactin has also been shown to interact with several factors encoded within the MHC on chromosome 6.

Embryonic development is also primarily controlled by transcriptional patterns that change during time. In model organisms like *C. elegans*, *Drosophila melanogaster*, and Zebrafish Cactin depletion has been shown to primarily compromise pathways involved in cell proliferation and differentiation shortly leading to embryonic lethality (Atzei et al., 2010b; Lin et al., 2000; Tannoury et al., 2010). Thus, these observations corroborate the idea that Cactin proteins promote transcription regulation.

In eukaryotes alternative splicing confers plasticity to the components involved in the immune response. The use of alternative splicing by T- and B-cells has emerged as a powerful mechanism to generate new protein isoforms to promptly respond to environmental changes (Ergun et al., 2013). Moreover, connections between aberrant splicing and susceptibility to cancer or degenerative diseases have been recently made (Hahn and Scott, 2012;

Wojtuszkiewicz et al., 2015). For example in the substantia nigra of patients with Parkinson's disease high rate of alternative splicing events have been correlated with the upregulation of the hCactin interactor SRRM2 (Shehadeh et al., 2010).

Viruses produce high amounts of proteins by alternative splicing of few initial transcripts. Upon infection viruses are known to modulate the host splicing machinery in order to promote viral RNA splicing and inhibit the cellular immune defence (Walsh and Mohr, 2011).

The hCactin interactor DHX8 has been shown to be one of the cellular proteins required for replication of the human immunodeficiency virus type 1 (HIV-1) upon infection (Dziuba et al., 2012), whereas SRRM2 has been identified as one of the cellular proteins involved in pre-mRNA splicing that were differentially phosphorylated upon HIV-1 entry in order to modulate host alternative splicing and facilitate virus replication and release (Wojcechowskyj et al., 2013). Moreover, CCDC8 has been found to inhibit HIV-1 assembly and promote degradation of its major structure protein Gag through CRL7-mediated polyubiquitination (Wei et al., 2015).

Thus, hCactin and its interactome are embedded in the complexity of the transcriptional regulation that also modulates immune response plasticity, highlighting the central role of pre-mRNA splicing in gene expression.

## 5.8 Conclusion

We have shown that hCactin is an essential nuclear protein necessary for maintaining genome stability and promoting cell proliferation in human cells. We have provided evidence suggesting that hCactin is an accessory splicing factor that functions with the RNA helicase DHX8 and the SR protein SRRM2 in promoting sister chromatid cohesion through Sororin pre-mRNA splicing. Yet, the exact molecular function exerted by hCactin and genetic interactions in this context have not been clarified.

We propose that hCactin, like its interactors DHX8 and SRRM2, promotes the second step of the splicing process and possibly control mRNA fate of specific factors (**Fig. 46**).

Moreover, our data also indicate that hCactin is not only involved in pre-mRNA splicing but also supports independent cellular processes through interaction with a plethora of factors, thus explaining the pleiotropic phenotypes observed upon hCactin depletion. We have also provided preliminary indication that hCactin may contribute to the alternative pre-mRNA splicing process through interaction with SRRM2 and the 3-M complex.

Last but not least, we have shown that, differently from its fission yeast ortholog Cay1, hCactin does not participate in maintaining telomere homeostasis in human cells. Yet, a basic conservation of function in pre-mRNA splicing and transcriptional control has likely been conserved throughout evolution.

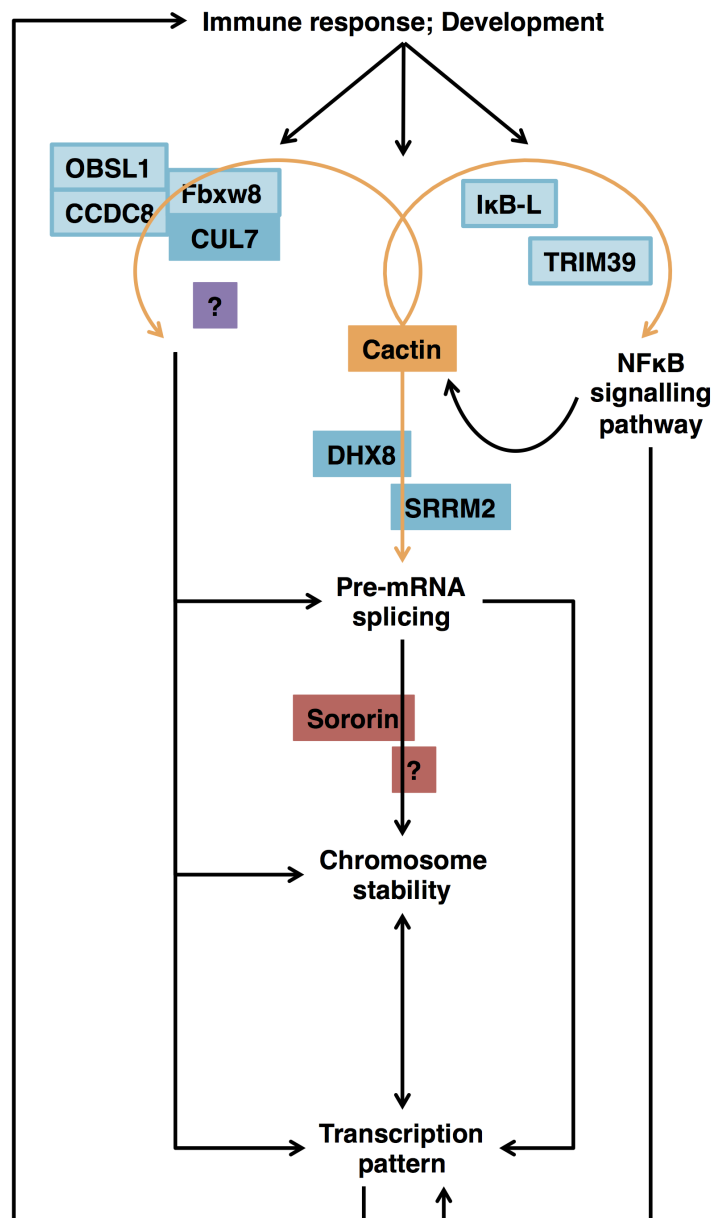


**Figure 46: Speculative model for functions of hCactin in promoting chromosome stability.**

hCactin interacts with the ATPase/RNA helicase DHX8 and the SR protein SRRM2 to promote pre-mRNA splicing of Sororin and other factors (question mark) essential for chromosome stability. hCactin interacts with TRIM39 and IκB-L in order to modulate the NFκB signalling pathway in response to inflammatory stimuli. hCactin also interacts with CUL7 and others factors (question mark) in different cellular pathways that ultimately contribute to establishing the cellular transcription landscape. See discussion for details.

## 5.9 Outlook

Data presented in this thesis and previous results obtained in fission yeast suggest that Cactin is a conserved accessory splicing factor that also exerts pleiotropic functions in regulating transcription and promoting genomic stability. Our data support the idea of hCactin functioning at the second catalytic step of pre-mRNA splicing interacting with important splicing factors that not only promote intron removal, but also play important roles in controlling mRNA fate.

Genome-wide chromatin- and RNA-immunoprecipitation analysis followed by DNA sequencing (ChIP-seq and Rip-seq) would help understand whether Cactin works directly as a transcription factor or whether it functions at the RNA level. In fact, we cannot exclude that protein-protein interactions involving Cactin are stimulated by protein-RNA interactions. Further analyses of constitutive and alternative splicing events in cells depleted for hCactin would help elucidate which set of genes are particularly controlled by Cactin and its interactome. This would allow a more restricted analysis of specific pre-mRNA splicing and transcription events and to gain a deeper insight into the molecular details of Cactin function(s).





## 6 MATERIAL AND METHODS

### 6.1 Human cell lines

U2OS	Human osteosarcoma cells (a gift from Massimo Lopes).
HeLa	Human cervical carcinoma cells (ATTC).
HEK293T	Human embryonic kidney cells expressing SV40 large T-antigen (ATTC).
RPE-1	Human retina pigmented epithelial cells expressing hTERT (a gift from Massimo Lopes).
Flp-In T-Rex 293	HEK293-derived cells featuring T-Rex system, a tetracycline-regulated mammalian expression system, and Flp-In system (Invitrogen, a gift from Ulrike Kutay).

**Table 2: Commercial cell lines.**

pB_Cac	Generated by clonal integration of N-terminal HA-Strep-tagged hCactin cDNA into the LTR promoter-based pBABE_Hygro vector (Addgene #1765).
pcDNA5_Cac	Generated by clonal integration of N-terminal HA-Strep-tagged hCactin cDNA into the Flp-In expression pcDNA5/FRT/TO_Hygro vector (Life Technologies).
pL_Sor	Generated by clonal integration of Sororin cDNA, PCR amplified from RNA prepared from HeLa cells, into the tetracycline-regulated mammalian expression pLVX_Puro vector (Clontech/Takara #631849).
pL_CUL7	Generated by clonal integration of N-terminal MYC-tagged CUL7 cDNA, PCR-amplified from the pcDNA3-MYC-CUL7 plasmid (Addgene #20695), into the tetracycline-regulated mammalian expression pLVX_Puro vector (Clontech/Takara #631849).

**Table 3: Plasmids for stable integration.**

The following stable cell lines were generated by transduction of U2OS, HeLa and HEK293T cells with retroviruses expressing pB\_Cac vector or empty vector control viruses according to standard procedures. Cells were selected with 200  $\mu$ g/ml Hygromycin (Fluka).

U2OS pB_EV	Empty vector control cells
U2OS pB_Cac	Constitutively expressing a N-terminal HA-Strep-tagged hCactin cDNA
HeLa pB_EV	Empty vector control cells
HeLa pB_Cac	Constitutively expressing a N-terminal HA-Strep-tagged hCactin cDNA
HEK293T pB_EV	Empty vector control cells
HEK293T pB_Cac	Constitutively expressing a N-terminal HA-Strep-tagged hCactin cDNA

**Table 4: Generated stable cell lines.**

The following stable cell lines were previously generated in our lab by transfection of Flp-In T-Rex 293 cells with the Flp-In expression pcDNA5\_Cac vector according to manufacturer's instructions (Flp-In System, Invitrogen #R780-07), resulting in integration of the N-terminal HA-Strep-tagged hCactin cDNA into a tetracycline-inducible expression cassette. Cells were selected with 200  $\mu\text{g/ml}$  Zeocin (Invitrogen).

Flp-In_EV	Empty vector control cells
Flp-In_Cac	Doxycycline-inducible expression of a N-terminal HA-Strep-tagged hCactin cDNA

**Table 5: Generated DOX-inducible Flp-In T-Rex 293 cell lines.**

The following stable cell lines were generated by infection of HeLa cells with lentiviruses expressing pL\_Sor or pL\_CUL7 vectors or empty vector control viruses according to manufacturer's instructions (Lenti-X Tet-One inducible Expression System, Clontech/Takara). Infected cells were selected with 1  $\mu\text{g/ml}$  Puromycin (Sigma-Aldrich). While HeLa pL\_EV and HeLa pL\_CUL7 are heterogeneous populations, the HeLa pL\_Sor has been generated by clonal selection.

HeLa pL_EV	Empty vector control cells
HeLa pL_Sor	Doxycycline-inducible expression of Sororin cDNA
HeLa pL_CUL7	Doxycycline-inducible expression of N-terminal MYC-tagged CUL7 cDNA

**Table 6: Generated DOX-inducible cell lines by random integration.**

## 6.2 Cell culture, cell transfection and cell treatments

### Cell culture

All cell lines were cultured in high glucose D-MEM (Invitrogen) supplemented with 10% TET-free FBS (Pan Bio Tech) and 100 U/ml Penicillin-Streptomycin (Sigma) in an atmosphere containing 6% CO<sub>2</sub> at 37°C.

### shRNA transfection

Cells were seeded in regular media 24h before transfection at 30-40% confluency. shRNA plasmids were transfected according to standard procedures using Lipofectamine 2000 (Invitrogen). 24h after transfection cells were selected with 1  $\mu\text{g/ml}$  Puromycin (Sigma-Aldrich).

Name	Plasmid	Target sequence 5'-3'	Source
shEV	pSUPER-Puro	-	-
shCac_A	pSUPER-Puro	TGGAGGATATCCAGGTCTACATG	-
shCac_B	pSUPER-Puro	ACATACAACCAGCTGCAGGTCAT	-
shCac_C	pSUPER-Puro	GCTTCGAGTGGAAACAAGTACAAC	-
shCac_D	pSUPER-Puro	ATGGAATTGGCCTATTGGCAAGA	-
shCac_E	pSUPER-Puro	GGAAATAGTTCCGTTTGTTC	-
shSF3A-3	pSUPER-Puro	GGAGGAGCTCAATGCCATT	(Tanackovic and Kramer, 2005)

**Table 7: shRNA sequences.**

### siRNA transfection

Cells were seeded in regular media 24h before transfection at 20% confluency. Oligonucleotides were transfected according to standard procedures using Lipofectamine RNAiMAX (Invitrogen). U2OS and U2OS-derived cell lines were transfected once with 20 nM siRNAs, whereas HeLa and HeLa-derived cell lines were transfected twice every 24h with 50 nM siRNAs. Cells were processed from 1 to 3 days after transfection.

Name	Target sequence 5'-3'	Source
siCtrl	AATTCTCCGAACGTGTACCGT	Qiagen #1027310
siCac_D	ATGGAATTGGCCTATTGGCAA	Qiagen - designed
siCac_E	AAATAGTTCCGTTTGTTC	Qiagen - designed
siCul7	CACGCTACTGTGAGCACTTTA	Qiagen #SI00357000
siOBSL1	CACTACGCTTCTCAGAGTAAA	Qiagen #SI04339951
siCCDC8	CAAGGTGCTCAGCTTGATAAA	Qiagen #SI05077086
siCK2 $\alpha$	CTGGTCGCTTACATCACTTTA	Qiagen #SI02660504
siCXorf56	CGGATTCTATTTATGCCCTA	Qiagen #SI03195731
siUBR5	CCAAATCTAGAGTGTATCCAA	Qiagen #SI03074225
siUSP9X	CCGCCAGATAGCACAACGATA	Qiagen #SI00066584
siDDX1	AAGGCACCGGATGGTTACATT	Qiagen #SI00299978
siDHX8	CCCAGAGAAGTGGGAGATCAA	Qiagen #SI03019373
siSRRM2	CTCGATCATCTCCGGAGCTAA	Qiagen #SI04173995
siSRPK1	TACCATGTGATCCGAAAGTTA	Qiagen #SI02223109

**Table 8: siRNA sequences.**

### Transient plasmid transfection

Cells were seeded in regular media 24h before transfection at 30% confluency. Generated DNA plasmids were transfected according to standard procedures using Lipofectamine 2000 (Invitrogen).

Plasmid	Description	Source
pcMV6_Cac	Generated by cloning of a synthesized C-terminal FLAG-tagged hCactin cDNA (GenScript) into a CMV promoter-based pcMV6 vector	-
pcDNA3_MYC-CUL7	CMV promoter-based vector expressing N-terminal MYC-tagged CUL7cDNA	Addgene #20695
pZW6	CMV promoter-based vector expressing C-terminal HA-tagged CK2 $\alpha$ cDNA	Addgene #27086
pZW16	CMV promoter-based vector expressing N-terminal HA-tagged CK2 $\alpha'$ cDNA	Addgene #27087
pZW12	CMV promoter-based vector expressing N-terminal MYC-tagged CK2 $\beta$ cDNA	Addgene #27088

**Table 9: Plasmids for transient transfections.**

### Cell treatments

The following compounds were added to the cells when indicated.

Compound	Final concentration	Time	Source
Hydroxyurea	2 mM	16h	Sigma-Aldrich
Camptothecin	100-500 nM	2-16h	Sigma-Aldrich
Bleomycin	5-10 $\mu$ g/ml	1-2h	Sigma-Aldrich
Halogenated nucleotide EdU	10 $\mu$ M	30 min	Invitrogen
Colcemid	200 nM	3-4h	Sigma-Aldrich
Thymidine	2 mM	20h	Sigma-Aldrich
Nocodazole	75 ng/ml	12h	Sigma-Aldrich
MG132	20 $\mu$ M	1-3h	Sigma-Aldrich
Cycloheximide	100 $\mu$ g/ml	1-6h	Sigma-Aldrich
Doxycycline	500 $\mu$ g/ml	24-72h	Sigma-Aldrich

**Table 10: Compounds used for cell culture treatments.**

### Cell synchronization in mitosis (Thymidine-nocodazole block)

Cells were treated for 20h with Thymidine to arrest them at the G1/S transition, released from arrest for 4h into regular media, and then treated with Nocodazole for 12h to arrest them in mitosis. Synchronised cells were collected by mitotic shake-off and released into fresh regular media. In order to analyse the first round of replication upon depletion of specific factors, cells were transfected with siRNAs during the 4h between Thymidine and Nocodazole block.

### Cell synchronisation in G0/G1 (Serum starvation)

Cells were seeded in high glucose D-MEM (Invitrogen) supplemented with 100 U/ml Penicillin-Streptomycin (Sigma) without serum for 48-72h to arrest them in G0/G1. Synchronised cells were then re-stimulated with regular media

containing 10% serum. In order to analyse the first round of replication upon depletion of specific factors, cells were transfected with siRNAs during serum starvation.

### **6.3 Protein extraction and western blotting**

#### **Protein fractionation**

About  $2 \times 10^6$  cells were harvested and resuspended in Solution A (10mM HEPES pH 7.7, 10 mM KCl, 1.5 mM  $MgCl_2$ , 0.34 M Sucrose, 10% Glycerol, 10 mM NaF, 1 mM DTT, 1 mM  $Na_2VO_3$ , 1XProtease and 1XPhosphatase inhibitor cocktails (Sigma-Aldrich)). Cell suspension was supplemented with Triton X-100 to final concentration of 0.1% and incubated for 5 min on ice. Cytoplasmic fraction was recovered by centrifugation in the supernatant. Nuclei were resuspended in Solution B (3 mM EDTA, 0.2 mM EGTA, 1mM DTT, 1XProtease and 1XPhosphatase inhibitor cocktails) and incubated on ice for 10 min. Nucleoplasmic fraction was recovered by centrifugation in the supernatant. Pellet was resuspended in Solution C (20 mM HEPES pH 7.7, 0.4 M NaCl, 1 mM EDTA, 1 mM EGTA, 1 mM DTT, 1 mM PMSF, 1XProtease and 1XPhosphatase inhibitor cocktails) and vigorously rocked at 4°C for 30 min. Insoluble fraction was recovered by centrifugation in the supernatant.

#### **Total SDS extracts**

Cells were harvested and lysed in 2XLaemmli buffer (4% SDS, 20% Glycerol, 120 mM Tris pH6.8) and boiled for 10 min. Total protein extracts were recovered by centrifugation in the supernatant. Protein concentration was determined by Lowry protein assay using BSA standards. In brief, sample aliquots and BSA standards were supplemented with 1 ml of Solution A (2%  $Na_2CO_3$  in 0.1N NaOH)/Solution B (0.5%  $CuSO_4 \cdot 5H_2O$  in 1% Sodium citrate) mixture (50:1), incubated 10 min at RT and subsequently supplemented with 100  $\mu$ l Folin&Ciocalteu's phenol reagent (Sigma-Aldrich), pre-diluted in  $H_2O$  (1:3). After 30 min incubation at RT in the dark, the absorbance at 750 nm was measured with a spectrophotometer.

#### **SDS-PAGE and western blotting**

30-50  $\mu$ g of protein were used for western blot analysis. SDS extracts were supplemented with 5XSDS loading buffer (250 mM Tris pH 6.8, 10% SDS, 30% Glycerol, 0.02% Bromophenol blue, 5%  $\beta$ -Mercaptoethanol), boiled for 5 min, and subjected to SDS-polyacrylamide gel electrophoresis (SDS-PAGE)

according to standard protocol. Proteins were subsequently transferred to a nitrocellulose membrane (Whatman) using a Trans-Blot SD Semidry Transfer Cell (BioRad) according to manufacturer's instructions. Blocking was performed in 5% Milk diluted in 1XPBS-containing Tween20 to final concentration of 0.1% (PBST 0.1%). The membrane was subjected to immunostaining with primary antibody and with HRP-conjugated secondary antibody diluted in 5% Milk or 5% BSA in PBST 0.1%. Washes were performed in PBST 0.1% by shaking. Secondary antibody was activated using ECL detection reagent (GE Healthcare) and chemo luminescent signal documented on a Fluor chem HD2 imager system (Alpha Innotech).

Antibody	Host and clonality	Source	Dilution
Cactin	Rabbit polyclonal	Abnovasc-17775 #PAB23952	1:1000
UPF1	Rabbit polyclonal	Custom antibody	1:1000
Golgin97	Mouse monoclonal	Molecular probes #A-21270	0.2 $\mu$ l/ml
LaminB1	Rabbit polyclonal	GeneTex #GTX103292	1:1000
LaminA/C	Rabbit polyclonal	GeneTex #GTX111677	1:1000
Actin	Mouse monoclonal	Abcam #ab8224	1:5000
pATM (Ser1987)	Mouse monoclonal	Cell Signaling #4526	1:500
pKAP1 (Ser824)	Rabbit polyclonal	Bethyl #A300-767A	1:1000
KAP1	Rabbit polyclonal	Bethyl #A300-274A	1:1000
pChk1 (Ser345)	Rabbit monoclonal	Cell Signalling #2348	1:500
Chk1	Mouse monoclonal	SCBT #sc-8408	1:1000
pRPA32 (Ser33)	Rabbit polyclonal	Bethyl #A300-246A	1:1000
RPA32	Rabbit polyclonal	Bethyl #A300-244A	1:1000
H2AX	Rabbit polyclonal	Bethyl #A300-082A	1:2000
$\gamma$ H2AX (Ser139)	Mouse monoclonal	Millipore #05-636	1:1000
CUL7	Rabbit polyclonal	GeneTex #GTX113906	1:1000
CyclinD1	Mouse monoclonal	SCBT #sc-20044	1:1000
CyclinB1	Rabbit polyclonal	GeneTex #GTX100911S	1:1000
CyclinE	Mouse monoclonal	SCBT #sc-247	1:1000
IRS1	Rabbit polyclonal	Bethyl #A301-158A	1:2000
TRF2	Mouse monoclonal	Millipore #05-521	1:1000
TRF1	Mouse monoclonal	Abcam #ab10579	1:1000
RAP1	Rabbit polyclonal	Bethyl #A300-306A	1:500
TPP1	Mouse monoclonal	Abnova #H0006557-M02	1:500
CUL1	Mouse monoclonal	SCBT #sc-17775	1:1000
Ubiquitin antibody	Mouse monoclonal	SCBT #sc-166553	1:1000
HA	Mouse monoclonal	SCBT #sc-57592	1:2000
MYC	Mouse monoclonal	Cell Signalling #2276	1:2000
FLAG	Mouse monoclonal	Sigma-Aldrich #F1804	1:1000

**Table 11: Antibodies used for WB analysis.**

## 6.4 Indirect immunofluorescence and DNA *in-situ* hybridisation

### Indirect immunofluorescence analysis

Indirect immunofluorescence (IF) analysis was performed according to standard procedures. Cells of interest were grown on coverslips until 70-80% confluency. If required, pre-extraction of soluble proteins was performed by incubating cells in cold CSK (300 mM Sucrose, 3 mM MgCl<sub>2</sub>, 100 mM NaCl, 10 mM PIPES pH 7, 0.5% Triton X-100) buffer for 7 min on ice. Cells were then fixed with 4% Formaldehyde diluted in 1XPBS for 10 min at RT and permeabilised with 0.5% Triton X-100 diluted in 1XPBS for 10 min at RT. Alternatively cells were fixed and permeabilised in a single step, without prior pre-extraction, with cold MeOH for 20 min at -20°C. Permeabilised cells were then blocked in 5% Milk diluted in 1XPBS containing Tween20 to final concentration of 0.1% (PBST 0.1%). Cells were incubated with primary and secondary antibodies diluted in 5% Milk diluted in PBST 0.1% on parafilm in a moist chamber. Washes were performed in PBST 0.1% by gentle shaking. Immunolabelled cells were additionally incubated in DAPI (100 ng/ml, Sigma-Aldrich) diluted in 1XPBS to counterstain cellular DNA. Coverslips were then mounted on microscope slides with Vectashield antifade medium (Vector Laboratories). Analysis and image acquisition was performed on an Olympus IX 81 microscope.

### IF combined with DNA fluorescence *in-situ* hybridisation analysis

Cells of interest were grown on coverslips until 70-80% confluency. After pre-extraction in CSK (described above), cells were fixed with 2% Formaldehyde diluted in 1XPBS for 10 min at RT and permeabilised with 0.5% Triton X-100 diluted in 1XPBS for 10 min at RT. Cells were re-fixed with chilled MeOH for 20 min at -20°C and then incubated for 30 min at 37°C in Blocking solution (5% BSA, 20 mM Glycine, 1XPBS) supplemented with RNaseA (20 µg/ml, Roche). Cells incubated in primary and secondary antibodies diluted in 5% BSA in 1XPBS at 37°C. Washes were performed in 1XPBS containing Tween20 to final concentration of 0.1% (PBST 0.1%) by gently shaking. Cells were again fixed with 4% Formaldehyde diluted in 1XPBS for 10 min at RT and then equilibrated in 10 mM Tris pH 7.2. A denaturation step was carried on by incubating coverslips in Hybridisation mix (10 mM Tris pH 7.2, 70% Formamide, 0.5% Blocking solution (Roche)) containing telomeric or centromeric PNA probe (1:2000 dilution of 10 µM stock) for 5 min at 80°C on a heating plate. To allow hybridisation coverslips were then incubated 2h at RT in a moist chamber. Cells were washed twice with Hybridisation wash 1 (10 mM Tris pH 7.2, 70% Formamide, 0.1% BSA, pH adjusted to 7.2) and

once with Hybridisation wash 2 (0.1 M Tris pH 7.2, 0.15 M NaCl, 0.08% Tween-20, pH adjusted to 7.2) for 10 min each by gentle shaking. Cellular DNA was then counterstained with DAPI (100 ng/ml, Sigma-Aldrich) diluted in Hybridisation wash 2. Coverslips were mounted with Vectashield antifade medium (Vector Laboratories). Analysis and image acquisition was performed on an Olympus IX71 microscope equipped with DeltaVision Multiplexed system.

Antibody	Host and clonality	Source	Dilution
Cactin	Rabbit polyclonal	Abnova #PAB23952	1:1000
HA	Mouse monoclonal	SCBT #sc-57592	1:1000
53BP1	Rabbit polyclonal	Abcam #ab21083	1:1000
LaminB1	Mouse monoclonal	SCBT #7292	1:500

**Table 12: Antibodies used for IF analysis.**

PNA probe	Sequence 5'-3'	Source
Telomeric: TelC-Cy3	Cy3-OO-CCCTAACCCCTAACCCCTAA	Panagene
Centromeric: Cent-FAM	FAM-AAACTAGACAAGCATT	PNAbio #3006

**Table 13: Fluorescent labelled probes used for DNA FISH analysis.**

## 6.5 Flow cytometric analysis

### Flow cytometric analysis for DNA content

Approximately  $0.5 \times 10^6$  cells were harvested, resuspended in chilled 70% EtOH by vortexing and fixed for at least 1h at  $-20^\circ\text{C}$ . Fixed cells were recovered by centrifugation, treated with RNaseA (0.25 mg/ml, Roche) diluted in 1XPBS for 20 at  $37^\circ\text{C}$  and then stained with Propidium iodide ( $20 \mu\text{g/ml}$ , Sigma-Aldrich) diluted in 1XPBS for 10 min at  $4^\circ\text{C}$ . Stained cells were analysed on a FACSCalibur flow cytometer (BD Bioscience) and using FlowJo software.

### Flow cytometric analysis for DNA content and phosphorylated H3

The protocol for this analysis was kindly provided by Mia Li (PhD student from the Matthias Peter laboratory). Approximately  $0.5 \times 10^6$  cells were harvested and fixed in 70% EtOH for 30 min at  $-20^\circ\text{C}$ . Fixed cells were recovered by centrifugation and permeabilised for 30 min with 5% FBS diluted in 1XPBS containing Triton X-100 to final concentration of 0.25%. Permeabilised cells were incubated in primary and secondary antibodies diluted in 5% FBS in 1XPBS containing Triton X-100 to final concentration of 0.1% (5% FBS/PBSTX 0.1%). Washes were also performed in 5% FBS/PBSTX 0.1%.



Immunostained cells were then treated with RNaseA (20  $\mu\text{g/ml}$ , Roche) and PI (50  $\mu\text{l/ml}$ , Sigma-Aldrich) diluted in 1XPBS. Cells were analysed on a FACSCalibur flow cytometer (BD Bioscience) and using FlowJo software.

### Flow cytometric analysis for DNA synthesis rate and antibody staining

This analysis was performed according to previously published protocol (Neelsen et al., 2013a). (Halogenated nucleotide EdU (Click-IT EdU Flow Cytometry Assay Kit, Invitrogen) to final concentration of 10  $\mu\text{M}$  was added to cultured cells of interest. After 30 min of incubation, cells were harvested and approximately  $0.5 \times 10^6$  cells were fixed in 4% Formaldehyde diluted in 1XPBS for 10 min on ice. Fixed cells were permeabilised in Saponin buffer (1% Saponin diluted in 1% BSA in 1XPBS) for 10 min and incubated in primary and secondary antibodies diluted in Saponin buffer. Washes were also performed with Saponin buffer. Cells were incubated in Click-It reaction mix containing Alexa Fluor 488 Azide (Click-IT EdU Flow Cytometry Assay Kit, Invitrogen #C10425). Cells were treated with 1% BSA diluted in 1XPBS containing RNaseA (0.1 mg/ml, Roche) and DAPI (1  $\mu\text{g/ml}$ , Sigma-Aldrich). Stained cells were analysed on a Fortessa flow cytometer (BD bioscience) and using FlowJo software.

Antibody	Host and clonality	Source	Dilution used
pH3 (Ser10)	Rabbit polyclonal	Millipore #06-570	1:500
$\gamma\text{H2AX}$ (Ser139)	Mouse monoclonal	Millipore #05-636	1:500

**Table 14: Antibodies used for flow cytometric analysis.**

## 6.6 Pulse Field Gel Electrophoresis for DSB detection

This analysis was performed according to previously published protocol (Toller et al., 2011).

### Plug preparation

2% Low Melting Temperature (LMT) agarose (Bio-Rad) were dissolved in 1XPBS equilibrated to 50°C for at least 15 min. Cells of interest were harvested and resuspended in 1XPBS to a final concentration of roughly  $0.5 \times 10^7$  cells/ml. Cell suspension was briefly equilibrated at 50°C, an equal volume of molten LMT agarose was added to the cell suspension followed by immediate mixing and transferred to the Plug Mold (Bio-Rad) for solidification. Solidified plugs were then ejected in Lysis buffer (100 nM EDTA pH 8.0, 0.2%

Sodium Deoxycholate, 1% Sodium Lauryl Sarcosine) containing ProteinaseK (1 mg/ml, Appli Chem) and incubated at 37°C for 36-72h. Plugs were then washed 3-4 times with Plugs washing buffer (20 mM Tris pH8.0, 50 mM EDTA pH 8.0) for at least 30 min each at RT on a nutator.

## PFGE

Plugs were embedded into a 0.9% Pulse Field Certified agarose (Bio-Rad) gel and subjected to pulse field electrophoresis (see table below for parameters) in an electrophoresis chamber (CHEF DR III apparatus, Bio-Rad). Pump power and cooling modules were set to 90% 14°C, respectively. Pulse field gel was then stained by gently shaking in 1xTBE containing EtBr (0.5 µg/ml) and documented on a Gel Doc 2000 imaging system (Bio-Rad). Double strand break (DSB) quantifications were performed by ImageJ software, normalizing DSB signals to unsaturated signal of DNA trapped in the well.

Block	I	II	III
Time (h)	9	6	6
Included angle (°)	120	117	112
(V/cm)	5.5	4.5	4.0
Switch (s)	30-18	18-9	9-5

**Table 15: Running parameters of PFGE for DSB detection.**

## 6.7 Metaphase spread

Cells of interest were grown to 60-70% confluency and treated for 3-4h with Colcemid, preventing mitotic spindle formation and arresting cells in metaphase. Mitotic cells were harvested by mitotic shake-off and incubated in pre-warmed Hypotonic solution (0.075 M KCl) for 9 min at 37°C. Metaphase chromosome were resuspended in cold MeOH/Acetic acid solution (3:1) by vortexing and fixed overnight at -20°C. Chromosomes were washed twice in cold MeOH/Acetic acid solution (3:1), spread on glass slides and air-dried overnight at RT. Chromosomes were subsequently counterstained with DAPI/1XPBS (100 ng/ml, Sigma-Aldrich) and slides mounted with Vectashield antifade medium (Vector Laboratories). Analysis and image acquisition was performed on an Olympus IX 81 microscope.

## 6.8 Nuclei acids analysis

### Genomic DNA isolation

Genomic DNA was isolated by standard Phenol/Chloroform extraction. Cells were harvested and incubated overnight in DNA buffer (0.2 M Tris pH 8.0, 0.1 M EDTA, 1.3% SDS) containing Proteinase K (0.4 mg/ml, Appli Chem) at 45°C. Nucleic acids were subjected to Phenol/Chloroform extraction and the recovered aqueous phase was treated with RNaseA (25 µg/ml, Roche) and incubated for 1h at 37°C. Aqueous phase was then subjected to a second Phenol/Chloroform extraction. Genomic DNA was precipitated in the final aqueous phase with Isopropanol, washed with 70% EtOH, air-dried at RT and rehydrated overnight in H<sub>2</sub>O at 4°C.

### Terminal Restriction Fragment (TRF) analysis and Southern blotting

For TRF analysis 10-20 µg of genomic DNA was digested overnight with *Hinf* I (NEB) and *Rsa*I (NEB) at 37°C. DNA samples were loaded on a 0.6% agarose gel and subjected to electrophoresis. Gel was then dried on a drier plate for 45 min at 50°C and incubated in Church buffer (0.25 M Sodium phosphate buffer pH 7.2, 1 mM EDTA, 1% BSA, 7% SDS) at 50°C for pre-hybridisation. Hybridisation in native conditions was performed overnight at 50°C using a radiolabelled double stranded telomeric DNA probe obtained by PCR amplification of telomeric specific oligonucleotides and subsequent labelling by random priming using α<sup>32</sup>P dCTP (Hartmann Analytic) dTTP, dATP, and Klenow fragment (NEB). Post-hybridisation washes were performed in 2XSSC+0.5%SDS and a final wash in 0.5XSSC+0.5%SDS at 50°C. Hybridised gel was then exposed to a phosphoimager screen and signal acquired on a Typhoon FLA 9000 imager (GE Healthcare). For hybridisation in denatured conditions gel was first incubated in Denaturation solution (1.5 M NaCl, 0.5M NaOH) and then in Neutralisation solution (0.5 M Tris pH 7.5, 3M NaCl) by gently shaking. Gel was re-hybridised as before.

### RNA isolation

RNA was isolated by the Nucleo Spin RNA Kit Plus (Macherey-Nagel) or using the TRIzol reagent (Invitrogen) according to manufacturer's instructions. Isolated DNA was subjected to one or two treatments with DNaseI (Qiagen) according to manufacturer's instructions, followed by overnight RNA precipitation in 100% EtOH at -20°C and RNA recovery in H<sub>2</sub>O.

### RT-PCR and qRT-PCR analysis

For PCR analysis 1  $\mu\text{g}$  of isolated RNA was reverse transcribed using Superscript II reverse transcriptase (Invitrogen) according to manufacturer's procedure using random primers.

For intron retention analysis, cDNA was amplified using a Taq DNA polymerase (Invitrogen) and the following specific primer pairs:

Name	Sequence	Product name
Sor_Exon5_FWD	CGTAAGAAGAAGAAAATGCCAG A	Sororin intron 5
Sor_Exon6_REV	TCAAACCTCGGCATTCATGG	
Sor_Exon1_FWD	AGTTATGTCTGGGAGGCGAA	Sororin intron 1
Sor_Exon3_REV	AGACGATGGGCTTTCTGACT	
CUL7_FWD	CGGCTTGGAGATAGCCACCA	CUL7 pre-mRNA
CUL7_REV	CGCTGCAGCTCCTTAGAGGT	

**Table 16: Primers used for RT-PCR analysis, previously designed (Watrin et al., 2014).**

For specific RNA species quantification, cDNA was PCR amplified on a Rotor-Gene Q instrument (Qiagen) using the Light Cyclor 489 SYBR Green I master mix (Roche) and the following primer pairs:

Name	Sequence	Product name
Sor_Exon1_FWD	AGTTATGTCTGGGAGGCGAA	Sororin pre-mRNA intron 1
Sor_Intron1_REV	ACAGGTTCTAGAGACAGCGAG	
Sor_Intron2_FWD	TCTCACTTCTCCCCTTGTG	Sororin pre-mRNA intron2
Sor_Exon3_REV	AGACGATGGGCTTTCTGACT	
Sor_Exon5_FWD	AAGTCAGGCGTTTCTACAGC	Sororin tot RNA
Sor_Exon5_REV	TCGAAGCCAAAGCAGGAC	
Sor_Exon3_FWD	CAGAAAGCCCATCGTCTTAAA	Sororin mRNA
Sor_Exon3_REV	GGCTCGTTTTCTTTCTCCAA	
CUL7_Intron1_FWD	GGGGAAGCAAATGGCAACAG	CUL7 pre-mRNA intron1
CUL7_Intron1_REV	GGACCTTCTTTTAGCCCCC	
CUL7_Intro4_FWD	TCCTCAAAGGTCAGGGTCA	CUL7 pre-mRNA intron4
CUL7_Intro4_REV	TTCATGGCTTATGCCCCAC	
CUL7_Exon24_FWD	TCAAGATTCGAGATGGCAGCA	CUL7 tot RNA
CUL7_Exon24_REV	CAGCTTGCAGGTACGTCTGA	
CUL7_Exon9_FWD	TGCGGTCCCCAAACACTGAT	CUL7 mRNA
CUL7_Exon10_REV	ACGGCATAGTCCCTGCTCAC	
cFOS_Exon2_FWD	CTGGCGTTGTGAAGACCATGAC	cFOS pre-mRNA intron2
cFOS_Intron2_REV	TCTGTAAGTGGCTCCTGCATC	
cFOS_Exon3_FWD	AGGAGGGAGCTGACTGATACA	cFOS pre-mRNA intron3
cFOS_Intron3_REV	GGGCCCTTATGCTCAATCTCC	
cFOS_Exon1_FWD	CACGATGATGTTCTCGGGCT	cFOS tot RNA
cFOS_Exon1_REV	ATGCTGGAGAAGGAGTCTGC	
cFOS_Exon1_FWD	CTTACTACCACTACCCGCA	cFOS mRNA
cFOS_Exon2_REV	GAAGTTGGCACTGGAGACGG	

**Table 17: Primers used for qRT-PCR analysis. Sororin and c-Fos primers were previously designed (Watrin et al., 2014) (Gu et al., 2013).**

Quantifications were obtained according to the comparative C<sub>T</sub> method (Schmittgen and Livak, 2008) using U6, Actin or GAPDH genes.

### **Northern blotting**

10-15  $\mu\text{g}$  of RNA were briefly denatured at 65°C and subjected to electrophoresis in 1.2% agarose/10% Formaldehyde gels. RNA was transferred overnight by capillary transfer onto a nylon membrane, and then crosslinked to the membrane using a UV-crosslinker. For TERRA detection the membrane was incubated in Church buffer (0.25 M Sodium phosphate buffer pH 7.2, 1 mM EDTA, 1% BSA, 7% SDS) at 55°C for pre-hybridisation. Hybridisation was then performed overnight at 55°C using strand-specific telomeric probe labelled by random priming using  $\alpha^{32}\text{P}$  dCTP (Hartmann Analytic) dTTP, dATP, and Klenow fragment (NEB). Post-hybridisation washes were performed in 2XSSC+0.5%SDS and a final wash in 0.5XSSC+0.5%SDS at 50°C. For Sororin RNA detection, pre-hybridisation, hybridisation and post-hybridisation washes were performed at 60°C. Sororin probe was made by random priming labelling of the PCR amplification product of Sororin cDNA from the pL\_Sor plasmid. For 18s ribosomal RNA detection, pre-hybridisation, hybridisation and post-hybridisation washes were performed at 50°C. 18s probe was made by oligonucleotide labelling using  $\gamma^{32}\text{P}$  dATP (Hartmann Analytic), dTTP, dGTP, dCTP and T4 PNK. Hybridised membranes were exposed to a phosphoimager screen and signal acquired on a Typhoon FLA 9000 imager (GE Healthcare).

### **Transcriptome analysis**

Roughly 5  $\mu\text{g}$  of isolated RNA was sent to Fasteris SA (Plan-les-Ouates, Switzerland) for high-throughput RNA sequencing using Illumina technology. The sequencing was performed with a single-end protocol providing reads of 100 bp. Reads were trimmed with Sickle software and aligned to the human genome (UCSC Hg19) using RUM software. A FPKM (Fragments Per Kilobase per Million mapped reads) estimate for each intron, exon and gene were then generated using only uniquely mapping reads. Relative intron expression was calculated for each intron by dividing its estimated expression for the corresponding gene. Files generated by RUM were further filtered and used to visualise the coverage of selected genes.

## 6.9 Streptavidin One-Step purification for MS analysis

Single-step in column purification of HA-Strep-tagged hCactin protein complexes was performed according to standard protocol. About  $1 \times 10^8$  cells of interest were harvested and resuspended in ice-cold HNN lysis buffer (50 mM HEPES, 150 mM NaCl, 50 mM NaF, 0.5% NP-40, 1 mM PMSF, 1XPhosphatase and 1XProtease inhibitor cocktails (Sigma-Aldrich), 10  $\mu\text{g}/\text{ml}$  Avidin (IBA)). After 10 min incubation on ice, lysate was recovered by centrifugation and loaded on Bio-Spin chromatography column (BioRad) containing 200  $\mu\text{l}$  of 50% slurry Strep-Tactin sepharose beads (IBA) previously blocked with BSA and equilibrated in HNN lysis buffer. Columns were washed twice with HNN lysis buffer and three times with HNN buffer (50 mM HEPES, 150 mM NaCl, 50 mM NaF). HA-Strep-tagged hCactin protein complexes were eluted three times with 0.5 mM Biotin (Sigma-Aldrich) diluted in HNN buffer and loaded on gradient protein gel (Invitrogen). Gels were fixed and stained with  $\text{AgNO}_3$  according to standard protocol and bands were excised and sent for mass spectrometry analysis to Alphalyse (Denmark).

## 6.10 Co-Immunoprecipitation

Roughly  $5 \times 10^6$  cells were harvested and resuspended in ice-cold Lysis buffer (50 mM Tris pH 7.4, 1.5 mM  $MgCl_2$ , 1 mM EDTA, 150 mM NaCl, 0.5% Triton X-100, 1 mM DTT, 1XPhosphatase and 1XProtease inhibitor cocktails (Sigma-Aldrich)). Lysate was incubated on ice for 30 min. Supernatant was recovered by centrifugation and pre-cleared by incubation with 20  $\mu$ l of 50% slurry protein beads (Protein A or G agarose beads, Santa Cruz Biotechnology) at 4°C on a wheel. 500  $\mu$ g of protein lysate was then incubated for 4h with 4 $\mu$ g of primary antibody at 4°C. Lysate was then supplemented with 30  $\mu$ l of 50% slurry protein beads and incubated overnight at 4°C. Protein beads were washed three times with IB buffer (50 mM Tris pH 7.4, 1.5 mM  $MgCl_2$ , 1 mM EDTA, 150 mM NaCl, 0.5% Triton X-100), once with Final wash buffer (50 mM Tris pH 7.4, 1.5 mM  $MgCl_2$ , 1 mM EDTA, 150 mM NaCl) and boiled in 50  $\mu$ l of 2XLaemmli buffer for 95°C. Co-immunoprecipitated proteins were recovered by centrifugation and subjected to western blot analysis.

Antibody	Host and clonality	Source
HA	Mouse monoclonal	SCBT #sc-57592
MYC	Mouse monoclonal	Cell Signalling #2276
FLAG	Mouse monoclonal	Sigma-Aldrich #F1804
Cactin (1)	Rabbit polyclonal	Abgent #AP5411a
Cactin (2)	Rabbit polyclonal	Bethyl #A303-349A
CUL7	Rabbit polyclonal	GeneTex #GTX113906

**Table 18: Antibodies used for IP and Co-IP analyses.**





## 7 BIBLIOGRAPHY

Aballay, A., Drenkard, E., Hilbun, L.R., and Ausubel, F.M. (2003). *Caenorhabditis elegans* innate immune response triggered by *Salmonella enterica* requires intact LPS and is mediated by a MAPK signaling pathway. *Curr Biol* *13*, 47-52.

Albanese, C., Johnson, J., Watanabe, G., Eklund, N., Vu, D., Arnold, A., and Pestell, R.G. (1995). Transforming p21ras mutants and c-Ets-2 activate the cyclin D1 promoter through distinguishable regions. *J Biol Chem* *270*, 23589-23597.

Alexander, R.D., Innocente, S.A., Barrass, J.D., and Beggs, J.D. (2010). Splicing-dependent RNA polymerase pausing in yeast. *Mol Cell* *40*, 582-593.

Allo, M., Buggiano, V., Fededa, J.P., Petrillo, E., Schor, I., de la Mata, M., Agirre, E., Plass, M., Eyra, E., Elela, S.A., *et al.* (2009). Control of alternative splicing through siRNA-mediated transcriptional gene silencing. *Nat Struct Mol Biol* *16*, 717-724.

Alt, J.R., Cleveland, J.L., Hannink, M., and Diehl, J.A. (2000). Phosphorylation-dependent regulation of cyclin D1 nuclear export and cyclin D1-dependent cellular transformation. *Genes Dev* *14*, 3102-3114.

Ameur, A., Zaghlool, A., Halvardson, J., Wetterbom, A., Gyllensten, U., Cavelier, L., and Feuk, L. (2011). Total RNA sequencing reveals nascent transcription and widespread co-transcriptional splicing in the human brain. *Nat Struct Mol Biol* *18*, 1435-1440.

An, J., Nakajima, T., Shibata, H., Arimura, T., Yasunami, M., and Kimura, A. (2013). A novel link of HLA locus to the regulation of immunity and infection: NFKBIL1 regulates alternative splicing of human immune-related genes and influenza virus M gene. *J Autoimmun* *47*, 25-33.

Anczukow, O., Rosenberg, A.Z., Akerman, M., Das, S., Zhan, L., Karni, R., Muthuswamy, S.K., and Krainer, A.R. (2012). The splicing factor SRSF1 regulates apoptosis and proliferation to promote mammary epithelial cell transformation. *Nat Struct Mol Biol* *19*, 220-228.

Ando, T., Kawabe, T., Ohara, H., Ducommun, B., Itoh, M., and Okamoto, T. (2001). Involvement of the interaction between p21 and proliferating cell nuclear antigen for the maintenance of G2/M arrest after DNA damage. *J Biol Chem* *276*, 42971-42977.

Arumugam, P., Gruber, S., Tanaka, K., Haering, C.H., Mechtler, K., and Nasmyth, K. (2003). ATP hydrolysis is required for cohesin's association with chromosomes. *Curr Biol* *13*, 1941-1953.

Atzei, P., Gargan, S., Curran, N., and Moynagh, P.N. (2010a). Cactin targets the MHC class III protein I $\kappa$ B-like (I $\kappa$ B $\Delta$ N) and inhibits NF- $\kappa$ B and interferon-regulatory factor signaling pathways. *J Biol Chem* *285*, 36804-36817.

Atzei, P., Yang, F., Collery, R., Kennedy, B.N., and Moynagh, P.N. (2010b). Characterisation of expression patterns and functional role of Cactin in early zebrafish development. *Gene Expr Patterns* *10*, 199-206.

Azzalin, C.M., Reichenbach, P., Khoriantseva, L., Giulotto, E., and Lingner, J. (2007). Telomeric repeat containing RNA and RNA surveillance factors at mammalian chromosome ends. *Science* *318*, 798-801.

- Bah, A., Wischniewski, H., Shchepachev, V., and Azzalin, C.M. (2012). The telomeric transcriptome of *Schizosaccharomyces pombe*. *Nucleic Acids Res* *40*, 2995-3005.
- Baldwin, K.L., Dinh, E.M., Hart, B.M., and Masson, P.H. (2013). CACTIN is an essential nuclear protein in *Arabidopsis* and may be associated with the eukaryotic spliceosome. *FEBS Lett* *587*, 873-879.
- Barberan-Soler, S., and Zahler, A.M. (2008). Alternative splicing regulation during *C. elegans* development: splicing factors as regulated targets. *PLoS Genet* *4*, e1000001.
- Bellare, P., Small, E.C., Huang, X., Wohlschlegel, J.A., Staley, J.P., and Sontheimer, E.J. (2008). A role for ubiquitin in the spliceosome assembly pathway. *Nat Struct Mol Biol* *15*, 444-451.
- Benard, C.Y., Kebir, H., Takagi, S., and Hekimi, S. (2004). mau-2 acts cell-autonomously to guide axonal migrations in *Caenorhabditis elegans*. *Development* *131*, 5947-5958.
- Berget, S.M. (1995). Exon recognition in vertebrate splicing. *J Biol Chem* *270*, 2411-2414.
- Bernard, P., Maure, J.F., Partridge, J.F., Genier, S., Javerzat, J.P., and Allshire, R.C. (2001). Requirement of heterochromatin for cohesion at centromeres. *Science* *294*, 2539-2542.
- Bessonov, S., Anokhina, M., Will, C.L., Urlaub, H., and Luhrmann, R. (2008). Isolation of an active step I spliceosome and composition of its RNP core. *Nature* *452*, 846-850.
- Beyer, A.L., Bouton, A.H., and Miller, O.L., Jr. (1981). Correlation of hnRNP structure and nascent transcript cleavage. *Cell* *26*, 155-165.
- Birkenbihl, R.P., and Subramani, S. (1992). Cloning and characterization of rad21 an essential gene of *Schizosaccharomyces pombe* involved in DNA double-strand-break repair. *Nucleic Acids Res* *20*, 6605-6611.
- Birkenbihl, R.P., and Subramani, S. (1995). The rad21 gene product of *Schizosaccharomyces pombe* is a nuclear, cell cycle-regulated phosphoprotein. *J Biol Chem* *270*, 7703-7711.
- Blencowe, B.J., Bauren, G., Eldridge, A.G., Issner, R., Nickerson, J.A., Rosonina, E., and Sharp, P.A. (2000). The SRm160/300 splicing coactivator subunits. *RNA* *6*, 111-120.
- Borges, V., Lehane, C., Lopez-Serra, L., Flynn, H., Skehel, M., Rolef Ben-Shahar, T., and Uhlmann, F. (2010). Hos1 deacetylates Smc3 to close the cohesin acetylation cycle. *Mol Cell* *39*, 677-688.
- Bose, T., Lee, K.K., Lu, S., Xu, B., Harris, B., Slaughter, B., Unruh, J., Garrett, A., McDowell, W., Box, A., *et al.* (2012). Cohesin proteins promote ribosomal RNA production and protein translation in yeast and human cells. *PLoS Genet* *8*, e1002749.
- Boucher, L., Ouzounis, C.A., Enright, A.J., and Blencowe, B.J. (2001). A genome-wide survey of RS domain proteins. *RNA* *7*, 1693-1701.
- Bradley, A., Zheng, H., Ziebarth, A., Sakati, W., Branham-O'Connor, M., Blumer, J.B., Liu, Y., Kistner-Griffin, E., Rodriguez-Aguayo, C., Lopez-Berestein, G., *et al.* (2014). EDD enhances cell survival and cisplatin resistance and is a therapeutic target for epithelial ovarian cancer. *Carcinogenesis* *35*, 1100-1109.
- Bridger, J.M., and Kill, I.R. (2004). Aging of Hutchinson-Gilford progeria syndrome fibroblasts is characterised by hyperproliferation and increased apoptosis. *Exp Gerontol* *39*, 717-724.

- Brooks, A.N., Choi, P.S., de Waal, L., Sharifnia, T., Imielinski, M., Saksena, G., Pedamallu, C.S., Sivachenko, A., Rosenberg, M., Chmielecki, J., *et al.* (2014). A pan-cancer analysis of transcriptome changes associated with somatic mutations in U2AF1 reveals commonly altered splicing events. *PLoS One* *9*, e87361.
- Brow, D.A. (2002). Allosteric cascade of spliceosome activation. *Annu Rev Genet* *36*, 333-360.
- Camozzi, D., Capanni, C., Cenni, V., Mattioli, E., Columbaro, M., Squarzone, S., and Lattanzi, G. (2014). Diverse lamin-dependent mechanisms interact to control chromatin dynamics. Focus on laminopathies. *Nucleus* *5*, 427-440.
- Carrillo Oesterreich, F., Preibisch, S., and Neugebauer, K.M. (2010). Global analysis of nascent RNA reveals transcriptional pausing in terminal exons. *Mol Cell* *40*, 571-581.
- Castedo, M., Perfettini, J.L., Roumier, T., Andreau, K., Medema, R., and Kroemer, G. (2004). Cell death by mitotic catastrophe: a molecular definition. *Oncogene* *23*, 2825-2837.
- Chan, Y.A., Hieter, P., and Stirling, P.C. (2014). Mechanisms of genome instability induced by RNA-processing defects. *Trends Genet* *30*, 245-253.
- Chen, A., Wu, K., Fuchs, S.Y., Tan, P., Gomez, C., and Pan, Z.Q. (2000). The conserved RING-H2 finger of ROC1 is required for ubiquitin ligation. *J Biol Chem* *275*, 15432-15439.
- Chen, H.W., Yang, C.C., Hsieh, C.L., Liu, H., Lee, S.C., and Tan, B.C. (2013). A functional genomic approach reveals the transcriptional role of EDD in the expression and function of angiogenesis regulator ACVRL1. *Biochim Biophys Acta* *1829*, 1309-1319.
- Chen, J., Shi, X., Padmanabhan, R., Wang, Q., Wu, Z., Stevenson, S.C., Hild, M., Garza, D., and Li, H. (2008). Identification of novel modulators of mitochondrial function by a genome-wide RNAi screen in *Drosophila melanogaster*. *Genome Res* *18*, 123-136.
- Chen, L., Bush, S.J., Tovar-Corona, J.M., Castillo-Morales, A., and Urrutia, A.O. (2014). Correcting for differential transcript coverage reveals a strong relationship between alternative splicing and organism complexity. *Mol Biol Evol* *31*, 1402-1413.
- Chen, Y., Zhang, L., and Jones, K.A. (2011). SKIP counteracts p53-mediated apoptosis via selective regulation of p21Cip1 mRNA splicing. *Genes Dev* *25*, 701-716.
- Chen, Z.H., Yu, Y.P., Michalopoulos, G., Nelson, J., and Luo, J.H. (2015). The DNA replication licensing factor miniature chromosome maintenance 7 is essential for RNA splicing of epidermal growth factor receptor, c-Met, and platelet-derived growth factor receptor. *J Biol Chem* *290*, 1404-1411.
- Chiba, T., Miyashita, K., Sugoh, T., Warita, T., Inoko, H., Kimura, M., and Sato, T. (2011). IkappaBL, a novel member of the nuclear IkappaB family, inhibits inflammatory cytokine expression. *FEBS Lett* *585*, 3577-3581.
- Chien, R., Zeng, W., Kawauchi, S., Bender, M.A., Santos, R., Gregson, H.C., Schmiesing, J.A., Newkirk, D.A., Kong, X., Ball, A.R., Jr., *et al.* (2011). Cohesin mediates chromatin interactions that regulate mammalian beta-globin expression. *J Biol Chem* *286*, 17870-17878.
- Chuang, P.T., Albertson, D.G., and Meyer, B.J. (1994). DPY-27: a chromosome condensation protein homolog that regulates *C. elegans* dosage compensation through association with the X chromosome. *Cell* *79*, 459-474.
- Ciccia, A., and Elledge, S.J. (2010). The DNA damage response: making it safe to play with knives. *Mol Cell* *40*, 179-204.

- Ciosk, R., Shirayama, M., Shevchenko, A., Tanaka, T., Toth, A., Shevchenko, A., and Nasmyth, K. (2000). Cohesin's binding to chromosomes depends on a separate complex consisting of Scc2 and Scc4 proteins. *Mol Cell* 5, 243-254.
- Clurman, B.E., Sheaff, R.J., Thress, K., Groudine, M., and Roberts, J.M. (1996). Turnover of cyclin E by the ubiquitin-proteasome pathway is regulated by cdk2 binding and cyclin phosphorylation. *Genes Dev* 10, 1979-1990.
- Company, M., Arenas, J., and Abelson, J. (1991). Requirement of the RNA helicase-like protein PRP22 for release of messenger RNA from spliceosomes. *Nature* 349, 487-493.
- Cooper, J.P., Nimmo, E.R., Allshire, R.C., and Cech, T.R. (1997). Regulation of telomere length and function by a Myb-domain protein in fission yeast. *Nature* 385, 744-747.
- Correa, R.G., Tergaonkar, V., Ng, J.K., Dubova, I., Izpissua-Belmonte, J.C., and Verma, I.M. (2004). Characterization of NF-kappa B/I kappa B proteins in zebra fish and their involvement in notochord development. *Mol Cell Biol* 24, 5257-5268.
- Cramer, P., Pesce, C.G., Baralle, F.E., and Kornblihtt, A.R. (1997). Functional association between promoter structure and transcript alternative splicing. *Proc Natl Acad Sci U S A* 94, 11456-11460.
- Dai, C., Tang, Y., Jung, S.Y., Qin, J., Aaronson, S.A., and Gu, W. (2011). Differential effects on p53-mediated cell cycle arrest vs. apoptosis by p90. *Proc Natl Acad Sci U S A* 108, 18937-18942.
- Damgaard, C.K., Kahns, S., Lykke-Andersen, S., Nielsen, A.L., Jensen, T.H., and Kjems, J. (2008). A 5' splice site enhances the recruitment of basal transcription initiation factors in vivo. *Mol Cell* 29, 271-278.
- Daum, J.R., Potapova, T.A., Sivakumar, S., Daniel, J.J., Flynn, J.N., Rankin, S., and Gorbsky, G.J. (2011). Cohesion Fatigue Induces Chromatid Separation in Cells Delayed at Metaphase. *Curr Biol* 21, 1018-1024.
- de Almeida, S.F., and Carmo-Fonseca, M. (2008). The CTD role in cotranscriptional RNA processing and surveillance. *FEBS Lett* 582, 1971-1976.
- de Lange, T. (2005). Shelterin: the protein complex that shapes and safeguards human telomeres. *Genes Dev* 19, 2100-2110.
- de Lange, T. (2009). How telomeres solve the end-protection problem. *Science* 326, 948-952.
- Dearth, R.K., Cui, X., Kim, H.J., Hadsell, D.L., and Lee, A.V. (2007). Oncogenic transformation by the signaling adaptor proteins insulin receptor substrate (IRS)-1 and IRS-2. *Cell Cycle* 6, 705-713.
- Destefano, M.A., and Jacinto, E. (2013). Regulation of insulin receptor substrate-1 by mTORC2 (mammalian target of rapamycin complex 2). *Biochem Soc Trans* 41, 896-901.
- Dias, D.C., Dolios, G., Wang, R., and Pan, Z.Q. (2002). CUL7: A DOC domain-containing cullin selectively binds Skp1.Fbx29 to form an SCF-like complex. *Proc Natl Acad Sci U S A* 99, 16601-16606.
- Diaz-Martinez, L.A., Gimenez-Abian, J.F., and Clarke, D.J. (2007). Regulation of centromeric cohesion by sororin independently of the APC/C. *Cell Cycle* 6, 714-724.
- Donjerkovic, D., and Scott, D.W. (2000). Regulation of the G1 phase of the mammalian cell cycle. *Cell Res* 10, 1-16.

- Dorsett, D. (2007). Roles of the sister chromatid cohesion apparatus in gene expression, development, and human syndromes. *Chromosoma* *116*, 1-13.
- Dorsett, D. (2011). Cohesin: genomic insights into controlling gene transcription and development. *Curr Opin Genet Dev* *21*, 199-206.
- Dreier, M.R., Bekier, M.E., and Taylor, W.R. (2011). Regulation of sororin by Cdk1-mediated phosphorylation. *Journal of Cell Science* *124*, 2976-2987.
- Dujardin, G., Lafaille, C., de la Mata, M., Marasco, L.E., Munoz, M.J., Le Jossic-Corcos, C., Corcos, L., and Kornblihtt, A.R. (2014). How slow RNA polymerase II elongation favors alternative exon skipping. *Mol Cell* *54*, 683-690.
- Duronio, R.J., and Xiong, Y. (2013). Signaling pathways that control cell proliferation. *Cold Spring Harb Perspect Biol* *5*, a008904.
- Dziuba, N., Ferguson, M.R., O'Brien, W.A., Sanchez, A., Prussia, A.J., McDonald, N.J., Friedrich, B.M., Li, G., Shaw, M.W., Sheng, J., *et al.* (2012). Identification of cellular proteins required for replication of human immunodeficiency virus type 1. *AIDS Res Hum Retroviruses* *28*, 1329-1339.
- English, M.A., Lei, L., Blake, T., Wincovitch, S.M., Sr., Sood, R., Azuma, M., Hickstein, D., and Liu, P.P. (2012). Incomplete splicing, cell division defects, and hematopoietic blockage in *dhx8* mutant zebrafish. *Dev Dyn* *241*, 879-889.
- Ergun, A., Doran, G., Costello, J.C., Paik, H.H., Collins, J.J., Mathis, D., Benoist, C., and ImmGen, C. (2013). Differential splicing across immune system lineages. *Proc Natl Acad Sci U S A* *110*, 14324-14329.
- Evan, G.I., Wyllie, A.H., Gilbert, C.S., Littlewood, T.D., Land, H., Brooks, M., Waters, C.M., Penn, L.Z., and Hancock, D.C. (1992). Induction of apoptosis in fibroblasts by *c-myc* protein. *Cell* *69*, 119-128.
- Ewing, R.M., Chu, P., Elisma, F., Li, H., Taylor, P., Climie, S., McBroom-Cerajewski, L., Robinson, M.D., O'Connor, L., Li, M., *et al.* (2007). Large-scale mapping of human protein-protein interactions by mass spectrometry. *Mol Syst Biol* *3*, 89.
- Fabrizio, P., Dannenberg, J., Dube, P., Kastner, B., Stark, H., Urlaub, H., and Luhrmann, R. (2009). The evolutionarily conserved core design of the catalytic activation step of the yeast spliceosome. *Mol Cell* *36*, 593-608.
- Fay, A., Misulovin, Z., Li, J., Schaaf, C.A., Gause, M., Gilmour, D.S., and Dorsett, D. (2011). Cohesin selectively binds and regulates genes with paused RNA polymerase. *Curr Biol* *21*, 1624-1634.
- Feytout, A., Vaur, S., Genier, S., Vazquez, S., and Javerzat, J.P. (2011). Psm3 acetylation on conserved lysine residues is dispensable for viability in fission yeast but contributes to Eso1-mediated sister chromatid cohesion by antagonizing Wpl1. *Mol Cell Biol* *31*, 1771-1786.
- Fontrodona, L., Porta-de-la-Riva, M., Moran, T., Niu, W., Diaz, M., Aristizabal-Corrales, D., Villanueva, A., Schwartz, S., Jr., Reinke, V., and Ceron, J. (2013). RSR-2, the *Caenorhabditis elegans* ortholog of human spliceosomal component SRm300/SRRM2, regulates development by influencing the transcriptional machinery. *PLoS Genet* *9*, e1003543.
- Foster, M.I., and Lehmann, A.R. (2000). A novel SMC protein complex in *Schizosaccharomyces pombe* contains the Rad18 DNA repair protein. *EMBO J* *19*, 1691-1702.

- Fox-Walsh, K.L., Dou, Y., Lam, B.J., Hung, S.P., Baldi, P.F., and Hertel, K.J. (2005). The architecture of pre-mRNAs affects mechanisms of splice-site pairing. *Proc Natl Acad Sci U S A* *102*, 16176-16181.
- Fullam, A., and Schroder, M. (2013). DExD/H-box RNA helicases as mediators of anti-viral innate immunity and essential host factors for viral replication. *Biochim Biophys Acta* *1829*, 854-865.
- Fumagalli, M., Rossiello, F., Clerici, M., Barozzi, S., Cittaro, D., Kaplunov, J.M., Bucci, G., Dobрева, M., Matti, V., Beausejour, C.M., *et al.* (2012). Telomeric DNA damage is irreparable and causes persistent DNA-damage-response activation. *Nat Cell Biol* *14*, 355-365.
- Gallego-Paez, L.M., Tanaka, H., Bando, M., Takahashi, M., Nozaki, N., Nakato, R., Shirahige, K., and Hirota, T. (2014). Smc5/6-mediated regulation of replication progression contributes to chromosome assembly during mitosis in human cells. *Mol Biol Cell* *25*, 302-317.
- Game, J.C., Birrell, G.W., Brown, J.A., Shibata, T., Baccari, C., Chu, A.M., Williamson, M.S., and Brown, J.M. (2003). Use of a genome-wide approach to identify new genes that control resistance of *Saccharomyces cerevisiae* to ionizing radiation. *Radiat Res* *160*, 14-24.
- Gandhi, R., Gillespie, P.J., and Hirano, T. (2006). Human Wapl is a cohesin-binding protein that promotes sister-chromatid resolution in mitotic prophase. *Curr Biol* *16*, 2406-2417.
- Gause, M., Misulovin, Z., Bilyeu, A., and Dorsett, D. (2010). Dosage-sensitive regulation of cohesin chromosome binding and dynamics by Nipped-B, Pds5, and Wapl. *Mol Cell Biol* *30*, 4940-4951.
- Gautam, A., Grainger, R.J., Vilardell, J., Barrass, J.D., and Beggs, J.D. (2015). Cwc21p promotes the second step conformation of the spliceosome and modulates 3' splice site selection. *Nucleic Acids Res* *43*, 3309-3317.
- Geisler, S.B., Robinson, D., Hauringa, M., Raeker, M.O., Borisov, A.B., Westfall, M.V., and Russell, M.W. (2007). Obscurin-like 1, OBSL1, is a novel cytoskeletal protein related to obscurin. *Genomics* *89*, 521-531.
- Gelot, C., Guirouilh-Barbat, J., Le Guen, T., Dardillac, E., Chailleux, C., Canitrot, Y., and Lopez, B.S. (2016). The Cohesin Complex Prevents the End Joining of Distant DNA Double-Strand Ends. *Mol Cell* *61*, 15-26.
- George, C.M., Bozler, J., Nguyen, H.Q., and Bosco, G. (2014). Condensins are Required for Maintenance of Nuclear Architecture. *Cells* *3*, 865-882.
- Gerlich, D., Koch, B., Dupeux, F., Peters, J.M., and Ellenberg, J. (2006). Live-cell imaging reveals a stable cohesin-chromatin interaction after but not before DNA replication. *Curr Biol* *16*, 1571-1578.
- Giannakouros, T., Nikolakaki, E., Mylonis, I., and Georgatsou, E. (2011). Serine-arginine protein kinases: a small protein kinase family with a large cellular presence. *FEBS J* *278*, 570-586.
- Giot, L., Bader, J.S., Brouwer, C., Chaudhuri, A., Kuang, B., Li, Y., Hao, Y.L., Ooi, C.E., Godwin, B., Vitols, E., *et al.* (2003). A protein interaction map of *Drosophila melanogaster*. *Science* *302*, 1727-1736.
- Goncalves, V., Henriques, A.F., Pereira, J.F., Costa, A.N., Moyer, M.P., Moita, L.F., Gama-Carvalho, M., Matos, P., and Jordan, P. (2016). Corrigendum: Phosphorylation of SRSF1 by SRPK1 regulates alternative splicing of tumor-related Rac1b in colorectal cells. *RNA* *22*, 166.

- Gorbsky, G.J. (2013). Cohesion fatigue. *Curr Biol* 23, R986-988.
- Goshima, G., Wollman, R., Goodwin, S.S., Zhang, N., Scholey, J.M., Vale, R.D., and Stuurman, N. (2007). Genes required for mitotic spindle assembly in *Drosophila* S2 cells. *Science* 316, 417-421.
- Govind, S. (1999). Control of development and immunity by rel transcription factors in *Drosophila*. *Oncogene* 18, 6875-6887.
- Govind, S., Brennan, L., and Steward, R. (1993). Homeostatic balance between dorsal and cactus proteins in the *Drosophila* embryo. *Development* 117, 135-148.
- Grainger, R.J., Barrass, J.D., Jacquier, A., Rain, J.C., and Beggs, J.D. (2009). Physical and genetic interactions of yeast Cwc21p, an ortholog of human SRm300/SRRM2, suggest a role at the catalytic center of the spliceosome. *RNA* 15, 2161-2173.
- Grainger, R.J., and Beggs, J.D. (2005). Prp8 protein: at the heart of the spliceosome. *RNA* 11, 533-557.
- Graveley, B.R., and Maniatis, T. (1998). Arginine/serine-rich domains of SR proteins can function as activators of pre-mRNA splicing. *Mol Cell* 1, 765-771.
- Greenwood, J., and Cooper, J.P. (2012). Non-coding telomeric and subtelomeric transcripts are differentially regulated by telomeric and heterochromatin assembly factors in fission yeast. *Nucleic Acids Res* 40, 2956-2963.
- Grosso, A.R., Martins, S., and Carmo-Fonseca, M. (2008). The emerging role of splicing factors in cancer. *EMBO Rep* 9, 1087-1093.
- Gruber, S., Haering, C.H., and Nasmyth, K. (2003). Chromosomal cohesin forms a ring. *Cell* 112, 765-777.
- Gu, B., Eick, D., and Bensaude, O. (2013). CTD serine-2 plays a critical role in splicing and termination factor recruitment to RNA polymerase II in vivo. *Nucleic Acids Res* 41, 1591-1603.
- Guacci, V., Koshland, D., and Strunnikov, A. (1997). A direct link between sister chromatid cohesion and chromosome condensation revealed through the analysis of MCD1 in *S. cerevisiae*. *Cell* 91, 47-57.
- Guenatri, M., Bailly, D., Maison, C., and Almouzni, G. (2004). Mouse centric and pericentric satellite repeats form distinct functional heterochromatin. *J Cell Biol* 166, 493-505.
- Gullerova, M., and Proudfoot, N.J. (2008). Cohesin complex promotes transcriptional termination between convergent genes in *S. pombe*. *Cell* 132, 983-995.
- Guo, H., Wu, F., Wang, Y., Yan, C., and Su, W. (2014). Overexpressed ubiquitin ligase Cullin7 in breast cancer promotes cell proliferation and invasion via down-regulating p53. *Biochem Biophys Res Commun* 450, 1370-1376.
- Hacker, I., Sander, B., Golas, M.M., Wolf, E., Karagoz, E., Kastner, B., Stark, H., Fabrizio, P., and Luhrmann, R. (2008). Localization of Prp8, Brr2, Snu114 and U4/U6 proteins in the yeast tri-snRNP by electron microscopy. *Nat Struct Mol Biol* 15, 1206-1212.
- Haering, C.H., Lowe, J., Hochwagen, A., and Nasmyth, K. (2002). Molecular architecture of SMC proteins and the yeast cohesin complex. *Mol Cell* 9, 773-788.

- Hagting, A., Den Elzen, N., Vodermaier, H.C., Waizenegger, I.C., Peters, J.M., and Pines, J. (2002). Human securin proteolysis is controlled by the spindle checkpoint and reveals when the APC/C switches from activation by Cdc20 to Cdh1. *J Cell Biol* *157*, 1125-1137.
- Hahn, C.N., and Scott, H.S. (2012). Spliceosome mutations in hematopoietic malignancies. *Nat Genet* *44*, 9-10.
- Hanson, D., Murray, P.G., Coulson, T., Sud, A., Omokanye, A., Stratta, E., Sakhinia, F., Bonshek, C., Wilson, L.C., Wakeling, E., *et al.* (2012). Mutations in CUL7, OBSL1 and CCDC8 in 3-M syndrome lead to disordered growth factor signalling. *J Mol Endocrinol* *49*, 267-275.
- Hartman, T., Stead, K., Koshland, D., and Guacci, V. (2000). Pds5p is an essential chromosomal protein required for both sister chromatid cohesion and condensation in *Saccharomyces cerevisiae*. *J Cell Biol* *151*, 613-626.
- Hartmann, T., Xu, X., Kronast, M., Muehlich, S., Meyer, K., Zimmermann, W., Hurwitz, J., Pan, Z.Q., Engelhardt, S., and Sarikas, A. (2014). Inhibition of Cullin-RING E3 ubiquitin ligase 7 by simian virus 40 large T antigen. *Proc Natl Acad Sci U S A* *111*, 3371-3376.
- Hauf, S., Waizenegger, I.C., and Peters, J.M. (2001). Cohesin cleavage by separase required for anaphase and cytokinesis in human cells. *Science* *293*, 1320-1323.
- Hayashi, M.T., Cesare, A.J., Fitzpatrick, J.A., Lazzarini-Denchi, E., and Karlseder, J. (2012). A telomere-dependent DNA damage checkpoint induced by prolonged mitotic arrest. *Nat Struct Mol Biol* *19*, 387-394.
- Hayles, J., Wood, V., Jeffery, L., Hoe, K.L., Kim, D.U., Park, H.O., Salas-Pino, S., Heichinger, C., and Nurse, P. (2013). A genome-wide resource of cell cycle and cell shape genes of fission yeast. *Open Biol* *3*, 130053.
- Hegele, A., Kamburov, A., Grossmann, A., Sourlis, C., Wowro, S., Weimann, M., Will, C.L., Pena, V., Luhrmann, R., and Stelzl, U. (2012). Dynamic protein-protein interaction wiring of the human spliceosome. *Mol Cell* *45*, 567-580.
- Heidinger-Pauli, J.M., Unal, E., Guacci, V., and Koshland, D. (2008). The kleisin subunit of cohesin dictates damage-induced cohesion. *Mol Cell* *31*, 47-56.
- Henderson, M.J., Munoz, M.A., Saunders, D.N., Clancy, J.L., Russell, A.J., Williams, B., Pappin, D., Khanna, K.K., Jackson, S.P., Sutherland, R.L., *et al.* (2006). EDD mediates DNA damage-induced activation of CHK2. *J Biol Chem* *281*, 39990-40000.
- Herman, M. (2001). *C. elegans* POP-1/TCF functions in a canonical Wnt pathway that controls cell migration and in a noncanonical Wnt pathway that controls cell polarity. *Development* *128*, 581-590.
- Herold, N., Will, C.L., Wolf, E., Kastner, B., Urlaub, H., and Luhrmann, R. (2009). Conservation of the protein composition and electron microscopy structure of *Drosophila melanogaster* and human spliceosomal complexes. *Mol Cell Biol* *29*, 281-301.
- Hirano, T., Kobayashi, R., and Hirano, M. (1997). Condensins, chromosome condensation protein complexes containing XCAP-C, XCAP-E and a *Xenopus* homolog of the *Drosophila* Barren protein. *Cell* *89*, 511-521.
- Hirose, Y., Tacke, R., and Manley, J.L. (1999). Phosphorylated RNA polymerase II stimulates pre-mRNA splicing. *Genes Dev* *13*, 1234-1239.



- Ho, C.Y., Murnane, J.P., Yeung, A.K., Ng, H.K., and Lo, A.W. (2008). Telomeres acquire distinct heterochromatin characteristics during siRNA-induced RNA interference in mouse cells. *Curr Biol* *18*, 183-187.
- Hoffman, B.E., and Grabowski, P.J. (1992). U1 snRNP targets an essential splicing factor, U2AF65, to the 3' splice site by a network of interactions spanning the exon. *Genes Dev* *6*, 2554-2568.
- Horsfield, J.A., Anagnostou, S.H., Hu, J.K., Cho, K.H., Geisler, R., Lieschke, G., Crosier, K.E., and Crosier, P.S. (2007). Cohesin-dependent regulation of Runx genes. *Development* *134*, 2639-2649.
- Hsin, J.P., and Manley, J.L. (2012). The RNA polymerase II CTD coordinates transcription and RNA processing. *Genes Dev* *26*, 2119-2137.
- Hu, B., Itoh, T., Mishra, A., Katoh, Y., Chan, K.L., Upcher, W., Godlee, C., Roig, M.B., Shirahige, K., and Nasmyth, K. (2011). ATP hydrolysis is required for relocating cohesin from sites occupied by its Scc2/4 loading complex. *Curr Biol* *21*, 12-24.
- Huang, V., and Li, L.C. (2014). Demystifying the nuclear function of Argonaute proteins. *RNA Biol* *11*, 18-24.
- Huber, C., Fradin, M., Edouard, T., Le Merrer, M., Alanay, Y., Da Silva, D.B., David, A., Hamamy, H., van Hest, L., Lund, A.M., *et al.* (2010). OBSL1 mutations in 3-M syndrome are associated with a modulation of IGFBP2 and IGFBP5 expression levels. *Hum Mutat* *31*, 20-26.
- Inoue, A., Hyle, J., Lechner, M.S., and Lahti, J.M. (2008). Perturbation of HP1 localization and chromatin binding ability causes defects in sister-chromatid cohesion. *Mutat Res* *657*, 48-55.
- Jain, D., and Cooper, J.P. (2010). Telomeric strategies: means to an end. *Annu Rev Genet* *44*, 243-269.
- Jeppsson, K., Kanno, T., Shirahige, K., and Sjogren, C. (2014). The maintenance of chromosome structure: positioning and functioning of SMC complexes. *Nat Rev Mol Cell Biol* *15*, 601-614.
- Jin, J., Samuvel, D.J., Zhang, X., Li, Y., Lu, Z., Lopes-Virella, M.F., and Huang, Y. (2011). Coactivation of TLR4 and TLR2/6 coordinates an additive augmentation on IL-6 gene transcription via p38MAPK pathway in U937 mononuclear cells. *Mol Immunol* *49*, 423-432.
- Jung, P., Verdoodt, B., Bailey, A., Yates, J.R., 3rd, Menssen, A., and Hermeking, H. (2007). Induction of cullin 7 by DNA damage attenuates p53 function. *Proc Natl Acad Sci U S A* *104*, 11388-11393.
- Jurica, M.S., Licklider, L.J., Gygi, S.R., Grigorieff, N., and Moore, M.J. (2002). Purification and characterization of native spliceosomes suitable for three-dimensional structural analysis. *RNA* *8*, 426-439.
- Jurica, M.S., and Moore, M.J. (2003). Pre-mRNA splicing: awash in a sea of proteins. *Mol Cell* *12*, 5-14.
- Kabir, S., Sfeir, A., and de Lange, T. (2010). Taking apart Rap1: an adaptor protein with telomeric and non-telomeric functions. *Cell Cycle* *9*, 4061-4067.
- Kagey, M.H., Newman, J.J., Bilodeau, S., Zhan, Y., Orlando, D.A., van Berkum, N.L., Ebmeier, C.C., Goossens, J., Rahl, P.B., Levine, S.S., *et al.* (2010). Mediator and cohesin connect gene expression and chromatin architecture. *Nature* *467*, 430-435.

- Kannan, R., Hartnett, S., Voelker, R.B., Berglund, J.A., Staley, J.P., and Baumann, P. (2013). Intronic sequence elements impede exon ligation and trigger a discard pathway that yields functional telomerase RNA in fission yeast. *Genes Dev* *27*, 627-638.
- Kanoh, J., and Ishikawa, F. (2001). spRap1 and spRif1, recruited to telomeres by Taz1, are essential for telomere function in fission yeast. *Curr Biol* *11*, 1624-1630.
- Kanoh, J., and Ishikawa, F. (2003). Composition and conservation of the telomeric complex. *Cell Mol Life Sci* *60*, 2295-2302.
- Karni, R., de Stanchina, E., Lowe, S.W., Sinha, R., Mu, D., and Krainer, A.R. (2007). The gene encoding the splicing factor SF2/ASF is a proto-oncogene. *Nat Struct Mol Biol* *14*, 185-193.
- Kaustov, L., Lukin, J., Lemak, A., Duan, S., Ho, M., Doherty, R., Penn, L.Z., and Arrowsmith, C.H. (2007). The conserved CPH domains of Cul7 and PARC are protein-protein interaction modules that bind the tetramerization domain of p53. *J Biol Chem* *282*, 11300-11307.
- Khodor, Y.L., Rodriguez, J., Abruzzi, K.C., Tang, C.H., Marr, M.T., 2nd, and Rosbash, M. (2011). Nascent-seq indicates widespread cotranscriptional pre-mRNA splicing in *Drosophila*. *Genes Dev* *25*, 2502-2512.
- Kim, S., Kim, H., Fong, N., Erickson, B., and Bentley, D.L. (2011). Pre-mRNA splicing is a determinant of histone H3K36 methylation. *Proc Natl Acad Sci U S A* *108*, 13564-13569.
- Kim, S.S., Shago, M., Kaustov, L., Boutros, P.C., Clendening, J.W., Sheng, Y., Trentin, G.A., Barsyte-Lovejoy, D., Mao, D.Y.L., Kay, R., *et al.* (2007). CUL7 is a novel antiapoptotic oncogene. *Cancer Res* *67*, 9616-9622.
- Kim, S.T., Xu, B., and Kastan, M.B. (2002). Involvement of the cohesin protein, Smc1, in Atm-dependent and independent responses to DNA damage. *Genes Dev* *16*, 560-570.
- Kishore, S., and Stamm, S. (2006). Regulation of alternative splicing by snoRNAs. *Cold Spring Harb Symp Quant Biol* *71*, 329-334.
- Klusza, S., Novak, A., Figueroa, S., Palmer, W., and Deng, W.M. (2013). Prp22 and spliceosome components regulate chromatin dynamics in germ-line polyploid cells. *PLoS One* *8*, e79048.
- Klutstein, M., Fennell, A., Fernandez-Alvarez, A., and Cooper, J.P. (2015). The telomere bouquet regulates meiotic centromere assembly. *Nat Cell Biol* *17*, 458-469.
- Kopan, R. (2012). Notch signaling. *Cold Spring Harb Perspect Biol* *4*.
- Kornblihtt, A.R., de la Mata, M., Fededa, J.P., Munoz, M.J., and Nogues, G. (2004). Multiple links between transcription and splicing. *RNA* *10*, 1489-1498.
- Krantz, I.D., McCallum, J., DeScipio, C., Kaur, M., Gillis, L.A., Yaeger, D., Jukofsky, L., Wasserman, N., Bottani, A., Morris, C.A., *et al.* (2004). Cornelia de Lange syndrome is caused by mutations in NIPBL, the human homolog of *Drosophila melanogaster* Nipped-B. *Nat Genet* *36*, 631-635.
- Krenn, V., and Musacchio, A. (2015). The Aurora B Kinase in Chromosome Bi-Orientation and Spindle Checkpoint Signaling. *Front Oncol* *5*, 225.
- Kruiswijk, F., Labuschagne, C.F., and Vousden, K.H. (2015). p53 in survival, death and metabolic health: a lifeguard with a licence to kill. *Nat Rev Mol Cell Biol* *16*, 393-405.

- Kueng, S., Hegemann, B., Peters, B.H., Lipp, J.J., Schleiffer, A., Mechtler, K., and Peters, J.M. (2006). Wapl controls the dynamic association of cohesin with chromatin. *Cell* *127*, 955-967.
- Kuhn, A.N., van Santen, M.A., Schwienhorst, A., Urlaub, H., and Luhrmann, R. (2009). Stalling of spliceosome assembly at distinct stages by small-molecule inhibitors of protein acetylation and deacetylation. *RNA* *15*, 153-175.
- Kurata, R., Nakaoka, H., Tajima, A., Hosomichi, K., Shiina, T., Meguro, A., Mizuki, N., Ohono, S., Inoue, I., and Inoko, H. (2010). TRIM39 and RNF39 are associated with Behcet's disease independently of HLA-B \*51 and -A \*26. *Biochem Biophys Res Commun* *401*, 533-537.
- Kurata, R., Tajima, A., Yonezawa, T., and Inoko, H. (2013). TRIM39R, but not TRIM39B, regulates type I interferon response. *Biochem Biophys Res Commun* *436*, 90-95.
- Kwek, K.Y., Murphy, S., Furger, A., Thomas, B., O'Gorman, W., Kimura, H., Proudfoot, N.J., and Akoulitchev, A. (2002). U1 snRNA associates with TFIIH and regulates transcriptional initiation. *Nat Struct Biol* *9*, 800-805.
- LaBonty, M., Szmygiel, C., Byrnes, L.E., Hughes, S., Woollard, A., and Cram, E.J. (2014). CACN-1/Cactin plays a role in Wnt signaling in *C. elegans*. *PLoS One* *9*, e101945.
- Lafont, A.L., Song, J., and Rankin, S. (2010). Sororin cooperates with the acetyltransferase Eco2 to ensure DNA replication-dependent sister chromatid cohesion. *Proc Natl Acad Sci U S A* *107*, 20364-20369.
- Lakin, N.D., and Jackson, S.P. (1999). Regulation of p53 in response to DNA damage. *Oncogene* *18*, 7644-7655.
- Lavoie, B.D., Hogan, E., and Koshland, D. (2004). In vivo requirements for rDNA chromosome condensation reveal two cell-cycle-regulated pathways for mitotic chromosome folding. *Genes Dev* *18*, 76-87.
- Le Hir, H., Gatfield, D., Izaurralde, E., and Moore, M.J. (2001). The exon-exon junction complex provides a binding platform for factors involved in mRNA export and nonsense-mediated mRNA decay. *EMBO J* *20*, 4987-4997.
- Le Hir, H., Izaurralde, E., Maquat, L.E., and Moore, M.J. (2000). The spliceosome deposits multiple proteins 20-24 nucleotides upstream of mRNA exon-exon junctions. *EMBO J* *19*, 6860-6869.
- Le Hir, H., and Seraphin, B. (2008). EJC's at the heart of translational control. *Cell* *133*, 213-216.
- Lee, K.M., and Tarn, W.Y. (2013). Coupling pre-mRNA processing to transcription on the RNA factory assembly line. *RNA Biol* *10*, 380-390.
- Lee, S.S., Fu, N.Y., Sukumaran, S.K., Wan, K.F., Wan, Q., and Yu, V.C. (2009). TRIM39 is a MOAP-1-binding protein that stabilizes MOAP-1 through inhibition of its poly-ubiquitination process. *Exp Cell Res* *315*, 1313-1325.
- Lee, Y., and Rio, D.C. (2015). Mechanisms and Regulation of Alternative Pre-mRNA Splicing. *Annu Rev Biochem* *84*, 291-323.
- Lehner, B., Semple, J.I., Brown, S.E., Counsell, D., Campbell, R.D., and Sanderson, C.M. (2004). Analysis of a high-throughput yeast two-hybrid system and its use to predict the function of intracellular proteins encoded within the human MHC class III region. *Genomics* *83*, 153-167.

- Lengronne, A., Katou, Y., Mori, S., Yokobayashi, S., Kelly, G.P., Itoh, T., Watanabe, Y., Shirahige, K., and Uhlmann, F. (2004). Cohesin relocation from sites of chromosomal loading to places of convergent transcription. *Nature* *430*, 573-578.
- Lens, S.M., Wolthuis, R.M., Klompaker, R., Kauw, J., Agami, R., Brummelkamp, T., Kops, G., and Medema, R.H. (2003). Survivin is required for a sustained spindle checkpoint arrest in response to lack of tension. *EMBO J* *22*, 2934-2947.
- Li, B., Oestreich, S., and de Lange, T. (2000). Identification of human Rap1: implications for telomere evolution. *Cell* *101*, 471-483.
- Li, X., and Manley, J.L. (2005). Inactivation of the SR protein splicing factor ASF/SF2 results in genomic instability. *Cell* *122*, 365-378.
- Li, Z.J., Pei, X.H., Yan, J., Yan, F., Cappell, K.M., Whitehurst, A.W., and Xiong, Y. (2014). CUL9 Mediates the Functions of the 3M Complex and Ubiquitylates Survivin to Maintain Genome Integrity. *Mol Cell* *54*, 805-819.
- Lin, P., Fu, J., Zhao, B., Lin, F., Zou, H., Liu, L., Zhu, C., Wang, H., and Yu, X. (2011). Fbxw8 is involved in the proliferation of human choriocarcinoma JEG-3 cells. *Mol Biol Rep* *38*, 1741-1747.
- Lin, P., Huang, L.H., and Steward, R. (2000). Cactin, a conserved protein that interacts with the *Drosophila* I kappaB protein cactus and modulates its function. *Mech Dev* *94*, 57-65.
- Lin, S., Coutinho-Mansfield, G., Wang, D., Pandit, S., and Fu, X.D. (2008). The splicing factor SC35 has an active role in transcriptional elongation. *Nat Struct Mol Biol* *15*, 819-826.
- Litterman, N., Ikeuchi, Y., Gallardo, G., O'Connell, B.C., Sowa, M.E., Gygi, S.P., Harper, J.W., and Bonni, A. (2011). An OBSL1-Cul7Fbxw8 ubiquitin ligase signaling mechanism regulates Golgi morphology and dendrite patterning. *PLoS Biol* *9*, e1001060.
- Liu, Y.C., and Cheng, S.C. (2015). Functional roles of DEXD/H-box RNA helicases in Pre-mRNA splicing. *J Biomed Sci* *22*, 54.
- Loomis, R.J., Naoe, Y., Parker, J.B., Savic, V., Bozovsky, M.R., Macfarlan, T., Manley, J.L., and Chakravarti, D. (2009). Chromatin binding of SRp20 and ASF/SF2 and dissociation from mitotic chromosomes is modulated by histone H3 serine 10 phosphorylation. *Mol Cell* *33*, 450-461.
- Lorenzi, L.E., Bah, A., Wischnewski, H., Shchepachev, V., Sonesson, C., Santagostino, M., and Azzalin, C.M. (2015). Fission yeast Cactin restricts telomere transcription and elongation by controlling Rap1 levels. *EMBO J* *34*, 115-129.
- Losada, A., Hirano, M., and Hirano, T. (2002). Cohesin release is required for sister chromatid resolution, but not for condensin-mediated compaction, at the onset of mitosis. *Genes Dev* *16*, 3004-3016.
- Losada, A., Yokochi, T., Kobayashi, R., and Hirano, T. (2000). Identification and characterization of SA/Scp3p subunits in the *Xenopus* and human cohesin complexes. *J Cell Biol* *150*, 405-416.
- Lukas, C., Savic, V., Bekker-Jensen, S., Doil, C., Neumann, B., Pedersen, R.S., Grofte, M., Chan, K.L., Hickson, I.D., Bartek, J., *et al.* (2011). 53BP1 nuclear bodies form around DNA lesions generated by mitotic transmission of chromosomes under replication stress. *Nat Cell Biol* *13*, 243-253.

- Lykke-Andersen, J., Shu, M.D., and Steitz, J.A. (2001). Communication of the position of exon-exon junctions to the mRNA surveillance machinery by the protein RNPS1. *Science* *293*, 1836-1839.
- Maduro, M.F., Lin, R., and Rothman, J.H. (2002). Dynamics of a developmental switch: recursive intracellular and intranuclear redistribution of *Caenorhabditis elegans* POP-1 parallels Wnt-inhibited transcriptional repression. *Dev Biol* *248*, 128-142.
- Maniatis, T., and Reed, R. (2002). An extensive network of coupling among gene expression machines. *Nature* *416*, 499-506.
- Martinez, P., Gomez-Lopez, G., Garcia, F., Mercken, E., Mitchell, S., Flores, J.M., de Cabo, R., and Blasco, M.A. (2013). RAP1 protects from obesity through its extratelomeric role regulating gene expression. *Cell Rep* *3*, 2059-2074.
- Martinez, P., Thanasoula, M., Carlos, A.R., Gomez-Lopez, G., Tejera, A.M., Schoeftner, S., Dominguez, O., Pisano, D.G., Tarsounas, M., and Blasco, M.A. (2010). Mammalian Rap1 controls telomere function and gene expression through binding to telomeric and extratelomeric sites. *Nat Cell Biol* *12*, 768-780.
- Mattioli, E., Columbaro, M., Capanni, C., Santi, S., Maraldi, N.M., D'Apice, M.R., Novelli, G., Riccio, M., Squarizoni, S., Foisner, R., *et al.* (2008). Drugs affecting prelamin A processing: effects on heterochromatin organization. *Exp Cell Res* *314*, 453-462.
- Mayas, R.M., Maita, H., and Staley, J.P. (2006). Exon ligation is proofread by the DExD/H-box ATPase Prp22p. *Nature Structural & Molecular Biology* *13*, 482-490.
- McCracken, S., Lambermon, M., and Blencowe, B.J. (2002). SRm160 splicing coactivator promotes transcript 3'-end cleavage. *Mol Cell Biol* *22*, 148-160.
- McCracken, S., Longman, D., Marcon, E., Moens, P., Downey, M., Nickerson, J.A., Jessberger, R., Wilde, A., Caceres, J.F., Emili, A., *et al.* (2005). Proteomic analysis of SRm160-containing complexes reveals a conserved association with cohesin. *J Biol Chem* *280*, 42227-42236.
- McManus, C.J., and Graveley, B.R. (2011). RNA structure and the mechanisms of alternative splicing. *Curr Opin Genet Dev* *21*, 373-379.
- McPheeters, D.S., Schwer, B., and Muhlenkamp, P. (2000). Interaction of the yeast DExH-box RNA helicase prp22p with the 3' splice site during the second step of nuclear pre-mRNA splicing. *Nucleic Acids Res* *28*, 1313-1321.
- Mehta, G.D., Kumar, R., Srivastava, S., and Ghosh, S.K. (2013). Cohesin: functions beyond sister chromatid cohesion. *FEBS Lett* *587*, 2299-2312.
- Men, X., Wang, L., Yu, W., and Ju, Y. (2015). Cullin7 is required for lung cancer cell proliferation and is overexpressed in lung cancer. *Oncol Res* *22*, 123-128.
- Merkhofer, E.C., Hu, P., and Johnson, T.L. (2014). Introduction to cotranscriptional RNA splicing. *Methods Mol Biol* *1126*, 83-96.
- Michaelis, C., Ciosk, R., and Nasmyth, K. (1997). Cohesins: chromosomal proteins that prevent premature separation of sister chromatids. *Cell* *91*, 35-45.
- Misulovin, Z., Schwartz, Y.B., Li, X.Y., Kahn, T.G., Gause, M., MacArthur, S., Fay, J.C., Eisen, M.B., Pirrotta, V., Biggin, M.D., *et al.* (2008). Association of cohesin and Nipped-B with transcriptionally active regions of the *Drosophila melanogaster* genome. *Chromosoma* *117*, 89-102.

- Moore, M.J., and Sharp, P.A. (1993). Evidence for two active sites in the spliceosome provided by stereochemistry of pre-mRNA splicing. *Nature* *365*, 364-368.
- Morrison, D.K. (2012). MAP kinase pathways. *Cold Spring Harb Perspect Biol* *4*.
- Mu, R., Wang, Y.B., Wu, M., Yang, Y., Song, W., Li, T., Zhang, W.N., Tan, B., Li, A.L., Wang, N., *et al.* (2014). Depletion of pre-mRNA splicing factor Cdc5L inhibits mitotic progression and triggers mitotic catastrophe. *Cell Death Dis* *5*, e1151.
- Murtaza, M., Jolly, L.A., Gecz, J., and Wood, S.A. (2015). La FAM fatale: USP9X in development and disease. *Cell Mol Life Sci* *72*, 2075-2089.
- Neelsen, K.J., Zanini, I.M., Herrador, R., and Lopes, M. (2013a). Oncogenes induce genotoxic stress by mitotic processing of unusual replication intermediates. *J Cell Biol* *200*, 699-708.
- Neelsen, K.J., Zanini, I.M., Mijic, S., Herrador, R., Zellweger, R., Ray Chaudhuri, A., Creavin, K.D., Blow, J.J., and Lopes, M. (2013b). Deregulated origin licensing leads to chromosomal breaks by rereplication of a gapped DNA template. *Genes Dev* *27*, 2537-2542.
- Newman, A.J., and Nagai, K. (2010). Structural studies of the spliceosome: blind men and an elephant. *Curr Opin Struct Biol* *20*, 82-89.
- Nguyen, M.H., Koinuma, J., Ueda, K., Ito, T., Tsuchiya, E., Nakamura, Y., and Daigo, Y. (2010). Phosphorylation and Activation of Cell Division Cycle Associated 5 by Mitogen-Activated Protein Kinase Play a Crucial Role in Human Lung Carcinogenesis. *Cancer Res* *70*, 5337-5347.
- Nilsen, T.W., and Graveley, B.R. (2010). Expansion of the eukaryotic proteome by alternative splicing. *Nature* *463*, 457-463.
- Nishiyama, T., Ladurner, R., Schmitz, J., Kreidl, E., Schleiffer, A., Bhaskara, V., Bando, M., Shirahige, K., Hyman, A.A., Mechtler, K., *et al.* (2010). Sororin mediates sister chromatid cohesion by antagonizing Wapl. *Cell* *143*, 737-749.
- Nonaka, N., Kitajima, T., Yokobayashi, S., Xiao, G., Yamamoto, M., Grewal, S.I., and Watanabe, Y. (2002). Recruitment of cohesin to heterochromatic regions by Swi6/HP1 in fission yeast. *Nat Cell Biol* *4*, 89-93.
- Nott, A., Le Hir, H., and Moore, M.J. (2004). Splicing enhances translation in mammalian cells: an additional function of the exon junction complex. *Genes Dev* *18*, 210-222.
- Nusse, R. (2012). Wnt signaling. *Cold Spring Harb Perspect Biol* *4*.
- Ohh, M., Kim, W.Y., Moslehi, J.J., Chen, Y., Chau, V., Read, M.A., and Kaelin, W.G., Jr. (2002). An intact NEDD8 pathway is required for Cullin-dependent ubiquitylation in mammalian cells. *EMBO Rep* *3*, 177-182.
- Ohlsson, R., Bartkuhn, M., and Renkawitz, R. (2010). CTCF shapes chromatin by multiple mechanisms: the impact of 20 years of CTCF research on understanding the workings of chromatin. *Chromosoma* *119*, 351-360.
- Ohno, M., and Shimura, Y. (1996). A human RNA helicase-like protein, HRH1, facilitates nuclear export of spliced mRNA by releasing the RNA from the spliceosome. *Genes Dev* *10*, 997-1007.

- Oka, Y., Varmark, H., Vitting-Seerup, K., Beli, P., Waage, J., Hakobyan, A., Mistrik, M., Choudhary, C., Rohde, M., Bekker-Jensen, S., *et al.* (2014). UBL5 is essential for pre-mRNA splicing and sister chromatid cohesion in human cells. *EMBO Rep* *15*, 956-964.
- Okabe, H., Lee, S.H., Phuchareon, J., Albertson, D.G., McCormick, F., and Tetsu, O. (2006). A critical role for FBXW8 and MAPK in cyclin D1 degradation and cancer cell proliferation. *PLoS One* *1*, e128.
- Painter, H.J., Campbell, T.L., and Llinas, M. (2011). The Apicomplexan AP2 family: integral factors regulating Plasmodium development. *Mol Biochem Parasitol* *176*, 1-7.
- Parelho, V., Hadjur, S., Spivakov, M., Leleu, M., Sauer, S., Gregson, H.C., Jarmuz, A., Canzonetta, C., Webster, Z., Nesterova, T., *et al.* (2008). Cohesins functionally associate with CTCF on mammalian chromosome arms. *Cell* *132*, 422-433.
- Patel, A.A., and Steitz, J.A. (2003). Splicing double: insights from the second spliceosome. *Nat Rev Mol Cell Biol* *4*, 960-970.
- Perez-Gonzalez, A., Pazo, A., Navajas, R., Ciordia, S., Rodriguez-Frandsen, A., and Nieto, A. (2014). hCLE/C14orf166 associates with DDX1-HSPC117-FAM98B in a novel transcription-dependent shuttling RNA-transporting complex. *PLoS One* *9*, e90957.
- Peters, J.M., Tedeschi, A., and Schmitz, J. (2008). The cohesin complex and its roles in chromosome biology. *Genes Dev* *22*, 3089-3114.
- Pickart, C.M. (2001). Mechanisms underlying ubiquitination. *Annu Rev Biochem* *70*, 503-533.
- Ponyeam, W., and Hagen, T. (2012). Characterization of the Cullin7 E3 ubiquitin ligase - Heterodimerization of cullin substrate receptors as a novel mechanism to regulate cullin E3 ligase activity. *Cell Signal* *24*, 290-295.
- Potts, P.R., Porteus, M.H., and Yu, H. (2006). Human SMC5/6 complex promotes sister chromatid homologous recombination by recruiting the SMC1/3 cohesin complex to double-strand breaks. *EMBO J* *25*, 3377-3388.
- Prokopenko, S.N., He, Y., Lu, Y., and Bellen, H.J. (2000). Mutations affecting the development of the peripheral nervous system in *Drosophila*: a molecular screen for novel proteins. *Genetics* *156*, 1691-1715.
- Pujol, N., Link, E.M., Liu, L.X., Kurz, C.L., Alloing, G., Tan, M.W., Ray, K.P., Solari, R., Johnson, C.D., and Ewbank, J.J. (2001). A reverse genetic analysis of components of the Toll signaling pathway in *Caenorhabditis elegans*. *Curr Biol* *11*, 809-821.
- Purvis, J.E., Karhohs, K.W., Mock, C., Batchelor, E., Loewer, A., and Lahav, G. (2012). p53 dynamics control cell fate. *Science* *336*, 1440-1444.
- Query, C.C., and Konarska, M.M. (2004). Suppression of multiple substrate mutations by spliceosomal prp8 alleles suggests functional correlations with ribosomal ambiguity mutants. *Mol Cell* *14*, 343-354.
- Rankin, S., Ayad, N.G., and Kirschner, M.W. (2005). Sororin, a substrate of the anaphase-promoting complex, is required for sister chromatid cohesion in vertebrates. *Mol Cell* *18*, 185-200.
- Rappsilber, J., Ryder, U., Lamond, A.I., and Mann, M. (2002). Large-scale proteomic analysis of the human spliceosome. *Genome Res* *12*, 1231-1245.

- Ratray, A.M., Nicholson, P., and Muller, B. (2013). Replication stress-induced alternative mRNA splicing alters properties of the histone RNA-binding protein HBP/SLBP: a key factor in the control of histone gene expression. *Biosci Rep* 33.
- Ray Chaudhuri, A., Hashimoto, Y., Herrador, R., Neelsen, K.J., Fachinetti, D., Bermejo, R., Cocito, A., Costanzo, V., and Lopes, M. (2012). Topoisomerase I poisoning results in PARP-mediated replication fork reversal. *Nat Struct Mol Biol* 19, 417-423.
- Reed, R. (2000). Mechanisms of fidelity in pre-mRNA splicing. *Curr Opin Cell Biol* 12, 340-345.
- Rein, K., and Stracker, T.H. (2014). The MRE11 complex: an important source of stress relief. *Exp Cell Res* 329, 162-169.
- Revil, T., Gaffney, D., Dias, C., Majewski, J., and Jerome-Majewska, L.A. (2010). Alternative splicing is frequent during early embryonic development in mouse. *BMC Genomics* 11, 399.
- Riedel, C.G., Katis, V.L., Katou, Y., Mori, S., Itoh, T., Helmhart, W., Galova, M., Petronczki, M., Gregan, J., Cetin, B., *et al.* (2006). Protein phosphatase 2A protects centromeric sister chromatid cohesion during meiosis I. *Nature* 441, 53-61.
- Rieder, C.L., and Maiato, H. (2004). Stuck in division or passing through: what happens when cells cannot satisfy the spindle assembly checkpoint. *Dev Cell* 7, 637-651.
- Rolef Ben-Shahar, T., Heeger, S., Lehane, C., East, P., Flynn, H., Skehel, M., and Uhlmann, F. (2008). Eco1-dependent cohesin acetylation during establishment of sister chromatid cohesion. *Science* 321, 563-566.
- Rosa, J., Canovas, P., Islam, A., Altieri, D.C., and Doxsey, S.J. (2006). Survivin modulates microtubule dynamics and nucleation throughout the cell cycle. *Mol Biol Cell* 17, 1483-1493.
- Rossiello, F., Herbig, U., Longhese, M.P., Fumagalli, M., and d'Adda di Fagagna, F. (2014). Irreparable telomeric DNA damage and persistent DDR signalling as a shared causative mechanism of cellular senescence and ageing. *Curr Opin Genet Dev* 26, 89-95.
- Rowland, B.D., Roig, M.B., Nishino, T., Kurze, A., Uluocak, P., Mishra, A., Beckouet, F., Underwood, P., Metson, J., Imre, R., *et al.* (2009). Building sister chromatid cohesion: smc3 acetylation counteracts an antiestablishment activity. *Mol Cell* 33, 763-774.
- Rubio, E.D., Reiss, D.J., Welcsh, P.L., Disteché, C.M., Filippova, G.N., Baliga, N.S., Aebersold, R., Ranish, J.A., and Krumm, A. (2008). CTCF physically links cohesin to chromatin. *Proc Natl Acad Sci U S A* 105, 8309-8314.
- Saretzki, G., Sitte, N., Merkel, U., Wurm, R.E., and von Zglinicki, T. (1999). Telomere shortening triggers a p53-dependent cell cycle arrest via accumulation of G-rich single stranded DNA fragments. *Oncogene* 18, 5148-5158.
- Sarikas, A., Hartmann, T., and Pan, Z.Q. (2011). The cullin protein family. *Genome Biol* 12, 220.
- Scanlan, M.J., Gordan, J.D., Williamson, B., Stockert, E., Bander, N.H., Jongeneel, V., Gure, A.O., Jager, D., Jager, E., Knuth, A., *et al.* (1999). Antigens recognized by autologous antibody in patients with renal-cell carcinoma. *Int J Cancer* 83, 456-464.
- Scheufele, F., Wolf, B., Kruse, M., Hartmann, T., Lempart, J., Muehlich, S., Pfeiffer, A.F., Field, L.J., Charron, M.J., Pan, Z.Q., *et al.* (2014). Evidence for a regulatory role of Cullin-RING E3 ubiquitin ligase 7 in insulin signaling. *Cell Signal* 26, 233-239.



- Schleiffer, A., Kaitna, S., Maurer-Stroh, S., Glotzer, M., Nasmyth, K., and Eisenhaber, F. (2003). Kleisins: a superfamily of bacterial and eukaryotic SMC protein partners. *Mol Cell* *11*, 571-575.
- Schmittgen, T.D., and Livak, K.J. (2008). Analyzing real-time PCR data by the comparative C(T) method. *Nat Protoc* *3*, 1101-1108.
- Schmitz, J., Watrin, E., Lenart, P., Mechtler, K., and Peters, J.M. (2007). Sororin is required for stable binding of cohesin to chromatin and for sister chromatid cohesion in interphase. *Curr Biol* *17*, 630-636.
- Schneider, M., Will, C.L., Anokhina, M., Tazi, J., Urlaub, H., and Luhrmann, R. (2010). Exon definition complexes contain the tri-snRNP and can be directly converted into B-like precatalytic splicing complexes. *Mol Cell* *38*, 223-235.
- Schnell, J.D., and Hicke, L. (2003). Non-traditional functions of ubiquitin and ubiquitin-binding proteins. *Journal of Biological Chemistry* *278*, 35857-35860.
- Schockel, L., Mockel, M., Mayer, B., Boos, D., and Stemmann, O. (2011). Cleavage of cohesin rings coordinates the separation of centrioles and chromatids. *Nat Cell Biol* *13*, 966-972.
- Schuldiner, O., Berdnik, D., Levy, J.M., Wu, J.S., Luginbuhl, D., Gontang, A.C., and Luo, L. (2008). piggyBac-based mosaic screen identifies a postmitotic function for cohesin in regulating developmental axon pruning. *Dev Cell* *14*, 227-238.
- Schwartz, S., Meshorer, E., and Ast, G. (2009). Chromatin organization marks exon-intron structure. *Nat Struct Mol Biol* *16*, 990-995.
- Schwer, B. (2008). A conformational rearrangement in the spliceosome sets the stage for prp22-dependent mRNA release. *Mol Cell* *30*, 743-754.
- Schwer, B., and Gross, C.H. (1998). Prp22, a DEXH-box RNA helicase, plays two distinct roles in yeast pre-mRNA splicing. *EMBO J* *17*, 2086-2094.
- Sepp, K.J., Hong, P., Lizarraga, S.B., Liu, J.S., Mejia, L.A., Walsh, C.A., and Perrimon, N. (2008). Identification of neural outgrowth genes using genome-wide RNAi. *PLoS Genet* *4*, e1000111.
- Serrano, A., Rodriguez-Corsino, M., and Losada, A. (2009). Heterochromatin protein 1 (HP1) proteins do not drive pericentromeric cohesin enrichment in human cells. *PLoS One* *4*, e5118.
- Sharma, S., Kohlstaedt, L.A., Damianov, A., Rio, D.C., and Black, D.L. (2008). Polypyrimidine tract binding protein controls the transition from exon definition to an intron defined spliceosome. *Nat Struct Mol Biol* *15*, 183-191.
- Shehadeh, L.A., Yu, K., Wang, L., Guevara, A., Singer, C., Vance, J., and Papapetropoulos, S. (2010). SRRM2, a potential blood biomarker revealing high alternative splicing in Parkinson's disease. *PLoS One* *5*, e9104.
- Shen, H., and Green, M.R. (2004). A pathway of sequential arginine-serine-rich domain-splicing signal interactions during mammalian spliceosome assembly. *Mol Cell* *16*, 363-373.
- Shen, H., and Green, M.R. (2006). RS domains contact splicing signals and promote splicing by a common mechanism in yeast through humans. *Genes Dev* *20*, 1755-1765.
- Shepard, P.J., and Hertel, K.J. (2009). The SR protein family. *Genome Biol* *10*, 242.

- Shi, Y., Reddy, B., and Manley, J.L. (2006). PP1/PP2A phosphatases are required for the second step of Pre-mRNA splicing and target specific snRNP proteins. *Mol Cell* *23*, 819-829.
- Shintomi, K., and Hirano, T. (2009). Releasing cohesin from chromosome arms in early mitosis: opposing actions of Wapl-Pds5 and Sgo1. *Genes Dev* *23*, 2224-2236.
- Shore, D., and Nasmyth, K. (1987). Purification and cloning of a DNA binding protein from yeast that binds to both silencer and activator elements. *Cell* *51*, 721-732.
- Sjogren, C., and Nasmyth, K. (2001). Sister chromatid cohesion is required for postreplicative double-strand break repair in *Saccharomyces cerevisiae*. *Curr Biol* *11*, 991-995.
- Skaar, J.R., Pagan, J.K., and Pagano, M. (2013). Mechanisms and function of substrate recruitment by F-box proteins. *Nat Rev Mol Cell Biol* *14*, 369-381.
- Sofueva, S., Yaffe, E., Chan, W.C., Georgopoulou, D., Vietri Rudan, M., Mira-Bontenbal, H., Pollard, S.M., Schroth, G.P., Tanay, A., and Hadjur, S. (2013). Cohesin-mediated interactions organize chromosomal domain architecture. *EMBO J* *32*, 3119-3129.
- Somma, M.P., Ceprani, F., Bucciarelli, E., Naim, V., De Arcangelis, V., Piergentili, R., Palena, A., Ciapponi, L., Giansanti, M.G., Pellacani, C., *et al.* (2008). Identification of *Drosophila* mitotic genes by combining co-expression analysis and RNA interference. *PLoS Genet* *4*, e1000126.
- Song, J., Lafont, A., Chen, J., Wu, F.M., Shirahige, K., and Rankin, S. (2012). Cohesin acetylation promotes sister chromatid cohesion only in association with the replication machinery. *J Biol Chem* *287*, 34325-34336.
- Soret, J., and Tazi, J. (2003). Phosphorylation-dependent control of the pre-mRNA splicing machinery. *Prog Mol Subcell Biol* *31*, 89-126.
- Staley, J.P., and Guthrie, C. (1998). Mechanical devices of the spliceosome: motors, clocks, springs, and things. *Cell* *92*, 315-326.
- Staley, J.P., and Woolford, J.L., Jr. (2009). Assembly of ribosomes and spliceosomes: complex ribonucleoprotein machines. *Curr Opin Cell Biol* *21*, 109-118.
- Strom, L., Karlsson, C., Lindroos, H.B., Wedahl, S., Katou, Y., Shirahige, K., and Sjogren, C. (2007). Postreplicative formation of cohesion is required for repair and induced by a single DNA break. *Science* *317*, 242-245.
- Strom, L., Lindroos, H.B., Shirahige, K., and Sjogren, C. (2004). Postreplicative recruitment of cohesin to double-strand breaks is required for DNA repair. *Mol Cell* *16*, 1003-1015.
- Sumara, I., Vorlaufer, E., Gieffers, C., Peters, B.H., and Peters, J.M. (2000). Characterization of vertebrate cohesin complexes and their regulation in prophase. *J Cell Biol* *151*, 749-762.
- Sundaramoorthy, S., Vazquez-Novelle, M.D., Lekomtsev, S., Howell, M., and Petronczki, M. (2014). Functional genomics identifies a requirement of pre-mRNA splicing factors for sister chromatid cohesion. *EMBO J* *33*, 2623-2642.
- Suzuki, M., Watanabe, M., Nakamaru, Y., Takagi, D., Takahashi, H., Fukuda, S., and Hatakeyama, S. (2015). TRIM39 negatively regulates the NFkappaB-mediated signaling pathway through stabilization of Cactin. *Cell Mol Life Sci*.
- Szatanek, T., Anderson-White, B.R., Faugno-Fusci, D.M., White, M., Saeij, J.P., and Gubbels, M.J. (2012). Cactin is essential for G1 progression in *Toxoplasma gondii*. *Mol Microbiol* *84*, 566-577.

- Takahashi, T.S., Yiu, P., Chou, M.F., Gygi, S., and Walter, J.C. (2004). Recruitment of Xenopus Scc2 and cohesin to chromatin requires the pre-replication complex. *Nat Cell Biol* 6, 991-996.
- Tanackovic, G., and Kramer, A. (2005). Human splicing factor SF3a, but not SF1, is essential for pre-mRNA splicing in vivo. *Mol Biol Cell* 16, 1366-1377.
- Tanaka, N., and Schwer, B. (2005). Characterization of the NTPase, RNA-binding, and RNA helicase activities of the DEAH-box splicing factor Prp22. *Biochemistry-US* 44, 9795-9803.
- Tang, Z., Sun, Y., Harley, S.E., Zou, H., and Yu, H. (2004). Human Bub1 protects centromeric sister-chromatid cohesion through Shugoshin during mitosis. *Proc Natl Acad Sci U S A* 101, 18012-18017.
- Tannoury, H., Rodriguez, V., Kovacevic, I., Ibourk, M., Lee, M., and Cram, E.J. (2010). CACN-1/Cactin interacts genetically with MIG-2 GTPase signaling to control distal tip cell migration in *C. elegans*. *Dev Biol* 341, 176-185.
- Tardiff, D.F., Lacadie, S.A., and Rosbash, M. (2006). A genome-wide analysis indicates that yeast pre-mRNA splicing is predominantly posttranscriptional. *Mol Cell* 24, 917-929.
- Teo, H., Ghosh, S., Luesch, H., Ghosh, A., Wong, E.T., Malik, N., Orth, A., de Jesus, P., Perry, A.S., Oliver, J.D., *et al.* (2010). Telomere-independent Rap1 is an IKK adaptor and regulates NF-kappaB-dependent gene expression. *Nat Cell Biol* 12, 758-767.
- Teo, J.L., and Kahn, M. (2010). The Wnt signaling pathway in cellular proliferation and differentiation: A tale of two coactivators. *Adv Drug Deliv Rev* 62, 1149-1155.
- Terret, M.E., Sherwood, R., Rahman, S., Qin, J., and Jallepalli, P.V. (2009). Cohesin acetylation speeds the replication fork. *Nature* 462, 231-234.
- Thunstrom, S., Sodermark, L., Ivarsson, L., Samuelsson, L., and Stefanova, M. (2015). UBE2A deficiency syndrome: a report of two unrelated cases with large Xq24 deletions encompassing UBE2A gene. *Am J Med Genet A* 167A, 204-210.
- Tilgner, H., Nikolaou, C., Althammer, S., Sammeth, M., Beato, M., Valcarcel, J., and Guigo, R. (2009). Nucleosome positioning as a determinant of exon recognition. *Nat Struct Mol Biol* 16, 996-1001.
- Toller, I.M., Neelsen, K.J., Steger, M., Hartung, M.L., Hottiger, M.O., Stucki, M., Kalali, B., Gerhard, M., Sartori, A.A., Lopes, M., *et al.* (2011). Carcinogenic bacterial pathogen *Helicobacter pylori* triggers DNA double-strand breaks and a DNA damage response in its host cells. *Proc Natl Acad Sci U S A* 108, 14944-14949.
- Tonkin, E.T., Wang, T.J., Lisgo, S., Bamshad, M.J., and Strachan, T. (2004). NIPBL, encoding a homolog of fungal Scc2-type sister chromatid cohesion proteins and fly Nipped-B, is mutated in Cornelia de Lange syndrome. *Nat Genet* 36, 636-641.
- Trembley, J.H., Wang, G., Unger, G., Slaton, J., and Ahmed, K. (2009). Protein kinase CK2 in health and disease: CK2: a key player in cancer biology. *Cell Mol Life Sci* 66, 1858-1867.
- Tseng, C.K., and Cheng, S.C. (2008). Both catalytic steps of nuclear pre-mRNA splicing are reversible. *Science* 320, 1782-1784.
- Tsunematsu, R., Nishiyama, M., Kotoshiba, S., Saiga, T., Kamura, T., and Nakayama, K.I. (2006). Fbxw8 is essential for Cul1-Cul7 complex formation and for placental development. *Mol Cell Biol* 26, 6157-6169.

- Tsutsumi, T., Kuwabara, H., Arai, T., Xiao, Y., and Decaprio, J.A. (2008). Disruption of the *Fbxw8* gene results in pre- and postnatal growth retardation in mice. *Mol Cell Biol* *28*, 743-751.
- Uhlmann, F., Wernic, D., Poupard, M.A., Koonin, E.V., and Nasmyth, K. (2000). Cleavage of cohesin by the CD clan protease separin triggers anaphase in yeast. *Cell* *103*, 375-386.
- Unal, E., Arbel-Eden, A., Sattler, U., Shroff, R., Lichten, M., Haber, J.E., and Koshland, D. (2004). DNA damage response pathway uses histone modification to assemble a double-strand break-specific cohesin domain. *Mol Cell* *16*, 991-1002.
- Unal, E., Heidinger-Pauli, J.M., and Koshland, D. (2007). DNA double-strand breaks trigger genome-wide sister-chromatid cohesion through Eco1 (Ctf7). *Science* *317*, 245-248.
- van Der Houven Van Oordt, W., Newton, K., Sreaton, G.R., and Caceres, J.F. (2000). Role of SR protein modular domains in alternative splicing specificity in vivo. *Nucleic Acids Res* *28*, 4822-4831.
- van der Lelij, P., Stocsits, R.R., Ladurner, R., Petzold, G., Kreidl, E., Koch, B., Schmitz, J., Neumann, B., Ellenberg, J., and Peters, J.M. (2014). SNW1 enables sister chromatid cohesion by mediating the splicing of sororin and APC2 pre-mRNAs. *EMBO J* *33*, 2643-2658.
- van der Sar, A.M., Stockhammer, O.W., van der Laan, C., Spaik, H.P., Bitter, W., and Meijer, A.H. (2006). MyD88 innate immune function in a zebrafish embryo infection model. *Infect Immun* *74*, 2436-2441.
- Villa, T., and Guthrie, C. (2005). The Isy1p component of the NineTeen complex interacts with the ATPase Prp16p to regulate the fidelity of pre-mRNA splicing. *Genes Dev* *19*, 1894-1904.
- Vitale, I., Galluzzi, L., Castedo, M., and Kroemer, G. (2011). Mitotic catastrophe: a mechanism for avoiding genomic instability. *Nat Rev Mol Cell Biol* *12*, 385-392.
- Wachtel, C., and Manley, J.L. (2009). Splicing of mRNA precursors: the role of RNAs and proteins in catalysis. *Mol Biosyst* *5*, 311-316.
- Wagner, J.D., Jankowsky, E., Company, M., Pyle, A.M., and Abelson, J.N. (1998). The DEAH-box protein PRP22 is an ATPase that mediates ATP-dependent mRNA release from the spliceosome and unwinds RNA duplexes. *EMBO J* *17*, 2926-2937.
- Wagner, S., Chiosea, S., Ivshina, M., and Nickerson, J.A. (2004). In vitro FRAP reveals the ATP-dependent nuclear mobilization of the exon junction complex protein SRm160. *J Cell Biol* *164*, 843-850.
- Wahl, M.C., Will, C.L., and Luhrmann, R. (2009). The spliceosome: design principles of a dynamic RNP machine. *Cell* *136*, 701-718.
- Waizenegger, I., Gimenez-Abian, J.F., Wernic, D., and Peters, J.M. (2002). Regulation of human separase by securin binding and autocleavage. *Curr Biol* *12*, 1368-1378.
- Wallace, J.A., and Felsenfeld, G. (2007). We gather together: insulators and genome organization. *Curr Opin Genet Dev* *17*, 400-407.
- Walsh, D., and Mohr, I. (2011). Viral subversion of the host protein synthesis machinery. *Nat Rev Microbiol* *9*, 860-875.
- Wang, Z., and Burge, C.B. (2008). Splicing regulation: from a parts list of regulatory elements to an integrated splicing code. *RNA* *14*, 802-813.

- Ward, A.J., and Cooper, T.A. (2010). The pathobiology of splicing. *J Pathol* *220*, 152-163.
- Watanabe, Y. (2010). Temporal and spatial regulation of targeting aurora B to the inner centromere. *Cold Spring Harb Symp Quant Biol* *75*, 419-423.
- Watrin, E., Demidova, M., Watrin, T., Hu, Z., and Prigent, C. (2014). Sororin pre-mRNA splicing is required for proper sister chromatid cohesion in human cells. *EMBO Rep* *15*, 948-955.
- Watrin, E., and Peters, J.M. (2009). The cohesin complex is required for the DNA damage-induced G2/M checkpoint in mammalian cells. *EMBO J* *28*, 2625-2635.
- Watrin, E., Schleiffer, A., Tanaka, K., Eisenhaber, F., Nasmyth, K., and Peters, J.M. (2006). Human Scc4 is required for cohesin binding to chromatin, sister-chromatid cohesion, and mitotic progression. *Curr Biol* *16*, 863-874.
- Wei, M., Zhao, X., Liu, M., Huang, Z., Xiao, Y., Niu, M., Shao, Y., and Kleiman, L. (2015). Inhibition of HIV-1 assembly by coiled-coil domain containing protein 8 in human cells. *Sci Rep* *5*, 14724.
- Wendt, K.S., Yoshida, K., Itoh, T., Bando, M., Koch, B., Schirghuber, E., Tsutsumi, S., Nagae, G., Ishihara, K., Mishiro, T., *et al.* (2008). Cohesin mediates transcriptional insulation by CCCTC-binding factor. *Nature* *451*, 796-801.
- Will, C.L., and Luhrmann, R. (2011). Spliceosome structure and function. *Cold Spring Harb Perspect Biol* *3*.
- Wlodaver, A.M., and Staley, J.P. (2014). The DExD/H-box ATPase Prp2p destabilizes and proofreads the catalytic RNA core of the spliceosome. *RNA* *20*, 282-294.
- Wojcechowskyj, J.A., Didigu, C.A., Lee, J.Y., Parrish, N.F., Sinha, R., Hahn, B.H., Bushman, F.D., Jensen, S.T., Seeholzer, S.H., and Doms, R.W. (2013). Quantitative phosphoproteomics reveals extensive cellular reprogramming during HIV-1 entry. *Cell Host Microbe* *13*, 613-623.
- Wojtuszkiewicz, A., Assaraf, Y.G., Maas, M.J., Kaspers, G.J., Jansen, G., and Cloos, J. (2015). Pre-mRNA splicing in cancer: the relevance in oncogenesis, treatment and drug resistance. *Expert Opin Drug Metab Toxicol* *11*, 673-689.
- Wu, K., Fuchs, S.Y., Chen, A., Tan, P., Gomez, C., Ronai, Z., and Pan, Z.Q. (2000). The SCF(HOS/beta-TRCP)-ROC1 E3 ubiquitin ligase utilizes two distinct domains within CUL1 for substrate targeting and ubiquitin ligation. *Mol Cell Biol* *20*, 1382-1393.
- Wu, L.P., and Anderson, K.V. (1998). Regulated nuclear import of Rel proteins in the *Drosophila* immune response. *Nature* *392*, 93-97.
- Xiao, X., Wang, Z., Jang, M., and Burge, C.B. (2007). Coevolutionary networks of splicing cis-regulatory elements. *Proc Natl Acad Sci U S A* *104*, 18583-18588.
- Xie, T., Rowen, L., Aguado, B., Ahearn, M.E., Madan, A., Qin, S., Campbell, R.D., and Hood, L. (2003). Analysis of the gene-dense major histocompatibility complex class III region and its comparison to mouse. *Genome Res* *13*, 2621-2636.
- Xu, X., Keshwani, M., Meyer, K., Sarikas, A., Taylor, S., and Pan, Z.Q. (2012). Identification of the degradation determinants of insulin receptor substrate 1 for signaling cullin-RING E3 ubiquitin ligase 7-mediated ubiquitination. *J Biol Chem* *287*, 40758-40766.
- Xu, X., Landesman-Bollag, E., Channavajhala, P.L., and Seldin, D.C. (1999). Murine protein kinase CK2: gene and oncogene. *Mol Cell Biochem* *191*, 65-74.

- Xu, X., Sarikas, A., Dias-Santagata, D.C., Dolios, G., Lafontant, P.J., Tsai, S.C., Zhu, W., Nakajima, H., Nakajima, H.O., Field, L.J., *et al.* (2008). The CUL7 E3 ubiquitin ligase targets insulin receptor substrate 1 for ubiquitin-dependent degradation. *Mol Cell* *30*, 403-414.
- Yan, J., Yan, F., Li, Z.J., Sinnott, B., Cappell, K.M., Yu, Y.B., Mo, J.Y., Duncan, J.A., Chen, X., Cormier-Daire, V., *et al.* (2014). The 3M Complex Maintains Microtubule and Genome Integrity. *Mol Cell* *54*, 791-804.
- Yazdi, P.T., Wang, Y., Zhao, S., Patel, N., Lee, E.Y., and Qin, J. (2002). SMC1 is a downstream effector in the ATM/NBS1 branch of the human S-phase checkpoint. *Genes Dev* *16*, 571-582.
- Yuryev, A., Patturajan, M., Litingtung, Y., Joshi, R.V., Gentile, C., Gebara, M., and Corden, J.L. (1996). The C-terminal domain of the largest subunit of RNA polymerase II interacts with a novel set of serine/arginine-rich proteins. *Proc Natl Acad Sci U S A* *93*, 6975-6980.
- Zhang, B., Jain, S., Song, H., Fu, M., Heuckeroth, R.O., Erlich, J.M., Jay, P.Y., and Milbrandt, J. (2007). Mice lacking sister chromatid cohesion protein PDS5B exhibit developmental abnormalities reminiscent of Cornelia de Lange syndrome. *Development* *134*, 3191-3201.
- Zhang, J., Shi, X., Li, Y., Kim, B.J., Jia, J., Huang, Z., Yang, T., Fu, X., Jung, S.Y., Wang, Y., *et al.* (2008). Acetylation of Smc3 by Eco1 is required for S phase sister chromatid cohesion in both human and yeast. *Mol Cell* *31*, 143-151.
- Zhang, L., Huang, N.J., Chen, C., Tang, W., and Kornbluth, S. (2012a). Ubiquitylation of p53 by the APC/C inhibitor Trim39. *Proc Natl Acad Sci U S A* *109*, 20931-20936.
- Zhang, L., Mei, Y., Fu, N.Y., Guan, L., Xie, W., Liu, H.H., Yu, C.D., Yin, Z., Yu, V.C., and You, H. (2012b). TRIM39 regulates cell cycle progression and DNA damage responses via stabilizing p21. *Proc Natl Acad Sci U S A* *109*, 20937-20942.
- Zhang, N., Panigrahi, A.K., Mao, Q., and Pati, D. (2011). Interaction of Sororin protein with polo-like kinase 1 mediates resolution of chromosomal arm cohesion. *J Biol Chem* *286*, 41826-41837.
- Zhang, N., and Pati, D. (2012). Sororin is a master regulator of sister chromatid cohesion and separation. *Cell Cycle* *11*, 2073-2083.
- Zhang, S., Shi, L., Yang, Q.H., Dong, X.H., Chi, S.Y., Liu, H.Y., and Tan, B.P. (2014). Molecular characterization and functional analysis of Cactin gene from *Litopenaeus vannamei*. *Fish Shellfish Immunol* *41*, 608-617.
- Zhou, H.L., Luo, G., Wise, J.A., and Lou, H. (2014). Regulation of alternative splicing by local histone modifications: potential roles for RNA-guided mechanisms. *Nucleic Acids Res* *42*, 701-713.
- Zhou, Z., Licklider, L.J., Gygi, S.P., and Reed, R. (2002). Comprehensive proteomic analysis of the human spliceosome. *Nature* *419*, 182-185.
- Zhu, W., Rainville, I.R., Ding, M., Bolus, M., Heintz, N.H., and Pederson, D.S. (2002). Evidence that the pre-mRNA splicing factor Clf1p plays a role in DNA replication in *Saccharomyces cerevisiae*. *Genetics* *160*, 1319-1333.

## 8 CURRICULUM VITAE

### Personal information

Name Isabella Martina Yvonne  
 Family name Zanini  
 Date of birth February 9th 1985  
 Place of origin Bellinzona  
 Nationality swiss  
  
 Address Institute of Biochemistry, ETHZ  
 Otto-Stern Weg 3, HPM E17.1  
 8093 Zurich, Switzerland



### Diplomas

Master of Science in Biology - Molecular & Cellular  
 Biology - University of Zurich  
 Bachelor of Science in Biology - University of Zurich  
 Cantonal High School Leaving Certificate - Biology &  
 Chemistry - Liceo Cantonale di Bellinzona

### Research experiences

Since 01.01.2012 Doctoral studies  
 Molecular Life Science PhD Program Zurich  
 Group of Prof. Claus M. Azzalin  
 Institute of Biochemistry, ETH Zurich  
 Doctoral thesis "*Functions of human Cactin in pre-mRNA  
 splicing and chromosome stability*"

07.2010 - 12.2011 Internship - Research assistant  
 Group of Prof. Massimo Lopes  
 Institute of Molecular Cancer Research, University Zurich

03-2010-07.2011 Master studies  
 Group of Prof. Massimo Lopes  
 Institute of Molecular Cancer Research, University Zurich  
 Master thesis "*DNA re-replication: molecular features and  
 cellular responses*"

**Education**

- 2010 - 2011      Master studies in Molecular and Cellular Biology  
University of Zurich
- 2006 -.2010      Bachelor studies in Biology  
University of Zurich
- 2004 - 2006      Veterinary studies  
University of Zurich
- 1999 - 2004      Maturità liceale cantonale  
Liceo di Bellinzona

**Meetings**

- 2014              "Swiss Meeting on Genome Stability and Chromatin Dynamics"  
Weggis, Switzerland  
Poster presentation
- 2012              EMBO Conf. "Telomeres and the DNA damage response"  
L'Isle sur la Sorgue, France
- 2014              C.R. Brupbacher Symposium  
Zurich, Switzerland  
Poster presentation

**Publications**

K. J. Neelsen<sup>1</sup>, **I. M. Y. Zanini**<sup>1</sup>, S. Mijic, R. Herrador, R. Zellweger, A. Ray  
chaudhuri, K. D. Creavin, J.J. Blow, and M. Lopes; *Deregulated origin  
licensing leads to chromosomal breaks by replication of gapped DNA  
template*. Genes Dev., 2013

<sup>1</sup> Shared first author

K. J. Neelsen, **I. M.Y. Zanini**, R. Herrador, and M. Lopes; *Oncogenes induce  
genotoxic stress by mitotic processing of unusual replication intermediates*. J.  
Cell Biol., 2013

**Languages**

Italian (mother tongue)  
English (full professional proficiency)  
German (professional working proficiency)  
French (limited working proficiency)



**Extra-curricular activities**

since 2009	Municipal counsellor in Gudo, Ticino
2013	Organisation of the Molecular Life Science PhD program student retreat
2006 - 2010	Supply teacher and Summer courses Associazione Mise, Ticino Areas of teaching "Biology & Chemistry"
2006 - 2008	Summer job, Accounting and office skills Rodoni sagl, Ticino